IAEA TECDOC SERIES

IAEA-TECDOC-1753

# New Technologies for Seawater Desalination Using Nuclear Energy

IAEA
International Atomic Energy Agency

# NEW TECHNOLOGIES FOR SEAWATER DESALINATION USING NUCLEAR ENERGY

The following States are Members of the International Atomic Energy Agency:

AFGHANISTAN
ALBANIA
ALGERIA
ANGOLA
ARGENTINA
ARMENIA
AUSTRALIA
AUSTRIA
AZERBAIJAN
BAHAMAS
BAHRAIN
BANGLADESH
BELARUS
BELGIUM
BELIZE
BENIN
BOLIVIA
BOSNIA AND HERZEGOVINA
BOTSWANA
BRAZIL
BRUNEI DARUSSALAM
BULGARIA
BURKINA FASO
BURUNDI
CAMBODIA
CAMEROON
CANADA
CENTRAL AFRICAN REPUBLIC
CHAD
CHILE
CHINA
COLOMBIA
CONGO
COSTA RICA
CÔTE D'IVOIRE
CROATIA
CUBA
CYPRUS
CZECH REPUBLIC
DEMOCRATIC REPUBLIC OF THE CONGO
DENMARK
DOMINICA
DOMINICAN REPUBLIC
ECUADOR
EGYPT
EL SALVADOR
ERITREA
ESTONIA
ETHIOPIA
FIJI
FINLAND
FRANCE
GABON
GEORGIA
GERMANY
GHANA
GREECE
GUATEMALA
HAITI
HOLY SEE
HONDURAS
HUNGARY
ICELAND
INDIA
INDONESIA
IRAN, ISLAMIC REPUBLIC OF
IRAQ
IRELAND
ISRAEL
ITALY
JAMAICA
JAPAN
JORDAN
KAZAKHSTAN
KENYA
KOREA, REPUBLIC OF
KUWAIT
KYRGYZSTAN
LAO PEOPLE'S DEMOCRATIC REPUBLIC
LATVIA
LEBANON
LESOTHO
LIBERIA
LIBYA
LIECHTENSTEIN
LITHUANIA
LUXEMBOURG
MADAGASCAR
MALAWI
MALAYSIA
MALI
MALTA
MARSHALL ISLANDS
MAURITANIA, ISLAMIC REPUBLIC OF
MAURITIUS
MEXICO
MONACO
MONGOLIA
MONTENEGRO
MOROCCO
MOZAMBIQUE
MYANMAR
NAMIBIA
NEPAL
NETHERLANDS
NEW ZEALAND
NICARAGUA
NIGER
NIGERIA
NORWAY
OMAN
PAKISTAN
PALAU
PANAMA
PAPUA NEW GUINEA
PARAGUAY
PERU
PHILIPPINES
POLAND
PORTUGAL
QATAR
REPUBLIC OF MOLDOVA
ROMANIA
RUSSIAN FEDERATION
RWANDA
SAN MARINO
SAUDI ARABIA
SENEGAL
SERBIA
SEYCHELLES
SIERRA LEONE
SINGAPORE
SLOVAKIA
SLOVENIA
SOUTH AFRICA
SPAIN
SRI LANKA
SUDAN
SWAZILAND
SWEDEN
SWITZERLAND
SYRIAN ARAB REPUBLIC
TAJIKISTAN
THAILAND
THE FORMER YUGOSLAV REPUBLIC OF MACEDONIA
TOGO
TRINIDAD AND TOBAGO
TUNISIA
TURKEY
UGANDA
UKRAINE
UNITED ARAB EMIRATES
UNITED KINGDOM OF GREAT BRITAIN AND NORTHERN IRELAND
UNITED REPUBLIC OF TANZANIA
UNITED STATES OF AMERICA
URUGUAY
UZBEKISTAN
VENEZUELA, BOLIVARIAN REPUBLIC OF
VIET NAM
YEMEN
ZAMBIA
ZIMBABWE

The Agency's Statute was approved on 23 October 1956 by the Conference on the Statute of the IAEA held at United Nations Headquarters, New York; it entered into force on 29 July 1957. The Headquarters of the Agency are situated in Vienna. Its principal objective is "to accelerate and enlarge the contribution of atomic energy to peace, health and prosperity throughout the world''.

IAEA-TECDOC-1753

# NEW TECHNOLOGIES FOR SEAWATER DESALINATION USING NUCLEAR ENERGY

INTERNATIONAL ATOMIC ENERGY AGENCY
VIENNA, 2015

## COPYRIGHT NOTICE



For further information on this publication, please contact:

Nuclear Power Technology Development Section
International Atomic Energy Agency
Vienna International Centre
PO Box 100
1400 Vienna, Austria
Email: Official.Mail@iaea.org


Printed by the IAEA in Austria
January 2015

IAEA Library Cataloguing in Publication Data

New technologies for seawater desalination using nuclear energy.
— Vienna : International Atomic Energy Agency, 2015.
p. ; 30 cm. — (IAEA-TECDOC series, ISSN 1011–4289 ; no. 1753)
ISBN 978–92–0–100115–3
Includes bibliographical references.

1. Nuclear saline water conversion plants. 2. Nuclear energy — Industrial applications. 3. Saline water conversion — Economic aspects. I. International Atomic Energy Agency. II. Series.

IAEAL 15–00952

# FOREWORD

As seawater desalination technologies are rapidly evolving and more States are opting for dual purpose integrated power plants (i.e. cogeneration), the need for advanced technologies suitable for coupling to nuclear power plants and leading to more efficient and economic nuclear desalination systems is obvious. The Coordinated Research Programme (CRP) New Technologies for Seawater Desalination using Nuclear Energy was organized in the framework of the Technical Working Group on Nuclear Desalination (TWG-ND). The TWG-ND was established in 2008 with the purpose of advising the IAEA Deputy Director General and promoting the exchange of technical information on national programmes in the field of seawater desalination using nuclear energy.

This CRP project was conducted within the Nuclear Power Technology Development Section of the IAEA. It was launched in 2009 and completed by 2011, with research proposals received from nine Member States: Algeria, Egypt, France, India, Indonesia, Pakistan, the Syrian Arab Republic, the United Kingdom and the United States of America.

The project aimed to review innovative technologies for seawater desalination which could be coupled to main types of existing nuclear power plant. Such coupling is expected to help making nuclear desalination safer and more economical, and hence more attractive for newcomer States interested in nuclear desalination. The project also aimed to collect ideas and suggestions necessary to update the IAEA desalination economic evaluation program (DEEP) software to become more robust and versatile. The specific objectives of the project were the introduction of innovative technologies and their economic viability, which could help make nuclear desalination a globally viable option for the safe and sustainable production of fresh water. The technologies under scrutiny in this CRP involve the low temperature horizontal tube multi-effect distillation, heat recovery systems using heat pipe based heat exchangers, and zero brine discharge systems. Additional objectives of the CRP were to analyse the economics of various desalination projects. Such analysis was expected to generate feedbacks, new ideas and suggestions to improve the IAEA DEEP software.

The outcome of the CRP was expected to enhance collaboration among researchers representing the nine Member States on various subjects related to seawater desalination using nuclear energy, including information exchange on feasibility studies and aspects of new technologies. The CRP was also to include the quest and analysis of potential new technologies that are expected to enhance the application of nuclear desalination, such as the re-use of waste heat from nuclear power plants and an update of the IAEA DEEP with new models to enhance its use, for example the addition of the model for bankable feasibility studies of desalination projects.

The aim of this publication is to summarize the outputs from the Member States which participated in this CRP. The publication follows the same objectives and scope as those established for the CRP. It also presents the Member States' results and highlights major advances, difficulties and recommendations in the area of seawater desalination using nuclear energy which are of importance to the nuclear communities at large and to scientists and engineers focusing on potential new technologies, technical considerations and economics of the overall nuclear power plant coupled to seawater desalination plants.

This publication has been prepared through the collaboration of all the participants to the CRP. The IAEA appreciates this support and thanks all the authors who provided their reviews and contributions. The IAEA officer responsible for this publication was I. Khamis of the Division of Nuclear Power.

*EDITORIAL NOTE*

# CONTENTS

## INTRODUCTION

Desalination refers to any of several processes that remove some amount of salt and other minerals from saline water. More generally, desalination may also refer to the removal of salts and minerals as in soil desalination.

The desalination industry is the lifeline for several countries and zones around the world, especially the Gulf countries, southern California, and the Caribbean islands. The industry has expanded considerably since the 1950s. The early production units, the fully immersed type evaporators, had a very poor overall performance and were built in a very small number. Operation of such units was plagued by scale formation, excessive corrosion, and high frequency of tube failure. The units were operated for periods of less than 4 weeks, followed by a similar period for cleaning and maintenance. Since then, various developments have been achieved in system design, construction, operation, and control, where use of alloy materials and special chemicals allows for plant operating factors close to 90%. The two most commonly used desalination technologies are MSF (multistage flash) and RO (reverse osmosis) systems. Being the most recent technology, RO has become dominant in the desalination industry over the last decade. In 1999, about 78% of global production capacity comprised of MSF plants and RO accounted for a modest 10%. But in 2008 [1], the total installed capacity of desalination plants was 61 million $m^3$ per day, and RO accounted for 53% of worldwide capacity, whereas MSF consisted of about 23%. Although MED (multieffect desalination) is less common than RO or MSF, it still accounts for a significant percentage of the global desalination capacity (8%). MED is only used on a limited basis (3%). Figure 1 shows the new global desalination plant capacity by technology in 2012 [2].

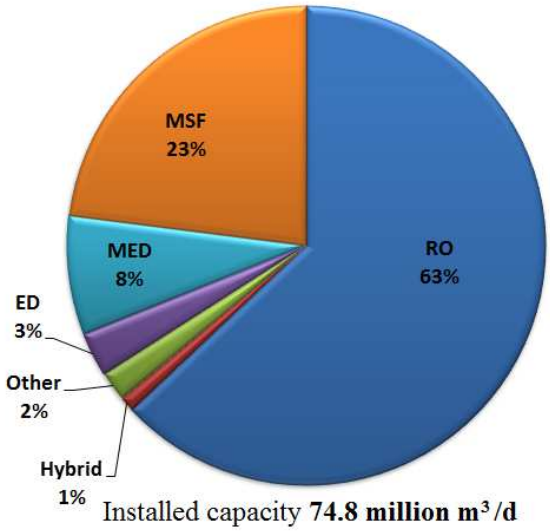


*FIG. 1. Global desalination plant capacity by technology (2012).*

As the number of installed plants worldwide has increased to more than 15 000 in 125 countries [3], there has been a decrease in the production cost of desalinated water obtained by RO, from \$1.92 per $m^3$ at Catalina Island, California in 1990 to a low point of \$0.47 at Tuas, Singapore in 2003, but then rising again to \$1.10 at Chennai, India in 2005, as seen from a survey of 20 plants over that period [4]. The full details are given in the Table 1.

Comparisons can be misleading, as many factors influence the product water cost such as plant size, feedwater characteristics, the recovery rate, pretreatment requirements and membrane life. The main reason for the recent upward trend has been the rise in the cost of construction and of power. The breakdown of production costs for a 100 000 $m^3$/day seawater RO plant is as shown in Fig. 2 [4]. Between 1980 and 2000 the amount of energy needed for seawater desalination was halved because of improvements in pumps and other equipment, and has been further halved with new energy recovery systems that regain 97% of the energy used [2]. In the Ashkelon and Tuas plants this has helped in achieving a production cost of \$0.47–0.5 1/$m^3$, the lowest cost recorded. However, the cost of water produced from desalination plant depends on the size, geographical location, infrastructure availability and other local factors.

TABLE 1. RO DESALINATION WATER COST IN THE YEAR OF BID [4]

| Year | Location | US\$/$m^3$ |
|---|---|---|
| 1990 | Catalina Island, California | 1.92 |
| 1991 | Santa Barbara, California | 1.53 |
| 1993 | Monterey, California | 1.57 |
| 1996 | Bahamas | 1.25 |
| 1997 | Dhekelia, Cyprus | 1.20 |
| 1999 | Larnaca, Cyprus | 0.80 |
| 2000 | Trinidad | 0.70 |
| 2000 | Tampa, Florida | 0.57 |
| 2001 | Ashkelon 1, Israel | 0.51 |
| 2002 | Ashkelon 1, Israel | 0.49 |
| 2003 | Tuas, Singapore | 0.47 |
| 2004 | Spain | 0.61 |
| 2004 | Tampa, remedied | 0.68 |
| 2005 | Cap Djinet, Algeria | 0.70 |
| 2005 | El Hamma, Israel | 0.70 |
| 2005 | Douaouda, Algeria | 0.72 |
| 2005 | Shoaiba, Saudi Arabia | 0.73 |
| 2005 | Perth, Western Australia | 0.90 |
| 2005 | Chennai, India | 1.10 |
| 2005 | Trinidad | 0.85 |

The future production cost of desalinated water will be heavily influenced by the cost of plant construction and the anticipated increasing cost of energy. This may be partly offset by improved production efficiencies if membranes can be developed that are less prone to fouling or the pretreatment processes are improved (e.g. with low cost MF/UF), for example: if the processes can operate at lower pressures, achieve higher rejection of contaminants or require less pretreatment of feedwater. All these aspects of desalination are the focus of much research.

Concomitant with the objectives of the IAEA programme A1 in support of nuclear desalination (in the IAEA terminology, nuclear desalination is defined to be the production of potable water from seawater in a facility in which a nuclear reactor is used as the source of energy for the desalination process) and pursuing the repeated resolutions in its general conferences to promote the development of nuclear desalination systems.

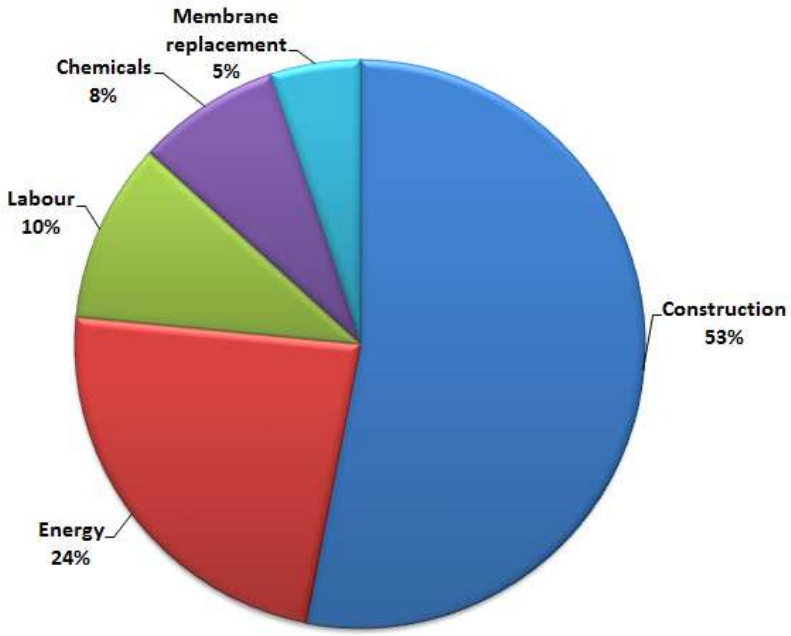


*FIG. 2. Costs of water production, 100 000 $m^3$/day SWRO desalination plant.*

The IAEA has, in the past, organized two CRPs [5]: on the optimization of coupling of nuclear reactors and desalination systems and on the economic research on, and the assessment of, selected nuclear desalination projects and case studies.

## 1.1. OBJECTIVES

As desalination is a very rapidly evolving field, and as more and more countries are opting for dual purpose integrated nuclear desalination systems, the need for advances in technologies leading to more efficient and economic systems is obvious. It seems that it is the time to go beyond techno-economic studies, and invest in promoting R&D on new technologies that can be employed in nuclear desalination systems to make nuclear desalination a viable option.

Hence, this CRP focused on the introduction of innovative technologies that may help making nuclear desalination safer and more economical. The new technologies are expected to enhance the harvesting of waste heat available in nuclear reactors (i.e. waste heat from the condenser of water cooled reactors, or from the precooler and intercooler of high temperature gas reactors (HTGR) and utilize it for seawater desalination. New technologies may involve technologies related to the desalination processes such as LTHT MED, others related to the efficient and maximizing heat recovery systems such as heat pipes, or the optimization of coupling configuration between nuclear reactors and desalination systems. Additional dimensions of the CRP are to analyse the economics of cogeneration systems (i.e. for electricity and water production), and improve the IAEA DEEP software.

## 1.2. SUBJECTS FOR INVESTIGATION

During this CRP, the following subjects were investigated:

- Desalination with nuclear energy:

  — Desalination technologies;
  — Combined water desalination and power generation.

- Promising technologies for desalination with nuclear energy:

  — Low temperature (LT) evaporation plants to enhance waste heat utilization;
  — Improved performance of RO plants at elevated temperature;
  — High temperature ultrafiltration (UF) for seawater feed pretreatment;
  — Hybrid desalination systems;
  — Heat pipe technology for improved waste heat recovery and safety of nuclear desalination.

- Competitiveness and sustainability of nuclear desalination:

  — New modelling approach for multiple effect evaporation plants;
  — New financial modelling for feasibility of cogeneration projects;
  — Life cycle assessment (LCA) for power and desalination plant impacts on climate change.

- New models for IAEA nuclear desalination tools:

  — Desalination economic evaluation program (DEEP);
  — New robust thermodynamic modules for DEEP.

- Techno-economic feasibility study of nuclear desalination (Algeria case study):

  — Background;
  — Site Selection;
  — Technology assessment;
  — Economic evaluation;
  — Conclusions.

## DESALINATION WITH NUCLEAR ENERGY

Worldwide availability of potable water greatly exceeds the amounts needed and used, but resources are not evenly distributed. There are regions where water is scarce, and where the population is already at the mercy of inadequate supplies. Seawater constitutes a practically unlimited source of supply. When desalted, it can contribute to the solution of growing water problems, wherever the sea is accessible. Desalination, as all industrial processes, requires energy. Fossil energy resources are limited, however, and their increasingly intensive use raises environmental concerns, including the threat of a gradual climate change with far-reaching consequences. At the same time, worldwide demand for energy is steadily growing, and adequate solutions are needed.

Nuclear desalination as designated by the IAEA is the production of potable water in a facility where a nuclear reactor is used as the source of energy for the desalination process. Electrical and/or thermal energy from the reactor is directly used by the desalination plants. An isolation loop is provided between the nuclear reactor and the desalination plant to ensure no radioactive contamination and high protection of desalinated water. Co-location of desalination and power plants has benefits of sharing the infrastructural facilities as in the case of hybrid plants. Dual purpose plants generating power and water have inherent design strategies for better thermodynamic efficiency besides economic optimization. Interest in using nuclear energy for the production of desalinated water is growing worldwide. This has been motivated by a wide variety of reasons such as economic competitiveness of nuclear energy to energy supply diversification etc.

### 1.3. DESALINATION TECHNOLOGIES

The two major types of desalination technologies used around the world can be broadly classified as either thermal desalination processes, in which feedwater is boiled and the vapour condensed as pure water (distillate), or membrane desalination processes, in which semi-permeable membranes are used to filter out the dissolved solids. Both technologies need energy to operate. Within these two types there are sub-categories (processes) using different techniques, as shown below and in Fig. 3:

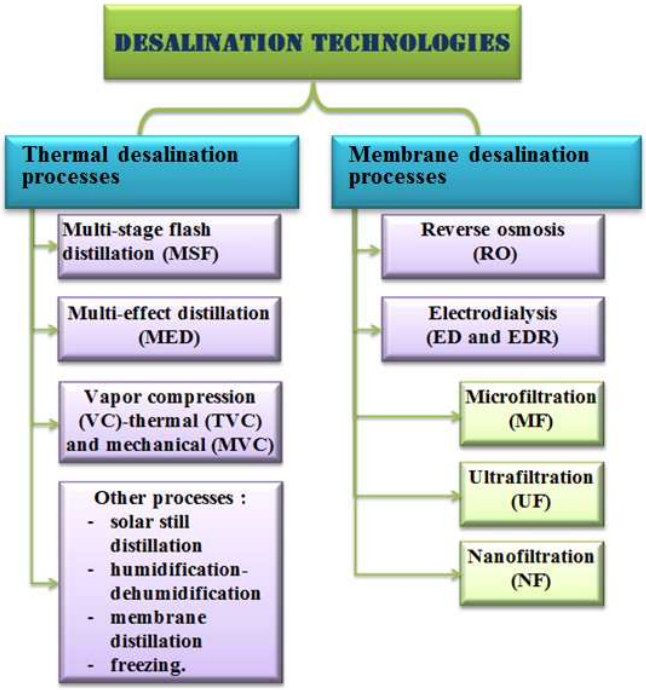


*FIG. 3. Classification of desalination technologies.*

- Thermal desalination processes:

  — MSF distillation;
  — Multieffect distillation (MED);
  — Vapour compression (VC), thermal (TVC) and mechanical (MVC);
  — Other processes include solar still distillation, humidification-dehumidification, membrane distillation, and freezing.

- Membrane desalination processes:

  — Reverse osmosis (RO);
  — Electro dialysis (ED and EDR).

Three other membrane processes that are not considered desalination processes, but that are relevant, are: microfiltration (MF), ultrafiltration (UF), and nanofiltration (NF). The ion exchange process is also not regarded as a desalination process, but is generally used to improve water quality for some specific purposes, e.g. boiler feedwater.

### 1.3.1. Thermal desalination processes

Thermal desalination processes account for about 50% of the entire desalination market. The remaining market share is dominated by the RO process. The main thermal desalination processes include MSF, MED/TVC/MVC. Other thermal desalination processes, e.g. solar stills, humidification-dehumidification, freezing, etc., are only found on a pilot or experimental scale. Thermal desalination processes consume a larger amount of energy than RO; approximately the electrical equivalent of 10–15 kWh/$m^3$ for thermal processes versus

5 kWh/$m^3$ for RO. The reliability and massive field experience in thermal desalination keep its production cost competitive compared to the RO process. Also, the large-scale production capacity for a single MSF unit (about 75 000 $m^3$/day) is sufficient to provide potable water for 300 000 inhabitants. An increase in production capacity for the MED system has been realized recently, with unit production capacities up to 30 000 $m^3$/day [6].

The following chapter covers various aspects of thermal desalination processes. It also includes a review of design and operation. The analysis of each process includes process descriptions, process models, and an illustration of system design and performance analysis.

*Multistage flash*

The single-effect evaporation system for seawater desalination has no practical use on an industrial scale. This is because the system has a thermal performance ratio (PR) of less than 1, i.e. the mass of water produced is less than the mass of heating steam used to operate the system. However, the understanding of this process is essential as it is a constituent of other single-effect vapour compression systems, as well as multiple effect evaporation processes. In a MSF process, seawater is heated by passing through a brine heater (Fig. 4). Heated seawater then flows into a stage, where the ambient pressure is lowered for the water to boil. Sudden introduction of the heated water into the chamber causes it to boil rapidly, almost flashing into steam. Generally, only a small percentage of this water is converted to steam/water vapour, depending on the pressure maintained in the stage, since flashing will continue only until the water cools down, releasing the heat of vaporization to below the boiling point. Remaining heated seawater passes to the next stage, which is at a lower atmospheric pressure, causing it to flash again. This is repeated so that the feedwater passes from one stage to another and is boiled repeatedly without additional heat. Typically, an MSF plant contains 4–40 stages, with 20–30 constantly being operated. The steam generated by flashing is converted to fresh water after condensing by making contact with cool tubes that run through stage. The tubes are cooled by the incoming seawater going into the brine heater. This, in turn, warms up the feedwater so that the amount of thermal energy needed in the brine heater to raise the temperature of the seawater is reduced.

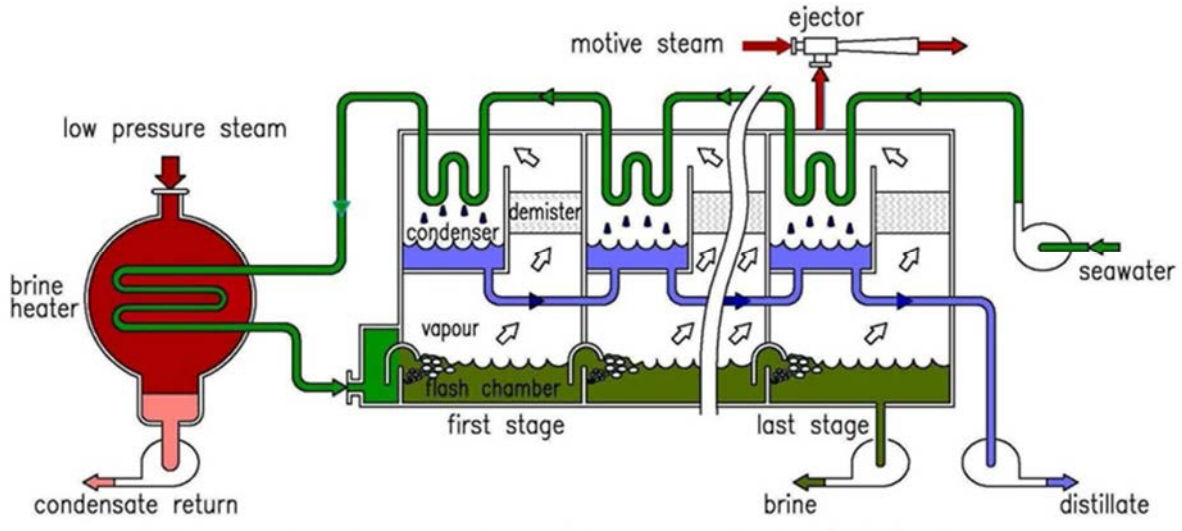


*FIG. 4. Schematic diagram of (MSF) distillation.*

*Multiple effect distillation*

The multiple effect distillation process can be found in various industries, i.e. sugar, paper and pulp, dairy, textiles, acids and desalination. Small MED plants with capacities of less than 500 $m^3$/day were introduced to the desalination industry in the 1960s. Subsequent developments lead to the increase in unit production capacity.

In 2006, MED capacity increased to a value of 36 000 $m^3$/day [6]. Most MED processes operate at LT of less than 70°C. This is because the evaporators adopt a horizontal tube thin film (HTTF) configuration, where the feed seawater is sprayed on the outside surface of the tubes. Therefore, LT operation limits the rate of scale formation on the outside surface of the evaporator tubes as well as allows the use of cheaper materials for heat exchangers. MED, like the MSF process, takes place through a series of small-scale processes, and the ambient pressure is reduced in successive effects (Fig. 5).

This permits the seawater feed to undergo boiling in multiple stages without supplying additional heat after the first chamber. In an MED plant, the seawater enters the first chamber and is raised to the boiling point after being preheated in the tubes. Seawater is either sprayed or distributed uniformly onto the surface of the evaporator tubes in a thin film to promote rapid boiling and evaporation. The feed seawater is heated by steam from a boiler, or another heat source, which is condensed on the opposite side of the tubes. The condensate from the boiler steam is recycled to the boiler for reuse. Only a portion of the seawater sprayed on to the tubes in the first effect is evaporated. The remaining seawater is collected and fed to the second. The vapour generated in the first chamber is fed to the second chamber as additional heating media and generates an approximately equal amount of vapour from the boiling seawater outside the tube surface while condensing and becoming product water. The process continues through several stages, with 80–16 stages being found in a typical large plant. Vapours from the last effect are condensed in the final condenser simultaneously preheating the feed seawater.

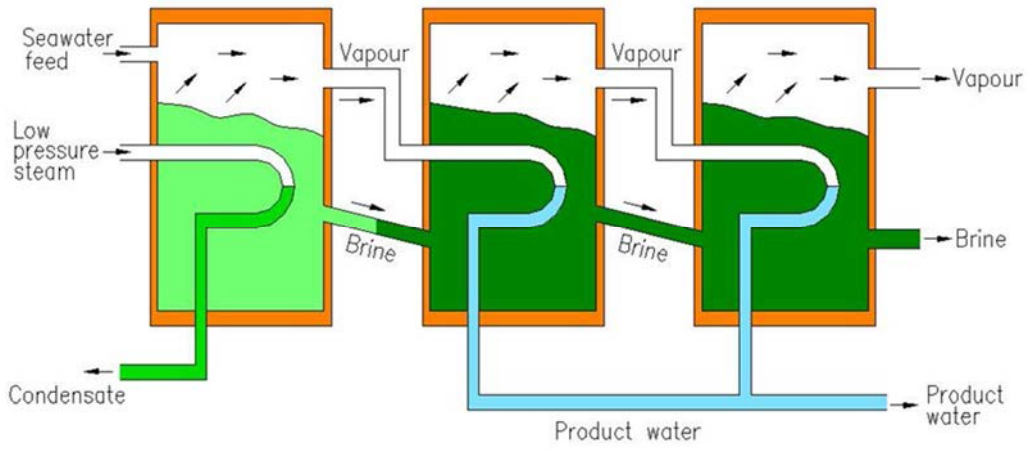


*FIG. 5. Schematic diagram of multieffect distillation (MED).*

Ophir and Lokiec [7] presented a recent evaluation of the MED process and how its economics are superior to other desalination processes. As mentioned before, LT operation allows use of low-grade energy. Another advantage is the use of relatively inexpensive construction material, which includes aluminium alloys for the heat transfer tubes, as well as carbon steel epoxy coated shells, for the evaporator shells.

Ophirand and Lokiec [7] reported water cost of 0.54 $/m$^3$ for a plant of 5 units, each producing 20 000 m$^3$/day.

*Vapour compression*

Vapour compression (VC) distillation process is generally used for small or medium-scale seawater desalting units. The heat for evaporating the water comes from the compression of vapour rather than the direct exchange of heat from steam produced in a boiler. Two methods are used to compress vapour in order to produce enough heat to evaporate incoming seawater: a mechanical compressor, usually electrically driven, or a thermo-compressor. VC units have been built in a variety of configurations to promote the exchange of heat to evaporate seawater. The MVC distillation is inherently the most thermodynamically efficient process of single-purpose thermal desalination plants.

Figure 6 illustrates a simplified method in which a mechanical compressor is used to generate the heat for evaporation. In this scheme, the heat required to evaporate part of the processed feed, which flows on one side of a heat transfer surface, is supplied through the simultaneous condensation of the distillate on the other side of the surface. The "heat pump" work, plus the fraction required for liquid pumping, is the only energy consumed by the process. No additional heat is required, and no cooling water is needed for the heat rejection, as in other distillation processes.

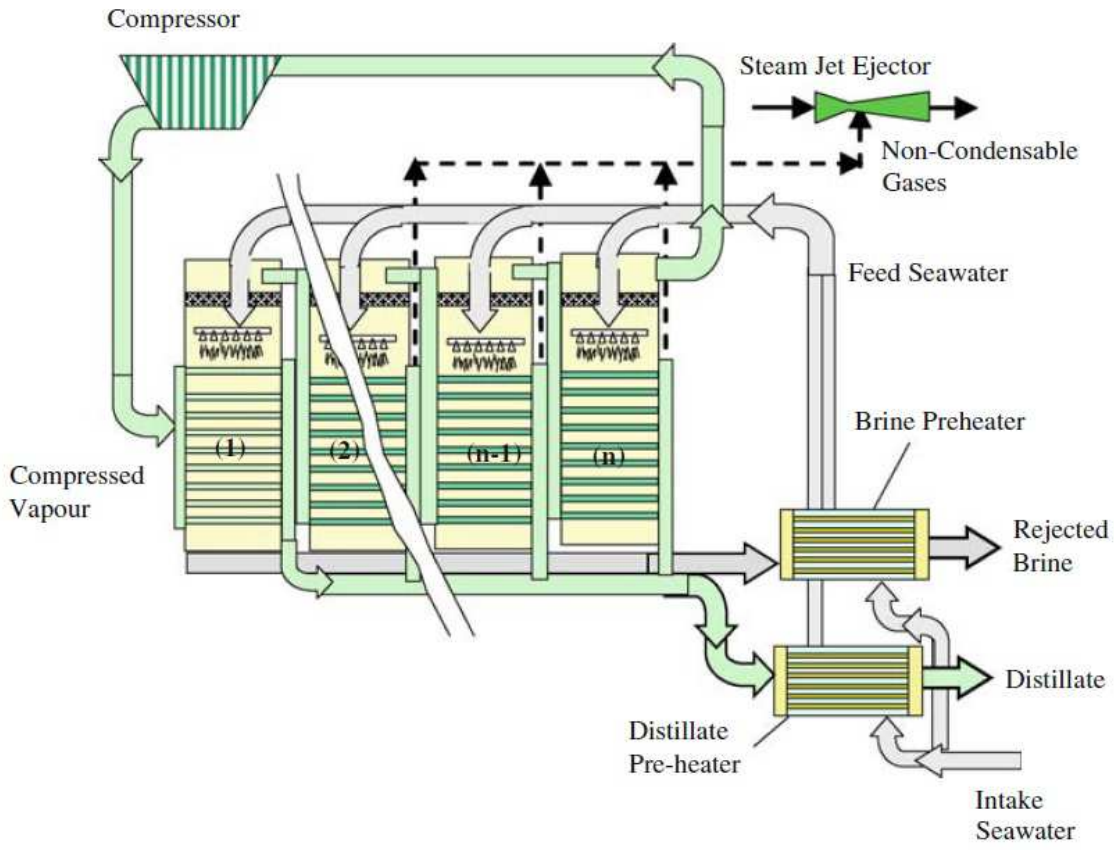


*FIG. 6. Schematic of MED with MVC.*

The heat generated by the compressor work is rejected in the outgoing product and brine streams that are discharged at a higher temperature than the seawater feed. Seawater is

sprayed on the outside of the heated tube bundle where it boils and partially evaporates, producing more vapour. The incoming seawater feed is preheated by means of two plate heat exchangers, by exchanging heat with the outgoing streams.

The reasons for using mechanical vapour recompression are:

— Low specific energy consumption;
— Gentle evaporation of the product due to LT differences;
— Short residence times of the product, as a single-effect system is most often used;
— High availability of the plants due to the simplicity of the process;
— Excellent partial load behaviour;
— Low specific operating costs.

The thermo vapour compressor (TVC) uses high-pressure motive steam to extract and compress low-pressure vapour from the last effect to an intermediate pressure. The motive steam enters TVC through a converging-diverging nozzle and expands to a pressure slightly lower than the suction vapour pressure. The high velocity expanding steam jet entrains the suction vapour and both get mixed in a mixing chamber of TVC. The mixed vapour is recompressed to an intermediate pressure through the diffuser converting kinetic energy to pressure energy. Figure 7 shows a schematic of TVC and Fig. 8 shows a schematic of MED-TVC.

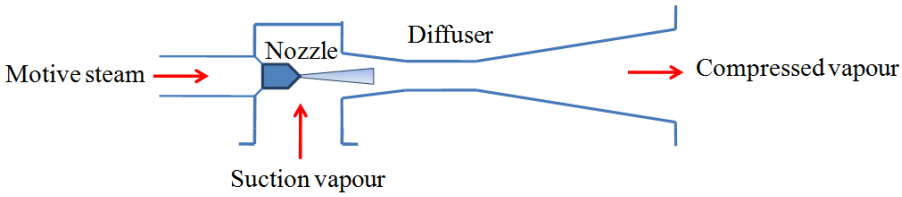


*FIG. 7. Schematic of TVC.*

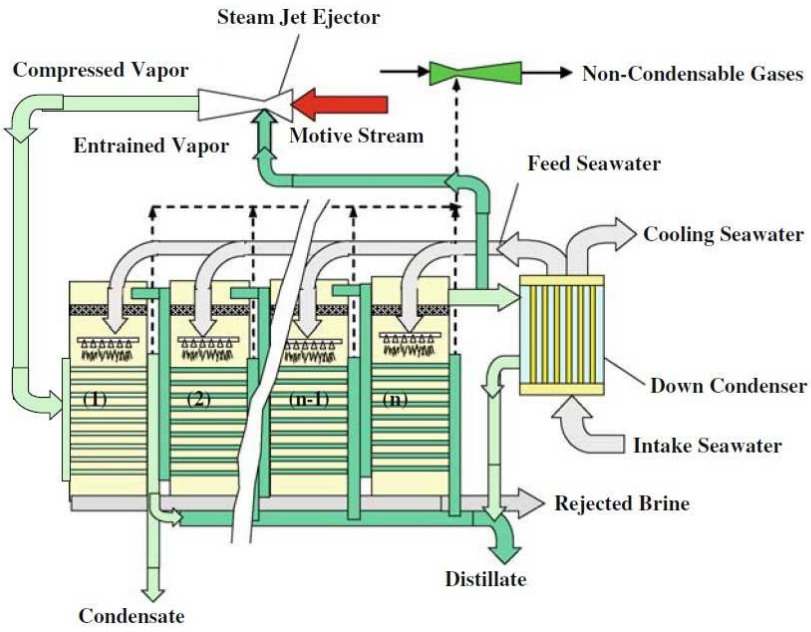


*FIG. 8. Schematic of MED with TVC.*

### 1.3.2. Membrane desalination processes

Membrane distillation is a membrane separation process which may overcome some limitations of other membrane technologies. In particular, high solute concentrations can be achieved, overcoming concentration polarization phenomena and producing ultrapure water as permeate. The process uses microporous hydrophobic membranes, impermeable to the transport of liquid water, while water vapour can be transported across them, having as driving force a vapour pressure difference between the two solutions at the membrane interfaces. Various polymeric hydrophobic membranes have been prepared with an appropriate microporosity on the order of approximately 0.2 mm, of interest for this process. The influence of the feed temperature, transmembrane temperature gradient, feed concentration, hydrodynamic conditions, etc., have been studied theoretically and tested experimentally. Various membrane configurations and operation techniques have been also suggested for optimizing transmembrane fluxes and energy consumption.

Membrane distillation has shown interesting potential in water desalination, fruit juice concentrations and in other various industrial productions. Furthermore, by using membrane distillation in integrated operations it is possible to achieve higher concentration values and better overall performance of the processes. Membranes and filters can selectively permit or prohibit the passage of certain ions, and desalination technologies have been designed around these capabilities. Membranes play an important role in separating salts in the natural processes of dialysis and osmosis. These natural principles have been adapted in two commercially important desalting processes: ED and RO. Although they have typically been used to desalinate brackish water, versions are increasingly being applied to seawater, and these two approaches now account for more than half of all desalination capacity. A growing number of desalination systems are also adding filtration units prior to the membranes to remove contaminants that affect long-term filter operation. The filtration systems include MF, NF and UF. Membrane desalination can be classified depending on the driving force (Table 2).

Power consumption of MSF, MED and RO is detailed in Table 3.

TABLE 2. MAIN FEATURES OF MEMBRANE DESALINATION PROCESSES

| Process | Size of particles retained | Driving force | Types of membranes |
|---|---|---|---|
| Reverse osmosis (RO) | <1nm | Pressure difference (10–80 bar) | Nonporous |
| Electro-dialysis (ED) | <1nm | Electrical potential difference | Nonporous or microporous |
| Pervaporation | <1nm | Concentration difference | Nonporous |
| Membrane distillation | <1nm molecules | Partial pressure difference | Microporous |
| Nanofiltration (NF) | 0.5–5.0 nm | Pressure difference (10–15 bar) | Microporous |

TABLE 3. SPECIFIC ENERGY CONSUMPTION BY THE THREE MAJOR DESALINATION PROCESSES [5]

| Desalination processes | Specific heat consumption ($kW \cdot h/m^3$) | Specific Electric consumption ($kW \cdot h/m^3$) |
|---|---|---|
| Multistage flash (MSF) | 100 | 3.5 |
| Multieffect distillation (MED) | 50 | 2.5 |
| Reverse osmosis (RO) | 0 | 4.5 |

*Reverse osmosis*

RO units are available in a wide range of capacities due to their modular design. Large plants are made of hundreds of units that are accommodated in racks. A typical maximum plant capacity is 128 000 $m^3$/day, and very small units (down to 0.1 $m^3$/day) are also used for marine purposes, houses, or hotels. PV power is used for small size RO units especially in remote places due to initial cost benefits. Osmosis is a natural phenomenon in which solvent passes through a semi permeable membrane from the side of lower solute (higher solvent) concentration to the side of higher solute (lower solvent) concentration until the concentrations of both sides are equal. At equilibrium, the height difference of solvent on the two sides of the membrane converted to pressure unit is equal to the osmotic pressure difference. If pressure higher than osmotic pressure in the concentrated side is applied externally on the concentrated solution, the flow reverses, i.e. solvent passes through the semi permeable membrane from higher to lower solute concentration side [1].

This phenomenon is called reverse osmosis (Fig. 9). As a result, concentrated solution becomes more concentrated and dilute solution becomes pure. Thus, water separation from solutions becomes possible.

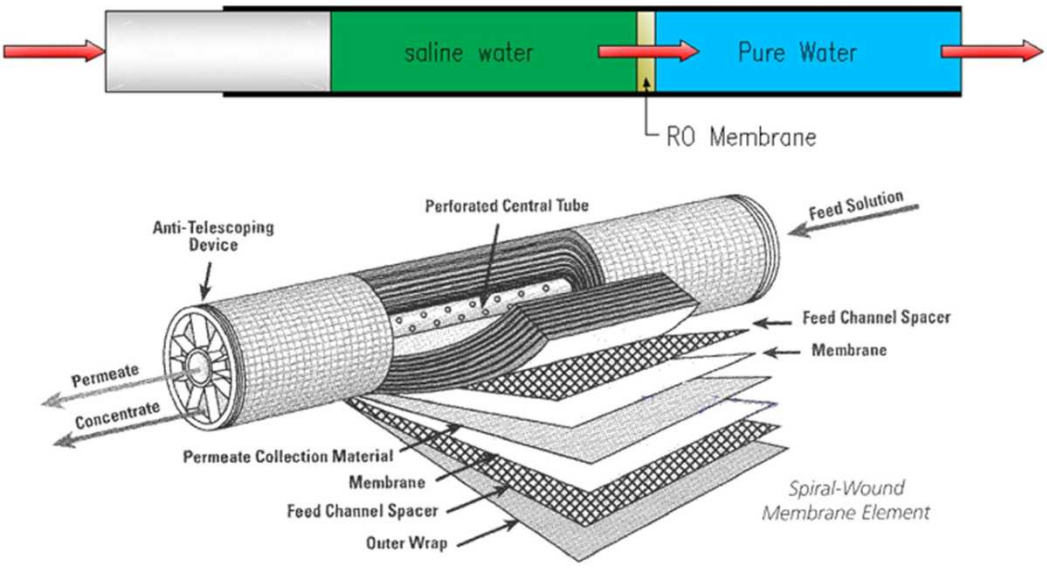


*FIG. 9. Pictorial view of osmosis and reverse osmosis.*

A typical RO system consists of four major subsystems (Fig. 10):

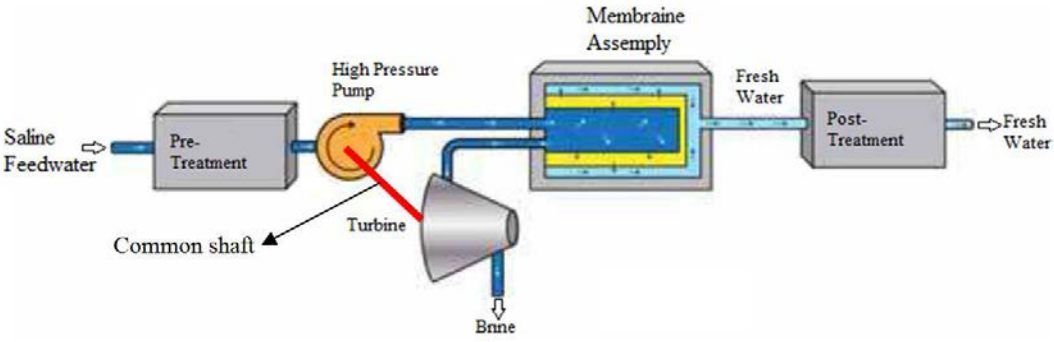


*FIG. 10. Major subsystems in a reverse osmosis system.*

— Pretreatment system;
— High-pressure pump;
— Membrane module;
— Post-treatment system.

Feedwater pretreatment is a critical factor in operating an RO system because membranes are sensitive to fouling. Pretreatment commonly includes sterilizing feedwater, filtering, and adding chemicals to prevent scaling and bio-fouling. Using a high-pressure pump, the pretreated feedwater is forced to flow across the membrane surface.

Osmotic pressure is a colligative property of the solvent which depends only on the number of dissolved species in solution and not their identity. Osmotic pressure depends upon concentration of solute, solution temperature and the type of ions present.

For dilute solutions, osmotic pressure is approximated by using Van't Hoff equation [8]:

$$\Pi = i \times C \times R \times T \qquad \text{Eq. (2.1)}$$

Where, $\Pi$ is the osmotic pressure in the atmosphere, $i$ is the osmotic coefficient (number of species in solution), $C$ is the concentration of species in g·moles/l, $R$ is the gas constant and $T$ is the temperature in Kelvin. Operating pressure for osmosis ranges from 17 to 27 bars for brackish water and from 55 to 82 bars for seawater. The energy efficiency of seawater RO heavily depends on recovering the energy from the pressurized reject brine. In large plants, the reject brine pressure energy is recovered by a turbine; commonly a Peloton wheel turbine recovering 20% to 40% of the consumed energy. The RO membrane is semi-permeable, possessing a high degree of water permeability, but presents an impenetrable barrier to salts. It has a large surface area for maximum permeate flow and is extremely thin so that it offers minimal resistance to water flow; but it is also sturdy enough to withstand the pressure of the feed stream [9]. Polymers currently used for manufacturing RO membranes are based on either cellulose acetates (cellulose diacetate, cellulose triacetate, or combinations of the two) or polyamide polymers. Two types of RO membranes commonly used commercially are spiralwound (SW) membranes and hollowfibre (HF) membranes. Other configurations, including tubular and plate-frame designs, are sometimes used in the food and dairy industries.

Seawater membrane elements are most commonly manufactured from a cellulose diacetate and triacetate blend or a thin-film composite usually made from polyamide, polysulphone, or polyurea polymers. A typical industrial SW membrane module is about 100–150 cm long and

20–30 cm in diameter. An HF membrane is made from both cellulose acetate blends and non-cellulose polymers such as polyamide. Millions of fibres are folded to produce bundles about 120 cm long and 10–20 cm in diameter. SW and HF membranes are used to desalt both seawater and brackish water. Knowing which membrane to use is a decision heavily influenced by the cost, feedwater quality, and product-water capacity factors of each membrane. The main membrane manufacturers are in the United States and Japan. The post-treatment system consists of sterilization, stabilization, and mineral enrichment of the product water. Because the RO unit operates at ambient temperature, corrosion and scaling problems are diminished compared to distillation processes. However, effective pretreatment of the feedwater is required to minimize fouling, scaling, and membrane degradation. In general, the selection of proper pretreatment and proper membrane maintenance are critical for the efficiency and life of the system [1].

*Electro dialysis*

The basic principles of the electro dialysis (ED) treatment process are similar to the ion exchange treatment process. Dissolved ions present in water have either a positive or negative charge and are attracted to electrodes with an opposite electric charge. ED differs from a normal ion exchange process as it utilizes both cation and anion selective membranes to segregate charged ions extracted from a water solution (Fig. 11). In ED, membranes that allow either cations or anions (but not both) to pass are placed between a pair of electrodes. An improvement to ED, referred to as electro dialysis reversal (EDR), utilizes the same concept with periodic automatic reversal of polarity and cell function to reverse the flow of ions across the membrane.

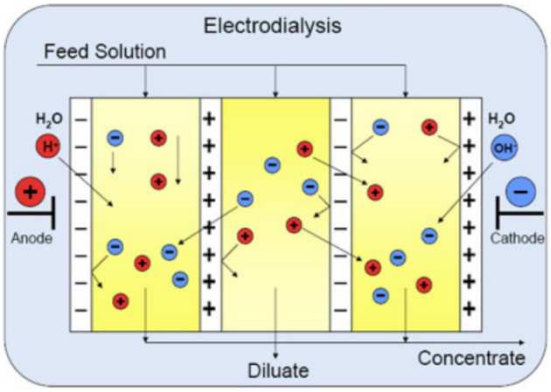


*FIG. 11. Ion exchange in electro dialysis unit.*

This returns anions across the anionic membranes and helps break up scale formed on the concentrating face of the membranes, minimizing membrane fouling. As with RO, a small pump is required to move the water through the membranes to overcome the resistance of the water as it passes through the narrow passages. Depending on the number of stages present within an ED unit, this treatment process can remove approximately 25% to 60% TDS with a resulting stream of approximately 15% to 30% of the raw water TDS, although higher water recovery rates (90%) are obtainable with low total dissolved salts (TDS) concentrations (<2000 mg/L). In general terms, electro dialysis installations are more expensive than RO, but are more resistant to membrane fouling, which in turn can reduce costs typically associated with membrane replacement or cleaning. For a coal bed natural gas water, treatment costs have been estimated to be under 15 cents per bbl for a 0.34 MGD (8000 bbl/day) treatment

process. ED treatment is more cost-effective and energy-efficient when treating low TDS water (e.g. TDS 4000–5000 mg/L) [10].

*Membrane distillation*

It is a relatively new membrane process in which two aqueous solutions, at different temperatures, are separated by a microporous hydrophobic membrane (Fig. 12).

In these conditions a net pure water flux from the warm side to the cold side occurs. The process takes place at atmospheric pressure and at temperature that may be much lower than the boiling point of the solutions. The driving force is the vapour pressure difference between the two solution membrane interfaces due to the existing temperature gradient.

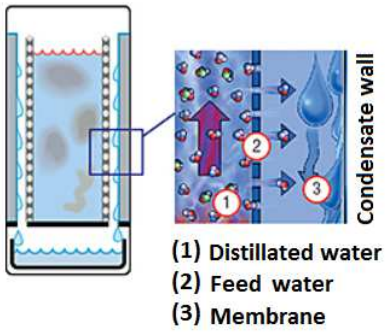


*FIG. 12. Membrane distillation.*

*Microfiltration*

It removes particles in the size range of approximately 0.1 to 10 micron. Suspended particles and large colloids are rejected while dissolved solids pass through the MF membrane. Applications include removal of bacteria, flocculated materials or suspended solids. Trans-membrane pressures are typically 0.7 bar.

*Ultrafiltration*

It provides macro molecular separation for particles in the range 1–100 nm. Rejected items are colloids, proteins, microbiological contaminants, bacteria, large organic molecules. Most UF membranes have molecular cut-off values between 1000 and 100 000 Daltons. Trans-membrane pressures are typically 1–7 bar.

*Nanofiltration*

Separation mechanism of NF and RO is same. It involves size exclusion as well as electro-static interaction and hence they are named as physico-chemical processes. In NF, organic molecules with molecular weight greater than 200–400 are rejected. Also, dissolved salts are rejected in the range of 20–98%. Bivalent anions have high rejections of 90–98%. Typical applications include removal of colour and total organic carbon from surface water, removal of hardness from well water and overall reduction of total dissolved solids. Trans-membrane pressures are typically 3.5–16.0 bar.

## 1.4. COMBINED WATER DESALINATION AND POWER GENERATION

### 1.4.1. Literature survey

New improved designs with reduced lower specific energy consumption and LT evaporation processes, which make use of waste heat or low-grade heat as energy source, are an attractive option for seawater desalination. A detailed literature survey was conducted for waste heat or low grade heat utilization for seawater desalination. Rautenbach et al. [11] studied gas turbine (GT) waste heat utilization for distillation and demonstrated the superiority of the MED process compared to standard MSF process. Discussion is limited to a case of practical importance: an already existing GT of nominal capacity of 10 MW, located near the seashore. Furthermore, the cost of heating steam from a waste heat boiler is compared with the cost of steam from other sources such as solar energy and fuel-fired boilers. Saari [12] described usability of LT waste heat for seawater desalination using a MED system. He has shown that waste heat energy that is cooled away from a process appears at two different temperature levels. Waste heat at 50°C, warmer than the ambient, can be utilized by MED processes and is competitive to utilize it at least as thoroughly as first-rate energy. At LTs, less than 20°C above ambient temperature, waste heat can be used technically and economically, depending on the pumping energy cost. Toelkes [13] described the Ebeye desalination project by utilizing diesel waste heat. The Ebeye seawater desalination project in the Marshall Islands produces 1100 $m^3$/day of pure distilled water utilizing waste heat discharged from an adjacent diesel generator station, operating at an average load of 3.2 MW. The only other energy requirement is electric power for process and seawater pumping at about 2.5 kW·h/$m^3$. The desalination plant consists of a 12 stage LT MED unit, operating at a top brine temperature of 70°C with simple polyphosphate feed pretreatment. The diesel generator station consists of two 2.4 MW diesel sets, with provision for addition of a third as demand increases. Heat is recovered from diesel's exhaust gases, jacket cooling water, lube oil and compressed air after coolers.

Senatore J.S. [14] described vapour compression distillation with maximum use of waste heat by using 4-effect vertical tube foam evaporator. Based on the techno-economics and site specific conditions, two types of vapour compression desalination system designs have been discussed: with low capital cost with low performance ratio (PR) and high capital cost with high PR. The low PR plant is designed with a maximum brine temperature of about 55$^o$C and PR of 7, requiring only a polyelectrolyte scale inhibitor. This design would employ a centrifugal compressor with a pressure ratio of ~1.2. The high PR plant operates at 121$^o$C maximum brine temperature and uses a higher-pressure ratio of 1.58. The author has shown the compressor can be extremely versatile, usable in both high or low PR VC processes, as it is well adapted to either a dual purpose (power and water) or a single purpose (water only) plant. High PR that is easily attainable in this design is becoming increasingly more attractive from an economic view, as the price of fuel continues to escalate. For example, at \$5.0/MBTU, fuel contribution to the total cost of water is \$1.4/$m^3$at a PR of 8 and is reduced to about \$0.35/$m^3$ at a PR of 31. Senatore has also presented the design and process descriptions for a 9000 $m^3$/day plant. This plant employs a 65 000 cubic feet per metre (CFM) centrifugal compressor driven by a diesel engine and operates across a 4-effect vertical tube foam evaporator. The design employs an exhaust gas and water jacket waste heat recovery scheme. Updated plant cost estimate and cost of product water are also presented.

Rautenbach and Arzt [15] presented an economical concept for desalination for a particular application by utilizing waste heat from a large stationary DG set. The desalination process

itself is of the horizontal tube (HT) multiple effect stack type, combined with a thermal vapour compressor. Some design aspects like the influence of non-condensable on overall heat transfer and the interdependence between GOR and a number of effects and the characteristics of the TVC have also been discussed quantitatively. Tay J.H. et al. [16] reported vacuum desalination using waste heat from a steam turbine exhaust. He described a vacuum desalination process at temperatures as low as 40°C.Using waste heat from a steam turbine, a pilot study was conducted in the laboratory to investigate the feasibility of using a vacuum desalination process for water supply. Based on experimental results, water boils at 40–90°C at the corresponding vacuum pressure of 0.1–0.7 bar, respectively. The consumption of heat from the waste steam is minimized as the superheated vapour is used to heat the influent seawater. Cohen M., et al. [17] presented the design and feasibility studies of using power plant residual heat for seawater desalination by using a LT flash concept. He described the possible integration of the low temperature flash (LTF) desalination technology in existing power stations. The LTF technology exploits the residual heat discharged by the cooling seawater for. A prototype LTF desalination unit has been operating at the ENEL power station in Piombino, Italy, since 1993, showing the industrial applicability of this technology. In the present study, an improved LTF design, with long tube and multistage evaporator has been applied to a typical IEC site located on the southern shore of the Mediterranean Sea. Studies have been carried out for both small-scale units, devoted to boiler make-up production, and for a large plant able to produce the whole water supply for the site. The investigation has shown very interesting perspectives for such an application, with extremely low steam and electrical consumption and a very competitive cost of produced water. Other advantages of LTF technology are related to the extreme plant availability, to the high purity of produced distillate, to the absence of any chemical consumption and environmental impact.

Cohen J., et al. [18] described utilization of waste heat from the flue gases scrubbing system by using MED technology. He has presented a thermal seawater desalination plant, which utilizes waste heat from a flue gas desulphurization (FGD) unit. This type of "low-grade" heat is suitable for LT desalination technologies such as MED technology. Two different alternatives for using the heat were analysed and compared. In these schemes, about 8500–10 000 $m^3$/day of high-quality water (~10 mg/l TDS) may be produced from one 575 MW generating unit. Moreover, a great amount of water is saved due to reduction in flue gas temperature and therefore reduction in water evaporation in the flue gas scrubber.

## PROMISING TECHNOLOGIES FOR DESALINATION WITH NUCLEAR ENERGY

Water scarcity is a global issue, affecting many countries every year. Apart from water conservation, pollution control and water reclamation, solutions for new sources of fresh water, including desalination, are also being considered to meet the water shortages. The rising concern over fossil fuel cost and its uncertain availability as well as other associated environmental concerns has prompted a search for alternative energy sources for the future desalination needs, including nuclear energy. Nuclear seawater desalination is becoming more favourable than conventional systems due to environmental concerns over the increasing concentration of GHG in the atmosphere, particularly carbon dioxide. The IAEA has been studying the feasibility of nuclear desalination since the late 1950s. Interest among Member States in the technology has been renewed recently, following a resolution adopted at the IAEA General Conference in 1959. A technical study report was prepared and submitted to the IAEA General Conference in September 1990. The IAEA had previously issued a number of technical publications on the technology [19–21].

They include:

- Desalination of water using conventional and nuclear energy, technical reports series No. 24 (1964) [19];
- Guide to the costing of water from nuclear desalination plants, technical reports series No. 80 (1967) [20];
- Heat utilization from nuclear reactors for desalting of seawater, IAEA-TECDOC-206 (1977) [21].

R&D work was carried out through CRPs to demonstrate more viable, reliable, cost effective and safe nuclear desalination systems in parallel to an electrical power plant. New ideas are pursued to alleviate environmental impact and prevent radioactive cross contamination to the product water, especially reducing tritium concentration in the product water [22]. An alternative and better economic option to produce desalted water is to harness the waste heat generated from the nuclear power reactor originally operating to produce either electricity or steam for other applications. In such a case, the waste heat available from the nuclear power plant will be looked at as the energy source for the desalination process, which was otherwise lost to the surrounding environment. Figure 13 shows a simplified diagram of the multipurpose nuclear power and desalination complex based on the VK-300 reactor (electricity generation and domestic heating and desalination).

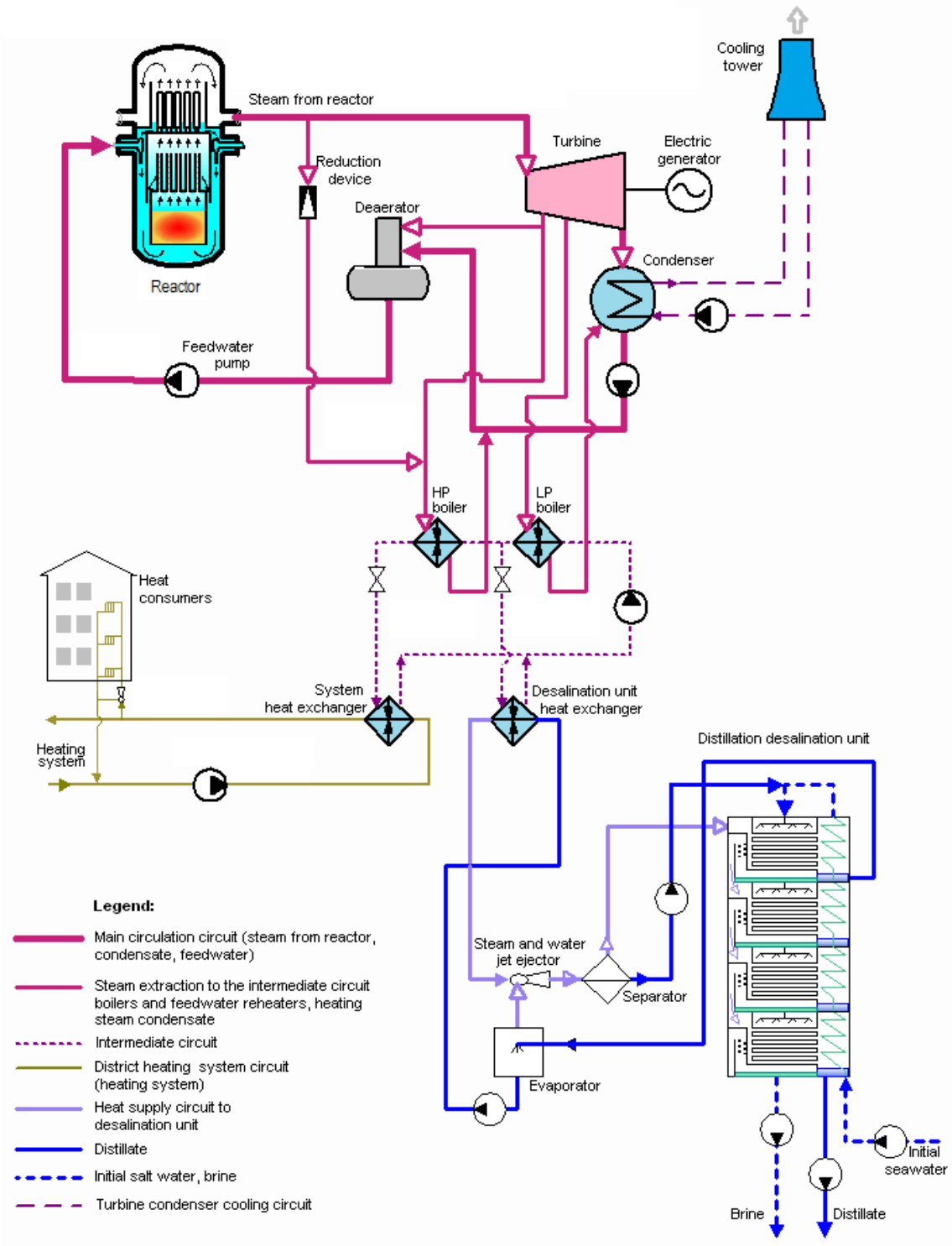


*FIG. 13. Simplified diagram of the multipurpose nuclear power and desalination complex based on VK-300 RF (electricity generation + domestic heating + desalination).*

## 1.5. LOW TEMPERATURE EVAPORATION PLANTS TO ENHANCE WASTE HEAT UTILIZATION

Low temperature evaporation (LTE) plants are MED type plants operating at very low temperatures. Thus, they can effectively utilize waste heat that has been rejected from nuclear

reactors for seawater desalination. The use of waste heat as an energy source is an attractive option to improve economic competitiveness and sustainability of seawater desalination plants.

The Bhabha Atomic Research Centre (BARC) has developed a 30 $m^3$/day LTE desalination plant coupled to a nuclear research reactor. The LTE plant uses the part of the heat rejected through the primary cooling system to run the desalination process. The product water is of a high purity level (conductivity <2 μS/cm), meeting the reactor make-up water requirements.

An intermediate heat exchanger is incorporated between the nuclear reactor and the desalination plant to ensure no radioactive contamination and protection of the desalinated water.

The nuclear research reactor (40 MW(th)) uses metallic natural uranium fuel, heavy water moderator, demineralized light water coolant and seawater as the secondary coolant. The heat generated in the fuel assemblies is removed by recirculation of demineralized water in a closed loop called primary cooling water (PCW) system using recirculation pumps. The heat from the primary coolant is transferred to the secondary coolant in a set of heat exchangers and ultimately rejected to the sea. The relevant process parameters of PCW and seawater (SW) systems are given as case I in the Table 4. When PCW pumps are not in operation for any reason, shut down cooling flow through the core is established automatically by one pass gravity flow from an overhead water storage tank.

TABLE 4. CHANGES IN FLOW AND TEMPERATURE OF PCW AND SW SYSTEMS AT 40 MW(th) OPERATION

| | | CASE–I | CASE–II | CASE–III |
|---|---|---|---|---|
| Core | PCW flow (l/min) | 17 700 | 17 700 | 17 700 |
| | PCW inlet temp. (°C) | 45 | 46 | 47.3 |
| | P`CW outlet temp. (°C) | 76.2 | 77.2 | 78.5 |
| Primary cooling water / seawater heat exchangers | PCW flow (l/min) | 3450 | 3285 | 3285 |
| | PCW inlet temp. (°C) | 76.3 | 77.2 | 78.5 |
| | PCW outlet temp. (°C) | 45 | 44.4 | 44.8 |
| | SW flow (l/min) | 6265 | 6175 | 6175 |
| | SW inlet temp. (°C) | 29 | 29 | 29 |
| | SW outlet temp. (°C) | 46.2 | 46 | 46.5 |
| Intermediate heat exchangers | PCW flow (l/min) | — | 1280 | 1280 |
| | PCW inlet temp. (°C) | — | 77.2 | 78.5 |
| | PCW outlet temp. (°C) | — | 65.8 | 78.5 |
| Seawater system | SW gross flow (l/min) | 3600 | 35 150 | 35 150 |
| | SW inlet temp. (°C) | 29 | 29 | 29 |
| | SW outlet temp. (°C) | 45.7 | 45 | 45 |

Case–I: parameters of existing reactor;
Case–II: parameters after proposed modifications;
Case–III: parameters considering non-availability of desalination unit.

The core outlet is led to an underground water storage tank (dump tank) from where it is pumped back to the storage tank. An intermediate heat exchanger is incorporated between the primary coolant water (PCW) and the desalination plant to ensure that no radioactive material reaches the desalted water. The intermediate circuit consists of a booster pump, the intermediate heat exchanger, the desalination plant and the associated piping and isolation valves.

The intermediate circuit water is maintained at a pressure higher than the PCW pressure in the intermediate heat exchanger so that ingression of activity to the inactive intermediate circuit is prevented in the event of leakage in the heat exchanger tubes. Flow controls for the feed seawater and product water have been provided to take care of the sudden changes in the power rating of the nuclear reactor. The sudden change in power rating leads to fluctuations in the temperature of the heating medium, resulting in changes in the production rate of fresh water.

### 1.5.1. Single effect low temperature evaporation plant

The desalination unit essentially consists of three portions i.e. heater, separator and condenser, (Fig. 14). In the heater shell, vertical tubes are used. Feed seawater enters the unit at the bottom of the tubes and partly evaporates by the time it comes out from the top. The generated vapours rise through the demisters and enter the HT bundle kept at the top of the vertical shell. Afterwards, they condense around the tubes cooled by the seawater flowing inside, producing desalinated water. The product water is then pumped out. The plant utilizes waste heat in the form of hot water in the range of 50–70°C to produce pure water from seawater.

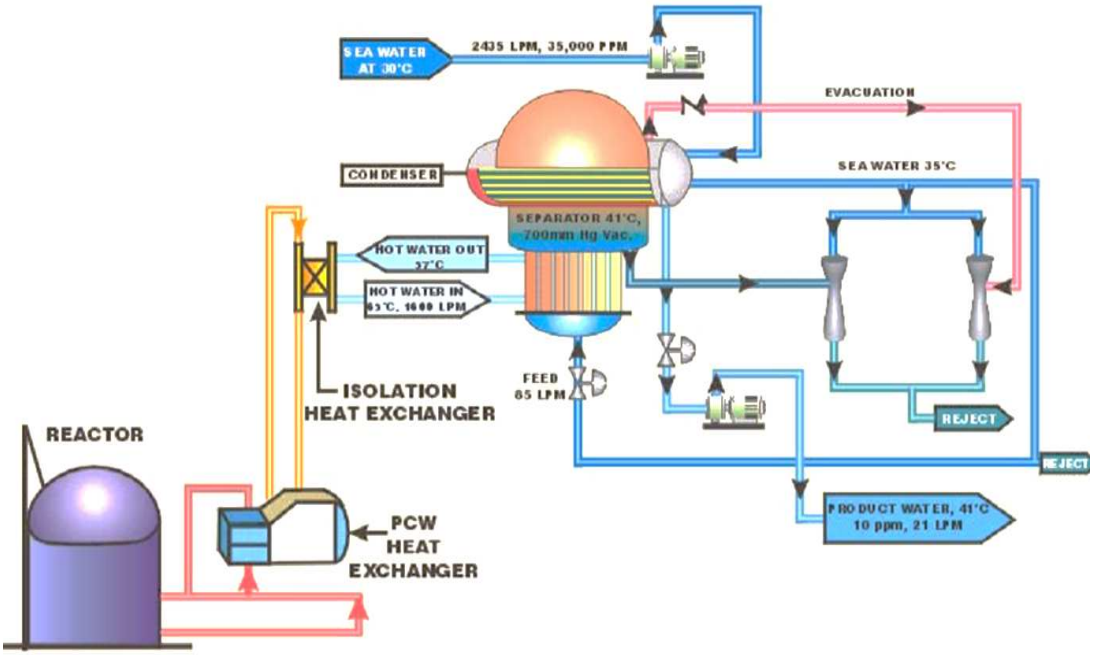


*FIG. 14. Schematic diagram of LTE desalination plant coupled to a reactor to use waste heat.*

Apart from the electric power requirement for the pump, no other energy or fuel is required. Seawater of about three times the product water is given as feed to the evaporator. One third of the feed seawater evaporates while the remaining two thirds of concentrated seawater are discharged.

This is done to maintain lower concentration of seawater to minimize the chances of scale formation in the evaporator tubes. Due to low evaporation temperature and low brine concentration, scale formation has been practically eliminated. The plant had been in round the clock operation for the past several years and consistently given designed output, indicating no deterioration in the heat transfer due to scaling/fouling. Vacuum is maintained and excess brine is drained by water jet ejectors having no moving parts. It produces very good quality pure water directly from seawater (10 μS/cm conductivity) and does not need any chemical pretreatment of seawater except chlorination. Moving parts are kept to a minimum, thus reducing maintenance and increasing reliability.

Seawater at ambient temperature (30°C) enters the condenser tubes. A part of this seawater from the outlet is taken as feed to the heater section which enters at the bottom of the tubes. About one third of the feed seawater evaporates. The remaining two thirds are discharged to avoid build-up of concentration. The hot water in the shell side, which enters at 65°C and leaves at 57°C, transfers heat to the seawater in the tube side, which boils at 41°C at 700 mmHg vacuum. After the seawater and vapour mixture coming out of tubes, the vapour rises through the separator section and enters the condenser section. Here, the vapour condenses to form the product water, which is pumped out. Water jet ejectors are used to create and maintain vacuum in the unit and to drain concentrated seawater from the unit. The product water is continuously monitored for its quality by an online conductivity meter. If the quality of the product water falls below the desired limit, the conductivity meter actuates a 3-way solenoid valve which diverts the product water back to the evaporator. As the hot water temperature to the desalination plant varied in the range of 53–65°C, depending upon the power rating of the reactor operation, experiments and performance analyses were conducted using a temperature range for the hot water corresponding to 20–40 MW(th) reactor rating. Table 5 gives the performance of the desalination plant at various hot water temperatures for reactor rating, varying from 20–40 MW(th). The conductivity of the product water obtained was in the range of 3–6 μS/cm (1.2–2.5 ppm TDS) throughout the operation of the desalination plant.

TABLE 5. OUTPUT OF LTE DESALINATION PLANT AT VARIOUS HOT WATER TEMPERATURES (HOT WATER FLOW RATE 1.0 $m^3$/min, VACUUM IN THE EVAPORATOR 700 mm hg, EVAPORATION TEMPERATURE 41°C)

| Sl. N | Hot water Temp (°C) | Product water flow rate ($m^3$/day) | Total dissolved solids in the product water (ppm) |
|---|---|---|---|
| 1 | 50 | 10.0 | 1.5 |
| 2 | 55 | 15.1 | 1.5 |
| 3 | 60 | 21.6 | 2 |
| 4 | 62 | 24.5 | 2 |
| 5 | 65 | 30.2 | 2.5 |

### 1.5.2. Two-effect low temperature evaporation plant

Based on the earlier experience, BARC has designed a two-effect LTE desalination plant (Fig. 15) to produce high-purity water of conductivity <2 μS/cm directly from seawater. Waste heat in the form of hot water at 65°C is used as heating media and circulated (78.0 $m^3$/h) in the shell side of the heater section of the evaporator at the first effect. Seawater at 4 $m^3$/h and 37°C is fed to the tube side of the first effect. Vacuum is created and maintained at 650 mm of Hg in this effect and 700 mm of Hg in second effect by a water jet ejector.

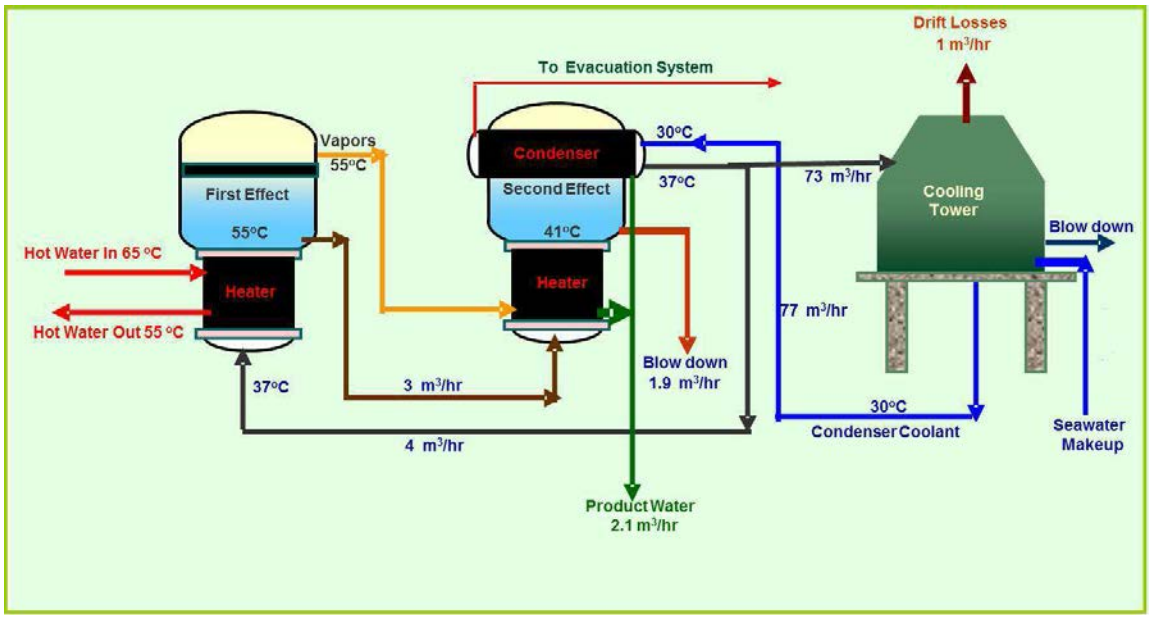


*FIG. 15. Two-effect LTE plant with cooling tower.*

Vapours from the first effect are used as the heating media in the second effect. Remaining concentrated seawater (3 $m^3$/h) from the first effect is used as feed for the second effect. In the second effect, seawater evaporates at 41°C. Vapour generated in the second effect rises through the demisters and enters the horizontal overhead condenser where it is condensed to produce fresh water. Raw seawater at 30°C from cooling tower basin is used as cooling media and is pumped through overhead condenser tubes of second effect (77 $m^3$/h). This cooling water is preheated up to 37°C. About 4.0 $m^3$/h of this cooling water from the condenser outlet is used as the feed to the first effect. The condensate from the heater and condenser section of second effect (2.1 $m^3$/h) is continuously pumped out. Concentrated water from the second effect (1.9 $m^3$/h) is removed as blow down.

## 1.6. IMPROVED PERFORMANCE OF REVERSE OSMOSIS PLANTS AT ELEVATED TEMPERATURE

RO membranes permit only fresh water to pass through, separating salt at a higher pressure than the osmotic pressure of seawater by means of a high-pressure pump. The recent R&D activities have been directed to save pumping power by the use of energy recovery devices and also to increase the productivity by using preheated seawater feed. The experts and the system designers have varying opinions about RO feed preheating systems. RO feed preheating increases system productivity and/or saves on power consumption. Effects, if any,

on the lifespan of membranes of the increasing feed temperature need to be assessed with long term studies.

A pilot plant of seawater RO plant is also operated on regular basis in BARC to perform studies on hybrid desalination systems and operation of UF-RO systems at elevated temperatures. The UF-RO plant has been coupled with a LTE as shown in Fig. 16.

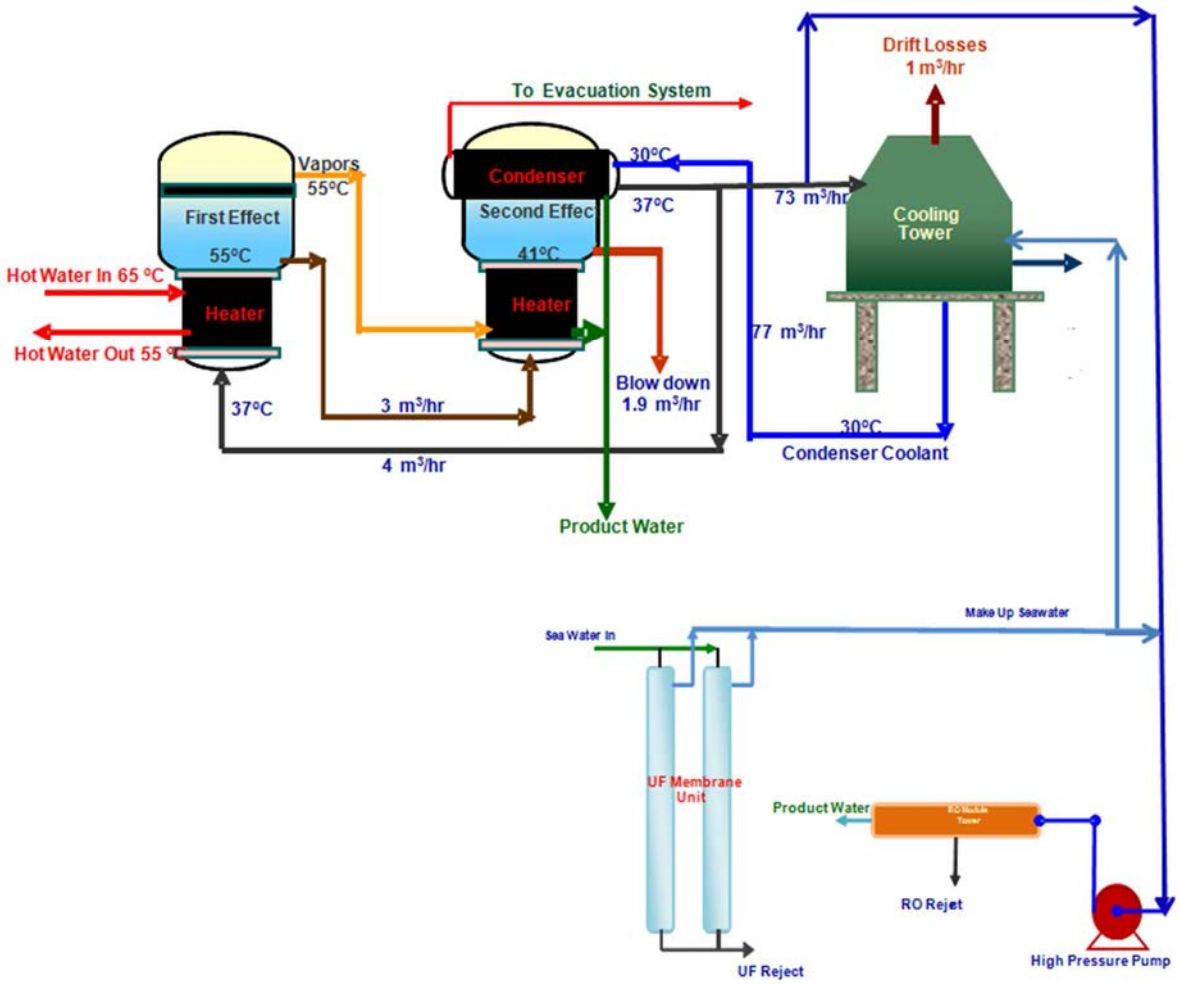


*FIG. 16. Flow coupling scheme of LTE-RO.*

Cooling tower make-up water to the LTE plant is delivered from the UF pretreatment system of the RO plant. By proper blending of UF pretreated seawater with the hot seawater from LTE condenser outlet the temperature of the RO feed was varied from 30°C to about 40°C. The experiments were carried out in two phases. In the first phase, experiments were carried out in the temperature range of 28–32°C for the RO feedwater from the thermal LTE plant by blending the condenser coolant recirculation stream with the UF treated seawater. In the second phase of the experiments, the RO plant feed temperature was increased up to 40°C for carrying out studies related to the effect of temperature on the operating parameters.

The result of such coupling on the performance of the RO flux is reported in Figs. 17, 18 and 19.

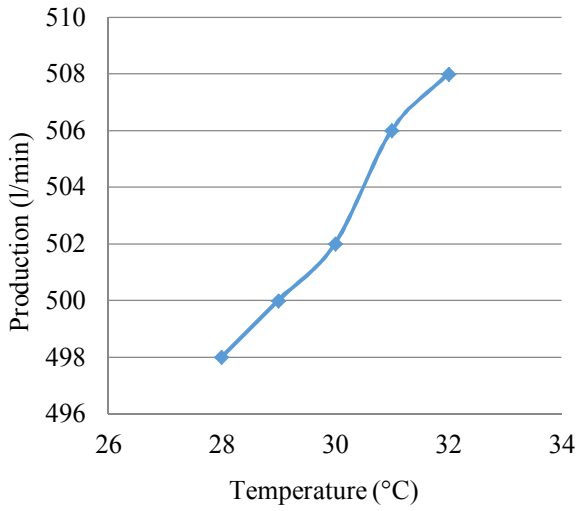


*FIG. 17. Effect of temperature on production rate.*

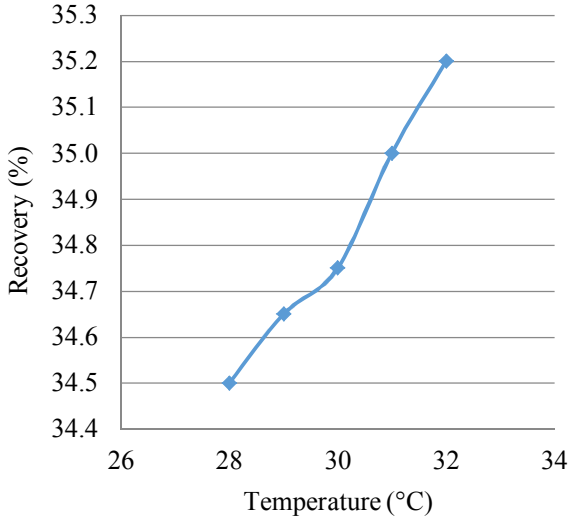


*FIG. 18. Effect of temperature on plant recovery.*

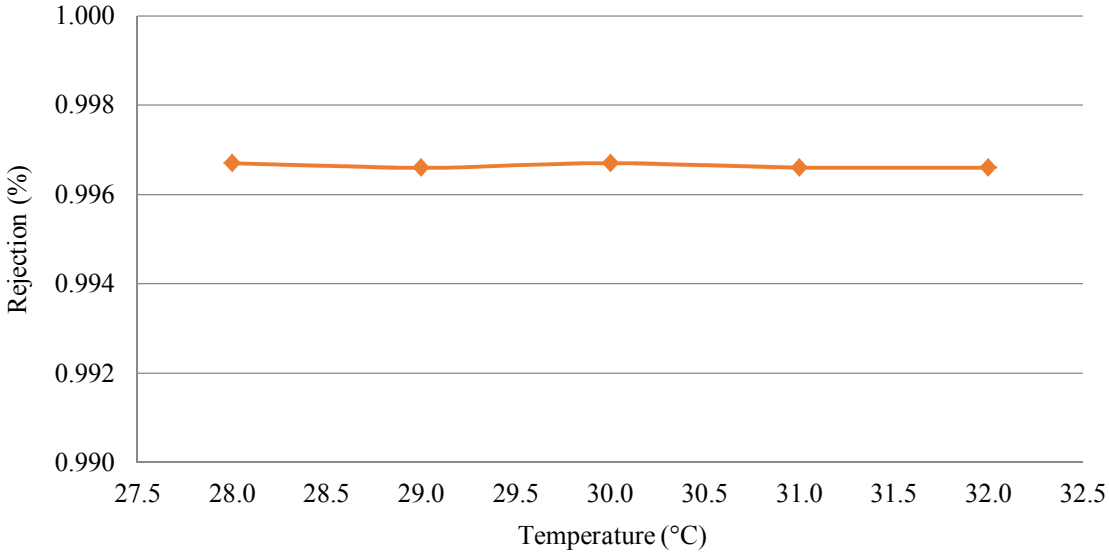


*FIG. 19. Effect of temperature on solute rejection.*

The experimental results indicate an increase in flux of about 0.3–0.7%. Though the trend of flux increase is in line with the single element experiments done in earlier CRP [23], the increase in temperature is not linear, in fact, it decreases with an increased flux in case of plant scale experiment compared to those obtained with single element experiments. This may be attributed to the fact that, for test cell or single element studies, recovery is either too meagre or rather nil, while in plant scale experiments, the average recovery is about 35%. In these conditions, water flux can be taken as directly proportional to membrane constant and solute flux is proportional to the constant concentration gradient. The observed variations in single element experiments are primarily attributable to effects of temperature on the transport properties alone and not to any secondary effects such as increase in the boundary layer concentration etc.

The percentage of recovery in the plant data has got a similar trend to those observed in earlier CRP with single element experiments. Solute rejection is not dependent on the increase in the temperature range considered in the first phase of the plant scale experiments (Fig. 19).

In the second phase of the experiments, the temperature was raised further, up to 40°C, in order to carry out studies related to the effect of temperature on the operating parameters. Experiments were conducted to assess the performance of BWRO (brackish water reverse osmosis) and SWRO (salt water reverse osmosis) membrane elements at elevated feed temperatures. FilmTech BW-30-4040 and SW-30-4040 membranes were used for the experiments. A positive displacement pump (40 l/min capacity, 70 bar pressure) was used to pressurize feedwater well above its osmotic pressure. Brackish feedwater of different salinities was prepared by dissolving sodium chloride (LR grade) in tap water (60 ppm TDS). For seawater, experiments have been carried out both with simulated seawater solution as well as actual seawater.

For simulated feed solutions, $CaCl_2$ and $MgSO_4$ were also added to maintain sodium, calcium, magnesium, chloride and sulphate equivalence of actual seawater. Figures 20 and 21 show that product flux and recovery increase with increasing temperature for BWRO membrane with simulated brackish water feed solution. With increasing feed salinity, the rate of increase in product flux (slope of the curve) declines, e.g. 1.06%, 0.86% and 0.66% for 5600 ppm, 13 000 ppm and 18 500 ppm respectively per °C rise of temperature.

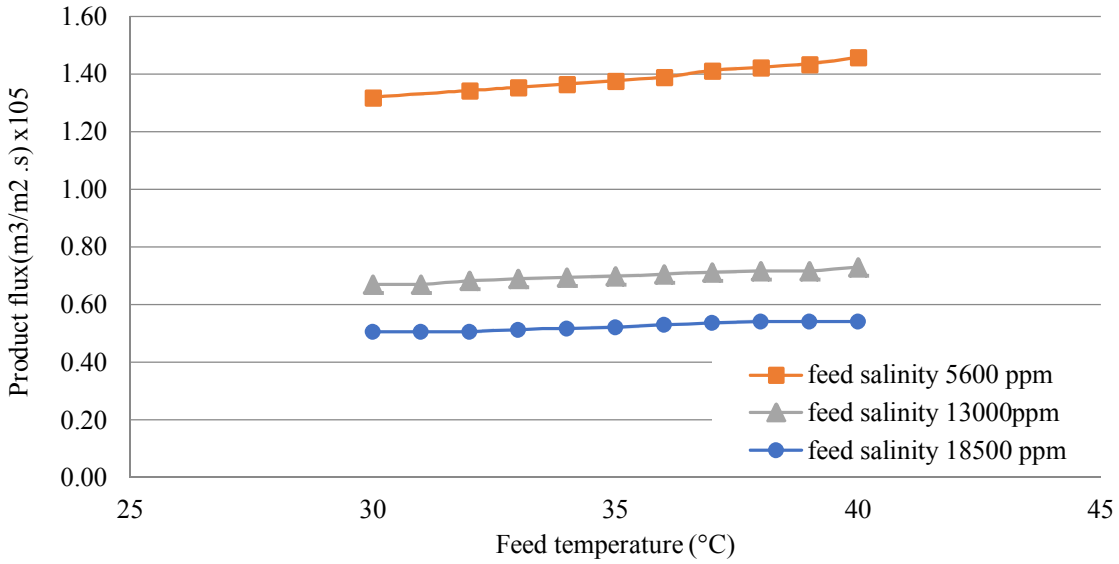


*FIG. 20. Variation of product flux with temperature at different salinities at 20 bar pressure for BWRO membrane.*

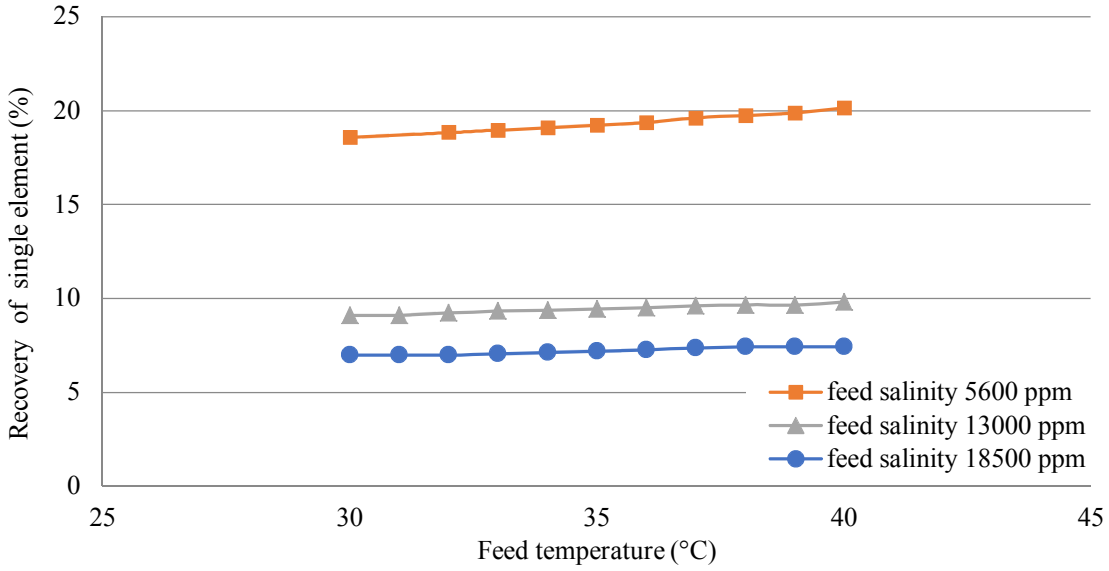


*FIG. 21. Variation of recovery with temperature at different salinities at a pressure of 20 bar for BWRO membrane.*

Figures 22 and 23 show the behaviour of actual seawater and simulated seawater at different salinities with increasing temperature for SWRO membrane. Here, akin to BWRO membrane, the same trend is observed: increase of flux at the rate of 2.6% and 1.6% for 23 000 ppm and 30 000 ppm per °C rise of temperature was observed.

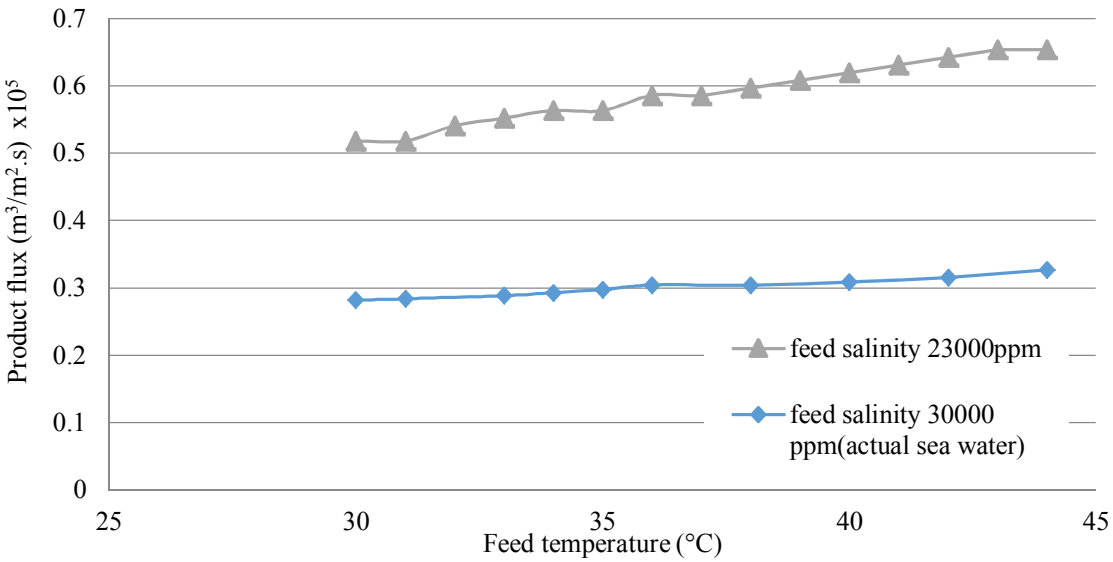


*FIG. 22. Variation of product flux with temperature at different salinities at 30 bar pressure for SWRO membrane.*

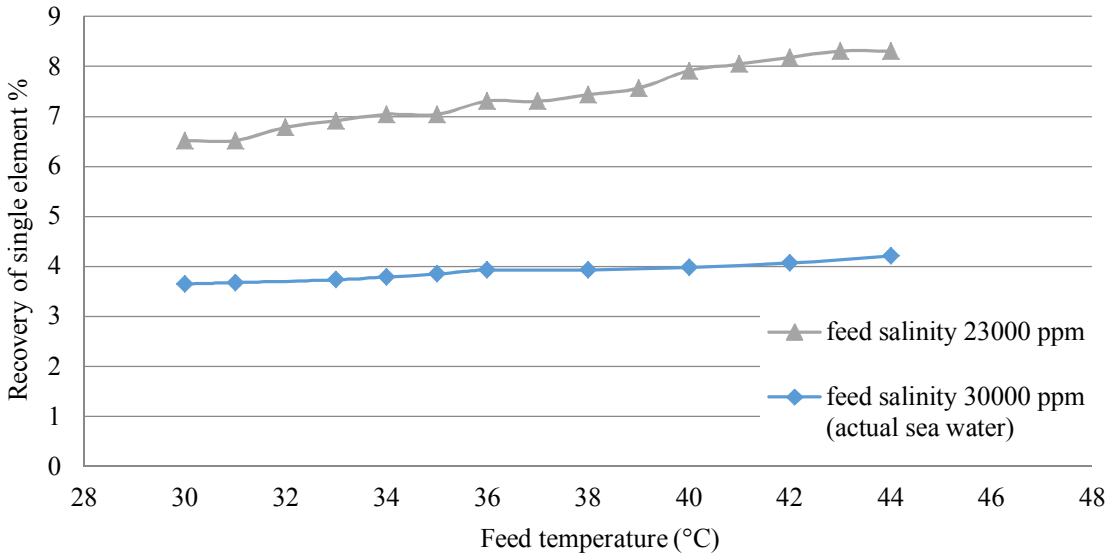


*FIG. 23. Variation of recovery with temperature at different salinities for a pressure of 30 bar for an SWRO membrane.*

## 1.7. HIGH TEMPERATURE ULTRAFILTRATION FOR SEAWATER FEED PRETREATMENT:

Experiments were also carried out for the UF membrane elements. Figures 24 and 25 show that increasing temperature has prominent effect on the UF membrane when compared to the RO membrane.

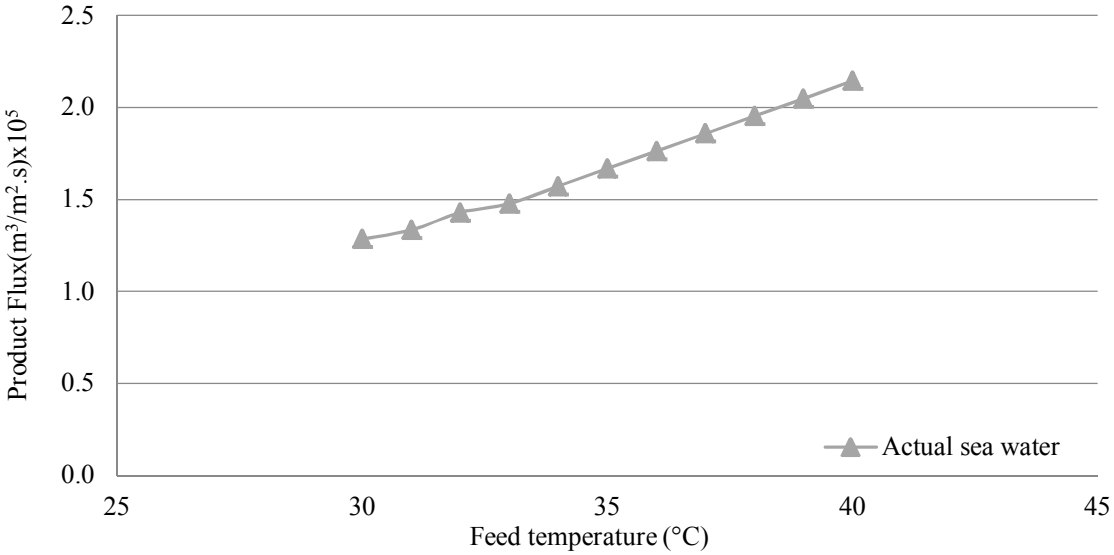


*FIG. 24. Variation of product flux with temperature at 2.5 bar pressure in hollow fibre UF membrane.*

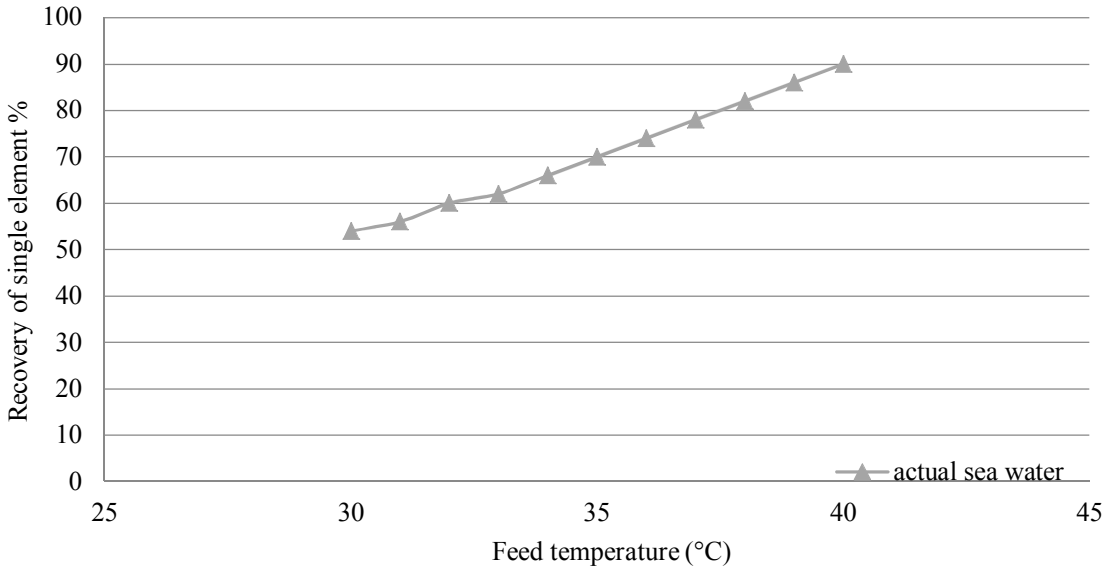


*FIG. 25. Variation of recovery with temperature at 2.5 bar pressure in hollow fibre UF membrane.*

## 1.8. HYBRID DESALINATION SYSTEMS

Hybrid desalination systems combining both thermal and membrane desalination processes with power generation systems are currently considered a good economic alternative to dual-purpose evaporation plants. Hybrid (membrane/thermal/power) configurations are characterized by flexibility in operation, less specific energy consumption, low construction cost, high plant availability and better power and water matching. A promising approach for pretreatment of seawater make-up feed to MSF and SWRO desalination processes using NF membranes has been introduced by the SWCC. NF membranes are capable of significantly reduce the number of scale forming ions from seawater, allow high temperature operation of thermal desalination processes, and subsequently increase water productivity. The main advantages of hybrid plants are: more flexible power-to-water ratio, efficient operation even with significant seasonal and daily fluctuations of the electric and water demand, reduction of primary energy consumption and increase of plant efficiency, thus improving economics and reducing environmental impacts. Blending the products of the thermal and SWRO allows for the use of a single stage SWRO instead of the two stage SWRO plant normally employed in standalone SWRO plants. Combining thermal and membranes desalination plants in the same site will allow the use of common intake and outfall facilities with less capital cost. An integrated pretreatment and post-treatment operation can reduce cost and chemicals. Figure 26 shows the contribution of different desalination units in the water demand along the year.

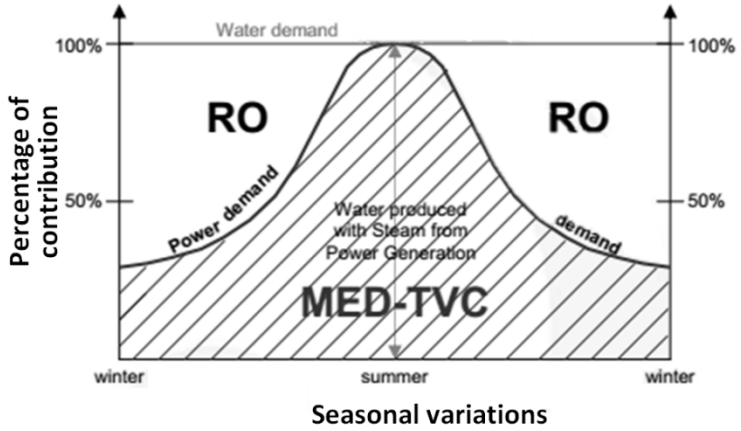


*FIG. 26. The different desalination units' contribution in the water demand along the year.*

### 1.8.1. Hybrid configuration options

Hybrid desalination systems are classified as simple hybrid and integrated hybrid.

*Simple hybrid configuration*
In the simple hybrid MSF/RO desalination power process, a seawater RO plant is combined with either a new or existing dual-purpose MSF/power plant to offer some advantages. Figure 27 shows the hybrid elements and the important connections for simple configuration.

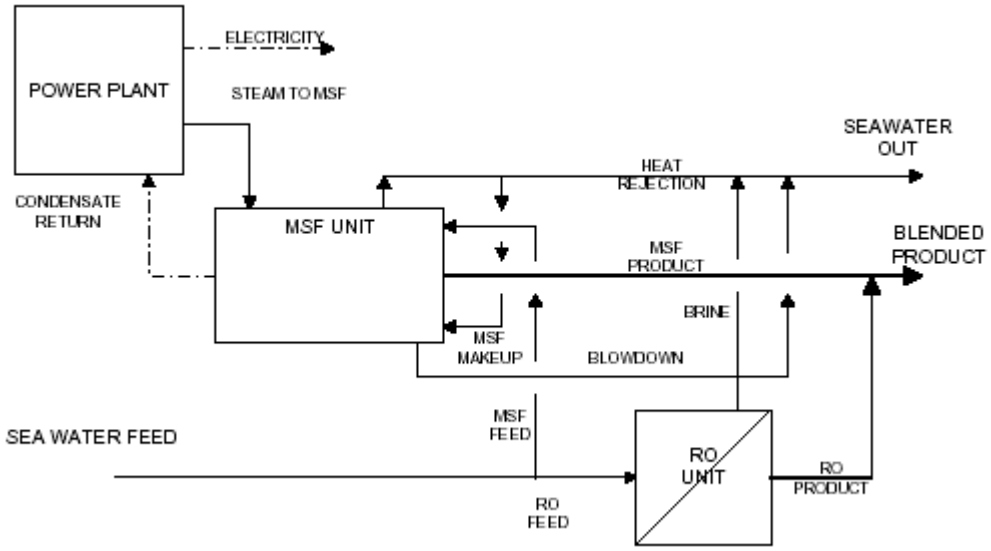


*FIG. 27. Simple hybrid (blend of RO and MSF product).*

In this configuration a seawater RO plant is combined with a new or existing dual purpose distillation (MSF or MED) and power plant obtaining the following advantages:

— Use of common and considerably smaller seawater intake;
— Obtain suitable product water quality by blending product water from RO and MSF plants;

— Allow higher temperature of distillate by blending product waters from RO and distillation plants;
— Use of a single stage RO process;
— Reduce strict requirements on boron removal from RO by blending MSF distillate with RO products;
— Extend lifetime of RO membrane;
— Reduce excess power and power to water ratio production from the desalting complex.

*Integrated hybrid configuration*

The fully integrated water and power plant with hybrid desalination processes, shown in Fig. 28, takes additional advantages of the following integration features:

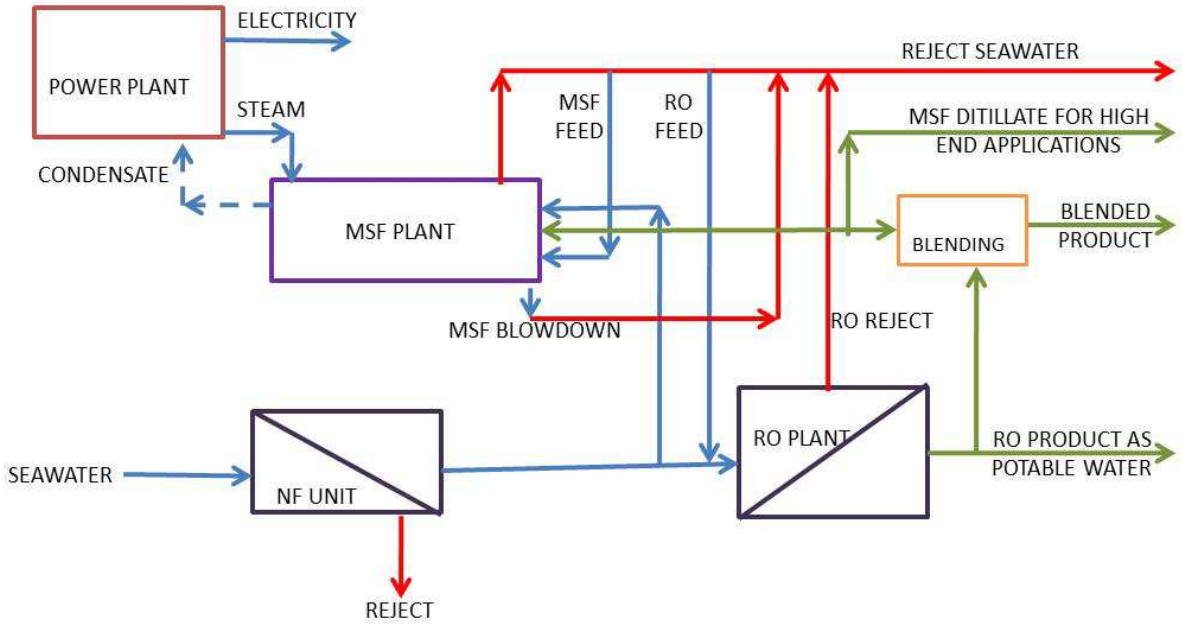


*FIG. 28. Integrated hybrid configuration.*

— Optimize and control the feedwater temperature to the RO plant by using cooling water from the heat-reject section of the MSF/MED or power plant condenser;
— Use the low-pressure steam from the MSF/MED plant to de-aerate or use de-aerated brine as a feedwater to the RO plant to minimize corrosion and reduce residual chlorine;
— Use of an integrated seawater pretreatment and post-treatment for the product water from both plants;
— Combine the reject brine from the RO plant with the brine recycle in the MSF or use as a feed to MED;
— Improve in GOR by using hybridization of NF as feed pretreatment for MSF and MED plants;
— Reduce strict requirements on boron removal from RO by blending MSF distillate with RO products.

### 1.8.2. Main advantages of hybrid systems

*Reduced seawater feed requirements*
The use of distillation plant cooling water in the rejection section as feed to the RO plant reduces both the seawater intake and rejects disposal system. Additionally the pretreatment costs and the required pumping power for feedwater are further reduced.

*Reduced RO membrane replacement*
Integrating SWRO unit with a MSF distiller provides the opportunity to blend the products of the two processes. Such arrangement allows operating the RO unit with relatively high TDS and consequently allows lowering the replacement rate of the membranes. If the useful life of the RO membrane can be extended from 3 to 5 years, the annual membrane replacement cost can be reduced by nearly 40 per cent. Blending the RO product water with the high purity distilled water allows meeting the product water quality standards with a single stage RO plant, while maintaining a long membrane life.

*Increased RO membrane performance as a function of feed temperature*
For all membranes, water production is a function of temperature and increases by 1.5–3% per degree Celsius for nearly all membranes, thereby reducing the required number of RO membrane modules. And if the useful life of the RO membrane can be extended from 3 to 5 years, the annual membrane replacement cost can be reduced by nearly 40%.

*Blending RO and distillation units*
Integrating a seawater reverse osmosis unit with a MSF distiller provides the opportunity to blend the products of the two processes. Such arrangement allows operating the RO unit with relatively high TDS and consequently allows lowering the replacement rate of the membranes. If the useful life of the RO membrane can be extended from 3 to 5 years, the annual membrane replacement cost can be reduced by nearly 40% [22]. Blending the products of the thermal and SWRO plants allows the use of a single stage SWRO instead of the two stage SWRO plant normally employed in standalone SWRO plants. Combining thermal and membranes desalination plant in the same site will allow using common intake and outfall facilities with less capital cost. An integrated pretreatment and post-treatment operation can reduce cost and chemicals. During cooler seasons, the preheated seawater leaving the heat rejection of the MSF distiller or the last effect of the MED plant can be used as feedwater for the RO plant.

*Increased recovery ratio*
The ratio of the desalinated water output volume to the seawater input volume used to produce it is called the water recovery ratio:

- In case of MSF-RO hybrid configuration, the overall seawater utilization and % recovery can be increased by utilizing MSF reject water as feed for RO plant. Also, the higher temperature of MSF reject water increases the flux in RO plant;
- In case of NF-MSF hybrid combination, utilizing NF as feed pretreatment for the MSF plant removes scale forming ions ($SO_4^{--}/Ca^{++}/Mg^{++}$) and the plant can be operated at top brine temperature (TBT), at more than 121°C. The increase in TBT increases the % recovery by increasing the flash range. MSF plants of higher concentration factor and high recovery can be designed;
- In case of NF-MSF-RO, removal of scale forming ions ($SO_4^{--}/Ca^{++}/Mg^{++}$) from the RO plant feed leads to higher % recovery in both RO and MSF plants. The overall

seawater utilization and % recovery can be increased further utilizing MSF reject water as feed for the RO plant. Also, the higher temperature of MSF reject water increases the flux in the RO plant.

### 1.8.3. Feedwater deaeration

A deaerator is a device that is widely used for the removal of oxygen and other dissolved gases from the feedwater to steam-generating boilers. In particular, dissolved oxygen in boiler feedwaters will cause serious corrosion damage in steam systems by attaching to the walls of metal piping and other metallic equipment and forming oxides (rust). Dissolved carbon dioxide combines with water to form carbonic acid that causes further corrosion. Most deaerators are designed to remove oxygen down to levels of <7 ppb and to eliminate carbon dioxide. There are many different horizontal and vertical deaerators available from a number of manufacturers, and the actual construction details will vary from one manufacturer to another. There are two basic types of deaerators, the tray-type and the spray-type:

— The tray-type (also called the cascade type) includes a vertical domed deaeration section mounted on top of a horizontal cylindrical vessel which serves as the deaerated boiler feedwater storage tank;
— The spray-type consists only of a horizontal (or vertical) cylindrical vessel which serves as both the deaeration section and the boiler feedwater storage tank.

*The tray-type*
The typical horizontal tray-type deaerator (Fig. 29) has a vertical domed deaeration section.

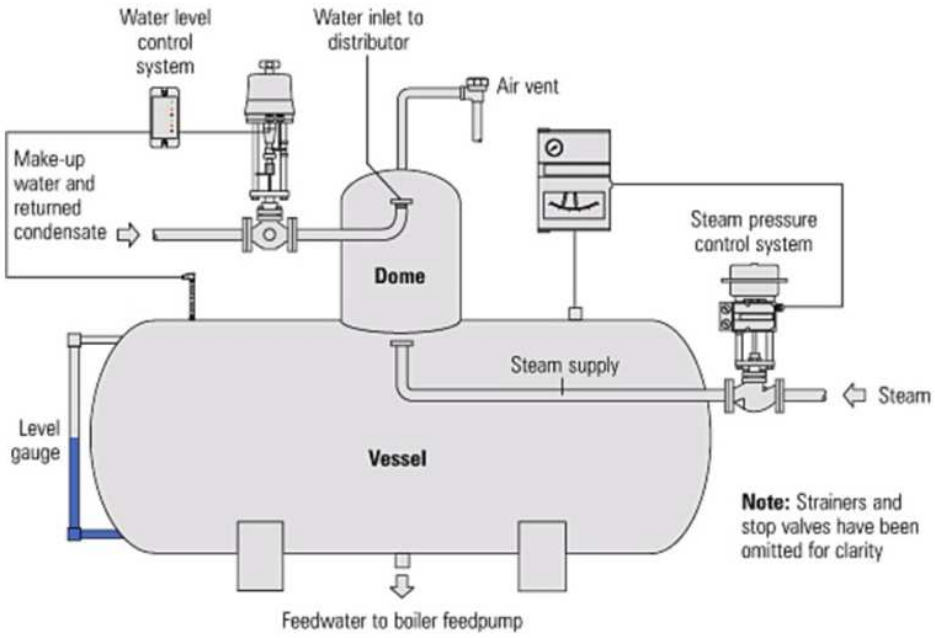


*FIG. 29. Schematic diagram of a typical tray-type deaerator.*

This deaeration section is mounted above a horizontal boiler feedwater storage vessel. The boiler feedwater enters the vertical deaeration section above the perforated trays and flows downward through the perforations. The low-pressure deaeration steam enters below the perforated trays and flows upward through the perforations. Some designs use various types

of packing material, rather than perforated trays, to provide good contact and mixing between the steam and the boiler feedwater. The steam strips the dissolved gas from the boiler feedwater and exits via the vent at the top of the domed section. Some designs may include a vent condenser to trap and recover any water entrained in the vented gas. The vent line usually includes a valve and just enough steam is allowed to escape with the vented gases to provide a small and visible telltale plume of steam. The deaerated water flows down into the horizontal storage vessel from where it is pumped to the steam generating boiler system. Low-pressure heating steam, which enters the horizontal vessel through a sparge pipe in the bottom of the vessel, is provided to keep the stored boiler feedwater warm. External insulation of the vessel is typically provided to minimize heat loss.

*The spray-type*

As shown in Fig. 30, the typical spray-type deaerator is a horizontal vessel which has a preheating section (E) and a deaeration section (F). The two sections are separated by a baffle (C).

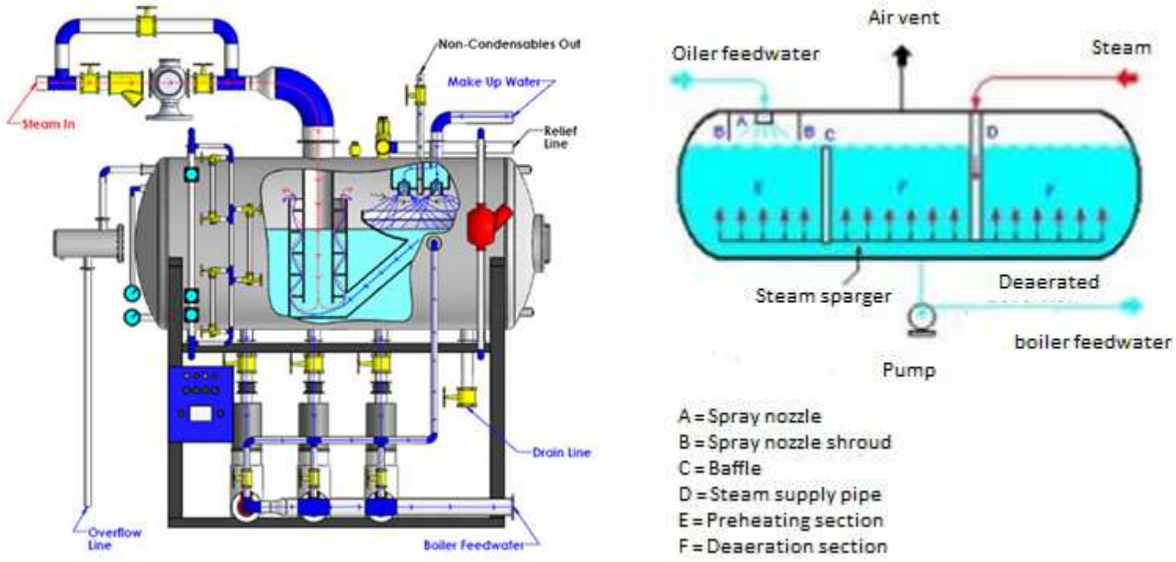


*FIG. 30. A schematic diagram of a typical spray-type deaerator.*

The low-pressure steam enters the vessel through a sparger in the bottom of the vessel. The boiler feedwater is sprayed into section (E) where it is preheated by the rising steam from the sparger. The purpose of the feedwater spray nozzle (A) and the preheating section (E) is to heat the boiler feedwater to its saturation temperature to facilitate stripping out the dissolved gases in the following deaeration section. The preheated feedwater then flows into the dearation section (F), where it is deaerated by the steam rising from the sparger system. The gases stripped out of the water exit via the vent at the top of the vessel. Again, some designs may include a vent condenser to trap and recover any water entrained in the vented gas. The vent line usually includes a valve and just enough steam is allowed to escape with the vented gases to provide a small and visible telltale plume of steam. The deaerated boiler feedwater is pumped from the bottom of the vessel to the steam generating boiler system. The deaerators in the steam generating systems of most thermal power plants use low pressure steam obtained from an extraction point in their steam turbine system. However, the steam generators in many large industrial facilities such as petroleum refineries may use whatever low-pressure steam is available.

Oxygen scavenging chemicals are very often added to the deaerated boiler feedwater to remove any last traces of oxygen that were not removed by the deaerator. The most commonly used oxygen scavenger is sodium sulphite ($Na_2SO_3$). It is very effective and rapidly reacts with traces of oxygen to form sodium sulphate ($Na_2SO_4$), which is non-scaling. Another widely used oxygen scavenger is hydrazine ($N_2H_4$).

### 1.8.4. Hybrid desalination with nanofiltration pretreatment

Membrane softening technology adapted to hybrid with distillation processes could lead to a significant increase in productivity and cost reduction of existing and future distillation plants. Similar to RO, NF bases itself on solution-diffusion as the main transport mechanism; however, NF membranes have fixed (negatively) charged functional groups. As a result, the selectivity of NF membranes for monovalent and bivalent anions is significantly different. The development of low-cost NF membranes that will remove, economically, the scaling salts from the MSF and SWRO plant feeds (Fig. 31), has been advocated by Awerbuch [24] and the research and development centre (RDC) of SWCC [25], which recently introduced a promising approach for pretreatment of seawater using NF membranes. Application of a NF technique for pretreatment of seawater resulted in the reduction of salt concentration and removal of most of the hardness, creating cations ($Ca^{+2}$, $Mg^{+2}$) and anions ($SO_4^{-2}$, $HCO_3^-$) which are responsible for the formation of the alkaline and non-alkaline scale on the heat transfer surfaces of thermal desalination processes.

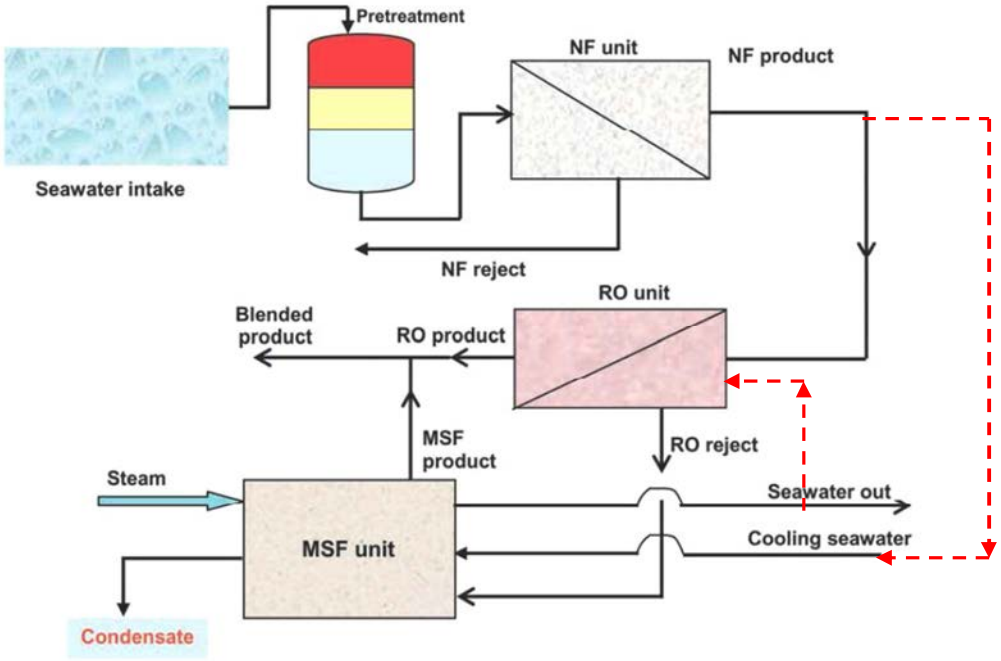


*FIG. 31. Schematic flow diagram of hybrid NF/RO/MSF desalination system.*

Similarly, the NF pretreatment process removes the hardness, causing ions from SWRO feed. Pretreatment of raw seawater by NF opens the possibility of safely increasing the top brine temperature (TBT) of thermal seawater desalination plants above their present TBT limit. Increase of TBT shall result in the increase of water production and PR. The hybridized MSF pilot plant was operated successfully for the first time up to a top brine temperature (TBT) of 130ºC, which is the design TBT limit of the unit, without injection of scale control additive

for a period of 1200 h, and the product recovery was increased up to 70% compared to 35% obtained from conventional operated MSF desalination plants. Successful evaluation tests were also performed at the same TBT of 130°C using a make-up to the MSF unit formed from a blend of nanofiltration product and seawater. The great potential of NF membrane softening technology was brought to focus by recent award by Sharjah electricity and water authority (SEWA) to Besix leading edge water technologies for the first commercial LET nanofiltration system to increase capacity of existing MSF plant from nominal 5 to 7.2 MIGD. This 40% increase in capacity of an MSF unit was a result of a two-year demonstration and simulation programme developed jointly with SEWA. The additional capacity is achieved without the requirement to build a new intake structure or new power plant; it can be installed in a very limited space, which would not allow the construction of a new desalination plant.

## 1.9. HEAT PIPE TECHNOLOGY FOR IMPROVED WASTE HEAT RECOVERY AND SAFETY OF NUCLEAR DESALINATION

Waste heat is generated in large quantities in various types of nuclear reactors. For example, the pebble bed modular reactor (PBMR), a high temperature gas-cooled-type reactor, produces up to 300 MW(th) of waste heat at about 67°C, which is a suitable temperature for the MED desalination process. Other types of nuclear reactors such as the pressurized water reactors (PWR), the Canadian CANDU reactors, and the Indian pressurized heavy water reactors (PHWR), dissipate almost two thirds of their net thermal power in the heat sink (typically nuclear reactors have an electrical efficiencies, of around 32% as average). In some specific cases, even high-power nuclear research reactors could produce sufficient waste heat to be considered as a source of energy for desalination [26].

In the case of research reactors, the waste heat can be used to produce the required high quality distilled water from seawater to meet the demands of the demineralized water makeup requirement of the reactor itself [26]. If not utilized, such waste heat energy will be dissipated to the ultimate heat sink (i.e. sea, river or air).

Efficient heat exchangers are required to harness the waste heat from various potential sections of the nuclear plant to be used in the water desalting process. Such heat exchangers should meet the minimum safety requirements to prevent contamination among the various sections of the plant and to ensure an efficient heat transfer process, making effective use of the available energy in the desalting process. At present, shell and tube heat exchangers are generally being used for desalination purposes. This type of heat exchanger has many disadvantages. To address these disadvantages, the use of heat pipe technology in desalination heat exchanger systems will be introduced in the following sections. Beyond the many advantages of heat pipe technology [26–30], the utilization of heat pipe heat exchangers is expected to affect not only the overall economics but also to enhance the public perception, specially of the nuclear seawater desalination at large, as it offers an efficient method to harvest the waste heat, and better handling of brine before discharge. Heat pipes can be used to build heat exchangers that can effectively harness most of the waste heat being generated in the various types of nuclear power reactors. Such waste heat is viewed as a free source of energy to produce fresh water. Due to its LT, waste heat is useful only when the low-temperature multieffect distillation (LT-MED) process is used. The application of heat pipes could be seen as a viable option to nuclear seawater desalination where the efficiency to harness waste heat might not only be enhanced to produce larger quantities of desalted potable water, but also to make nuclear desalination more environmentally friendly.

In case of nuclear desalination, concerns over a possible contamination of the product water require special attention [31–33]. In specific, tritium is the major concern as it is able to penetrate various materials and possibly end up into the product water. With the application of appropriate safety measures (addressed on a later chapter), the experience from Kazakhstan, India, Japan and the United States, shows that nuclear desalination complies with various health standards. Indeed, public health problems have never occurred due to the tritium levels in the desalinated water. Moreover, the MSF-RO facility in Kalpakkam has delivered desalinated water outside the facility with tritium content below the detectable limit. Similarly, a number of non-electrical applications of nuclear power have reported background tritium levels in the product water or steam. Tritium is produced in nuclear reactors either as a direct product of nuclear fission or as a result of reactions between neutrons with elements present in the reactor, such as lithium and boron. It is a soft beta emitter and presents no dangerous hazard for external exposure. However, it is considered a health hazard if inhaled, digested via food, or entered the body as tritiated water above a certain dose level. In general, the quality assurance of desalinated water against any radioactive contamination is usually guaranteed through two types of measures: regulatory and technical ones. Heat pipes may also be used to improve conditioning of the brine before discharging to the environment. In general, brine disposal can be an environmental and economic issue in some areas. Furthermore, brine disposal should be studied and engineered to reduce the harmful effects to the environment thus guaranteeing that sensitive fauna and flora species of local seawater salinity are protected.

### 1.9.1. Heat pipe technology and applications

Heat pipes are hermetically sealed tubes containing a working fluid in both the liquid and vapour phases and a wick to allow for the return of the condensed working fluid to the evaporator (Fig. 32a). If the system permits, cheaper heat pipes (without wicks) can be utilized provided that the evaporator section is lower than the condenser section (at least by an angle of 5° [30, 34, 35]) thus allowing the working fluid in liquid phase to return from the condenser to the evaporator by gravity (Fig. 32b).

In some engineering applications, horizontal evaporator positioning is desirable (electronics cooling, concentrated solar collectors, etc.). This has been possible so far by utilizing loop or wicked heat pipes. Taking into account the relatively high space requirements for loop heat pipes and the cost of wicked heat pipes, horizontal wickless heat pipes are more desirable due to their lower cost and space requirements.

However, for heat pipes to function with horizontal evaporator orientation, the return of the working fluid condensate back to the evaporator section has to be secured so that the wickless heat pipe can fully function. Jouhara et al [36] reported and designed a heat pipe with a condenser section at an angle of 12 degree from the evaporator axis.

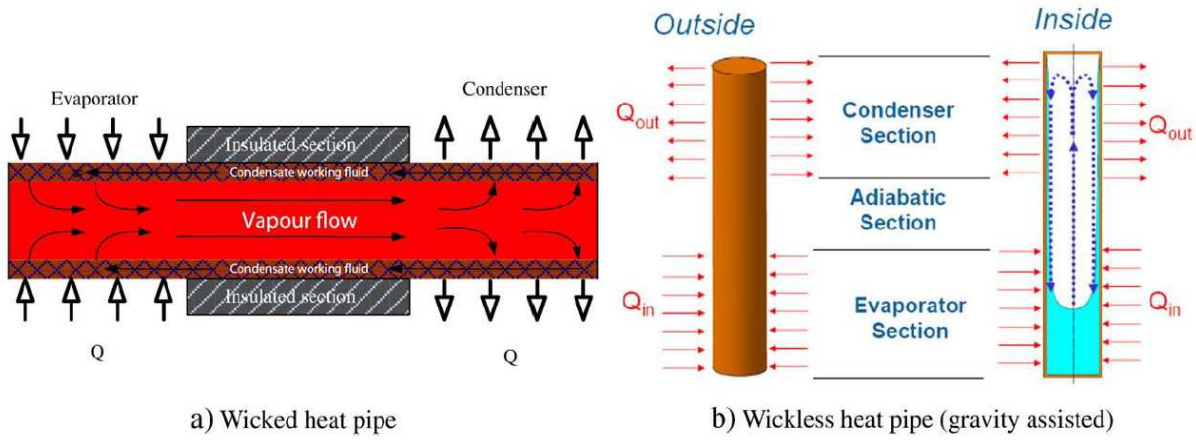


*FIG. 32. The concept of a heat pipe.*

Therefore, when the evaporator angle is at 0 degrees (horizontal positioning), the condenser will be at 12 degrees, which is large enough to secure the return of the condensate working fluid back to the evaporator, hence full operation capability of the heat pipe (Fig. 33).

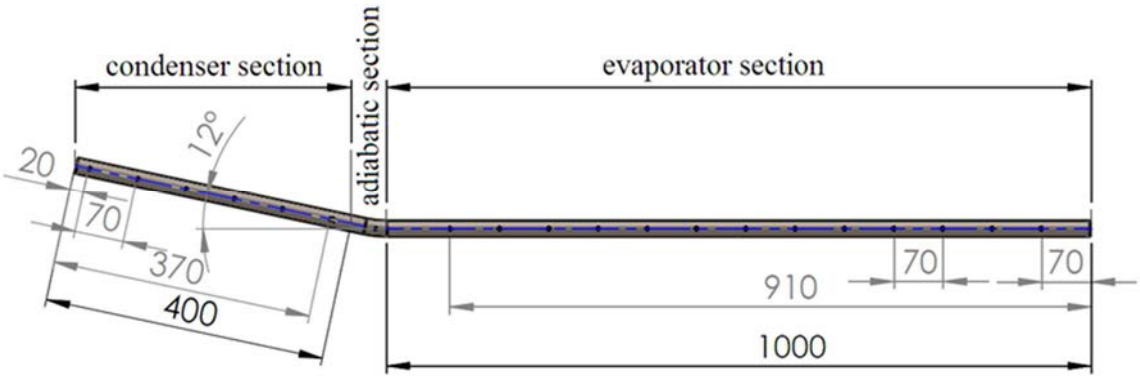


*FIG. 33. Wickless heat pipe with an inclined condenser section.*

The selection of the heat pipe working fluid and its shell and wick material depends largely on their chemical compatibility and the heat pipe working temperature ranges, [34–37]. The amount of heat that can be transported by these devices is normally several orders of magnitude greater than that transported by pure conduction through a solid metal [28, 30, 34]. Heat pipes can be used in bundles to create heat exchangers, which are passive (no external power requirement) and contain no moving parts. They can be manufactured in a wide variety of sizes, and can be made compact and suitable for a wide range of thermal applications as a result of their high efficiency. Indeed, such advantages of heat pipe-based heat exchangers resulted in their use in a wide range of applications. Many of these applications are related to space technology [38], thermal storage [39], harnessing of renewable energy [27, 28, 40–43] and in waste heat recovery of various processes [27, 37, 44].

Heat pipe based heat exchangers are likely to replace the conventional shell and tube heat exchangers in the evaporators and the condensers of the desalination plants. The benefits that heat pipe technology brings into the nuclear seawater desalination process are:

— Efficient transfer of heat energy between two systems while the systems are physically separated. That eliminates the risk of mixing between the steam from the nuclear reactor and the seawater in the evaporator section and from the condensed fresh water and the brine in the condenser section of the desalination system;
— Much needed contingency plan to the process. In the heat pipe based heat exchanger, the system will remain safely operational even if a number of heat pipes stopped functioning;
— High efficiency of the heat pipe heat exchangers, they will have much smaller size when compared to equivalent conventional heat exchangers;
— Major reduction in the fouling problem (the fouling problem is only an issue on the external surfaces of the heat pipes);
— No need for any pumping power as the heat pipe is a passive heat transfer device.

*Applications of heat pipes*

- Applications of heat pipes as heat exchangers

Based on safety considerations, coupling between the nuclear power plant and the desalination processes requires the usage of metallic barriers in the form of heat exchangers. Sometimes these are based on pressure reversal concept to prevent any radiation contamination between primary and secondary loops of the nuclear desalination system. For example, the MED plant is normally coupled to a nuclear reactor as bypass to the main heat sink (river or sea). A typical configuration of backpressure coupling desalination to a nuclear power plant can be seen in Fig. 34. Yet other turbine coupling scheme may include the coupling of a nuclear reactor to a thermal desalination plant using the backpressure turbine and a low-pressure turbine in parallel. In such cases, the conditions of the exhaust steam of the backpressure turbine (mass flow rate, temperature and pressure) are adjusted to the steam requirements of the thermal desalination plant.

Figure 35 represents a schematic diagram of a conventional single effect desalination process [45] where the steam is used to evaporate the seawater and the feed liquid is used to condensate it. There are a few concerns with the utilization of such typical design in the nuclear desalination process (Fig. 34). These concerns are related to the integrity of the separating surfaces between the fluids.

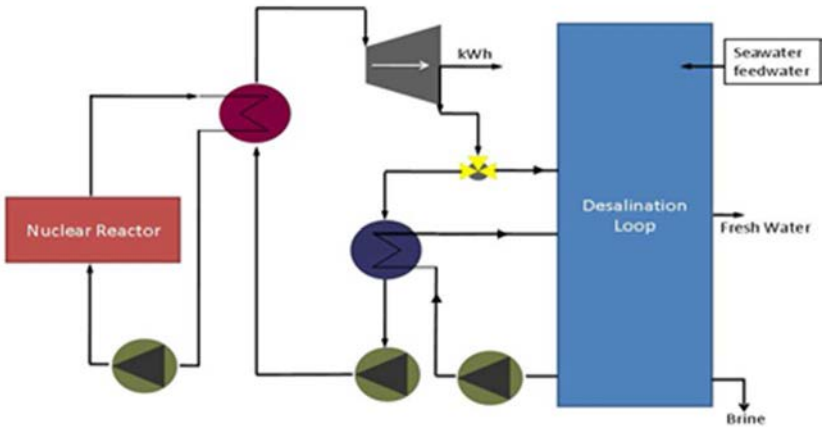


*FIG. 34. Typical coupling scheme of MED desalination plant to a nuclear reactor.*

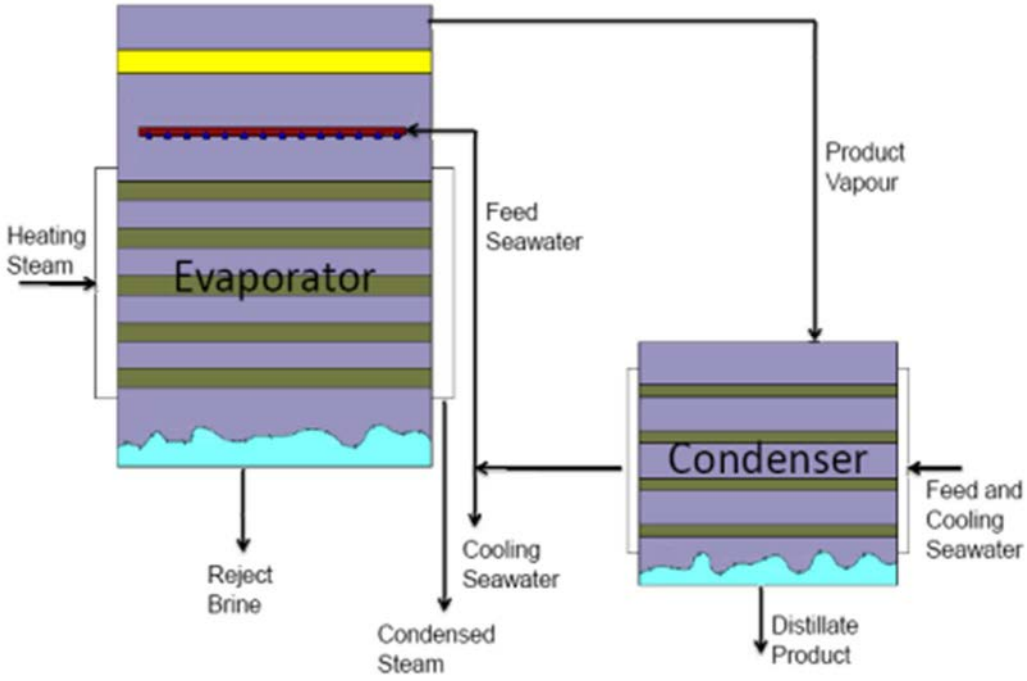


*FIG. 35. Conventional single effect desalination.*

Examples of these concerns are as follows:

- In the evaporator section, if a leak happens in any of the steam tubes of the shell and tube heat exchanger, it will lead to an interaction and mixing between the steam and the seawater (as a consequence, the whole system has to be shut down for maintenance and decontamination);
- The same scenario applies to the condenser section, where a leak will cause the fresh water produced to be contaminated by the feed seawater (the whole desalination process has to stop for maintenance;
- Fouling issues are of concerns (on the internal and external surfaces of the tubes) when using shell and tube heat exchanger, as this reduces the effectiveness of the heat exchange capacity of the system.

By utilizing heat pipe technology, the previous concerns will be addressed. A schematic of the proposed heat pipe-based system is illustrated in Fig. 36. In the proposed system, heat pipes transmit the heat energy from the steam flow (from the nuclear plant) to the seawater feed chamber where it will be used to evaporate the seawater. The condensed steam from the steam chamber will then return to the nuclear plant. As illustrated in Fig. 36, the steam chamber and the seawater feed are physically separated and heat pipes sections in the separation zone are usually well insulated (adiabatic sections). The same function of the heat pipe heat exchanger is illustrated for the waste heat recovery from the resulting brine (Figs. 36 and 37).

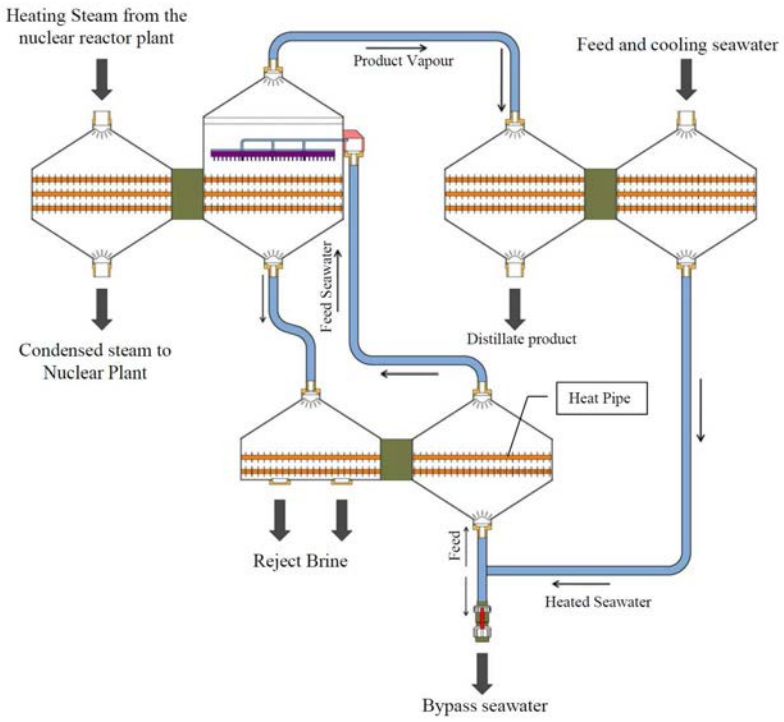


*FIG. 36. Heat pipe-based single effect desalination plant.*

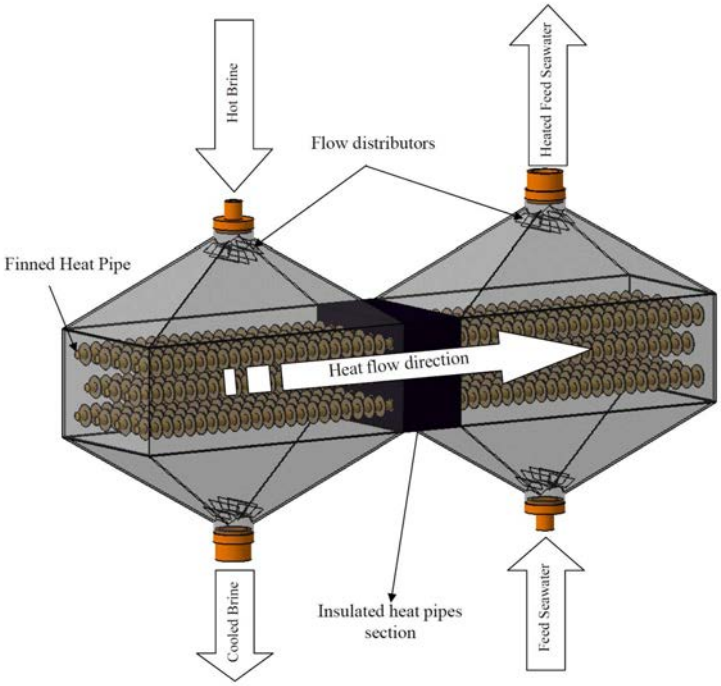


*FIG. 37. Typical heat pipe based heat exchanger to recover heat from the hot brine to the seawater feed stream.*

The proposed heat pipe based system will have the following advantages:

— As the evaporator has two physically separated chambers for the steam and the seawater flow, a leak in any of the chambers will not affect the other chamber thus

eliminating the risk of contamination. In the extreme case of a leak in any of the heat pipes, the heat pipe shell will keep an active barrier between the steam seawater in the evaporator zone and between the fresh water vapour/condensate and the feed seawater in the condenser zone. The same scenario can be said for the brine and the seawater feed for the brine system in Figs. 36 and 37;

— As the evaporator has two physically separated chambers for the steam and the seawater flow, a leak in any of the chambers will not affect the other chamber thus eliminating the risk of contamination. In the extreme case of a leak in any of the heat pipes, the heat pipe shell will keep an active barrier between the steam seawater in the evaporator zone and between the fresh water vapour/condensate and the feed seawater in the condenser zone. The same scenario can be said for the brine and the seawater feed for the brine system in Figs. 36 and 37;

— It allows for a process contingency plan, which means that if a number of heat pipes would stop to function, the system would remain operational, at a reduced capacity, until the next scheduled maintenance stage;

— As the heat pipe has an extremely high effective thermal conductivity, by placing two temperature sensors on the hot and the cold sides of the heat pipe, the temperature difference will be an indication of the operational status, thus providing an easy detection of any faulty heat pipe;

— The ultrahigh effective thermal conductivity of the heat pipes means that the system will be totally passive (no need for pumping power for the heat energy transmission between the hot and the cold fluids);

— Fouling can only take place on the external surfaces of the tubes as the heat pipe is a sealed device.

The previous points and many others justify the use of heat pipe-based heat exchangers in the nuclear desalination systems. The heat pipe units shown in Fig. 36 can be customized for the desired system capacity and conditions.

- Application of heat pipes as an auxiliary loop to prevent contamination

Nuclear desalination requires specific and stringent safety measures to ensure that public health will not be at risk. These measures are designed to provide product safety and prevent radioactive contamination. Such contamination may occur due to diffusion of radio nuclides through physical barriers separating the nuclear and desalination loops. Far more probable and, due to the higher amount of radioactive release; more hazardous pathway is a possible leakage from the nuclear to the desalination loop. Irradiation corrosion and other types of corrosion of the reactor structure present a very real problem, because they can lead to material cracking and subsequent leakage [46]. To prevent the above risks, an intermediate loop was introduced between the nuclear and the desalination loop [47]. This intermediate loop must have a higher pressure than the nuclear one in order to ensure that should a leak occurs it will be directed from the intermediate to the nuclear side, not the other way around. Search for small ruptures though, is very difficult, so it is important always to maintain the higher intermediate pressure. The intermediate loop includes an additional heat exchanger towards the desalination loop and acts as physical barrier preventing radionuclide

contamination of the desalination loop. This procedure is similar to the radiation safety principles applied to the schemes of using nuclear energy for district heating. Tritium is the primary concern from the radiation product safety aspect. It is a radioactive hydrogen isotope which is highly penetrative and able to oxidize forming tritiated water, effectively following the same pathways as natural water. As a potential hazard to public health, tritium in drinking water is regulated by various national and international standards and guidelines. Most of them differ in the limits set, but they all follow the calculation pattern used in the WHO guideline. The WHO limit for tritium in drinking water is based on the ICRP recommendation for an effective dose limit of 1 mSv per year for any combination of internal and external radiation doses [47], as well as the dose coefficient of $1{,}8 \times 10^{-11}$ Sv/Bq for ingestion of tritium by an adult member of the public [48]. The WHO regulatory recommendation starts with 10 per cent of the ICRP's effective dose limit of 1 mSv. Given the fact that other radiation sources will contribute to the committed effective dose 0,1 mSv per year through drinking water is a reasonable value. The guideline level for tritium activity *GL*, is calculated as:

$$GL = \frac{RDL}{DCF \times q} \qquad \text{Eq. (3.1)}$$

Where *RDL* is the reference dose level (= 0,1 mSv), *DCF* is the dose conversion factor for ingestion by adults (= $1{,}8 \times 10^{-11}$ Sv/Bq), and $q$ is the annual ingested volume of drinking water (= 730 l/year).

The subsequent guideline level of 7610 Bq/l is rounded up to 10 000 Bq/l, referring to the total beta activity in a water sample and not just tritium. It is used by many of the WHO member states as a basis for regulation as well as other UN agencies, some of which are presented in Table 6. The limit though, does not exclude the as low as reasonably achievable (ALARA) principle in efforts to further reduce the level of radionuclides in drinking water [49].

For comparison, the reported levels of tritium in the drinking water from the nuclear desalination plants were below the detectable limit in Kalpakkam [50] and 6 Bq/l in Aktau [49]. Nevertheless, monitoring of tritium levels is recommended for the nuclear plant as well as the intermediate safety loop between the nuclear and desalination plants, but it is absolutely necessary for the desalination plant.

TABLE 6. ALLOWED TRITIUM LEVELS IN DRINKING WATER

| Country/International Organizations | Tritium limit (Bq/l) |
|---|---|
| Australia | 76 103 |
| Finland | 30 000 |
| Canada | 7000 |
| EU* | 100 |
| Kazakhstan | 7700 |
| Switzerland | 10 000 |
| United States of America | 740 |
| WHO** | 10 000 |

**This value is not a limit, but rather an alarm level;*

The drinking water quality can be monitored in the reservoirs, which hold the water prior to its release into the drinking water network. This is common for all desalination plants, allowing for a chemical and bacteriological analysis. In the case of nuclear desalination, tritium activity measurement must be included in this analysis. Depending on the reactor type, tritium is observed as a result of nuclear reactions in the fuel, coolant or moderator (Table 7). Most of the tritium is transported close to the desalination loop with the coolant. Unlike other, heavier radio nuclides, tritium cannot be removed by the RO membranes. Hence, an intermediate loop between the reactor and the desalination plant is designed to prevent tritium contamination of the desalination water [51].

TABLE 7. TYPICAL TRITIUM PRODUCTION PER REACTOR TYPE AND SOURCE (GBq/GW(e)/year)

| | Fuel | Coolant | Moderator | Total |
|---|---|---|---|---|
| LWR-PWR | $5.18 \times 10^5$ | $3.70 \times 10^4$ | N/A | $5.55 \times 10^5$ |
| LWR-BWR | $5.18 \times 10^5$ | Low | N/A | $5.18 \times 10^5$ |
| HWR | $5.18 \times 10^5$ | $1.85 \times 10^6$ | $5.18 \times 10^7$ | $5.42 \times 10^7$ |
| GCR | $5.18 \times 10^5$ | Low | $(0 – 1.85) \times 10^5$ | $(5.18 – 7.03) \times 10^5$ |
| GCR-HTGR | $5.18 \times 10^5$ | $1.85 \times 10^5$ | $(0.18 – 7.40) \times 10^4$ | $(5.2 – 5.9) \times 10^5$ |
| FBR | $7.40 \times 10^5$ | $7.40 \times 10^4$ | N/A | $8.14 \times 10^5$ |

Tritium usually stays in the reactor fuel. Only a fraction of tritium escapes from the core diffusing into the primary coolant. Part of this fraction then diffuses to the secondary cooling circuit through the surface of the heat exchanger. Further, through the surface of the intermediate heat exchanger, it may also diffuse to the water–steam circuit. Diffusing and penetrating through reactor vessel walls, heat exchanger and steam generator surfaces, machinery and pipelines, a small portion of tritium may get transferred into the desalination loop [51]. Large part of the tritium in the nuclear coolant oxidizes into tritiated water, which is similar to natural water and cannot permeate through metallic barriers. Thus, the use of the added intermediate loop (Fig. 38) with higher pressure is considered a sufficient radiation protection, minimizing the tritium contamination potential. It should be noted that pressure barriers are likely to be a regulatory requirement as part of the established “defence in depth” principle for nuclear power plants.

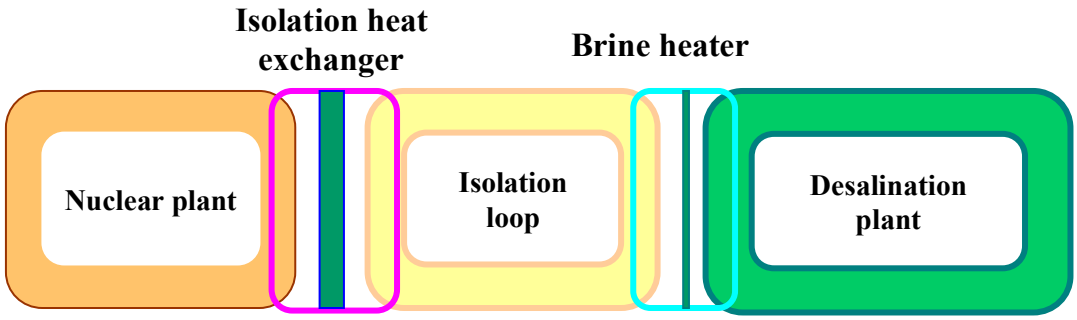


*FIG. 38. Nuclear desalination coupling with an intermediate isolation loop.*

In principle, heat pipes should provide lower tritium permeation rates. If we assume the same material, surface, temperature and pressure conditions for the heat exchanging area in a given nuclear desalination facility, the difference in reducing tritium permeation would be defined by the surface area. Heat pipes, with their higher thermal transfer efficiency, need a smaller surface for the same energy transfer and reduce the diffusive surface for tritium. However, there will always be a certain amount of tritium in the desalination loop, mainly due to diffusion of gaseous tritium through physical barriers. This cannot be totally prevented, although the diffusion rate will differ for different materials. It is important that the quantity of tritium diffused does not compromise the compliance with a set of health and safety protection limits.

Diffusion of gaseous tritium cannot be completely prevented by using physical barriers; however a large part of the formed tritium is in the form of tritiated water [52]. The latter is similar to natural water and cannot permeate through metallic barriers, making an intermediate loop with higher pressure a sufficient and effective radiation protection. The experience so far confirms this [51, 52]. As discussed above, heat pipe heat exchangers offer many additional advantages for product water safety in nuclear desalination. For example, having a higher thermal efficiency, such systems require a reduced heat transfer surface potentially reducing tritium penetration. The tritium transfer rate *Qtr* to the next circuit is calculated with the following formula:

$$Qtr = Che \times Jhe \times She \times Ghe \qquad \text{Eq. (3.2)}$$

Where: *Che*, *Jhe*, *She* and *Ghe* would represent, respectively, the concentration of tritium in the nuclear loop, the permeation flux (Fig. 39) of the heat pipe material, the combined surface of the heat pipes and the flow rate of the heat pipe system. It can be seen from the above equation that a reduction in the heat-exchanging surface will result in proportional reduction in tritium migration in the desalination loop. In addition, heat pipes can provide higher operational safety.

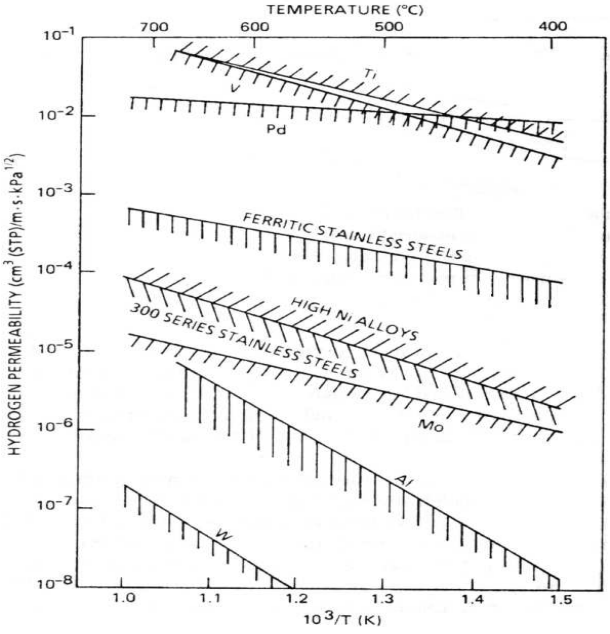


*FIG. 39. Hydrogen permeability as a function of temperature for selected metals and alloys.*

Leaks can be detected and located, while a physical barrier to the desalination loop is still provided. Furthermore, heat pipe systems offer system design simplicity, hence, eliminating the need for an intermediate loop, or a second heat exchanger and/or a pump which would be needed to provide higher intermediate pressure. In such set up, any operational and maintenance costs associated with the intermediate loop are avoided. In addition, the safety factor is still maintained at the necessary level preventing meaningful tritium migration into the desalination loop. In summary, the intermediate loop may be substituted with heat pipe systems. As a result, although tritium migration to the desalination loop will not be completely prevented due to the diffusion of gaseous tritium, one can still expect that heat pipes may prove as one of the effective tools for applying the ALARA principle on radiation safety in nuclear desalination.

Furthermore, implementation of such technology may present additional benefits for easier and more constant regulatory compliance concerning radionuclide contamination of the desalination loop, which will certainly reflect positively on the public confidence and in the product quality.

- Application of heat pipes as a measure to alleviate environmental impacts

Temperature is one of the most important single environmental factors, which affects the survival, growth and reproduction of aquatic organisms [53]. Distillation and desalination processes are typically associated with an increased brine temperature that affects the ultimate heat sink i.e. seawater. Higher brine temperature is responsible for higher corrosion rate of the desalination structure and subsequent adverse environmental impacts through increased discharge of toxic materials. Increasing seawater temperatures can potentially cause increased evaporation rates that may further elevate seawater salinity, and also causing adverse effects on organisms and enhanced uptake of toxic pollutants, decreased solubility levels of oxygen and nitrogen in the seawater [54]. Illustrating this, a study performed on Mediterranean seagrass Posidonia oceanica [55], reported that for the same salinity levels, survival rates decreased with higher temperatures. Also, the abundance and diversity of plankton species is likely to decrease, resulting from lower oxygen and nitrogen levels in the seawater [45]. Such an impact on primary production may lead to overall habitat deterioration. Finally, temperature increases have the potential to kill marine organisms especially, benthic communities, such as corals, which are very sensitive to temperature changes. On the other hand, 1°C increment on discharge temperature is of no ecological impact [56]. Yet, combined effect of discharging of effluents from power desalination plants, with increasing temperatures, contribute to an increase in the receiving seawater temperature which can often be observed several hundred meters away from the discharge point, depending on the technique used for discharging [57].

Jouhara [27] and later Jouhara et. al [28] have reported the economics and the characteristics of wraparound loop heat pipe (WLHP) based heat exchangers for the first time in the literature. Jouhara and Ezzuddin [58] have studied the thermal performance of a single WLHP and analysed the nature of heat transfer mechanisms within the heat pipe (Fig. 40). The output of the work provided significant information on the thermal characteristics of this type of loop heat pipes, which will play an important role in optimizing full-scale heat energy recovery heat exchangers that utilize this heat pipe configuration.

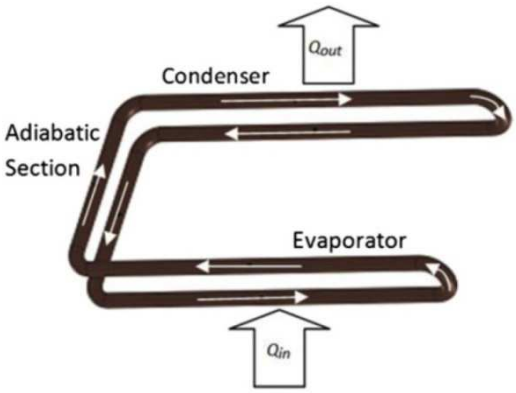


*FIG. 40. The WLHP design.*

Therefore, the issue of thermal energy (i.e. heat) dissipation from nuclear desalination in the normal heat sinks (i.e. rivers, lakes, or oceans) is of great environmental concern. Removal of the excess heat from the brine will improve the protection of the aquatic ecosystems and at the same time allow for a more effective preheating of the feedwater which reduces the energy required during the desalination process itself. The overall advantages of such heat recovery process will result in improved economics, offsetting the high cost and high energy consumption of the current process.

### 1.9.2. Experimental investigation

In order to demonstrate the thermal performance of a heat pipe that is capable of functioning as heat exchanger for applications in nuclear desalination, a fully instrumented experimental apparatus was built to test a 1m long, 22 mm outer diameter heat pipe. This apparatus is illustrated in Fig. 41. The chosen working fluid for the heat pipe was water while a copper shell was selected. The results demonstrate that for power throughputs of higher than 200 W, an average value of the overall thermal resistance of the heat pipe of about 0.1°C/W is achieved, as shown in Fig. 42. This means that to transport 1 W of heat energy between the two ends of the heat pipe, a temperature difference of about 0.1°C is required. This thermal resistance is almost about 300 times that for solid copper tube and demonstrates clearly the fact that the heat pipe is simply a thermal superconductor.

It should be noted that by using heat transfer enhancing mechanisms, the thermal resistance of the heat pipe can be further reduced and values as low as 0.05°C are achievable [28, 30, 34, 59].

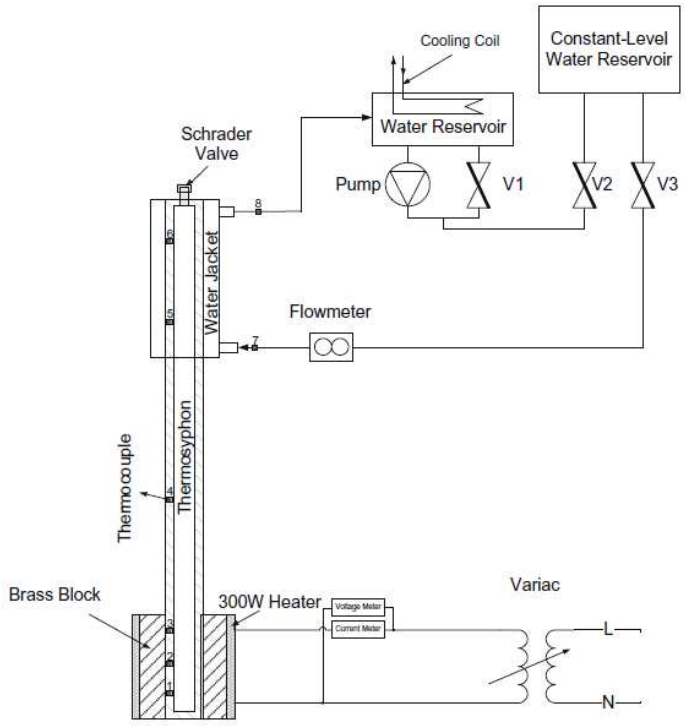


*FIG. 41. Schematic diagram of experimental apparatus rig attribute.*

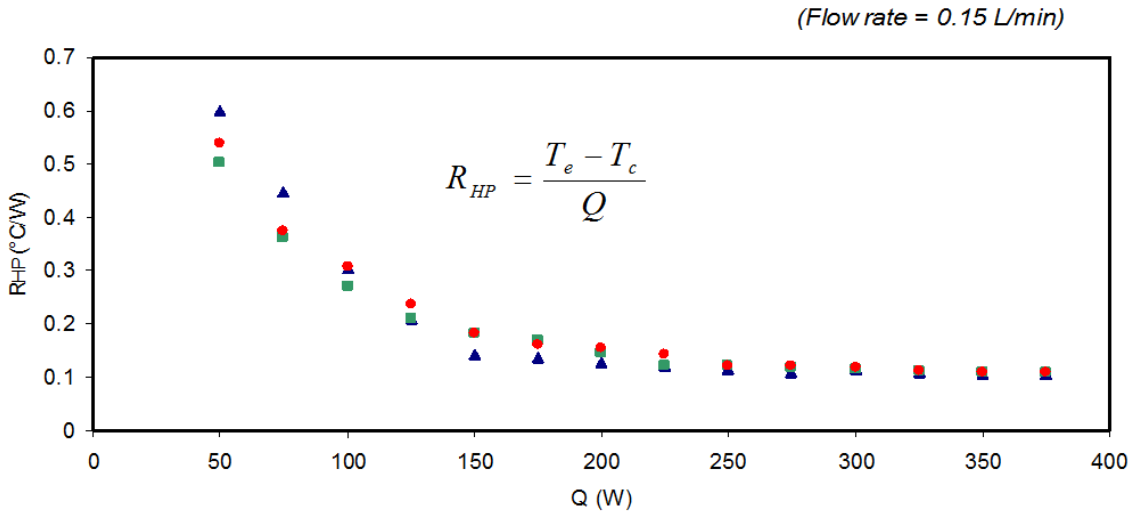


*FIG. 42. Heat pipe thermal resistance vs. power throughput.*

### 1.9.3. Conclusions

The use of heat pipes is likely to improve the economics, heat transfer efficiency and greater radiation safety of the product water due to lower tritium diffusion. For the same reason of a smaller heat exchange surface, the probability of tritiated fluid leaks in the desalination loop will be reduced. At the same time, application of heat pipes instead of the standard intermediate loop can decrease the capital, operating and maintenance costs. Heat pipes are expected to play an important role in making nuclear seawater desalination more economical as they are expected to recover a great percentage of waste heat. In addition to that, lower thermal discharges will improve the environmental performance of the nuclear desalination

plant. Experimental investigation on the thermal performance of a single heat pipe illustrated the reason behind calling this type of heat transfer devices a “thermal superconductor”. This type of investigations will have to be repeated on the selected type of heat pipes in order to achieve the desired performance for the heat exchanger that utilizes this heat pipe configuration. Finally, the reliability of water supply from the plant should increase due to the robustness of the heat pipe system. For example, possible leaks can be detected and located immediately, while a physical barrier to the desalination loop is still provided. Uninterrupted water supply has not only the benefit of higher revenue, but also higher safety of the product water and enhanced public support for the nuclear desalination plant. These points present a very good case for the use of heat pipe-based heat exchangers in the nuclear desalination systems.

## 1.10. SALTS RECOVERY FROM BRINE

The problem of disposing saline water from desalination plants (MED, RO) and chemicals industry is aggravating day by day. On one hand, there is continuous increase in number of desalination plants catering to the fresh water demands of the community and industry is on the other hand loading the saline water in the environment. The greatest environmental concern associated with the brine discharge of surface water relates to potential harm that concentrate disposal may pose to bottom-dwelling organisms located in the discharge area. Studies indicate that the extent of the vulnerability of marine environment to salinity differs from place to place. Another impact on marine environment is realized when different products used in chemical cleaning of desalination plants and pretreatment cleaning are disposed of in the sea [46]. The idea of nil liquid discharge emerges as a solution to reduce the impact of desalination plants on environment. KANUPP operates two desalination plants: RO and MED type nuclear desalination demonstration plant (NDDP). NDDP has been thermally coupled to KANUPP to alleviate the impact on environment. Salient features of the desalination plant at KANUPP are shown in Table 8.

TABLE 8. SALIENT FEATURES OF DESALINATION PLANTS AT KANUPP

| | RO | NDDP |
|---|---|---|
| Year of operation | 2000** | 2010 |
| Purpose | Industrial | Industrial |
| Capacity ($m^3$/day) | 454** | 1 600 |
| Source of water | Deep well | Sea |
| Recovery rate | 45%** | 28.8% |
| Disposal method | Discharge to sea | Discharge to sea |
| Any specific regulation followed regarding waste disposal | NEQS*, Pakistan | NEQS*, Pakistan |

** NEQS: national environmental quality standards;*
*** Values obtained from KANUPP-STR-03-12.*

### 1.10.1. Experimental investigation

RO and NDDP brine samples were collected and were analysed at the in-house chemical analysis facility at KANUPP (Table 9). The total salt load discharge to sea in Table 10 is indicative of the potential in the salt recovery process.

TABLE 9. THE RESULTS OF RO BRINE SAMPLE ANALYSIS

| Parameters | Result (ppm) |
|---|---|
| TDS | 46 000 |
| Total hardness | 7800 |
| Calcium | 2004 |
| Magnesium | 632 |
| Sodium | 13 000 |
| Chloride | 23 345 |
| Sulphate | 2793 |
| Manganese | 0.58 |
| pH value @ 25˚C | 6.92 |
| Theoretical TDS | 46 480 |
| Calcium hardness | 5010 |
| Mg hardness | 2598 |
| Bicarbonate | ND* |

* *ND: non-detectable*

TABLE 10. RO REJECT BRINE QUALITY DATA, OUTPUT VOLUME AND INDICATIVE ANNUAL SALT LOAD

| Item | Quantity |
|---|---|
| Reject brine aver. salinity as TDS in g/l | 46 |
| Reject brine output volume, $m^3/y$ | 212 000 |
| Annual salt load discharge, TPA | 9750 |

TABLE 11. ANALYSIS OF REJECT BRINE FROM NDDP AT KANUPP

| Parameter | Feedwater (ppm) | Brine blow down (ppm) |
|---|---|---|
| Calcium | 1450 | 2042 |
| Magnesium | 450 | 634 |
| Sodium | 11 800 | 16 615 |
| Sulphate | 3000 | 4228 |
| Chloride | 21 000 | 29 580 |

TABLE 12. ANNUAL REJECT BRINE QUALITY DATA FOR THE NDDP AT KANNUPP

| Constituent | Mass (tons) | Mass fraction |
|---|---|---|
| Calcium | 2932 | 0.032 |
| Magnesium | 910 | 0.01 |
| Sodium | 23 860 | 0.26 |
| Sulphate | 6067 | 0.066 |
| Chloride | 42 476 | 0.462 |
| Others | 15 659 | 0.7 |

TABLE 13. INDICATIVE ANNUAL PRODUCT YIELD FROM NDDP AT KANNUPP

| Salt | Mass fraction | Mass produced (tons) | Indicative price ($/ton) | Value (M$/year) |
|---|---|---|---|---|
| $CaSO_4$ | 0.093 | 8550 | 150 | 1.28 |
| NaCl | 0.661 | 60 750 | 70 | 4.25 |
| $Mg(OH)_2$ | 0.024 | 2206 | 400 | 0.90 |
| $CaCl_2$ | 0.012 | 1103 | 220 | 0.25 |
| Others | 0.21 | 19 300 | 500 | 9.65 |

Thus by processing 212 000 $m^3$/year of reject brine, it is possible to produce commercial salts worth 1.61 M$. Analysis of reject brine from NDDP, annual reject brine quality data for NDDP and indicative annual product yield from NDDP at KANUPP are presented in Tables 11, 12 and 13 respectively and by processing 1 436 000 $m^3$/year of reject brine, it is possible to produce commercial salts worth 16.33 M$.

A literature survey was conducted to find out trends regarding nil liquid discharge. There are three ways to deal with brines from desalination plants: zero liquid discharge, deep well injection and seawater discharge (Fig. 43). Among these, the first option is more environmental friendly if the components are designed in perspective of least impact on environment. All the seawater desalination technologies which are used nowadays are essential for the human civilization, unfortunately they are not environmentally friendly and produce harmful brine discharges with salt contents of about 50–60 g/l, which are thrown in the coastal areas, gradually killing the natural maritime faunae and flora and causing other serious environmental hazards. Such brines are waste products, because there is no economic use of them. On the contrary, seawater brines with salts' concentration more than 150 g/l are a valuable raw material, suitable for their processing into salts' products. However, with the existing desalination methods alone it is impossible to receive brines with such a high concentration level because of the 'calcium barrier'. The problem is that in the seawater there are large amounts of calcium salts, which simply form sediment if the concentration of the brine in the desalination plant is higher than 65 g/l.

The key element of this process is the process of calcium removal (softening) of the brines. The process is performed in a continuous manner, while one group of columns with sorbents removes calcium, the saturated sorbent from the second column group is regenerating and vice-versa. The sorbents are produced in such a manner that concentrated natrium chloride brine obtained in the result of desalination is enough for the recovery of their sorption capacity, i.e. the process does not require any chemical reagents. The brines are then passed to the thermal distillation unit, to obtain the drinking water and the highly concentrated (150 g/l TDS) tail brines. The highly concentrated brines are ready for recovery of valuable mineral by-products (such as gypsum, high purity table salt, magnesium–potassium liquid concentrates); the final process takes place in the crystallization chamber to receive dry products.

The brine will be passed through ion-exchange water softener to break the calcium barrier as much to inhibit salt deposition in the thermal concentrator. Various methods including precipitation [60] and adsorption have been used for calcium removal. Adsorption is considered an attractive one when the effective, low-cost materials are used as adsorbents.

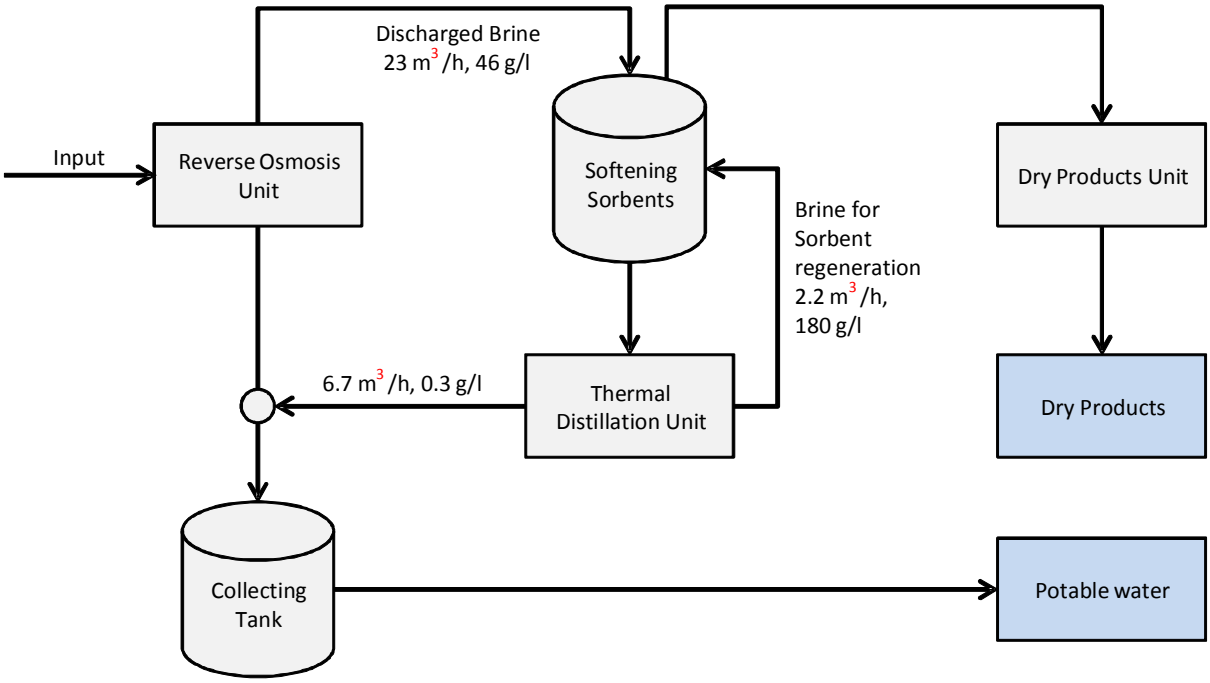


*FIG. 43. Schematic of zero discharge seawater brine recycling*

Several adsorbents, such as clay minerals [61], resins [62], and zeolite [63], have been used to remove calcium. Among these adsorbents, zeolite is recognized to be an attractive one for its high ion-exchange capacity, selectivity and compatibility with the natural environment. Zeolites are hydrated alumina–silicates (as shown in Table 14) that possess a three dimensional framework structure, which is formed by $AlO_4$ and $SiO_4$ tetrahedron connected by sharing an oxygen atom. When an $AlO_4$ tetrahedron is substituted for a $SiO_4$ tetrahedron, a negative charge appears which is neutralized by the exchangeable cations ($Na^+$, $K^+$, $Ca^+$, $Mg^{+2}$) appears [64].

TABLE 14. TYPICAL CONSTITUENTS OF ALUMINA–SILICATE ZEOLITE

| Constituents | Values ( % w/w ) |
|---|---|
| $SiO_2$ | 34 |
| $Al_2O_3$ | 28 |
| $Na_2O$ | 18 |
| Others | 20 |

The resin is selected because it is regenerated with concentrated brine or heating, thereby, no discharge of spent regeneration chemicals to environment. The initial and final metal concentrations will be determined by atomic absorption spectrophotometer. The following equation may be used to compute sorbent uptake capacity at equilibrium (*Qe*) in mg/g [65]:

$$Q_e = (C_o - C_e) \times V/w \qquad \text{Eq. (3.3)}$$

Where $C_o$ is the initial metal concentration in mg/l, $C_e$ is the final metal concentration in mg/l. Molecular sieve (sodium aluminium silicate) 0.5 nm having beads size 2 nm was found suitable for the removal of calcium from brine. Calcium removal capacity of up to 70 mg/g was recorded.

### 1.10.2. Conclusions

Nil discharge seawater brine recycling is technically feasible to reduce environmental effects of brine discharges to sea, etc. Detailed economic feasibility is required for the specific site. It may help in getting license from environmental protection agency. Molecular sieve 5 A (sodium aluminium silicate) may be used to remove calcium up to 70 mg/g. Ca selectivity of resin increases with increase in ph. Maximum calcium removal around 12.5 ph. Due to high energy requirement of thermal distillation unit, use of solar evaporation pond is proposed.

## 1.11. NEW MODELING APPROACH FOR MULTIPLE EFFECT EVAPORATION PLANTS

The CEA is the French alternative energies and atomic energy commission. It is a public body established in October 1945. A leader in research, development and innovation, the CEA mission statement has two main objectives: to become the leading technological research organization in Europe and to ensure that the nuclear deterrent remains effective in the future. The CEA is active in four main areas: low-carbon energies, defence and security, information technologies and health technologies. The CEA expressed interest in participating to the CRP. A research proposal, aiming at using CEA software tools to develop optimized nuclear desalination systems was established and submitted to the IAEA. The studies will focus on the development of optimized nuclear desalination systems producing large amounts of desalinated water while minimizing the impact on the efficiency of power conversion. The following technologically mature desalination processes will be considered for the study:

1. Multieffect evaporators (MEE);
2. Reverse osmosis (RO).

Each of these systems will be modelled using innovative techniques developed in CEA. Models will be first validated (against experimental results published in literature, or obtained through bilateral collaborations involving CEA) and then applied to optimize the energy use in the integrated power and water plants. This section discusses the modelling of multieffect evaporators. Modelling refers here to the (mathematical) representation of the transient behaviour of the process. It aims at predicting the variations of temperatures, pressures, species concentrations, mass and energy flows, in different locations throughout the desalination unit. The subject of process modelling has become increasingly important in recent years, for many reasons. The performance requirements for process plants have become increasingly difficult to satisfy. Stronger competition, tougher environmental and safety regulations and rapidly changing economic conditions have been key factors in tightening product quality specifications. A further complication is that modern plants have become more difficult to operate because of the trend toward complex and highly integrated processes. For such plants, it is difficult to prevent disturbances from propagating from one unit to other interconnected units. Models can be used for a variety of purposes including process design, control strategy definition and operation optimization. They can also be implemented in simulators and serve as a support for operator training. Process models can be derived in an analytical, semi-empirical or empirical manner.

Opting for analytical models rather than empiric or semi-empiric ones offers two important advantages:

1. They provide physical insight into process behaviour;
2. They are applicable over wide ranges of conditions.

However, they are generally expensive and time-consuming to develop. Some assumptions and simplifications should thus be introduced to ensure that the model equations can be solved. In the context of this work, an analytical approach was chosen to model MEEs. The basic mass, momentum and energy conservation principles were applied to different control

volumes around the plant. A new technique was introduced: it consists of representing process components such as pumps, tanks, heat exchangers, etc. using a network of links and well-stirred control volumes. The resulting system of ordinary differential equations (ODE) and the related algebraic equations were solved using different variants of the Euler (numerical) method. A C++ program was built based on the methods developed in the context of this work. Extendable classes, grouping components with common behaviour were implemented applying object oriented programming (OOP) techniques. The resulting optimized code was used to simulate a large number of interconnected process subsystems. This report presents the general modelling principles and the related mathematical formalism. The application of the models and their validation will be discussed later in a separate document. Paragraph 4.1.1 provides a brief review of the state of the art of MEE plant modelling. Paragraph 4.1.2 describes the new models introduced, to represent the components of a typical MEE plant, and to evaluate the thermo physical properties of different kinds of fluids. It also presents the ODE solving techniques implemented in the C++ code. Paragraph 4.1.3 concludes with a summary of the results obtained in the context of this work and an overview of the studies to be carried out in the future.

### 1.11.1. Multieffect evaporation process modelling in literature

The dynamic modelling of MEEs is a relatively recent R&D area. A quick review of the most recent papers about the subject is provided below.

In 1997, Narmine et al. developed a dynamic model for the MEE process to study the transient behaviour of the system. This model allowed the study of system start-up, shutdown, load changes and troubleshooting. Each effect of the process was represented by a number of variables related by the energy and material balance equations for the feed, product and brine flow. The equations were solved simultaneously to predict the system time dependent parameters under various transients. In 2003, El-Khatib et al. used a dynamic model of the process and the MATLAB software to develop a multi-input multi-output (MIMO) control strategy for MEE-MVC (multieffect evaporation with mechanical vapour compression). Numerical computations confirmed the interest of using proportional-integral-derivative (PID) controllers to minimize the effects of the inlet flow rate disturbances and secure a target value for the distillate. In 2005, Dardour et al. developed a software tool simulating the behaviour of horizontal tube multieffect evaporators (HT-MEE) during transient conditions, such as plant start-up and shutdowns, gradual changes in important parameters and unusual. The software was first used to simulate the steady-state and the dynamic behaviour for a couple of existing water plants. The computation results showed good agreement and accuracy compared to actual plants data. Later, in 2007, it served as a support for a study on the utilization of waste heat from GT-MHR and PBMR reactors for nuclear desalination. The new modelling approach assumes that the desalination plant components can be represented using networks of well-stirred volumes and links. Well-stirred volumes evaluate the instant temperatures, pressures and salinities in different regions. Links calculate the flows of mass and energies between different volumes. As an example, the following counter-current heat exchanger figure provides an illustration of the modelling technique (Fig. 44). The internal fluid is described by 4 (thermal hydraulic) volumes (U1 to U4) related by 3 (thermal hydraulic) links (A1 to A3). The internal heat transfer coefficient is evaluated by these links (A1 to A3). (Thermal) links (U1T1 to U4T4) calculate the amount of heat exchanged between the thermal hydraulic volumes (U1 to U4) and the masses (T1 to T4) which represent the tube structure. A similar approach is considered for the shell side.

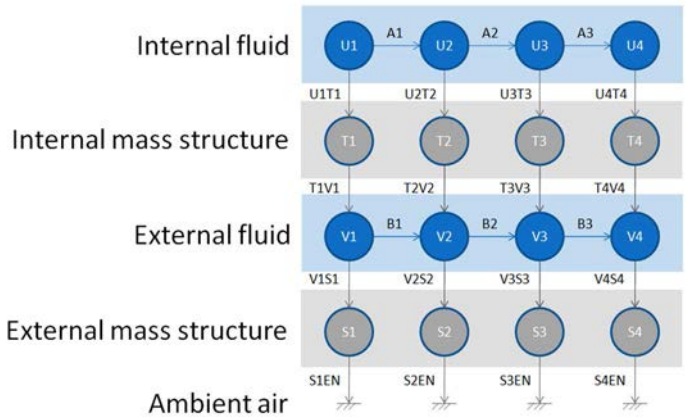


*FIG. 44. Volume-link representation of a counter current heat exchanger.*

Annex I describes the models associated to the following circuits: non-condensable gas extraction (vacuum system), seawater preheat, distilled water and brine extraction, and multieffect evaporators. The methods adopted for the evaluation of the thermo physical properties correlations of (sub-cooled and saturated) pure water, and dry air as well as the numerical techniques used for the calculation of the different well-stirred volumes are discussed in Annex I.

### 1.11.2. Conclusions

The new models introduced are associated to the following circuits: non-condensable gas extraction, seawater preheat, distilled water and brine extraction, and multieffect evaporators. They represent components like booster pumps, variable speed pumps, shell and tube heat exchangers, plate-type heat exchangers, evaporators and condensers. The thermo physical properties correlations of (sub-cooled and saturated) pure water, and dry air, are based on the engineering equation solver (EES) software built-in functions. The properties of saline water are deduced from the characteristics of pure water assuming the dissolved salts–water solution to be ideal. The physical models, the related correlations, the explicit and implicit variants of the Euler (numerical) method, were used to build a C++ code implementing an OOP approach. This program is now being used to simulate the dynamics of an existing MEE plant. The simulation results will be compared to experimental data. Once validated, the model will be enriched to include options like mechanical and thermal vapour compression, and then applied to plants operated by our partners. Many of the unitary operations used in MSF and RO plants (tanks, ducts, tees, pumps, heat exchangers, etc.) were already modelled in the context of this study. U unified modelling approach for both thermal and membrane-based desalination processes can be developed on the base of the work, extending the MEE models and validating the new modules.

## 1.12. NEW FINANCIAL MODELING FOR FEASIBILITY OF COGENERATION PROJECTS

An Excel-based financial modelling tool was used to perform net present value (NPV) calculations for cogeneration projects. Multiple case studies were conducted to demonstrate the model outputs for determining the feasibility of cogeneration projects at site-specific locations. The U.S. case study is for the northwestern coastal Florida region. Additional data was provided by IAEA CRP collaborators for a partial or complete analysis of cogeneration

options in their respective country sites; these were Indonesia, Algeria and India. The main model input parameters included:

- Overnight capital cost;
- Discount rate (financing scheme);
- Aggregate capacity of desalination operation;
- Sales of product water and electricity to premium consumers (herein referred to as "exports").

Additional parameters include: plant life, debt fraction, electricity and water plant capacities, plant load factors, construction period, annual fixed maintenance costs, decommissioning costs, and percentage share of customers by specific consumer sectors (agricultural, commercial, tourism, industrial, residential, export). All parameters can be adjusted using an Excel interface with corresponding sheets. Baseline values were used to standardize the cases, so that differences in outputs can be related to location-based factors. The chosen values reflect different sized cogeneration operations and different financing schemes. Cases were run with open-loop and closed-loop cooling configurations to show the comparison of coastal and inland scenarios. Coastal locations, which employ open loop cooling scenarios to cool the nuclear reactor, were found to be more profitable than inland closed loop cooling options. Closed loop cooling requires large amounts of makeup water, which would (wholly or partially) be provided by freshwater product from the desalination plant, resulting in a decreased amount of sellable product water to consumers. Open loop cooling scenarios were assumed for the case studies and were found to be more profitable for all analysed scenarios. This study found that profitability increases when there are low overnight costs and low discount rates on equity (below 12%). The rate of return on investment was found to be 20% greater on average for water production than for electricity production, and cases with 50% of produced water exports attained the largest region of profitability.

### 1.12.1. Cogeneration financial model description

Financial analysis tools for cogeneration projects demonstrate the feasibility and profitability of site-specific projects. Argonne's Excel-based financial model for cogeneration plants can be used to provide a quick and rough analysis of overall project profitability (i.e. financial feasibility). To demonstrate the financial tool, results of several select case studies are outlined in this report. The case study location for the US is Citrus County, Florida. Additional cases were based on information provided by CRP participants. Cases were run with baseline values and region-specific parameters. An appendix is also included which outlines the input parameters used, along with additional user reference materials. Recommendations for integrating Argonne's cost analysis methods into the IAEA's DEEP model are also outlined. DEEP is a spread sheet tool originally developed for the IAEA by General Atomics and later expanded in scope by the IAEA, in what came to be known as the DEEP-2 version. The models have been thoroughly reviewed and upgraded and a new version, DEEP-3.0, has been released. The program allows designers and decision makers to compare performance and cost estimates of various desalination and power configurations. The new version, DEEP-4.0, adds a new user interface emphasizing its user friendliness for both newcomers and experts.

In addition to carrying out a NPV cost analysis for project feasibility, the model outputs address the following questions:

— What demand conditions will result in sufficient revenue to cover the costs of operations, debt service and return on equity (ROE)?
— How can projects become more profitable?
— What discount rate (i.e. financing arrangement) is economically viable?

A NPV is the difference between the present value of the future cash flows from an investment and the amount of investment. Present value of the expected cash flows is computed by discounting them at the required rate of return. An NPV analysis will be used to compare costs and revenues of providing electricity and water to premium regional consumers. Costs and revenues have a discount rate determined at the start of operations. The NPV equation for cost calculation is:

$$\mathrm{NPV} = [\mathrm{Income}] - [\mathrm{Expenditures}] = [\mathrm{Sales\ Revenues}] - \begin{bmatrix} \{\text{Equity Share of the Capital Costs}\} + \\ \{\text{Variable Costs}\} + \{\text{Plant Decommissioning Costs}\} \\ + \{\text{Fixed Costs}\} + \{\text{Loan Payments}\} \end{bmatrix}$$

In the formula: equity share of capital costs are amounts paid to investor for construction; variable costs are maintenance and consumable costs; fixed costs are labour costs; loan payments are payments of interest and capital. If a cogeneration is profitable, the NPV is greater than zero. Model output variables include: profitability analysis, payback period analysis and cost of nuclear (per kW). Graphic outputs include: demand for electricity and water, profitability region, effects of discount rate on break even demand, effect of overnight capital cost, effect of exports and closed loop vs. open loop cooling.

### 1.12.2. Case studies for cogeneration projects

*Florida*

More than 12 000 desalination plants operate around the world today and have the capacity of producing 11 billion gallons of water each day (Fig. 45). In 2005, the U.S. contained more than 1100 facilities with the capacity of about 1.5 billion gallons per day. In 2010, almost 100% of the municipal desalination facilities in the country use reverse osmosis and other similar membrane treatment technologies. Florida, the largest U.S. producer of desalinated potable water, cannot meet its future demand for water by relying solely on the development of traditional ground and surface water sources. The state's water demand is expected to grow by greater than 25% to about 8.7 billion gallons per day by the year 2025. Florida has a growing water demand in its central and coastal regions. Central Florida currently operates more than 20 RO plants, serving approximately 730 000 people producing over 40 MGD. For an overview of the energy demands in the region, documents authored by the regional provider (Progress Energy Corporation) and site-specific proposals for nuclear energy projects have been reviewed. Location decisions were based on an assessment of site criteria, which include: land, access to water from the gulf and the electric transmission system. The Levy county site, eight miles north of the Crystal River energy complex in Citrus County, will serve as the base case for Florida due to its favourable coastal location (Fig. 46). Premium regional consumers (water exports) are located in neighbouring counties to the north and east of the Levy site. A sensitivity analysis was performed for the Florida case study to show how changes in the model affect present value (PV).

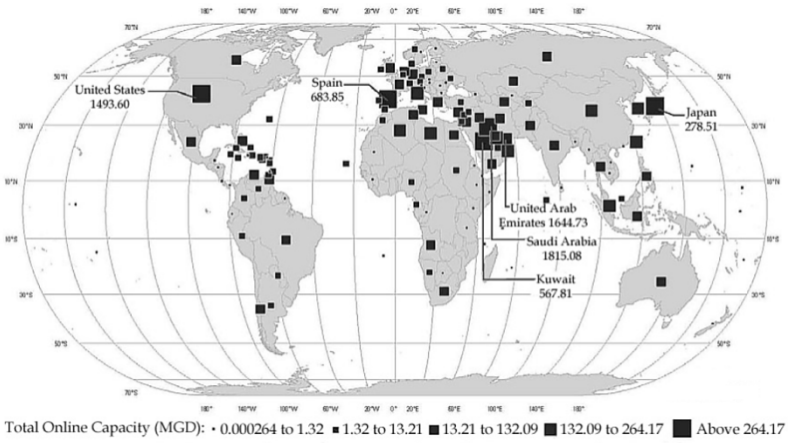


*FIG. 45. Total desalination capacity by country (adapted from GWI, 2006).*

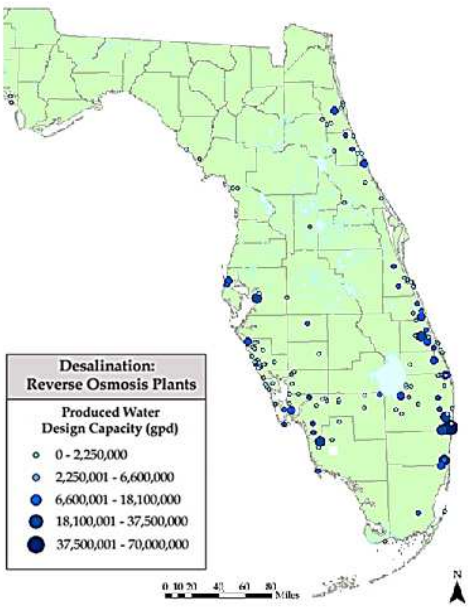


*FIG. 46. Illustrates case study area in context with operational RO desalination plants in Florida.*

A cogeneration project producing water at 100 000 m³/day was found to be profitable in the northern coastal region of Florida. Profitability is determined by both discount rate and plant-cooling configuration (i.e. open or closed cooling). An 8% discount rate was found to be profitable (Fig. 47); rates of 14% eliminated the region of profitability, while rates of 12% still maintain some profitability (Fig. 48).

The effects of discount rate on profitability are similar in all cases (lower discount rates result in profitable projects). Overnight capital costs were modelled at $2 500 000 per MW ($2500 per kW·h) and $3 500 000 ($3500 per kW·h) for all cases, while one case was run with a closed-loop cooling configuration to demonstrate the effects on profitability (Fig. 49). Exports were set at 50% for energy and water for all cases.

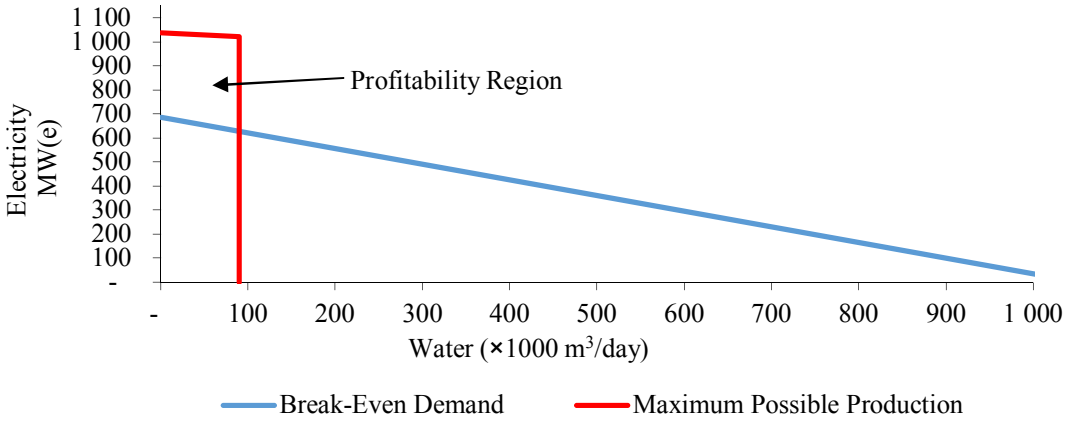


*FIG. 47. Region of profitability for an open loop, 100 000 m³/day capacity plant with an 8% discount rate.*

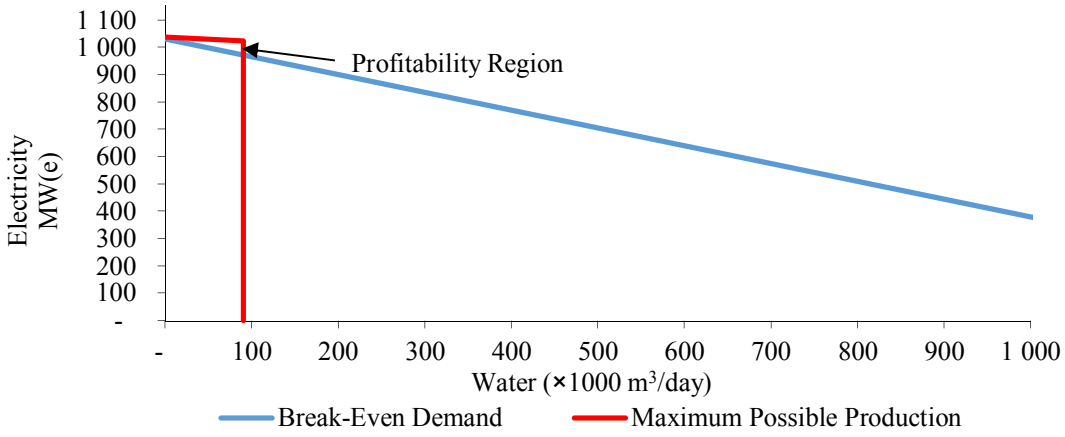


*FIG. 48. Region of profitability for an open loop 100 000 m³/day plant with a 12% discount rate, 50% exports.*

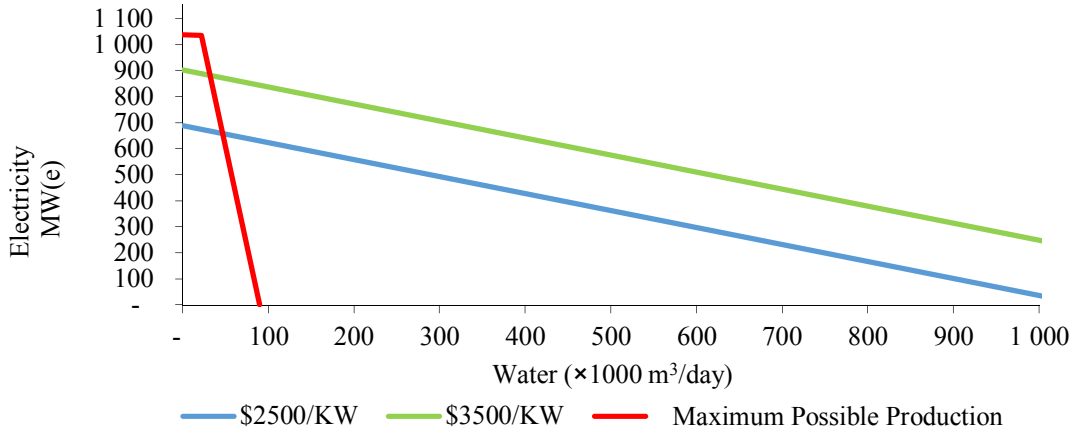


*FIG. 49. Effect of overnight cost (nuclear power plant only) scenarios on breakeven demand for a closed loop 100 000 m³/day plant, 8% discount rate, 50% exports.*

The maximum possible production (MPP) of electricity and water represents the feasible amount of product water and electricity that will be available for final consumers. All Florida cases were modelled using 1154 MW power plant capacities. For the lowest 100 000 $m^3$/day scenario, 1024 MW will be available for final electricity consumers. For the same 100 000 $m^3$/day plant, 90 000 $m^3$/day will be available for final water consumers (at the default value of 90% availability). The required demand to break even when only the desalination plant is built can be seen in Fig. 50. Figure 51 shows the required demand to break even when only the power plant is built. Investment rates are considered by multiplying NPV by capacity and dividing by constant costs (i.e. expected maintenance and decommissioning cost, variable costs, and discount rate) to provide a profitability analysis for investing in additional MW of electricity or $m^3$/day of product water. When plant capacity is increased from 100 000 to 400 000 $m^3$/day with a discount rate of 8%, the region of profitability grows (Fig. 52). For the 400 000 $m^3$/day scenario, the maximum production capacity will be 979 MW to final electricity consumers and 360 000 $m^3$/day will be available to final water consumers.

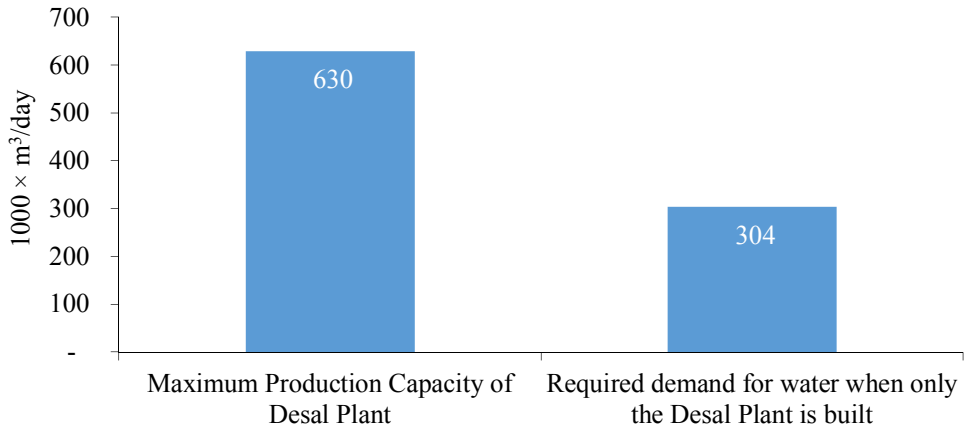


*FIG. 50. Required demand and maximum production capacity for water when only the desalination plant is built at an 8% discount rate, 100 000 $m^3$/day.*

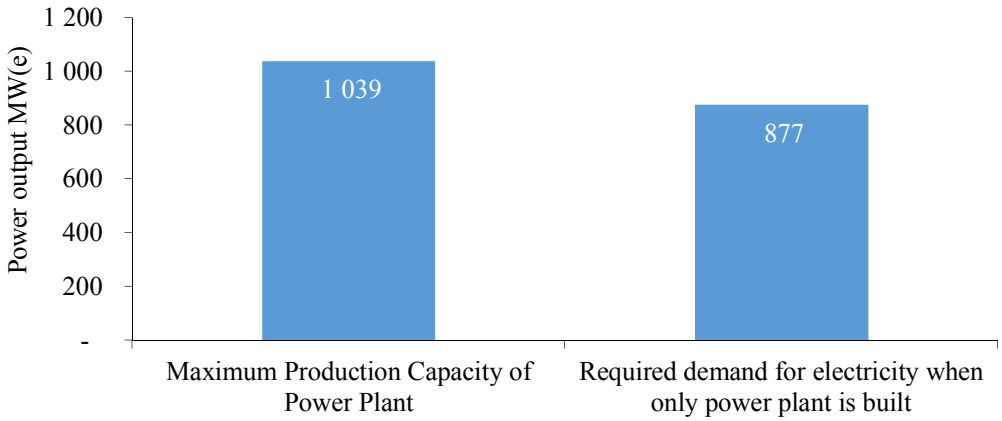


*FIG. 51. Required demand and maximum production capacity for energy when only the power plant is built at an 8% discount rate.*

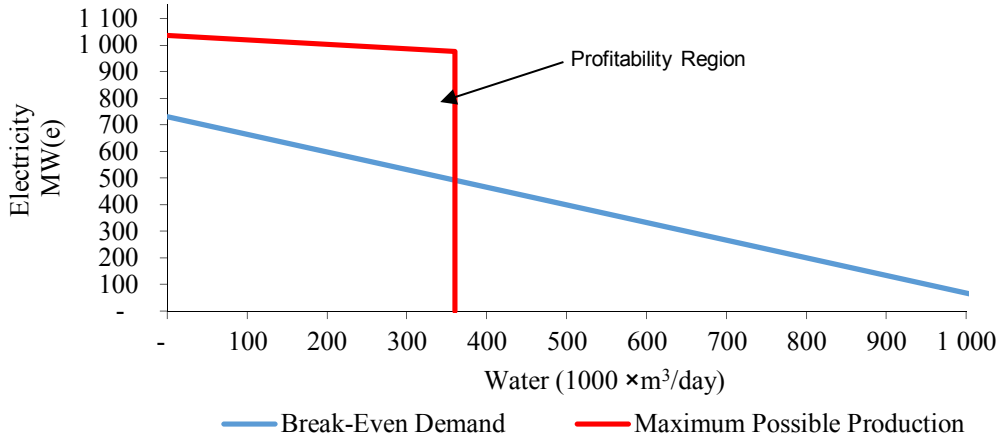


*FIG. 52. Region of profitability for an open loop 400 000 m³/day plant with an 8% discount rate.*

When configured for closed loop cooling (locating the plant inland), the plant requires makeup water (2.748 m³/MW(e)·h) for production. The region of profitability for both closed loop and open loop projects at a discount rate of 8% can be seen in Fig. 53. Geographic location is a considerable factor when trying to reduce the amount of makeup water required for cooling in order to increase profitability. When plant capacity is increased from 400 000 to 700 000 m³/day at a discount rate of 8%, the region of profitability grows again (Fig. 54). For the 700 000 $m^3$/day scenario, the maximum production capacity will be 934 MW for final electricity consumers and 630 000 $m^3$/day will be available for final water consumers. A plant with the capacity of 700 000 m³/day is only profitable with up to a 13% discount rate, above 14%, all costing scenarios are not profitable.

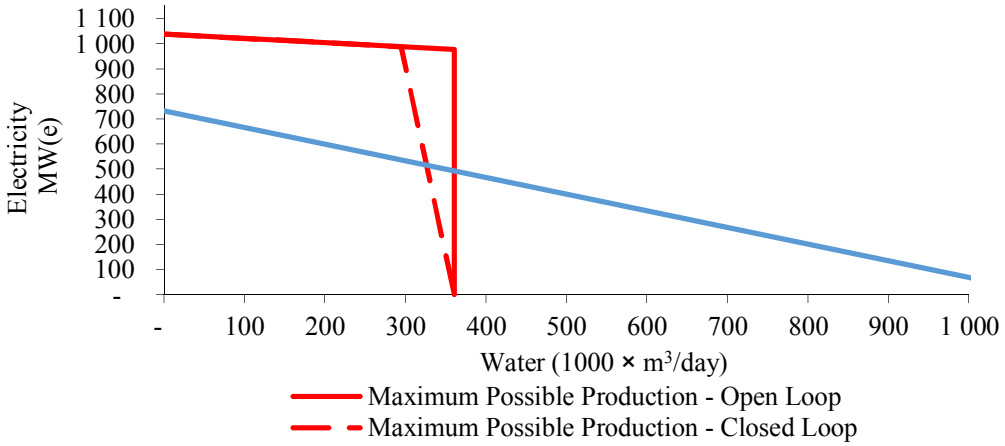


*(*) Because of the relatively low capital cost of cooling towers, the breakeven demand does not perceptibly change between closed and open-loop designs for the power plant.*

*FIG. 53. Open loop region of profitability compared to closed loop (dashed) for a 400 000 m³/day plant with an 8% discount rate. 2.748 $m^3$ of water is needed to produce 1 MW(e)·h of electricity.*

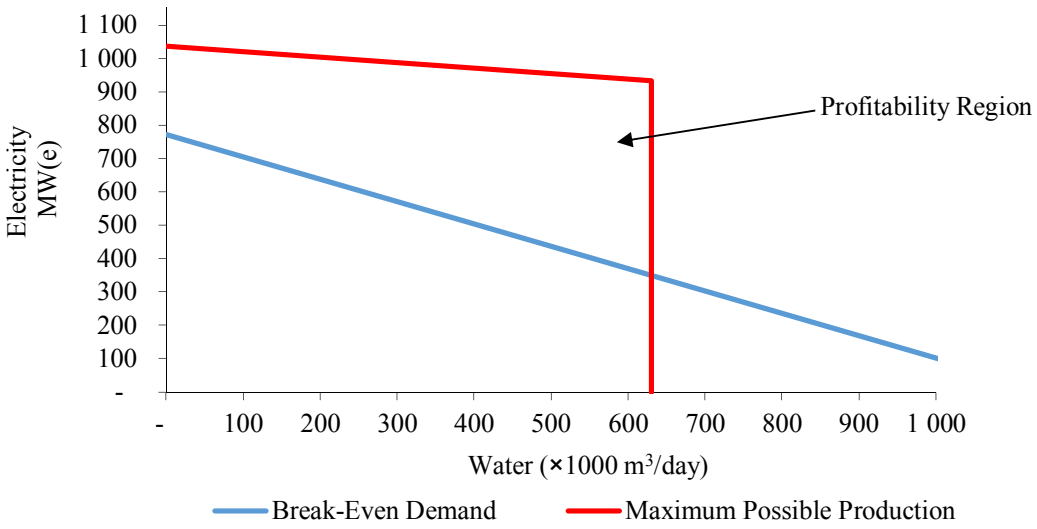


*FIG. 54. Region of profitability for open loop 700 000 m³/day plant with an 8% discount rate.*

From the baseline model input values, Table 15, the best-case scenario for Florida was a 700 000 $m^3$/day plant with 50% exports and an 8% discount rate. The worst-case scenario is 100 000 $m^3$/day with a 20% discount rate and no exports. A coastal region allows for open loop cooling, increasing the region of profitability. Table 16 shows the sensitivity analysis for various parameters and Table 17 shows the maximum production according to total capacity.

TABLE 15. BASELINE MODEL INPUT VALUES

| Water plant capacity (m³/day) | Discount rate on equity |
|---|---|
| 100 000 | 8% |
| 400 000 | 14% |
| 700 000 | 20% |

TABLE 16. SENSITIVITY ANALYSIS FOR VARIOUS PARAMETERS

| Parameters | Value | Sensitivity |
|---|---|---|
| Plant life | 40 years | Economic life of power plant |
| Discount rate | 8%, 14%, 20% | Profitable between 8 and 12% when capacity is 100 000 $m^3$/day and 400 000 m³/day. 700 000 m³/day is profitable up to 13%. |
| Construction period | 2 years | Typical value |

TABLE 17. MAXIMUM PRODUCTION ACCORDING TO CAPACITY

| | Water plant capacity | Maximum possible production* | |
|---|---|---|---|
| Capacity | 100 000 $m^3$/day | 1024 MW(e) | 90 000 $m^3$/day |
| | 400 000 $m^3$/day | 979 MW(e) | 360 000 $m^3$/day |
| | 700 000 $m^3$/day | 934 MW(e) | 630 000 $m^3$/day |
| Capital and fixed costs | | | |
| Overnight capital cost | $2 500 000 to $3 500 000 per MW(e) | Rate of returns for electricity decrease as overnight cost increases. | |

**(Outputs for sale to final consumers at 8% discount rate)*

*Indonesia*

A case study for Indonesia was conducted with a plant capacity of 1000 MW(e) and 120 000 m³/day, a discount rate of 10%, an overnight capital cost of $3 500 per kW·h and 0% exports (Fig. 55). The maximum production capacities for the nuclear power and water plants are 882 MW(e) and 108 000 m³/day, respectively. We find that an increase in the region of profitability occurs when the discount rate is reduced to 8% (Fig. 56). When the discount rate is reduced, the rate of return increases for both electricity and water.

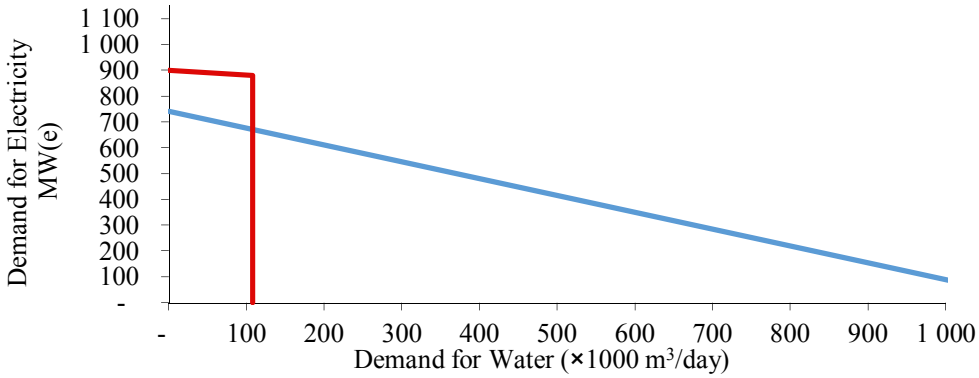


*FIG. 55. Profitability for a 1000 MW(e), 120 000 m³/day plant with a 10% discount rate and no exports.*

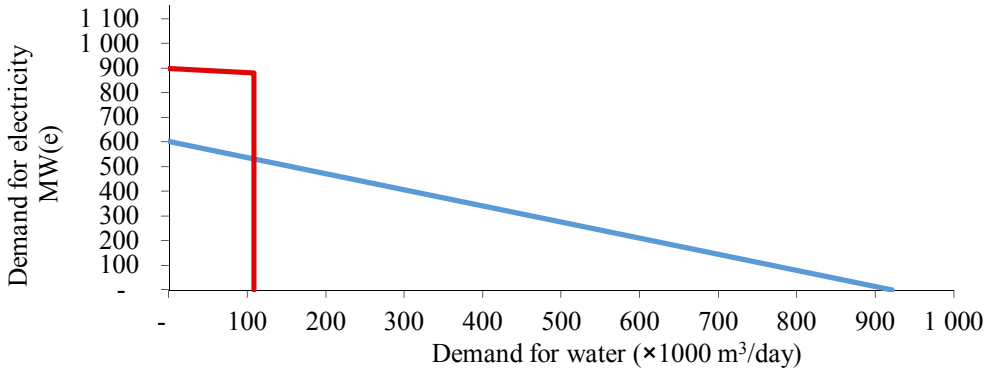


*FIG. 56. Profitability for a 1000 MW(e), 120 000 m³/day plant with an 8% discount rate and no exports.*

*Algeria*

A plant capacity of 120 000 m³/day at an 8% discount rate and 1000 MW(e) of electricity was modelled for the Algerian case study. Exports are included to compensate for some potable and industrial water needs of Skikda as outlined in the Algerian progress report. The maximum production capacity for electricity is 882 MW(e) and for water 108 000 m³/day. The region of profitability is shown in Fig. 57, with a best-case scenario being open loop cooling with 50% exports.

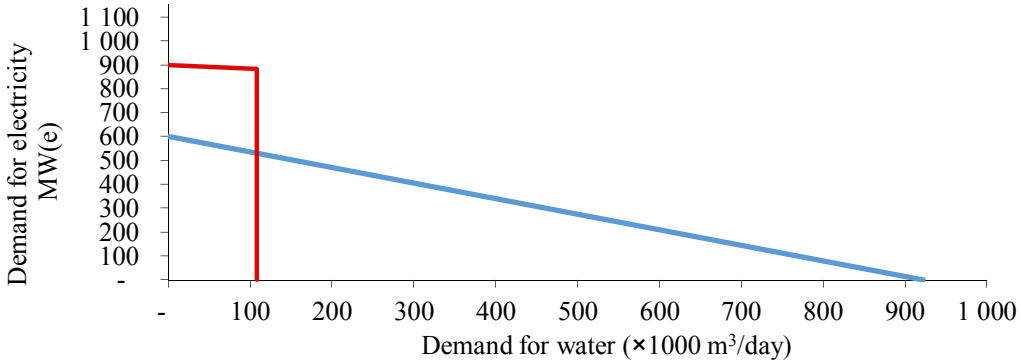


*FIG. 57. Profitability for a 1000 MW(e), 120 000 m³/day plant with an 8% discount rate.*

*India*

A nuclear plant capacity of 200 MW(e) and a water plant capacity of 6300 m³/day at a 6% discount rate were modelled for the India NDDP, Kalpakkam case study. Exports are included at 50% for premium regional consumers. When the model is running, the maximum production capacity for electricity will be 180 MW(e) and 5670 m³/day for water. With a low plant capacity the region of profitability narrows but remains positive due to the correspondingly low discount rate. For a demonstration of the difference in closed loop verses open loop cooling, profitability and MPP would decrease below breakeven demand with a closed loop configuration, while open loop maintains a region of profitability (Fig. 58).

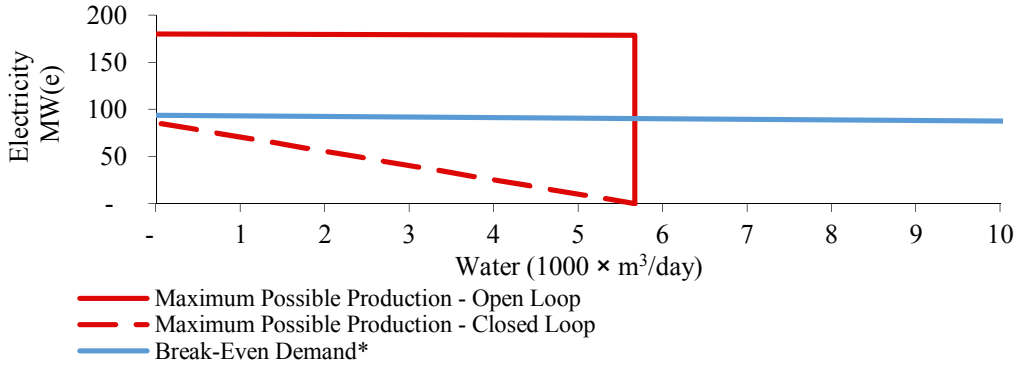


** Because of the relatively low capital cost of cooling towers, the breakeven demand does not perceptibly change between closed and open-loop designs for the power plant.*

*FIG. 58. Open and closed loop cooling with 200 MW(e) capacity at 6300 m³/day, 6% discount rate and 50% exports. 2.748 $m^3$ of water is needed to produce 1 MW(e)·h of electricity*

### 1.12.3. Conclusions

*Integration of the financial feasibility model with IAEA DEEP*
DEEP model could integrate NPV cost analysis capabilities by utilizing already existing model inputs to perform additional functions. Power law calculations can be used to provide PV outputs for the user by incorporating similar inputs to Argonne's model and the DEEP model. Similar inputs include: electricity capacity (MW(e)), water capacity ($m^3$/day), interest rate, discount rate, construction duration, plant life, decommissioning cost, annual, fixed maintenance cost/management and labour salaries. Argonne's unique inputs: overnight capital costs, fixed maintenance cost (per MW(e) and $m^3$/day), exports and customer class. Functions from the Argonne model can be added to the DEEP model for project profitability outputs and long term NPV analysis. Potential output values the DEEP model could incorporate include:

— Operating profit per unit sales;
— Operating profit per year;
— Present value of operating profits;
— Total operating cash inflow in PV;
— NPV of the project.

*Case studies conclusions*
The Excel-based financial model was used to determine long-term profitability for cogeneration project planning. The model incorporates NPV cost analysis to determine the benefits for regional premium consumers and initial investors. The case studies demonstrate several optimal cost settings for increasing the region of profitability for 'best-case' scenarios. Best-case scenario configurations include:

— Discount rates below 14%, with a best case of 8%;
— Open loop cooling systems which reduce the amount makeup water required for cooling;
— Large plant capacity for both water and electricity with a greater return on investment for water;
— Exports to regional premium consumers with a best-case scenario of 50% exports.

Worst-case scenario configurations result in reduced regions of profitability or less capacity of electricity and water for premium regional consumers. Worst-case scenario settings include:

— Discount rates above 12%;
— Closed loop cooling systems which lower the region of profitability below the break even demand point;
— Exports below 50%, with the least optimal at 0%.

Argonne's financial modelling tool and the DEEP model provide cost analysis calculations for cogeneration project planning. Best-case scenarios can help planners determine the long term success of projects. By incorporating functions from Argonne's model, the DEEP model can be expanded to perform additional NPV calculations, allowing for an even more robust analysis tool. Financial modelling for cogeneration projects is an extremely important and effective way to help determine project feasibility at early stages by providing long term cost benefit analysis for stakeholders and investors.

## 1.13. LIFE CYCLE ASSESSMENT FOR POWER AND DESALINATION PLANT IMPACTS ON CLIMATE CHANGE

The LCA is used as a tool for evaluation of potential environmental impacts of a product, process, or activity. An LCA study involves data collection and calculation to quantify relevant inputs and outputs or environmental loads of a product system. Environmental loads represent resources consumed and emissions released into the environment. One of the most significant contributors to environmental loads of most systems is energy that is essential to operate and run unit processes for the production of products and services in all industrial systems. While seawater desalination is a promising option, the technology requires a large amount of energy which is typically generated from fossil fuels. The combustion of fossil fuels emits GHG and, is implicated in climate change. In addition to environmental emissions from electricity generation for desalination, GHG are emitted in the production of chemicals and membranes for water treatment.

The Egyptian nuclear power plants authority under the coordinated research project (CRP) agreement with the IAEA developed an economic assessment tool for power and desalination plants impacts on climate change with the goal to provide decision makers with simple, soundly based, indicators of cost performance for a range of different electricity generation and water production technologies and fuels. The LCA software package for energy production system is important in order to improve environmental performance of an electricity generation system itself as well as to provide industries with a basic database required to carry out LCA studies for their own products. Building LCA software package for power production is valuable for effective environmental management of power producers as well as industrial systems that use electricity. In addition, since the power production sector is being subjected to increasingly stringent environmental regulations, establishing environmental loads data for power production is important to identify and improve its environmental aspects. Main objectives of this study were:

- Build a computer program by using the EES tool to present and analyse the life cycle greenhouse emission cost for the electricity generation and the water production chains (coal, natural gas, oil and nuclear);
- Perform sensitivity analysis for the computer program (program verification) to find the effectiveness of assumptions and to find the key factors (variables) influencing the life cycle energy use and greenhouse emissions;
- Calculate the global warming potential (GWP) per kW(e)·h of electricity production in $CO_2$ equivalents unit;
- Calculate annual GHG emissions for 1000 MW(e) power plant (coal, NG, oil, nuclear);
- Calculate the global worming potential (GWP) per $m^3$ of water production in $CO_2$ equivalents unit;
- Calculate annual GHG emissions for 200 000 $m^3$/day MED, MSF and RO desalination plants;
- Calculate the cost of the GHG for electricity generation and water production.

The results in the present study are generic, since the comparison of results presents an overview of emissions that can be usually expected. However, variations exist according to site-specific conditions (e.g. technology, carbon content of fuel, climatic conditions etc.).

### 1.13.1. Life cycle assessment methodology

LCA seeks to make general statements about the GHG emissions of a particular type of coal, oil, natural gas and nuclear life cycles stages.

For electricity generation, LCA would account for GHG emissions at the following stages:

- Energy resource exploration, extraction and processing;
- Raw materials extraction for technology and infrastructure;
- Production of infrastructure and fuels;
- Production and construction of technology;
- Transport of fuel;
- Other related transport activities (e.g. during construction, decommissioning);
- Conversion to electricity or heat or mechanical energy; and waste management and waste management infrastructure (e.g. radioactive waste depositories, ash disposal).

The rate of emission of GHG is influenced by numerous factors. Main parameters for fossil fuel power plants are:

- Fuel characteristics such as carbon content and calorific value;
- Type of mine;
- Fuel extraction practices (affecting transport requirements and methane releases);
- Transmission losses for natural gas;
- Conversion efficiency;
- Fuel mix for electricity needs associated with fuel supply and plant construction/ decommissioning.

Main parameters for nuclear power (light-water reactors) are:

1. Energy use for fuel extraction, conversion, enrichment and construction/ decommissioning;

2. Fuel enrichment by gas centrifuge, which is an less intensive energy process that can decrease GHG releases by an order of magnitude when compared to enrichment by diffusion;

3. Emissions from the enrichment step, which are highly country-specific since they depend on the local fuel mix.

Some basic features of the methodology are:

1. Covers the complete fuel life cycle chain (fuel extraction and conversion, transportation, electricity generation and waste management). All chains are described on a "cradle to grave" basis, with each step in the cycle being decomposed into construction, operation and dismantling.

2. Covers not only direct (concentrated) emissions from the life cycle, but also indirect (grey or diffuse) ones that are considered in order to provide as complete as possible representation of the total environmental fluxes;

3. Considers material inputs in connection with all steps of a fuel cycle, also construction efforts and materials for the infrastructure are included in the analysis;

4. Considers consistent set of data for material (concrete, steel) used in construction, production and decommissioning was developed to be used by all energy chains;

5. Uses electricity inputs resulting from the Egyptian generation mixes;

6. Considers only air pollutants ($CO_2$, $CH_4$, $NO_x$, $H_2S$, $NH_3$, CO, $CH_2O$, NMHCs, $SO_x$ and particulates);

7. Considers the impact of carbon dioxide emissions. A range of costs has been considered, i.e. \$50 per $CO_2$equ.·tonne.

LCA computer program uses a simplified version of the process analysis technique to perform the assessment of full energy chains. Process analysis is a microanalysis in which a complex system is divided into subsystems and well-defined process steps. Figure 59 shows the computer program flow chart.

The energy uses of some upstream fuel life cycles processes were gathered from various literature sources. Electricity production for use in upstream process was assumed to be the generation mix of Egypt. The LCA for the fuel life cycles of electricity generation (coal, natural gas, fuel oil and nuclear) are computed by using the engineering equation solver software, EES. The computer program to estimate the masses flow and the GHG emissions of the coal, natural gas, oil and nuclear fuel life cycles are listed in Annex III. The life cycle primary energy use is estimated as the sum of the energy consumed in the life cycle processes, which includes energy consumed in exploration, extraction, processing, manufacturing, decommissioning, severe accidents and disposal of all the materials associated with the power generation system. Tracing the primary sources of energy, a major GHG, namely, $CO_2$, $CH_4$, $NO_x$, and others gases $H_2S$, $NH_3$, CO, $CH_2O$, NMHCs, $SO_x$ and particulates are estimated. The different fuel life cycles analysis results are compared. Carbon Dioxide $CO_2$, Methane $CH_4$ and Nitrous Oxide $N_2O$ are the main contribution to atmospheric warming.

The specific contribution of $CH_4$ and $N_2O$ has been assessed respectively as 21 and 310 times that of $CO_2$. The GHG are classified under global warming category and the GWP per functional unit is calculated in $CO_2$ equivalents unit. Also, the climate warming rise temperature in the area centred by the power plant is calculated. Figure 60 shows the computer program input data and output results.

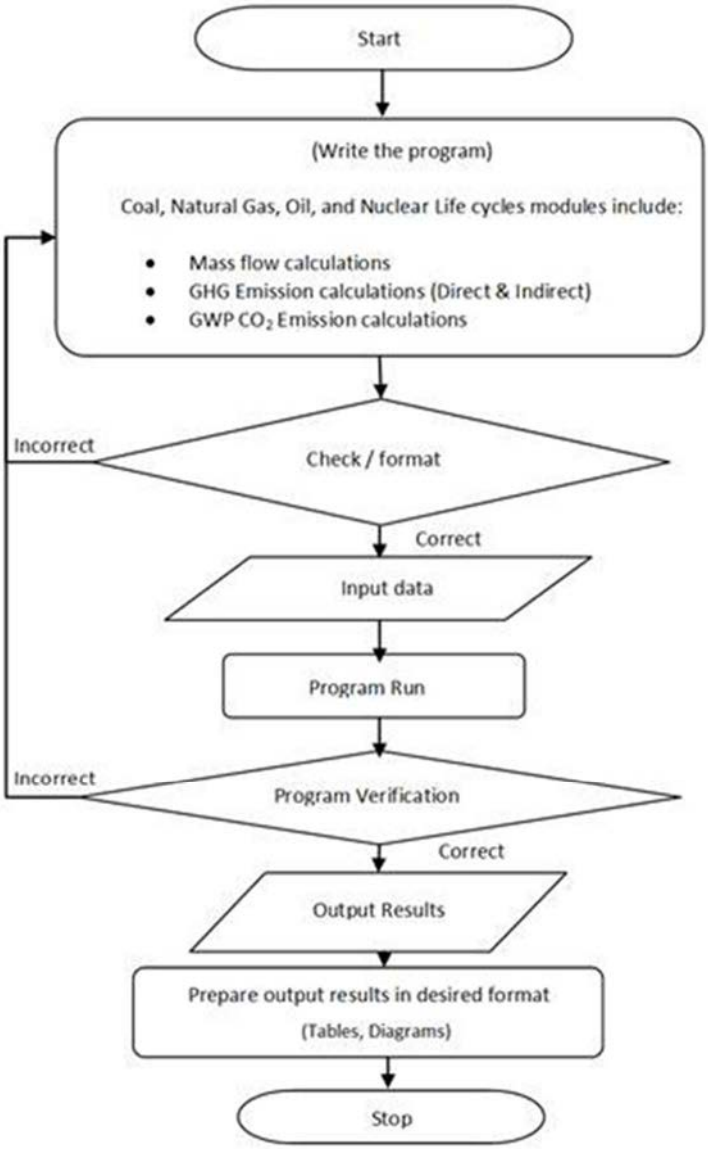


*FIG. 59. LCA computer program flow chart.*

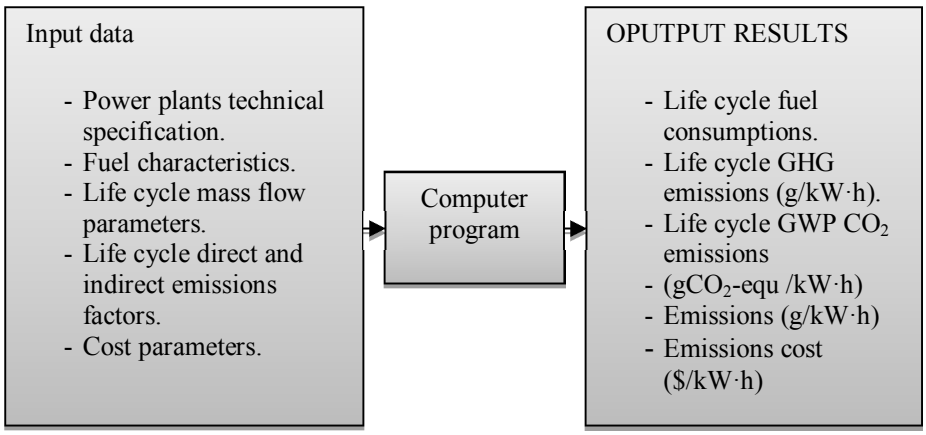


*FIG. 60. Computer program input/output.*

### 1.13.2. Life cycle chain calculations

LCA calculations for coal, natural gas, crude oil and nuclear fuel are detailed in Annex III. Figure 61 describes the general life cycle for power generation stations, including all the processes in the life cycle of the product, starting from the extraction of raw materials from nature and finishing with the delivery of electricity. The direct and indirect emissions are calculated as well as global warming potential and GHG cost estimation.

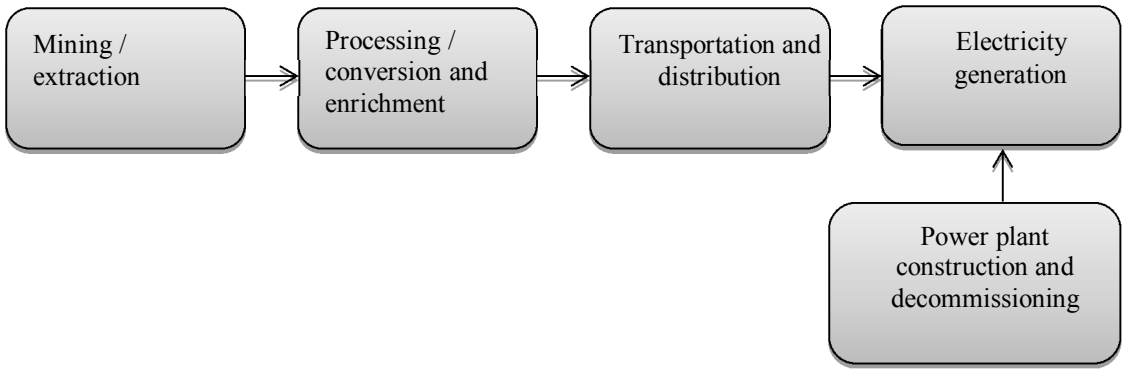


*FIG. 61. Life cycle chain of a power generation station.*

### 1.13.3. Greenhouse gas emission

While seawater desalination is a promising option, the technology requires a large amount of energy which is typically generated from fossil fuels. The combustion of fossil fuels emits GHG and, is implicated in climate change. In addition to environmental emissions from electricity generation for desalination, GHG are emitted in the production of chemicals and membranes for water treatment. European Commission Directorate General for Transport and Energy (DG TREN) reported the total GHG emissions in Europe.

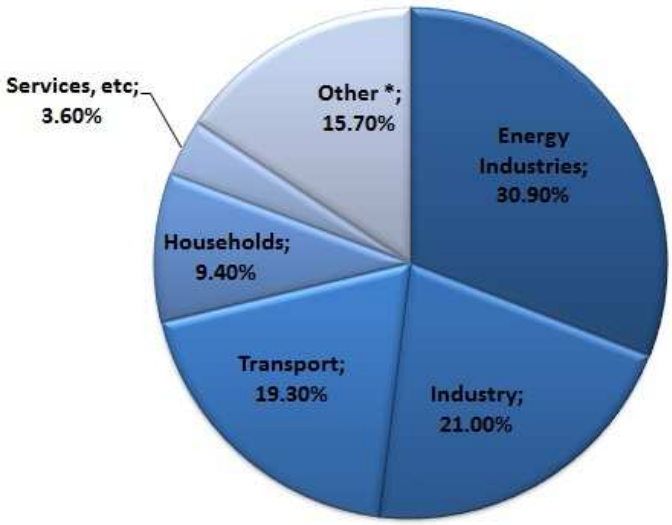


** Emissions from fuel combustion in agriculture/forestry/fisheries, Other (not elsewhere specified), fugitive emissions from fuels, solvent and other product use, agriculture, waste, other*

*FIG. 62. Greenhouse gas emissions by sector (2006).*

Emissions data is downloaded from European environment agency (EEA), which is the main provider for EU wide GHG emissions data. EEA prepares and maintains the complete EU greenhouse gas emissions inventory, which is based on data reported by Member States through the EU greenhouse gas monitoring mechanism and the UNFCCC process. Figure 62 shows GHG emissions by sector, (2006).

The change of greenhouse emission by sector in Europe country since 1990 up to 2006 is reported, we can find that the GHG emission was decreasing (Fig. 63).

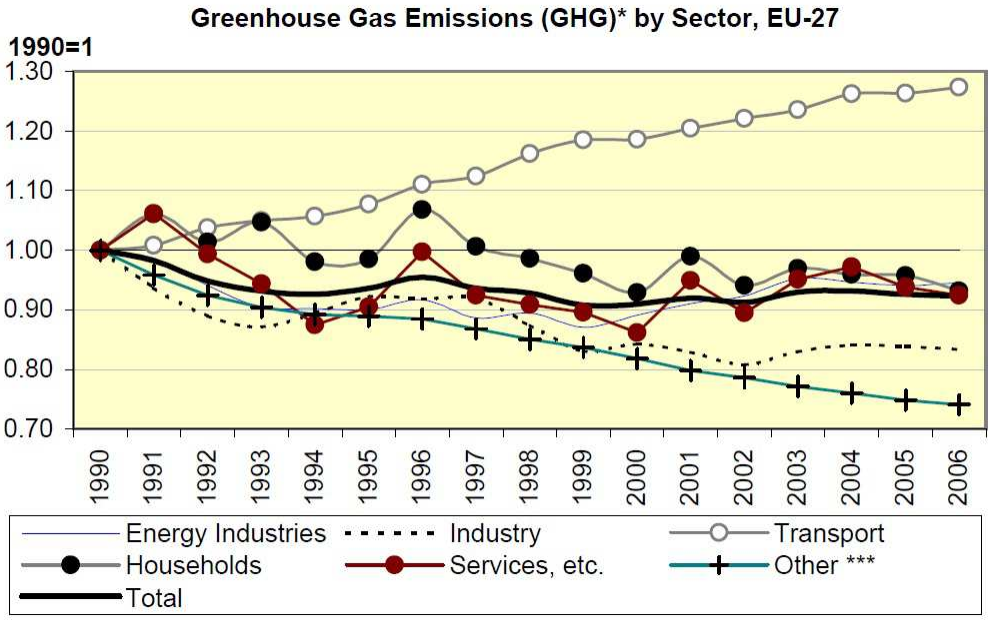


*FIG. 63. GHG emissions by sector (1990–2006).*

### 1.13.4. Sensitivity analysis

A sensitivity analysis was performed to find the effectiveness of assumptions made in this study and to find the key factors (variables) influencing the life cycle energy use and GHG emissions. To compare the magnitude of the variations, reference cases are defined as follows:

- Standalone coal power plant; coal lower heating value 22.1 MJ/kg corresponding to a plant efficiency of 35%, capacity factor of 75%, and fuel consumption 465.4 g/kW(e)·h and life time of 25 years;
- Standalone natural gas power plant; Natural gas lower heating value (LHV) 37.49 MJ/$m^3$ corresponding to a plant efficiency of 37%, capacity factor of 75%, and fuel consumption 0.2595 $m^3$/kW(e)·h and life time of 25 years;
- Standalone oil power plant; LHV 43 MJ/kg corresponding to a plant efficiency of 37%, capacity factor of 75%, and fuel consumption 226.3 g/kW(e)·h and life time of 25 years;
- PWR nuclear power plant; burn up 45 MW(e)·day/kg corresponding to a plant efficiency of 33%, capacity factor of 80%, and fuel consumption 2.806 kg/GW(e)·h and life time of 40 years;

— Combined cycle natural gas power plants; natural gas LHV 37.49 MJ/$m^3$ corresponding to a plant efficiency of 50%, capacity factor of 75%, and fuel consumption 0.2595 $m^3$/kW(e)·h and life time of 25 years;
— Combined cycle oil power plants; LHV 43 MJ/kg corresponding to a plant efficiency of 50%, capacity factor of 75%, and fuel consumption 226.3 g/kW(e)·h and life time of 25 years;
— MED desalination plant; power consumption 7.28 kW(e)·h/$m^3$ and plant availability 80%;
— MSF desalination plant; power consumption 14.45 kW(e)·h/$m^3$ and plant availability 80%;
— RO desalination plant; power consumption 2.85 kW(e)·h/$m^3$ and plant availability 80%.

*Power plant greenhouse gas emissions*

Figure 64 shows that the greenhouse emissions from coal, natural gas, oil and nuclear fuel life cycles are 1146, 693.4, 884.8 and 61.4 g$CO_2$equ./kW·h respectively. The greenhouse potential (GWP) GHG emissions for the natural gas and oil combined cycle of plant efficiency 50% are calculated to be 500 and 610 g$CO_2$equ./kW·h, respectively (emissions are the same for the combined cycle and standalone stages except the plant operation). The present study results of different fuel life cycles predicted here were compared with other studies. The comparison was listed in the Table 18. It shows that the present study results for the fossil fuel (coal, natural gas and oil) are close to the other results. There are some variations between the present study for nuclear fuel life cycle and others; this is due to different assumptions for decommissioning and enrichment processes.

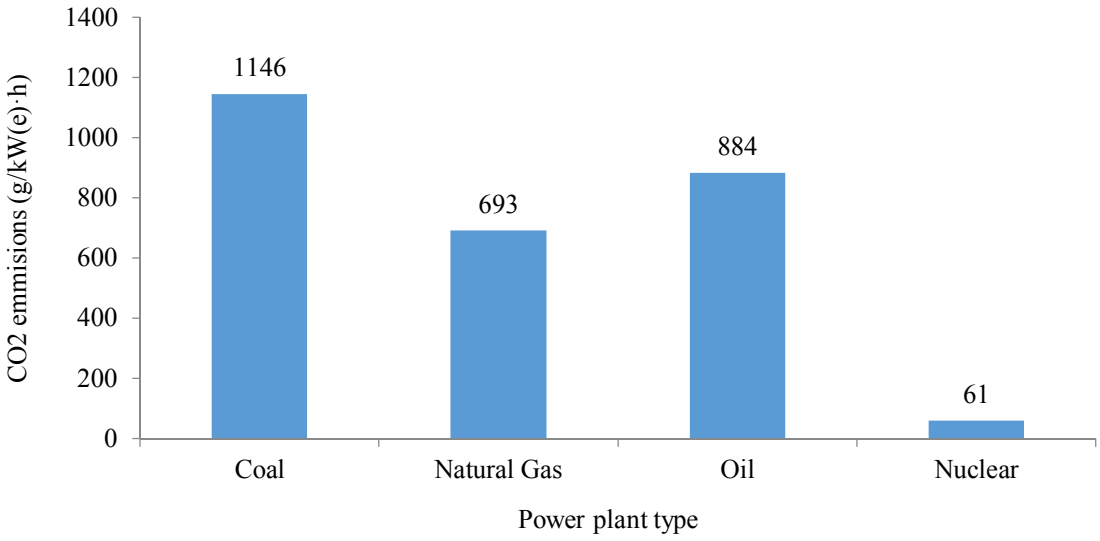


*FIG. 64. Life chain $CO_2$ equivalent emissions (g/kW(e)·h) for different power plant types.*

TABLE 18. COMPARATIVE FUEL LIFE CYCLE GREENHOUSE GAS EMISSIONS ($gCO_2equ./kW(e)\cdot h$)

| Energy source | Investigation results | | | | | | |
|---|---|---|---|---|---|---|---|
| | Present study | Pamela[19] 2000 | Paual[14] 2002 | IAEA,[38] 2006 | NREL,[20] 1999 | Vasilis[7] 2006 | Storm,[39] 2005 |
| Coal: (standalone) | 1146 | | 1041*** | 860–1290 | 1200–1300 | | |
| Natural gas: (standalone) | 693.4 | | | 460–1234 | 640 | | |
| Natural gas: (NGCC) | 500 | 499 | 470*** | | | | |
| Oil: (standalone) | 884.8 | | 875*** | 700–900 | | 932 | |
| Nuclear: | 61.4 | | | 9–30* | | 16–55* | 100** |

** Without decommissioning; ** Diffusion enrichment; *** USA average.*

*Desalination plant greenhouse gas emissions*

Figure 65 shows that the greenhouse emissions to produce 1 $m^3$ from MED plant operating in coal, natural gas, oil, combined cycle natural gas, combined cycle oil and nuclear fuel life cycles are 8687, 5230, 6708, 3790, 4624 and 465 $gCO_2equ./kW(e)\cdot h$ respectively. Figure 66 shows that the greenhouse emissions to produce 1 $m^3$ from MSF plant operating in coal, natural gas, oil, combined cycle natural gas, combined cycle oil and nuclear fuel life cycles are 16 560, 9970, 12 788, 7225, 8814 and 887 $gCO_2equ./kW(e)\cdot h$ respectively. Figure 67 shows that the greenhouse emissions to produce 1 $m^3$ from RO plant operating in coal, natural gas, oil, combined cycle natural gas, combined cycle oil and nuclear fuel life cycles are 3266, 1966, 2522, 1425, 1738 and 175 $gCO_2equ./kW(e)\cdot h$ respectively.

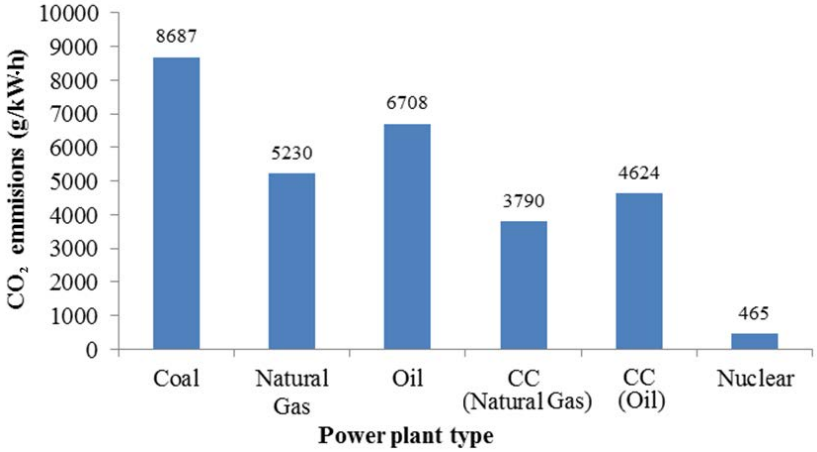


*FIG. 65. MED greenhouse gas emissions estimation.*

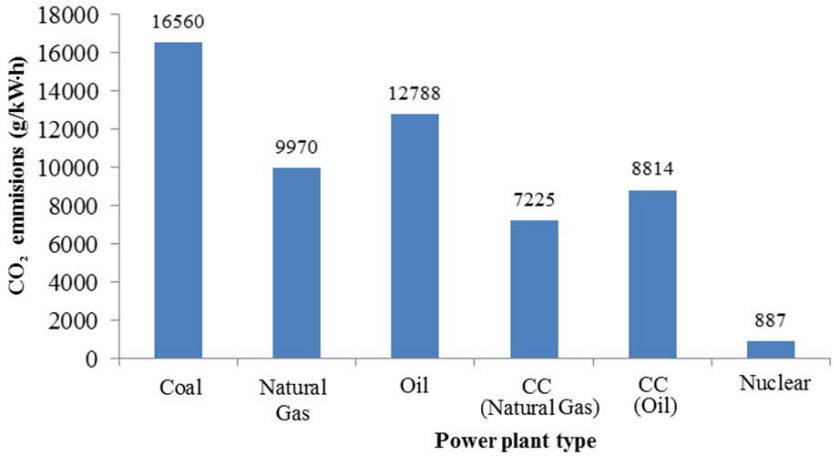


*FIG. 66. MSF greenhouse gas emissions estimation.*

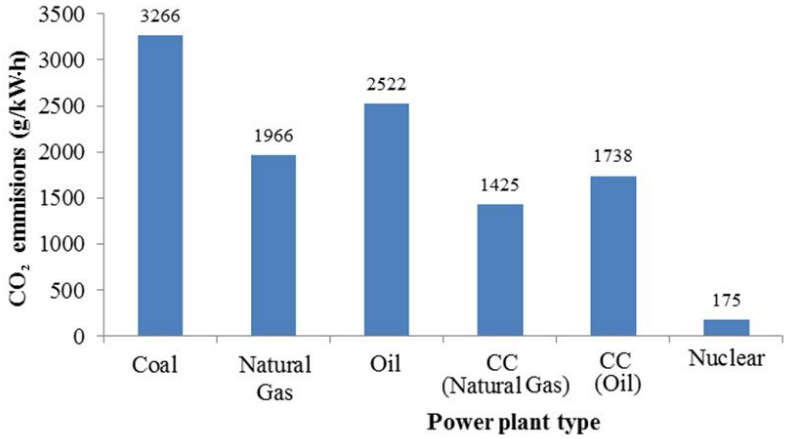


*FIG. 67. RO greenhouse gas emissions estimation.*

*Power and desalination plants greenhouse gas emissions costs*

Figure 68 shows the power and desalination plant greenhouse emissions estimated costs for different energy recourses (coal, natural gas, oil, combined cycle natural gas, combined cycle oil and nuclear).

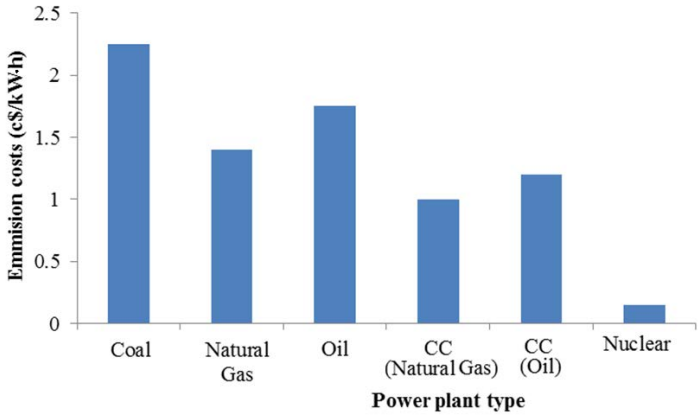


*FIG. 68. Electricity generation emission costs.*

### 1.13.5. Conclusions

There are a number of technical options that could be implemented in order to achieve the proposed reduction target. As for emissions related to electricity generation and water production, perhaps the most important factor over the near term is the improvement in efficiency of using energy at all the stages of the fuel cycle. A life cycle framework is necessary for a complete description of the sustainability of electricity generation and water production technologies. An evaluation of alternative energy technologies for their potential to decrease GHG emissions requires careful analyses of all the processes in the fuel life cycles. The LCA for the fuel life cycles of electricity generation and water production are computed by using the EES software. The computer program was developed to estimate the masses flow and the GHG emissions of the fuel life cycles. A sensitivity analysis was performed to find the effectiveness of assumptions made in this study and to find the key factors (variables) influencing the life cycle energy use and GHG emissions. The sensitivity analysis shows that the amount and the cost of the greenhouse emissions depends on power and desalination plants efficiency, capacity and availability factor, plant lifetime and fuel consumption.

## NEW MODELS FOR IAEA NUCLEAR DESALINATION TOOLS

### 1.14. DESALINATION ECONOMIC EVALUATION PROGRAM

The attractiveness of using nuclear energy for seawater desalination on large scale has led the IAEA to develop and distribute freely the DEEP. The IAEA DEEP software has been used worldwide for the economic evaluation of desalination plants coupled with various energy sources (nuclear, fossil fuelled or renewable). DEEP was originally derived from the desalination cost evaluation package developed in the eighties by General Atomics on behalf of the IAEA. The old version, named "Co-generation and desalination economic evaluation" spread sheet, (CDEE) which was used for feasibility studies related to nuclear desalination in the IAEA and other member states. Subsequently, with its increasing popularity, a user-friendly version was issued by the IAEA towards the end of 1998 under its current name of DEEP. The DEEP is a tool, which can be used for performance and cost evaluation of various power and water co-generation configurations. The new version, DEEP-4.0, adds a new user interface emphasizing its user friendliness for both newcomers and experts. DEEP software is usually used for the following:

1. Calculation of the levelized cost of electricity and desalted water as a function of quantity, site specific parameters, energy source, and desalination technology;
2. Side-by-side comparison of a large number of design alternatives on a consistent basis with common assumptions;
3. Quick identification of the lowest cost options for providing specified quantities of desalted water and/or power at a given location.

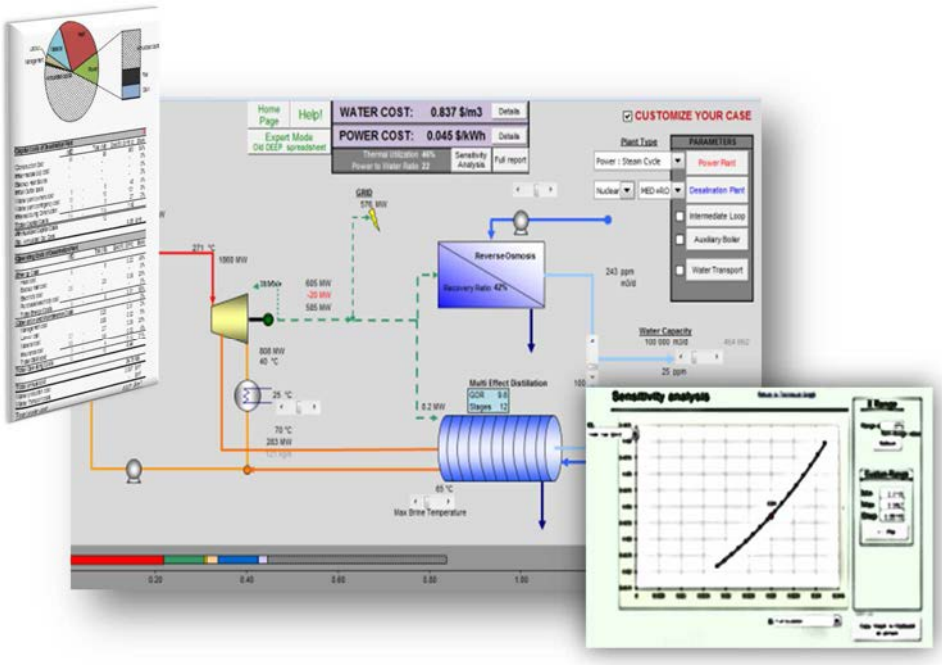


*FIG. 69. DEEP 4.0 user interface.*

Throughout the years, the software was updated constantly. Such updates included the user interface, model structure and economic models. The current version of the software, DEEP-4.0, has the following main features:

1. Development of an intuitive graphical user interface containing all the basic reference coupling schemes in a single unified template. This template includes beginner and expert mode, error checking and helpful messages that assist the user in tracing the logical errors produced by the input of erroneous values;
2. 'On-the-fly' comparison of different technologies and configurations without having to rerun the program;
3. Versatile sensitivity analysis to show the impact between important parameters and results.

The new version of DEEP is suitable for analysis among different plant types (steam, gas, combined cycle and heat only plants), different fuels (nuclear, oil, coal) and various desalination options including MED, MSF, RO and hybrid options. It also includes formulation of different alternatives such as different turbines configurations, backup heat, intermediate loop, water transport costs and carbon tax.

## 1.15. NEW ROBUST THERMODYNAMIC MODULES FOR DEEP

The Syrian Atomic Energy Commission (AECS) joined the CRP to focus on the modification of DEEP software and the development a precise model that estimates the performance and evaluates the economics of the MED/TVC system. Additionally the development of a module in DEEP for desalination with solar energy is investigated. The work plan includes the following tasks:

- Thermodynamic analysis of MED and calculation of GOR;
- Thermodynamic analysis of the TVC is preformed along with the TVC/MEE design, which include the thermodynamic analysis of the evaporator (effects) and the steam jet ejector. This also will include the calculation of gain output ratio;
- Thermodynamic analysis of the MED/MVC and calculation of GOR;
- Programming the modules for MED with both TVC and MVC cases;
- Comparative analysis of the GOR for MED, MED/TVC and MED/MVC including power consumptions;
- Investigation of *s*olar collector and solar cells to be used as power source for desalination and comparison with the nuclear were made.

### 1.15.1. MED vapour compression thermodynamic models

*Multieffect distillation and GOR calculations in DEEP*

MED plant consists of a series of evaporator (effects) with each subsequent effect operated at a lower pressure (Fig. 70). This permits the feed seawater to undergo multiple boiling without supplying additional heat after the first effect.

In MED plants, the seawater enters the first effect and is heated to the boiling point after being preheated in tubes. Seawater is either sprayed or otherwise distributed onto the surface

of evaporator tubes in a thin film to promote rapid boiling and evaporation. The tubes are heated by steam from a boiler, or other source, which is condensed on the inside of the tubes. The condensate is recycled to the boiler for reuse. Only a portion of the seawater applied to the tubes in the first effect is evaporated. The remaining feedwater is fed to the second effect, where it is again applied to a tube bundle. In turn, these tubes are heated by the vapours generated in the first effect. This vapour is condensed to form the product water, while giving up heat to evaporate a portion of the remaining seawater feed in the next effect. This continues for several effects, with up 20 effects being found in a typical large plant. The main parameter defines this process is gain output ratio:

$$GOR = \frac{M_d}{M_h} \qquad \text{Eq. (5.1)}$$

Where, $M_d$: distillate flow rate, and $M_h$: steam flow rate.

In order to validate DEEP calculations a detailed model for the GOR was developed as a Macro and compared to the DEEP models. Both models and results of comparison are included in Annex IV.

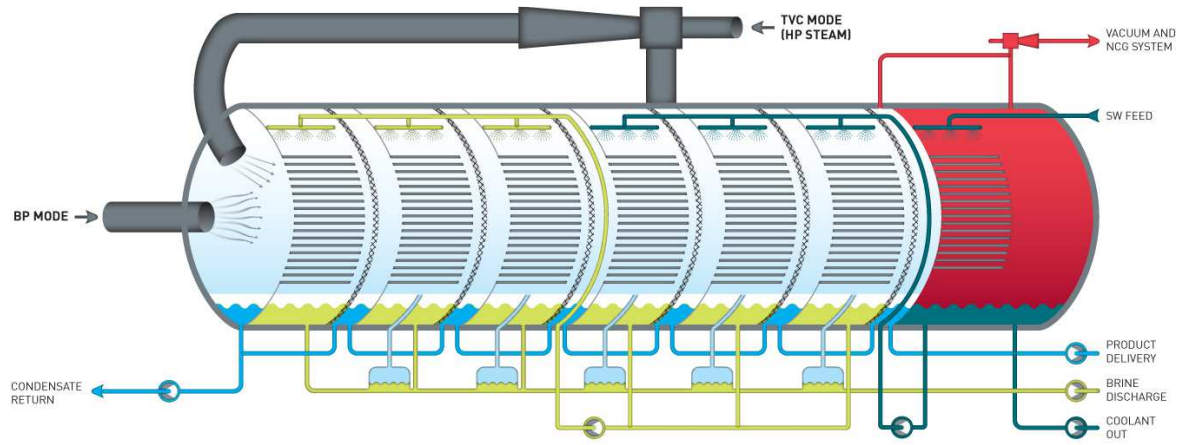


*FIG. 70. MED plant.*

*MED/TVC model*

MED/TVC desalination technology utilizes a steam-jet compressor as the heat pump. Steam-jet compressors use motive steam at pressures ranging between 0.3 to 1.0 MPa. Total efficiency of the steam-jet equation is:

$$\eta = \frac{Total\ energy\ output}{Total\ energy\ input} \qquad \text{Eq. (5.2)}$$

Where:

The total energy output = kinetic energy + pressure energy + flow energy

The total energy input = entrained vapour energy + motive steam energy

Therefore the total efficiency is found to be:

$$\eta = \frac{\frac{1}{2}(m_m + m_1) \times v_2^2 + m_1 \times \frac{R \times T_m}{M_w} + m_m \times \frac{R \times T_m}{M_w} + m_1 \left(\frac{\gamma}{\gamma - 1}\right)\left[\left(\frac{P_2}{P_1}\right)^{\frac{\gamma-1}{\gamma}} - 1\right] + m_m \left(\frac{\gamma}{\gamma - 1}\right) \times \frac{R \times T_m}{M_w}\left[\left(\frac{P_2}{P_m}\right)^{\frac{\gamma-1}{\gamma}} - 1\right]}{\frac{1}{2}m_1 \times v_1^2 + \frac{1}{2}m_m \times v_m^2 + m_1 \times \frac{R \times T_1}{M_w} + m_m \times \frac{R \times T_m}{M_w}}$$

Eq. (5.3)

Where: $P_2$ is the outlet pressure, $P_1$ is the inlet pressure, $P_m$ is the inlet pressure of motive steam, $v_1$ and $v_2$ are the inlet and outlet velocity of propelled stream, respectfully, $v_m$ is the inlet velocity of motive stream, $m_1$ is the inlet mass flow rate of propelled stream, $m_m$ is the inlet mass flow rate of motive stream, $T_1$ is the temperature of propelled stream, $T_m$ is the temperature of motive stream and $\gamma$ is the gas adiabatic factor. Gain output ratio for TVC/MED is defined as:

$$GOR = MD \times 2330/Q_{th} \qquad \text{Eq. (5.4)}$$

Figure 71 represents the user interface for the proposed TVC module in DEEP.

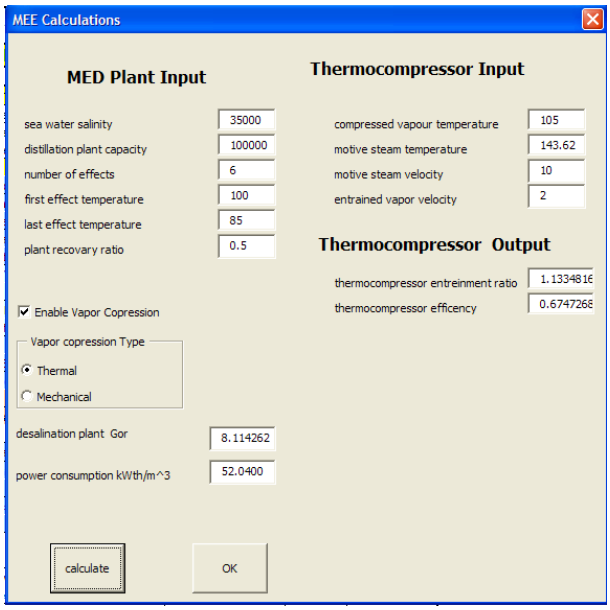


*FIG. 71. The TVC panel.*

*MED/MVC model*

The energy and material balances of system (energy, water and salts) are done in the same manner of the MED and compressor work analysis is added to the MED in order to understand the system. To calculate the compressor work, first the compressor ideal work ($a$) is given:

$$\alpha = \frac{\chi}{\chi - 1} \times (P_d \times v_d - P_v \times v_v) \qquad \text{Eq. (5.5)}$$

Where: $\chi = 1.327$, $P_d$ is the pressure at the compressor outlet, $v_d$ is the specific volume of the steam at the compressor outlet, $P_v$ is the pressure at the compressor inlet, $v_v$ is the specific volume of the steam at the compressor inlet. Then the real work $W$ is calculated from the following equation:

$$W = \frac{a}{\eta} \qquad \text{Eq. (5.6)}$$

Where $\eta$ is the compressor adiabatic efficiency. To estimate the plant GOR, the mechanical work must be converted to thermal value by multiplying it by the electric power conversion coefficient, where its value is usually taken as 3, and then we have the thermal power required

$$Q_{Th} = 3 \times w \times M_d \qquad \text{Eq. (5.7)}$$

and

$$GOR = \frac{M_d \times 2330}{Q_{th}} \qquad \text{Eq. (5.8)}$$

Where $M_d$ is the amount of produced water. Figure 72 represents the user interface for the proposed MVC module in DEEP.

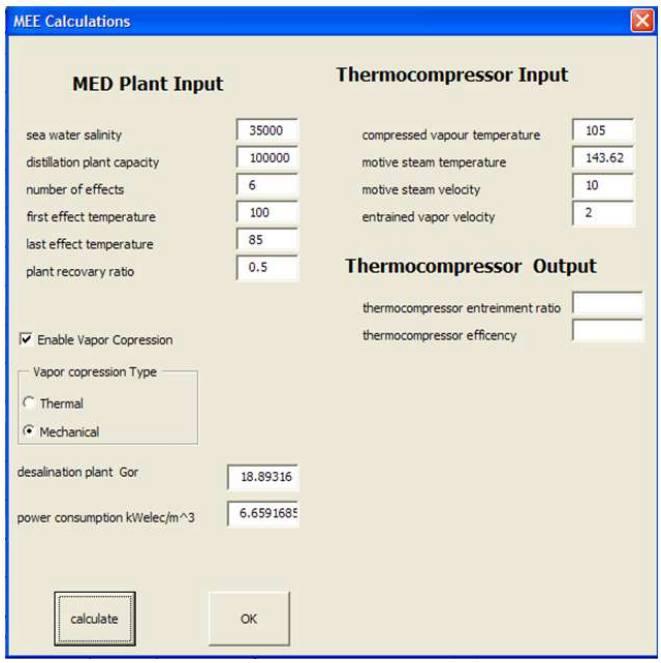


*FIG. 72. The MVC panel.*

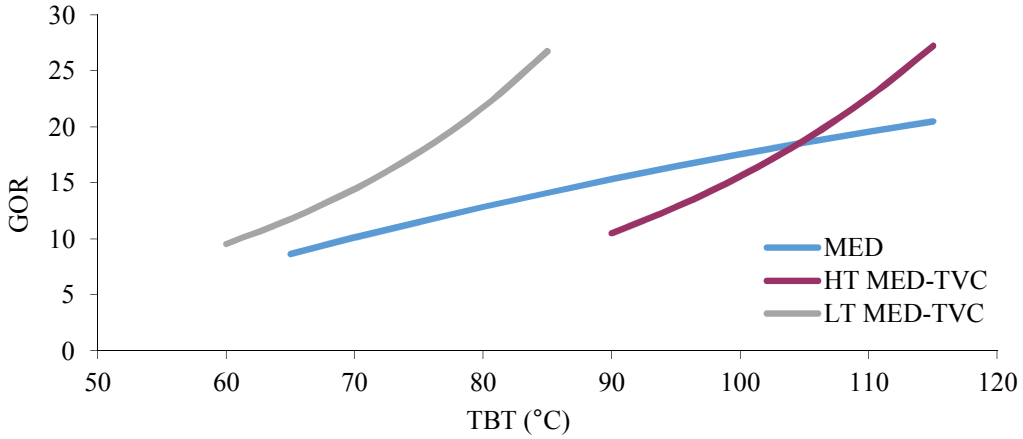


*FIG. 73. The comparison of GOR for MED, TVC and MVC.*

Comparison of the value GOR for MED, TVC and MVC against the TBT were done as shown in Fig. 73 above. And the same were done for the power consumption as in Fig. 74.

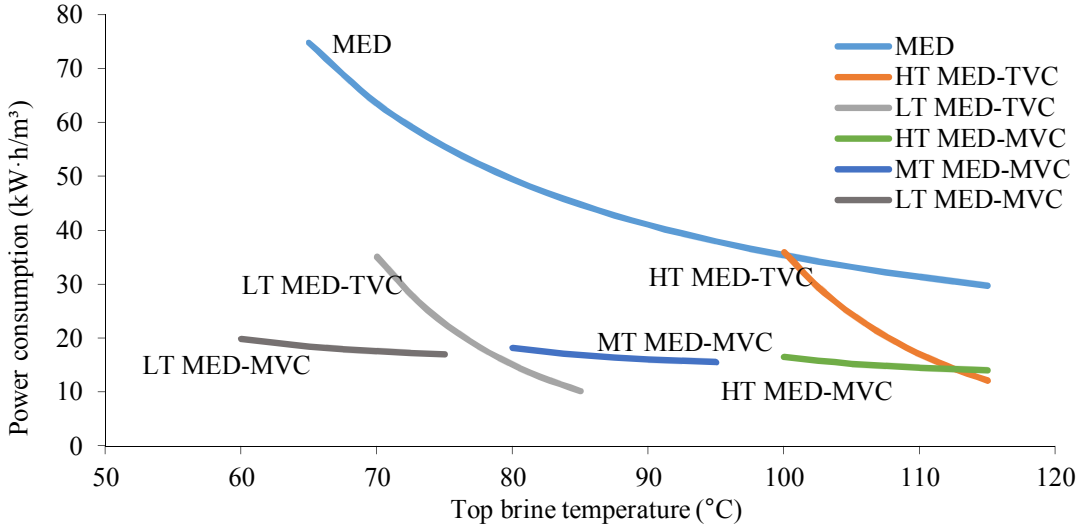


*FIG. 74. Power consumption vs. top brine temperature for MED, TVC and MVC.*

Nuclear energy has a lower power cost per kW than Solar PV cells and even Solar thermal collectors in general, if even by a small margin, as can be seen in Fig. 75. That cost is reflected on the water cost to cool down the reactor, cheaper for nuclear energy as can be seen in Figs. 76 and 77.

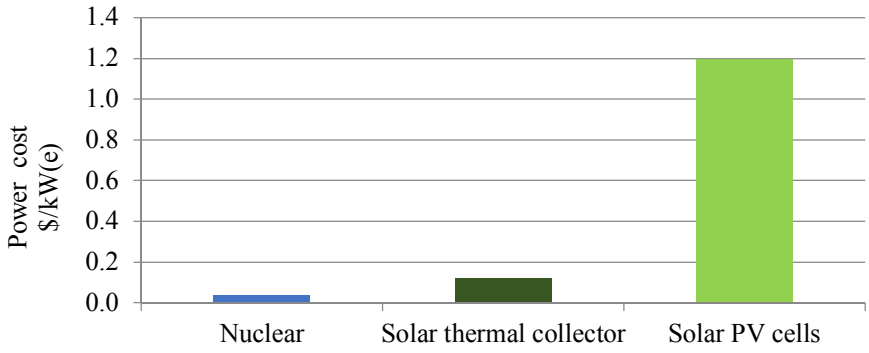


*FIG. 75. Power cost of nuclear, solar thermal collector and solar PV cells (in $/kW(e)).*

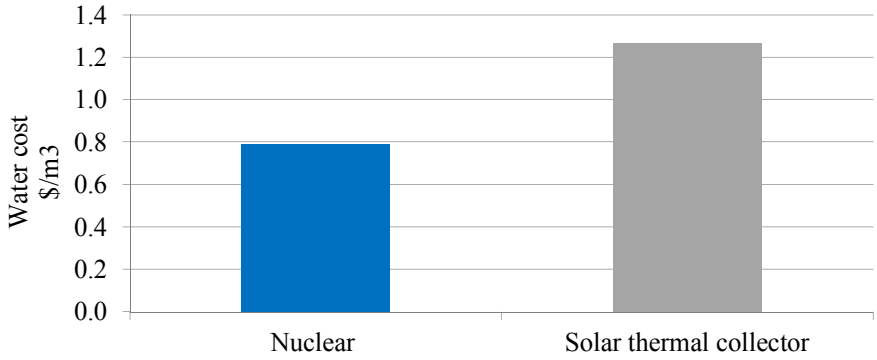


*FIG. 76. Water cost ($/m$^3$) for MED plant with nuclear power or thermal solar panels as energy source.*

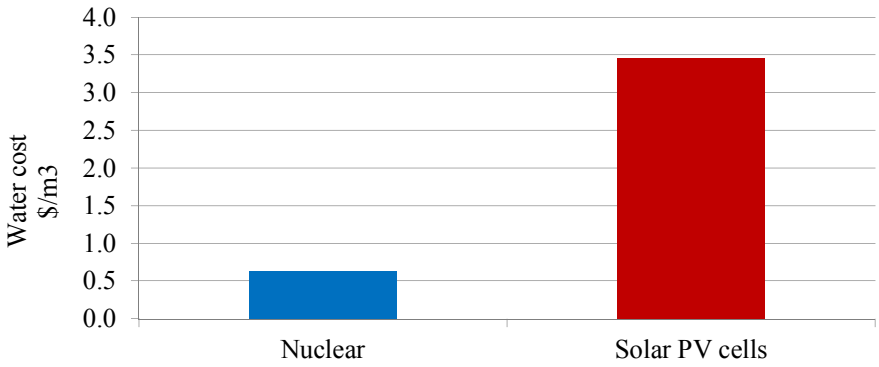


*FIG. 77. Water cost ($/m$^3$) for RO plant with nuclear power or photovoltaic panels as energy source.*

### 1.15.2. New module for water desalination with solar power as energy source

A new module for desalination with solar thermal power was developed for DEEP. Screen caps of the user interface are shown in Annex IV. The solar heating system consists of solar collector, heat exchanger, water tank and a circulation pump. The active area of the solar collector is considered as the main factor and can be calculated as follows:

$$A = \frac{Q}{\eta \times G} \qquad \text{Eq. (5.9)}$$

Where: $\eta$ is the output ratio of the collector, and $Q$ is the required thermal power to heat up the feedwater. It is given in the following equation:

$$Q = M \times C \times \Delta T \qquad \text{Eq. (5.10)}$$

Where $M$ is the mass flow rate of the water [kg/s], $C$ is the heat capacity of the water and, $\Delta T$ is the water temperature difference. $G$ is the solar intensity received by a horizontal surface and it is in general defined by the sum of the direct, diffused solar radiation and the solar radiation reflected from the ground.

$$G = G_{b,t} + G_{d,t} + G_{gr,t} \qquad \text{Eq. (5.11)}$$

Where $G_{b,t}$ is the direct solar intensity on the slope surface and it is given in equation, below:

$$G_{b,t} = r_b \times G_b \qquad \text{Eq. (5.12)}$$

Where $r_b$ is a constant related to the angle of the falling solar radiation on the surface, and $G_b$ is the vertical solar intensity on horizontal surface. Furthermore $G_{d,t}$ is the diffusion solar intensity on the slope surface and it is given in the equation:

$$G_{d,t} = G_d \times \cos^2\left(\frac{S}{2}\right) \qquad \text{Eq. (5.13)}$$

Where $S$ is the angle of the surface slope and $G_d$ is the vertical diffusion solar intensity on horizontal surface. $G_{gr,t}$ is the solar radiation reflected from the ground and it is calculated as follows:

$$G_{gr,t} = \rho_{gr} \times G \times \sin^2\left(\frac{S}{2}\right) \qquad \text{Eq. (5.14)}$$

Where $\rho_{gr}$ is the ground reflection constant.

The above methodology was programmed and case studies were run for different solar panel providers, either solar thermal and photovoltaic panels, as shown in Annex IV. The specific solar heating system cost \$0.047 /kW(th) for capacity of MED plant 100 000 $m^3$/day.

### 1.15.3. Conclusion

As it is well known that the thermal desalination is more important because in general nuclear power plants have waste heat coming out of the steam turbine therefore thermal desalination can make use of this waste heat. This work has shown that the thermal desalination processes vary one to the other. The thermal vapour compression with multieffect distillation can compete with all the other thermal desalination type, MED/TVC reduces water cost sometimes to 60%. Because of limited capacity of solar units, the capital costs and operating costs are not as well established as for the other processes. For solar stills, the cost of water production is high due to the low productivity of these stills. However, this type of desalination is only used in remote areas where there is no access to conventional energy resources.

# TECHNO–ECONOMIC FEASIBILITY STUDY OF NUCLEAR DESALINATION: ALGERIA CASE STUDY

It is anticipated that by 2025, 33% of the world population, or more than 1.8 billion people, will live in countries or regions without adequate supplies of water unless new desalination plants become operational. In many areas, the rate of water usage already exceeds the rate of replenishment. Nuclear reactors have already been used for desalination on relatively small-scale projects. In total, more than 150 reactor-years of operating experience with nuclear desalination has been accumulated worldwide. Eight nuclear reactors coupled to desalination projects are currently in operation in Japan. India commissioned the ND demonstration project in the year 2008 and the plant has been in continuous operation supplying demineralised (DM) quality water to the nuclear power plant and potable quality to the reservoir. Pakistan has launched a similar project in 2010. However, the great majority of the more than 7500 desalination plants in operation worldwide today use fossil fuels with the attendant emission of carbon dioxide and other GHG. Increasing the use of fossil fuels for energy-intensive processes such as large-scale desalination plants is not a sustainable long-term option in view of the associated environmental impacts. Thus, the main energy sources for future desalination are nuclear power reactors and renewable energy sources such as solar, hydro, or wind, but only nuclear reactors are capable of delivering the copious quantities of energy required for large-scale desalination projects. Algeria is participating in an IAEA's CRP in the subject related to "New technologies for seawater desalination using nuclear energy'' with a project entitled "Optimization of coupling nuclear reactors and desalination systems for an Algerian site Skikda". This project is a contribution to the IAEA CRP to enrich the economic data corresponding to the choice of technical and economical options for coupling nuclear reactors and desalination systems for specific sites in the Mediterranean region.

## 1.16. BACKGROUND

Algeria, situated in the centre of North Africa, has a strongly growing population, with 36 275 358 inhabitants in 2011. The geographic location of Algeria signifies that it is in a position to play an important strategic role in the implementation of renewable energy technology in the north of Africa. The climate is transitional between maritime (north) and semi-arid to arid (middle and south). The mean annual precipitation varies from 500 mm (in the north) to 150 mm (in the south). The average annual temperature is around 12°C. Algeria has for decades relied on rainfall for the water policy and strategy, but that proved to be not an adequate solution considering the actual water deficit. The water needs for different sectors is increasing and this will worsen since it is projected that population will double in the next 20 years. During the last two decades, the problem of water became a major concern in Algeria what required an important commitment of the authorities for its solution. With the overall water potentialities estimated at 17 billion $m^3$/year in 2006, that is to say 600 $m^3$/inhabitant/year, the situation of the country's water resources worsened and placed the country among those which live a water shortage.

This water shortage is due to several worsening factors: long periods of dryness, disparities between the urban and rural zones, an increase in population, an unequal distribution of water resources, an increase in pollution, and modifications of the physical environment. These factors destabilized the already precarious balance of the environment. The north of the country, where the three quarters of the population reside, has 12 billion $m^3$/year estimated

water resources, mainly surface waters. These resources are very limited compared to the high demand expressed by the population in this area. The use of non-conventional solutions, mainly sea/brackish water desalination, becomes imperative and inevitable solution to supply fresh water. Since Algeria has a coastal band of 1200 km, seawater desalination is considered to be a viable and a very advantageous solution, which can safely assure the water needs of the population despite the climatic variations. Taking into account the existing water resources and the total water demand, the Algerian Government adopted a strategy to implement a non-conventional water programme to face the various needs (domestic, agriculture and industry) in the future. This programme is translated by the installation of 13 seawater desalination units with a total capacity of 2.3 million $m^3$/day. This capacity will reach 2.5 million $m^3$/day in 2016.

Consequently, the seawater desalination will become in the next years an expanding industry. As this virtually unlimited water resource consumes a huge amount of energy, and because the power in Algeria is derived from fossil origin source, a diversification of energy sources is foreseen for the future, It should be noted that the primary energy sources, oil and natural gas, upon which the country is relying to meet its energy and electricity needs are non-renewable and expected to be depleted in a few decades. Further, the use of fossil fuel for seawater desalination does not seem to be cost effective. For this purpose, nuclear power and renewable energies are two alternatives that are considered in the government energy policy to increase the electricity production nationwide. As an indication, in 2008 the electricity consumption per capita was about 850 kW·h which is well below the world average consumption is equivalent to 2250 kW·h. In Algeria, the installed capacity in 2010 is 11 332 MW and 10 320 MW in the interconnected system. During the last decade, growth in consumption was almost stable around an average annual rate of 5.6%. As the needs for fresh water and electricity increase rapidly in Algeria, the Algerian authorities considered the feasibility of nuclear desalination as a source of low cost potable water. Therefore, the Algerian Government plans to carry out a comprehensive study to assess the potential use of nuclear energy for producing electricity and desalinated water.

## 1.17. SITE SELECTION

The potential site planned to host the nuclear seawater desalination unit is located in the town of Skikda, 510 km east of Algiers (Fig. 78).


*FIG. 78. Potential site location.*

This site is situated near the industrial zone of Skikda City, where all facilities (electric mains network, potable water supply, access roads to the chosen site) are available and suitable for safe and reliable operation of a nuclear desalination unit.

The climate of the site concerned by this study is of the Mediterranean type. The Skikda region, hosting the potential site of nuclear desalination plant, is among the rainiest in Algeria. Heavy rains with an average total annual fall of 830 mm/year are recorded in winter. The number of rainy days is 112 and the humidity is 70%. Usually the main directions of winds at the Skikda region are north-northwest. These winds frequently blow in winter and are sometimes violent. Table 19 illustrated the values of the main climatic parameters recorded in the region for the period 1993–1999.

TABLE 19. MAIN CLIMATIC PARAMETERS OF SKIKDA CITY FROM 1993 TO 1999

| Year | 1993 | 1994 | 1995 | 1996 | 1997 | 1998 | 1999 |
|---|---|---|---|---|---|---|---|
| Total annual fall (mm) | 606.3 | 730.4 | 629.0 | 758.0 | 750.0 | 842.0 | 435.8 |
| Rainy days (number of) | 98 | 82 | 106 | 122 | 111 | 117 | 97 |
| Average temperature (°C) | 17.9 | 19.0 | 19.6 | 18.4 | 19.0 | 18.5 | 19.5 |

From a socio-economic point of view, the region of Skikda is intended for agricultural, forestry and tourism, but actually its economy is based on industry. The groundwater resources of the site are exploited by an important number of wells, some for potable water and others to supply industrial water to the industrial zone of Skikda.

### 1.17.1. Population Forecast

The population of Skikda city and neighbouring regions is around 786 154 inhabitants in1998, meanwhile this figure is expected to reach 1 044 517 inhabitants in 2020. Table 20 illustrates the population forecast for Skikda city and its neighbouring regions up to 2020.

TABLE 20. POPULATION FORECAST FOR SKIKDA CITY (INHABITANTS)

| Year | 2010 | 2015 | 2020 |
|---|---|---|---|
| Population of Skikda | 973 800 | 979 200 | 1 044 500 |

### 1.17.2. Future water demand

The evaluation of water needs/resources for the period of 2003–2020 at Skikda and its neighbouring regions was carried out by considering two scenarios according to the rainfall. The scenarios selected are average period and dry period. This evaluation considers several factors (the population increase, the irrigated perimeter increase, the reuse of waste water, the realization of desalination units, and the rehabilitation of the networks to reduce water losses to less than 20%).These resources are evaluated according to two scenarios by considering that all the investments to the projected infrastructures will be carried out.

- **Scenario 1**: average period corresponding to an average contribution of the rainfall.
- **Scenario 2**: dry period corresponding, on one hand to a deficit of 50% of the inter-annual average contribution of rainfall, and on the other hand with a reduction in precipitations for the long term.

Table 21 and Fig. 79 summarize the analysis of the evaluation of the water needs/resources for the period indicated according to scenario 1, and Table 22 and Fig. 80 according to scenario 2.

TABLE 21. ESTIMATED WATER NEEDS/RESOURCES FOR AVERAGE PERIOD (1 $Hm^3$=10 000×$m^3$)

| Horizon Year | Population (estimated inhabitants) | Needs ($Hm^3$) | Resources ($Hm^3$) |
|---|---|---|---|
| 2010 | 974 000 | 231 | 181 |
| 2015 | 979 000 | 257 | 225 |
| 2020 | 1 045 000 | 268 | 316 |

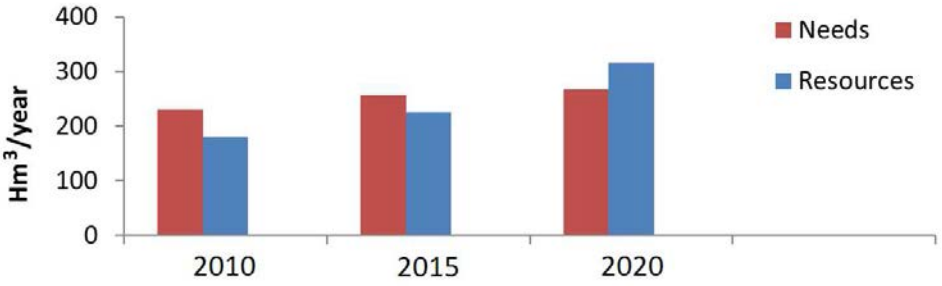


*FIG. 79. Assessment of water needs/resources (scenario 1).*

TABLE 22. ESTIMATED WATER NEEDS/RESOURCES FOR DRY PERIOD

| Horizon Year | Population (estimated inhabitants) | Needs ($Hm^3$) | Resources ($Hm^3$) |
|---|---|---|---|
| 2010 | 974 000 | 268 | 121 |
| 2015 | 979 000 | 301 | 163 |
| 2020 | 1 045 000 | 314 | 223 |

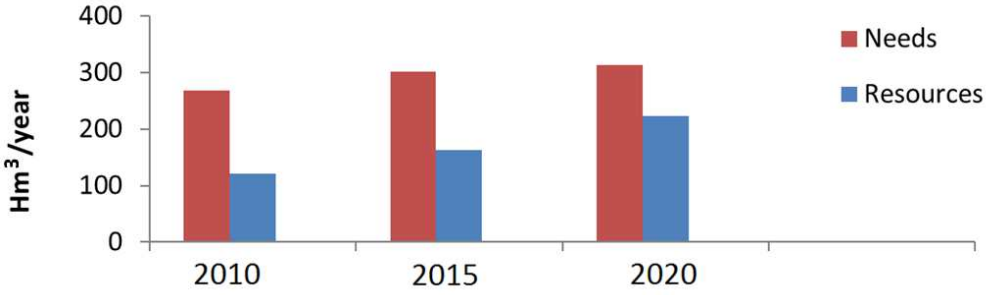


*FIG. 80. Assessment of water needs/resources (scenario 2).*

### 1.17.3. Future electricity demand

The total power installed on the inter-connected national network existing at the end of 2009 was 9109 MW€ [2733 MW€ from steam turbines (ST), 3826 MW€ from GT, 2277 MW€ from combined cycle (CC) and 273 MW€ from hydraulics (HT)]. This energy capacity is produced by the following five companies:

— The States' company "Sonelgaz Production Electricité–SPE" (62%);
— "SharikatKahrabaaSkikda–SKS" (15%), (private company);
— "Sharikat Kahraba Awamaad'arzew–KAHRAMA" (6%), (private company);
— "SharikatKahrabaBerouaghia–SKB" (7%), (private company);
— "SharikatKahrabaHadjret En Nouss–SKH" (10%), (private company).

As an indication, the total power installed on the national interconnected network at the end of 2005 was 6451 MW€ [2740 MW€ from steam turbines (ST), 3436 MW€ from GT and 275 MW€ from hydraulic turbines (HT)]. An increase of 41.2% of the total capacity has been realized in 2009. Currently an additional 2550 MW€ energy production capacity is under construction. For the period 2013–2015, it was decided the reinforcement of the energy production by another additional capacity of 2400 MW€. All the additional capacities decided and in the course of construction over the period 2010–2015 add up to 4950 MW€. For the development of electricity production means, two scenarios are projected: average and high scenarios. The two scenarios correspond to the electric demand forecasts supported by specific technical and socio-economic assumptions. This projected development is given on the basis of a strategy privileging the use of natural gas as the principal fuel, in coherence with the national energy policy directions which also considers the introduction of solar, wind and nuclear energies, with nuclear energy taken into account beyond 2020. The selected technologies for electricity production are: GT (100–200 MW€ range) and combined cycles (400 MW€ range).

As indicated in Fig. 81, the average scenario is based on load forecasts corresponding to a moderate economic growth with a maximum power demand of 13 680 MW in 2019 and a volume of production equal to 79 630 GW€·h. The high scenario is based on load forecasts corresponding to a constant economic revival, with a maximum power demand of 16 270 MW€ in 2019 and a production volume of 94 470 GW€·h.

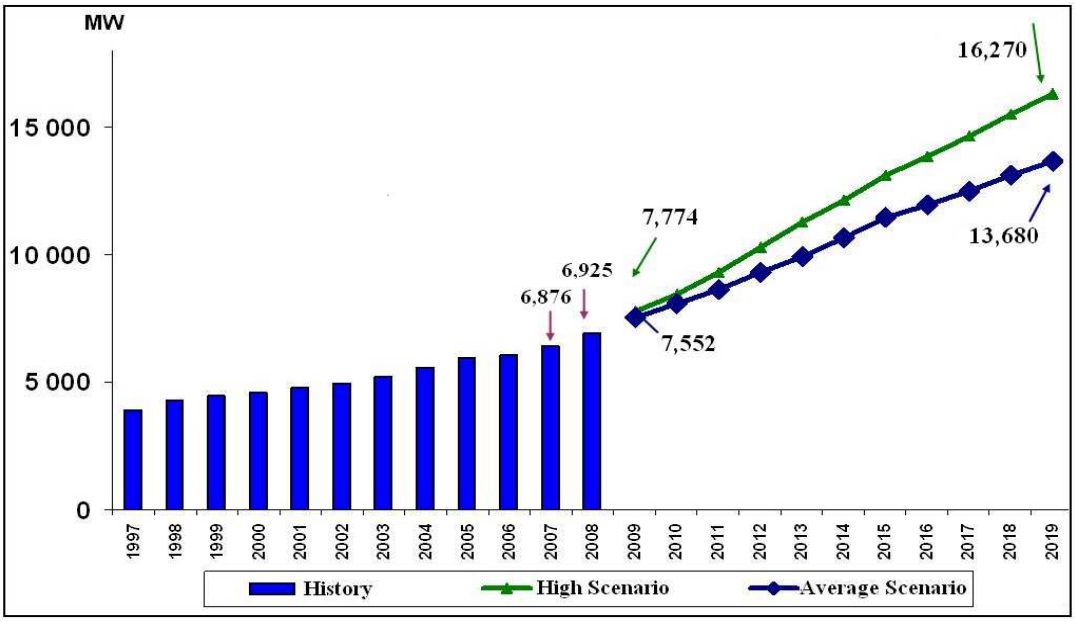


*FIG. 81. Evolution of maximal power demand on the national inter-connected network.*

## 1.18. TECHNOLOGY ASSESSMENT

As a result of the socio-economic vocation of the Skikda region and to the high exploitation of groundwater resources for agricultural purposes rather than for domestic needs, the implementation of a seawater desalination unit is considered more than necessary to cope with the development strategy of this region. The production capacity of the desalination unit is intended to take charge the water supply of Skikda and its neighbouring regions as well as the industrial water needs of the nearby industrial zone of Skikda. This capacity is about 120 000 $m^3$/day, which is distributed as follows: 96 000 $m^3$/day for the potable water needs of Skikda and its neighbouring regions, and 24 000 $m^3$/day to meet the water needs of the Skikda industrial zone.

The technologies used for desalination are those that are widely used currently in the world and which meet inherently to the technical and economic requirements such as: RO, MED and RO-MED. Due to the evolution in the current energy demand and that projected for 2019, it is essential in Algeria to think for other ways of energy production such as nuclear power in the context of diversification of energy sources. For this purpose, the size of nuclear power plant chosen for this study must be consistent with the evolution of the energy capacity installed in the country. Therefore, two scenarios are proposed. The first scenario calls for the use of a nuclear power 1000 MW€ coupled to desalination processes selected and the second scenario uses the small and medium reactors (SMR), gas turbine modular helium reactor (GT-MHR) and pebble bed modular reactor (PBMR), also coupled to desalination processes selected.

## 1.19. ECONOMIC EVALUATION

Calculations are performed using the desalination economic evaluation program software (DEEP-3.1) (possibility of reproducing the results using latest version of DEEP-4.0), which has been developed originally by General Atomics under contract, and has been used in the IAEA's feasibility studies. DEEP output includes the levelized cost of water and power, a breakdown of cost components, energy consumption and net saleable power for each selected option. Specific power plants can be simulated by adjustment of input data including design power, power cycle parameters and costs. In this part of the present study, we are carrying out economic evaluation and comparison of various energy source options coupled with different seawater desalination processes. The various case studies include the cost and performance models of several types of nuclear and fossil energy sources. For the site considered, the following parameters (Tables 22, 23) are the DEEP hypothesis related to desalination processes and power plants.

Considering the number of cases, which have been evaluated by DEEP code, different cases relevant to the selected site are studied. For this purpose, we use DEEP software to estimate and compare the cost of water produced by nuclear and fossil energies. In this study, we propose three scenarios. The energy sources outputs that are candidates in the three scenarios are based on the indicative programme of electricity generation developed in Algeria. The outputs related to nuclear energy are in respect with the threshold fixed to 10% of the maximum power installed. The cogeneration option is taken into account in this study.

TABLE 23. DEEP-BASED HYPOTHESIS RELATED TO DESALINATION PROCESSES

| Desalination plant | | | |
|---|---|---|---|
| Seawater temperature (°C) | 24 | | |
| Salinity, TDS ppm | 39 400 | | |
| Purchased electricity cost ($/kW€·h) | 0.04 | | |
| Production capacity ($m^3$/day) | 120 000 | | |
| Technology | RO | MED | RO–MED |
| Plant life (year) | 25–30 | 25–30 | 30 |
| Specific construction cost [$/($m^3$/day)] | 900 | 900 | 900 |
| Module capacity ($m^3$/day) | 24 000 | 24 000 | 24 000 |

TABLE 24. DEEP HYPOTHESIS RELATED TO DESALINATION PROCESSES

| | Power plant | | | | | | | |
|---|---|---|---|---|---|---|---|---|
| | GT-MHR | PBMR | AP1000 | PWR900 | VVER1000 / V320 | NGCC 400 | NGT 100 | NGT 200 |
| Currency reference year | 2006 | | | | | | | |
| Interest rate (%) | 5–8 | | | | | | | |
| Net electrical power MW€ | 286.2 | 1149 | 1117 | 951 | 1040 | 412.9 | 146 | 241 |
| Net thermal power MW(th) | 592.2 | 2600 | 3400 | 2727 | 2846 | 700–843€ | 406 | 670 |
| Efficiency (%) | 48.3 | 43.2 | 32.7 | 33.0 | 36.5 | 59–49€ | 36 | 36 |
| Number of power plant (units) | 01 | 01 | 01 | 01 | 01 | 01 | 01 | 01 |
| Plant availability (%) | 91.2 | 91.2 | 93.0 | 91.2 | 90.0 | 95.0 | 90.0 | 97.7 |
| Construction lead time (year) | 04 | 02 | 03 | 05 | 4.5 | 02 | 02 | 02 |
| Plant life (year) | 40–60 | 40–60 | 60 | 40 | 50 | 40 | 40 | 40 |
| Construction specific cost $/kW€ | 1073 | 1650 | 1100 | 1763 | 1120 | 600–878€ | 525 | 419 |
| Fossil fuel price ($/bbl) | - | - | - | - | - | 60 | 60 | 60 |
| Nuclear fuel cost $/MW(th) | 7.4 | 5.0 | 3.4 | 7.2 | 2.7 | - | - | - |
| $CO_2$ emission (g/kW·h) | - | - | - | - | - | 363–0€ | 222 | 222 |
| Carbon tax ($/t) | - | - | - | - | - | 50 | 50 | 50 |

*€ Value corresponding to carbon capture technology*

- Scenario 1

This scenario corresponds to the period 2020–2030. The nuclear power reactors proposed for this scenario have an output of 1000 MW€. This corresponds to the use of the 'Advanced PWR AP1000', 'pressurized water reactor PWR900' and 'water-water energy reactor VVER1000/V320' which respectively produce 1117, 951 and 1040 MW€.

As shown in Fig. 82, the AP1000-RO with a 30 years desalination plant lifetime and 5% interest rate appears as the most economical option as it produces water at a 0.473 $/m$^3$.

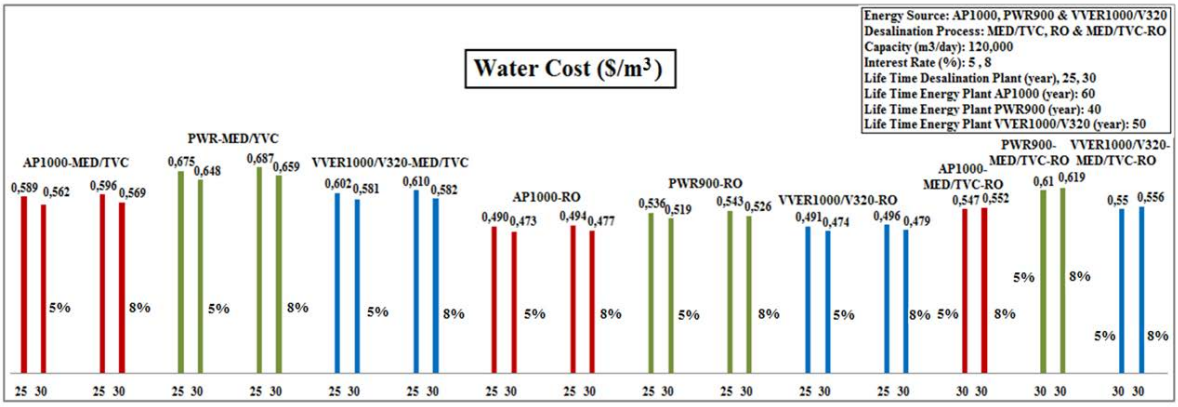


*FIG. 82. Comparative results of coupling AP1000, PWR900 and VVER1000/V320 with desalination systems.*

The high cost corresponding to PWR900-MED/TVC with 25 years desalination lifetime and 8% interest rate. The cost reduction between two configurations is about 31%. The hybrid system coupled to AP1000 is the most competitive option compared to the other hybrid systems considered. The average reduction of cost is 12% between the low and the high prices.

- Scenario 2

This scenario also corresponds to the same period 2020–2030 but the energy sources candidates in this scenario have a size corresponding to small and medium reactors. The nuclear reactors selected for this case are gas turbine modular helium reactor and pebble bed modular reactor with respectively 286 MW and 115 MW outputs. In this scenario, two values are considered for the lifetime of the energy plant: 40 and 60 years. As indicated in Fig. 83(a), the best option corresponding to 60 years energy plant lifetime is the GT-MHR-MED/TVC with 30 years lifetime desalination plant and 5% interest rate. This option produces water at a cost of $0.502 /m$^3$. As indicated in Fig. 83(b), the best option corresponding to a 40 years energy plant lifetime is GT-MHR-MED/TVC with also 30 years of desalination plant lifetime and 5% interest rate. This option produces water at a cost of $0.501 /m$^3$. There is similar tendency on the evolution of water cost produced by the configurations studied for both 40 and 60 lifetimes of energy source. In general, the difference in the cost between configurations corresponding to 40 and 60 lifetimes of energy source is due to fixed charges which are invariable despite the high increase in the energy plant lifetime.

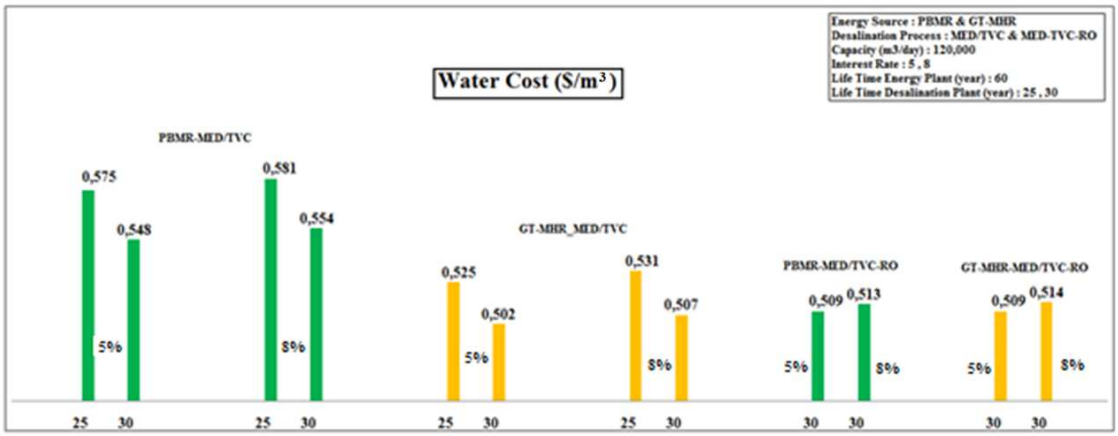


*FIG. 83(a). Comparative results of coupling GT-MHR and PBMR with desalination systems corresponding to 60 years energy plant lifetime.*

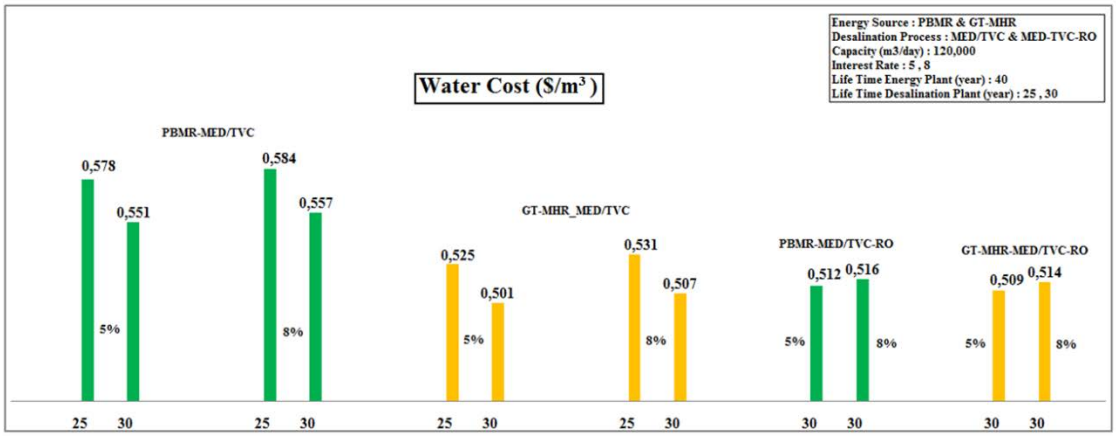


*FIG. 83 (b). Comparative results of coupling GT-MHR and PBMR with desalination systems corresponding to 40 years energy plant lifetime.*

- Scenario 3

The energy sources candidates in this scenario have an output corresponding to a strategy privileging option related to fossil energy in Algeria: natural gas combined cycle 400 MW, natural gas turbine 100 MW€ and natural gas turbine 200 MW€. In this scenario, we consider two options: with and without carbon tax. By considering configurations with and without carbon tax, we find that the configuration NGCC400-RO is the most competitive. In introducing the plant lifetime variable and the interest rate variable, it appears that the option with the lowest cost corresponds to a lifetime equal to 30 years and 5% interest rate (without carbon tax). This option produces water at a cost equal to \$0.769 /$m^3$. When we consider 25 and 30 desalination plant lifetimes, it appears that the difference between the most economic options is estimated to 2.2%. For configurations with carbon tax, we see the same tendency in the evolution of the water cost. The most economical option is NGCC400-RO whose cost is \$0.798 /$m^3$, with 30 years desalination plant lifetime and 5% interest rate. For all the configurations corresponding to NGCC400-RO, the influence of the interest rate on the water cost produces an average gap equal to 0.4% (Figs 84 and 85).

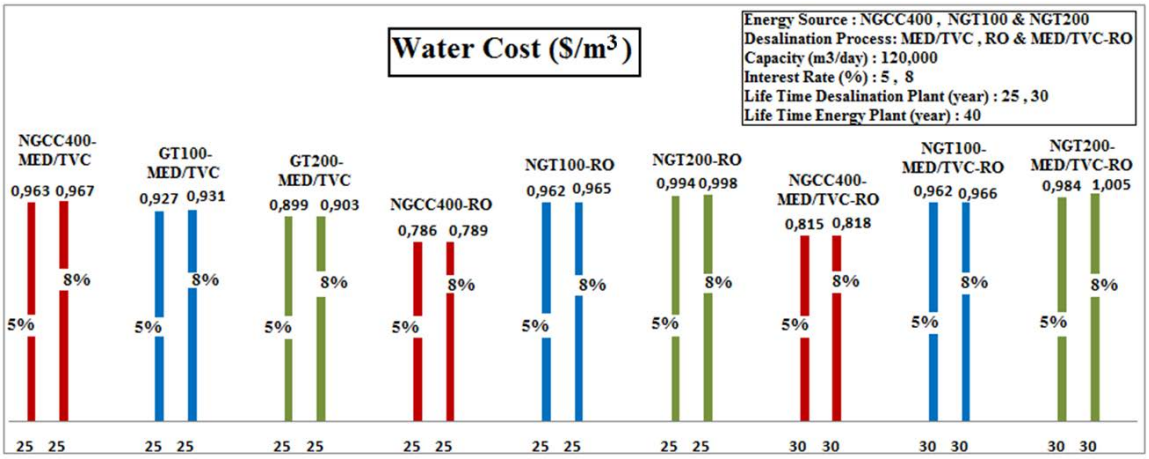


*FIG. 84(a). Comparative results of coupling NGCC400, NGT100 and NGT200 with desalination systems corresponding to 25 years lifetime without carbon tax.*

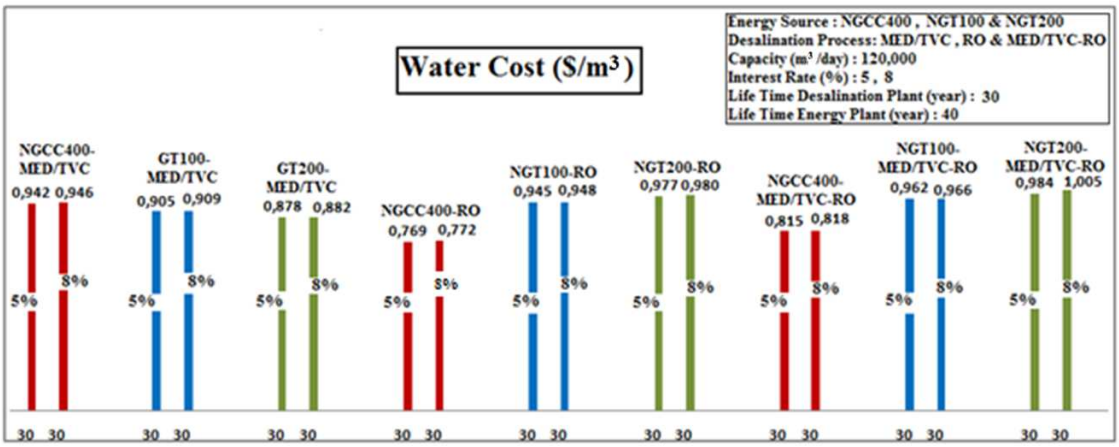


*FIG. 84(b). Comparative results of coupling NGCC400, NGT100 and NGT200 with desalination systems corresponding to 30 years lifetime without carbon tax.*

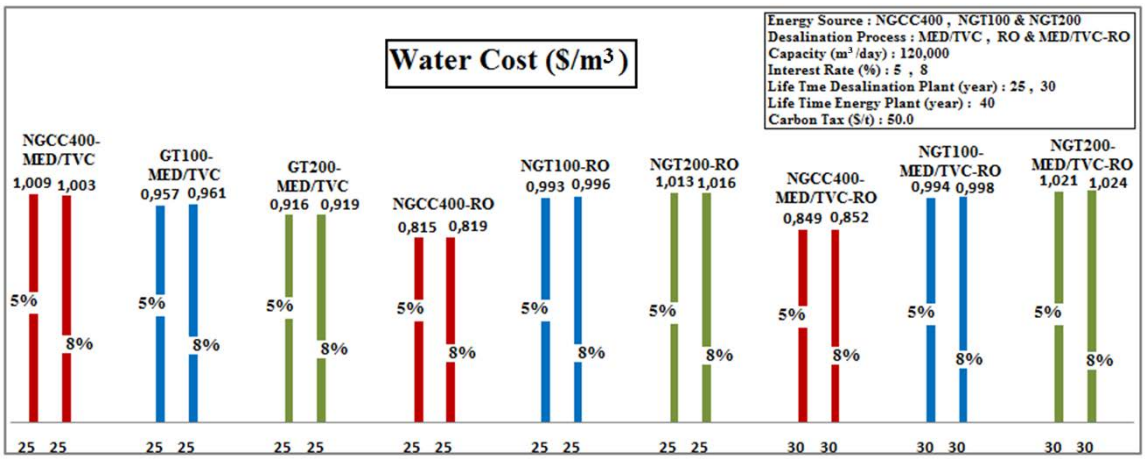


*FIG. 85(a).Comparative results of coupling NGCC400, NGT100 and NGT200 with desalination systems corresponding to 25 years lifetime with carbon tax.*

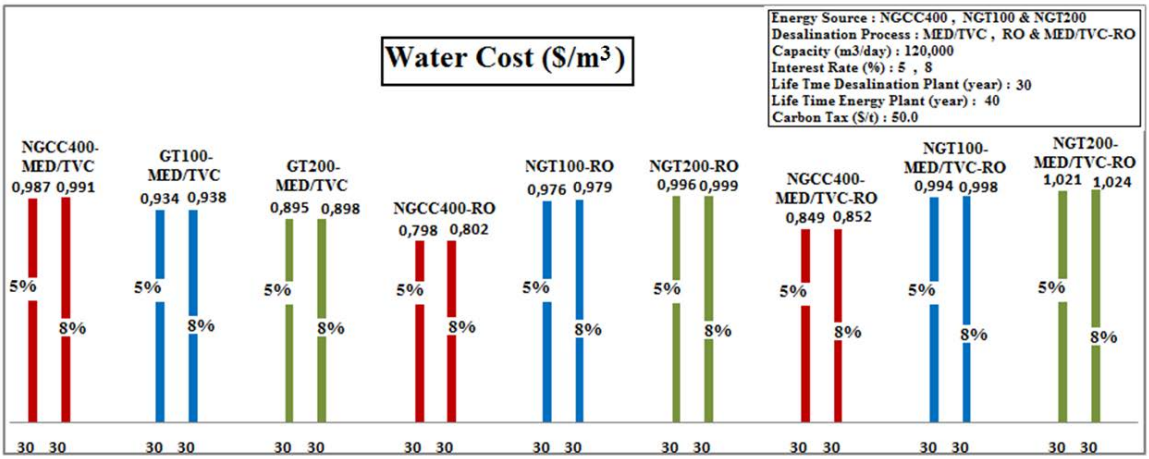


*FIG. 85(b). Comparative results of coupling NGCC400, NGT100 and NGT200 with desalination systems corresponding to 30 years lifetime with carbon tax.*

In this scenario, an additional variable is introduced. It is about the technology of carbon capture. The energy source considered in our case is the NGCC-400. By considering all configurations in this case, as shown in Figs 86(a) and 86(b), we see that the configuration NGCC400-RO with 30 years desalination plant lifetime and 5% interest rate is the most competitive option. In introducing the carbon capture variable, it appears that the difference between most economic options is estimated to be 1%.

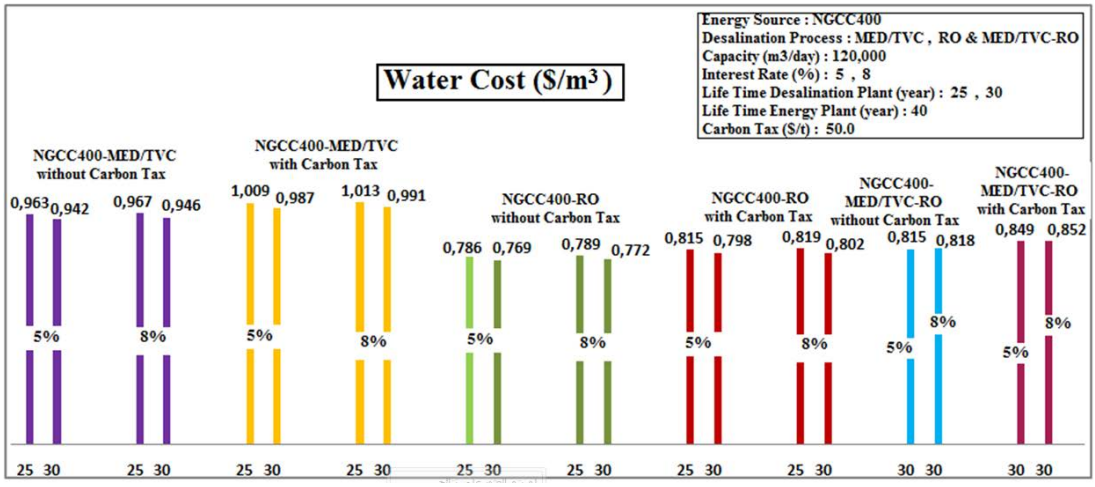


*FIG. 86(a). Comparative results of coupling NGCC400 with desalination systems corresponding to 25–30 years lifetime without and with carbon tax.*

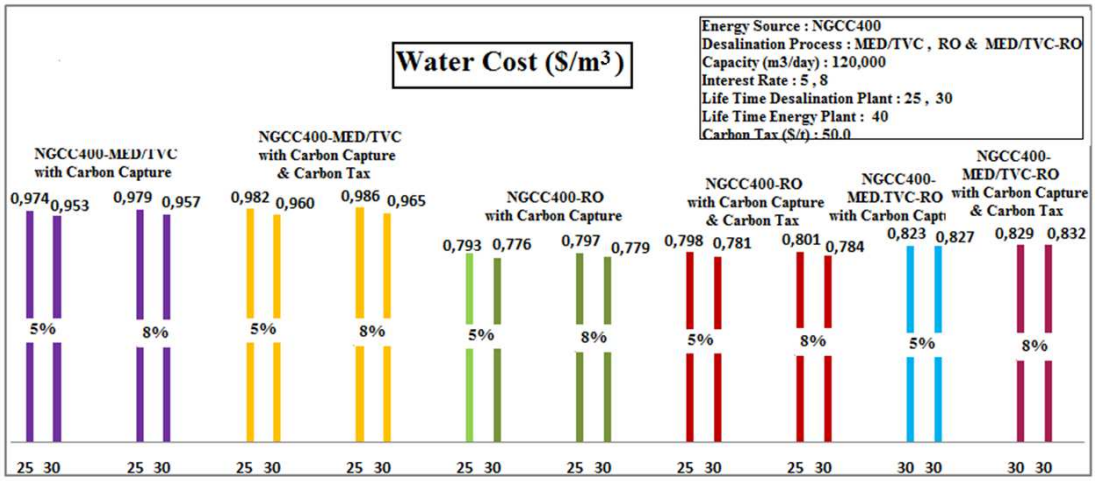


*FIG. 86(b). Comparative results of coupling NGCC400 with desalination systems corresponding to 25–30 years lifetime with carbon capture and carbon tax.*

## 1.20. CONCLUSIONS

Desalination has become an imperative and inevitable solution for Algeria to overcome its current shortage of potable water. So the objective of this study is the preliminary feasibility study necessary to evaluate the potentialities of using nuclear energy for electricity and potable water production. For this study different variables are introduced taking into account the development introduced in fossil and nuclear energy production technologies. The site considered in this case is in a region, where water needs compared to strong demand during the last years went in crescendo because of the population increase and agricultural and industrial vocation of this area. The production capacity of the nuclear desalination plant satisfies water demand of Skikda city and its neighbouring regions, for two to three decades beyond 2025. In addition, the electricity produced by this plant allows the satisfaction of its own needs and improves the reliability of the local electric mains network. Calculations are performed using the desalination economic evaluation program software DEEP-3.1. The economic evaluation and the comparison of the various energy source options coupled with different seawater desalination processes have been carried out. The various case studies include the cost and performance models of several types of nuclear and fossil energy sources. Energy sources used in this study are in compliance with the strategy adopted in the programme requirements in terms of electricity generation for the period 2010–2019 and that corresponding to the next decade. When comparing between configurations of scenarios 1 and 2, we find that the difference in water cost varies from 6 to 15%. Similarly, by comparing the configurations using nuclear energy with those based on fossil fuels, we find that the difference in water cost varies from 39 to 33%. It proves that nuclear desalination option is more competitive compared to desalination based on fossil energy. Finally, for a better estimation of water cost, other aspects must be also considered such as: environment, transport and other economic considerations.

# CONCLUSIONS

There is a great interest in using nuclear energy for producing desalinated water. This interest is growing worldwide, motivated by a wide variety of reasons such as the economic competitiveness of nuclear energy and energy supply diversification. It seems that it is the time to go beyond techno-economic studies, and invest in promoting R&D on new technologies that can be employed in nuclear desalination systems to make nuclear desalination a viable option. One of the distinct results of this CRP was the close collaboration established and information sharing among participants to the CRP.

The range of desalination technologies available to couple with nuclear power stations was presented, their pros and cons compared via an economic evaluation and comparison of the various energy source options coupled with different seawater desalination processes. In particular, LT desalination technologies such as HT multieffect distillation and hybrid desalination systems are found to be especially efficient, with reduced pretreatment costs and required pumping power in addition to having an increased desalinated water recovery ratio when compared to other processes. The use of heat pipes as heat transfer devices has been proposed and they do seem like a reasonable alternative, as when equipping heat exchangers, they allow for a complete flow separation as well as boosting lower operation and maintenance costs, reducing the risk of leaks in the desalination loop.

New modelling approaches were suggested by participants from France and USA. The suggested model by the French authority for nuclear energy was intended to set up a simulation programme for different desalination plants. The US-suggested model was an Excel-based financial modelling tool which was used to perform NPV calculations for cogeneration projects. The simulation model is useful for the development of nuclear desalination simulator in the future. However, the second model has already been used for multiple case studies to demonstrate the model outputs for determining the feasibility of cogeneration projects at site-specific locations. A sensitivity analysis was also performed to investigate the impacts of desalination units on climate change. It was found that the amount and the cost of the greenhouse emissions depends on a range of variables, including the power required, the efficiency, plant lifetime and fuel consumption.

An update to the DEEP was also done, with the purpose of increasing the model's robustness and reliability to predict the cost of different power plants. A major update of DEEP was based on the US-suggested model for NPV analysis. Several predictions were done with the software and it was found that the costs for the distinct types of units change wildly depending on the application. The comparison with solar stills was not possible due to lack of significant data available

The biggest case study available was that of Skikda, in Algeria, a plant that was constructed due to the lack of potable water in Algeria. It was proven that nuclear desalination option is more competitive compared to desalination based on fossil energy mainly based on the pollution caused by the latter as well as higher cost per litre of water.

Overall the CRP was a very successful event, for both the showcase of new technology and applications of current models in real-life power plants. A great part of the CRP work was directed towards modification of DEEP software and the development of a precise model, which estimates the performance and evaluates the economics of the MED/TVC system. Hybrid nuclear desalination systems do seem to be the way forward for both energy and drinkable water production.

## REFERENCES


[1] AL-KARAGHOULI, A., KAZMERSKI, L.L., Renewable Energy Opportunities in Water Desalination, Golden, Colorado, **80401** (2011).

[2] DESALDATA, Global Desalination Plant Capacity by Technology (2012), www.desaldata.com.

[3] R.F.SERVICE, Desalination Freshens Up. Science, (2006) 1088–1090.

[4] ADHAM, S., Desalination. Proc. Membrane Specialty Conf, II (2007).

[5] INTERNATIONAL ATOMIC ENERGY AGENCY, Economics of Nuclear Desalination: New Developments and Site Specific Studies: Final Results of a Coordinated Research Project, 2002–2006, IAEA, Vienna (2007).

[6] ETTOUNEY, H., Seawater Desalination: Conventional and Renewable Energy Processes, in: Cipollina A, Micale G, Rizzuti L, editors, Seawater Desalination: Conventional and Renewable Energy Processes, Springer (2009) 17.

[7] OPHIR, A., LOKIEC, F., Advanced MED process for most economical sea water desalination, Desalination, **182** 1–3 (2005) 187–198.

[8] CALIFANO, S., Pathways to Modern Chemical Physics, Springer (2012).

[9] AVLONITIS, S.A., KOUROUMBAS, K., VLACHAKIS, N., Energy consumption and membrane replacement cost for seawater RO desalination plants, Desalination, **157** (2003) 151–158.

[10] ALL CONSULTING, Electrodialysis in Water Treatment (2012), http://www.all-llc.com/page.php?5

[11] RAUTENBACH, R., ARZT, B., Gas turbine waste heat utilization for distillation, Desalination, **52** 2 (1985) 105–122.

[12] SAARI, R., Usability of low temperature waste heat for sea water desalination, Desalination, **39** (1981) 147–158.

[13] TOELKES, W.E., The Ebeye desalination project — total utilization of diesel waste heat, Desalination, **66** (1987) 59–68.

[14] SENATORE, S.J., Vapour compression distillation with maximum use of waste heat, Desalination, **38** (1981) 3–12.

[15] RAUTENBACH, R., ARZT, B., Waste heat utilization of large diesel engines by thermocompression and low temperature multiple effect evaporation, Desalination, **44** 1–3 (1983) 121–128.

[16] TAY, J.H., LOW, S.C., JEYASEELAN, S., Vacuum desalination for water purification using waste heat, Desalination, **106** 1–3 (1996) 131–135.

[17] COHEN, M., IANOVICI, I., BRESCHI, D., Power plant residual heat for seawater desalination, Desalination, **152** 1–3 (2003) 155–165.

[18] COHEN, J., JANOVICH, I., MUGINSTEIN, A., Utilization of waste heat from a flue gases up-stream gas scrubbing system, Desalination, **139** 1–3 (2001) 1–6.

[19] INTERNATIONAL ATOMIC ENERGY AGENCY, Desalination of Water Using Conventional and Nuclear Energy: A Report on the Present Status of Desalination and the Possible Role Nuclear Energy May Play in this Field, IAEA, Vienna (1964).

[20] INTERNATIONAL ATOMIC ENERGY AGENCY, Guide to the Costing of Water from Nuclear Desalination Plants: Work Done on IAEA Research Contract, IAEA, Vienna (1967).

[21] HOOPER, T., SMITH, J., Heat Utilization from Nuclear Reactors for Desalting of Seawater, IAEA, Vienna (1977).

[22] AWERBUCH, L., SHERMAN, M., RANDALL, S–H., VAN DER MAST, V., Hybrid Desalting Systems, 4th World Congress on Desalination and Water Reuse, Kuwait (1989).

[23] INTERNATIONAL ATOMIC ENERGY AGENCY, Optimization of the Coupling of Nuclear Reactors and Desalination Systems: Final Report of a Coordinated Research Project, 1999–2003 IAEA, Vienna (2005).
[24] AWERBUCH, L., Power–Desalination and the importance of hybrid ideas, World Congress on Desalination and Water Reuse, Madrid (1997) 181–192.
[25] HAMED, O.A., Overview of hybrid desalination systems — current status and future prospects, Desalination, **186** (2005) 207–214.
[26] INTERNATIONAL ATOMIC ENERGY AGENCY, Status of Nuclear Desalination in IAEA Member States, IAEATECDOC–1524, Vienna (2007).
[27] JOUHARA, H., Economic assessment of the benefits of wraparound heat pipes in ventilation processes for hot and humid climates, International Journal of Low-Carbon Technologies, **4** 1 (2009) 52–60.
[28] JOUHARA, H., GODFRIN, G., PEREZ, J., MESKIMMON, R., Experimental study of loop heat pipes used in air-to-air heat exchanger for energy efficient dehumidification in air handling units, SEEP (2009).
[29] JOUHARA, H., ANASTASOV, V., KHAMIS, I., Potential of heat pipe technology in nuclear seawater desalination, Desalination, **249** 3 (2009) 1055–1061.
[30] JOUHARA H., ROBINSON, A.J., Experimental investigation of small diameter two-phase closed thermosyphons charged with water, FC–84, FC–77 and FC–3283, Applied Thermal Engineering, **30** 2–3 (2010) 201–211.
[31] KHAMIS, I., JOUHARA, H., ANASTASOV, V., Heat pipes as an extra measure to eliminate radioactive contamination in nuclear seawater desalination, Desalination and Water Treatment, **13** 1–3 (2010) 82–87.
[32] ANASTASOV, V., KHAMIS, I., JEM Spotlight: Nuclear desalination — environmental impacts and implications for planning and monitoring activities, Environmental Monitoring, **12** (2009) 50–57.
[33] ANASTASOV, V., KHAMIS, I., Environmental Issues Related to Nuclear Desalination, 11th International Conference on Energy and Environment, Cairo, (2009).
[34] FAGHRI, A., Heat Pipe Science and Technology, Taylor & Francis Group (1995).
[35] DUNN, P., REAY, D.H., Heat Pipes. 4th ed, Pergamon Press, Oxford (1978).
[36] JOUHARA, H., AJJI, Z., KOUDSI, Y., EZZUDDIN, H., MOUSA, N., Experimental investigation of an inclined-condenser wickless heat pipe charged with water and an ethanol/water azeotropic mixture, Energy, **61** (2013) 139–147.
[37] H. JOUHARA AND A.J. ROBINSON, An experimental study of small-diameter wickless heat pipes operating in the temperature range 200ºC to 450ºC, Heat Transfer Engineering, **30** 13 (2009) 1041–1048.
[38] RIEHL, R.R., DUTRA, T., Development of an experimental loop heat pipe for application in future space missions, Applied Thermal Engineering, **25** 1 (2005) 101–112.
[39] LIN, M.C., CHUN, L.J., LEE, W.S., CHEN, S.L., Thermal performance of a two-phase thermosyphon energy storage system, Solar Energy, **75** 4 (2003) 295–306.
[40] FILIPPESCHI, S., On periodic two-phase thermosyphons operating against gravity, International Journal of Thermal Sciences, **45** 2 (2006) 124–137.
[41] MATHIOULAKIS, E., BELESSIOTIS, V., A new heat pipe type solar domestic hot water system, Solar Energy, **72** 1 (2002) 13–20.
[42] MORRISON, G.L., ROSENGARTEN, G., BEHNIA, M., Mantle heat exchangers for horizontal tank thermosyphon solar water heaters, Solar Energy, **67** 1–3 (1999) 53–64.

[43] WEBSTER, T.L., COUTIER, J.P., PLACE, J.W., TAVANA, M., Experimental evaluation of solar thermosyphons with heat exchangers, Solar Energy, **38** 4 (1987) 219–231.
[44] VASILIEV, L.L., Heat pipe research and development in the U.S.S.R, Heat Recovery Systems and CHP, **9** 4 (1989) 313–333.
[45] EL-DESSOUKY, H.T., ETTOUNEY, H.M., Fundamentals of Salt Water Desalination, Elsevier Science (2002).
[46] BLENINGER, T., JIRKA, G.H., Modelling and environmentally sound management of brine discharges from desalination plants, Desalination, **221** 1–3 (2008) 585–597.
[47] INTERNATIONAL ATOMIC ENERGY AGENCY, Nuclear Heat Applications: Design Aspects and Operating Experience, IAEATECDOC–1056, Vienna (1998).
[48] INTERNATIONAL COMMISSION ON RADIOLOGICAL PROTECTION, Age-dependent doses to members of the public from intake of radionuclides: Part 4 Inhalation dose coefficients, Annals of the ICRP, **25** 3–4 (1995).
[49] CANADIAN NUCLEAR SAFETY COMMISSION, Standards and Guidelines for Tritium in Drinking Water, Canadian Nuclear Safety Commission, (2008).
[50] BARC, Communication Received from BARC, India Concerning the Environmental Impact of the Nuclear Desalination Facility, IAEA, Vienna (2008).
[51] MCKAY, H., Tritium immobilization, European Applied Research Reports, Nuclear Science Technology, **1** (1979) 599–711.
[52] MURALEV, D., Experience in the application of nuclear energy for desalination and industrial use in Kazakhstan, Nuclear heat applications: Design aspects and operating experience (1998) 361–368.
[53] KINNE, O., Marine Ecology: pt. 1–2, Environmental factors, Wiley–Interscience, (1971).
[54] MIRI, R., CHOUIKHI, A., Ecotoxicological marine impacts from seawater desalination plants, Desalination, **182** 1–3 (2005) 403–410.
[55] SÁNCHEZ-LIZASO, J.L., ROMERO, J., RUIZ, et al., Salinity tolerance of the Mediterranean seagrass Posidonia oceanica: recommendations to minimize the impact of brine discharges from desalination plants, Desalination, **221** 1–3 (2008) 602–607.
[56] LATTEMANN, S., HÖPNER, T., Environmental impact and impact assessment of seawater desalination, Desalination, **220** 1–3 (2008) 1–15.
[57] ALAMEDDINE, I., EL-FADEL, M., Brine discharge from desalination plants: a modelling approach to an optimized outfall design, Desalination, **214** 1–3 (2007) 241–260.
[58] JOUHARA, H., EZZUDDIN, H., Thermal performance characteristics of a wraparound loop heat pipe (WLHP) charged with R134A, Energy, **61** (2013) 128–138.
[59] JOUHARA, H., MERCHANT, H., Experimental investigation of a thermosyphon based heat exchanger used in energy efficient air handling units, Energy, **39** 1 (2012) 82–89.
[60] SHEIKHOLESLAMI, R., BRIGHT, J., Silica and metals removal by pretreatment to prevent fouling of RO membranes. Desalination, **143** 3 (2002) 255–267.
[61] GASO, G., MENDEZ, A., Sorption of Ca2+, Mg2+, Na+ and K+ by clay minerals, Desalination, **182** 1–3 (2005) 333–338.
[62] MURAVIEV, D., NOGUEROL, J., VALIENTE, M., Separation and concentration of calcium and magnesium from sea water by carboxylic resins with temperature-induced selectivity, Reactive and Functional Polymers, **28** 2 (1996) 111–126.

[63] MURAVIEV, D., KHAMIZOV, R.K., TIKHONOV, N.A., MORALES, J.G., Clean ('green') ion-exchange Technologies, High Ca-Selectivity ion-exchange material for self-sustaining decalcification of mineralized waters process, Ind. Eng. Chem. Res., **43** 8 (2004) 1868–1874.
[64] AL-ANBER, M., AL-ANBER, Z.A., Utilization of natural zeolite as ion-exchange and sorbent material in the removal of iron, Desalination, **225** 1–3 (2008) 70–81.
[65] QIN, C., WANG, R., MA, W., Characteristics of calcium adsorption by Ca-Selectivity zeolite in fixed-pH and in a range of pH, Chemical Engineering Journal, **156** 3 (2010) 540–545.
[66] KESTIN, J., SENGERS, J.V., KANGMAR-PARSI, B., LEVELT SENGERS, J.M.H., Thermo physical properties of fluid H2O, Journal of Physics and Chemistry, **13** (1984) 175.

# ANNEX I
# NEW MODELING APPROACH FOR MULTIEFFECT EVAPORATION PLANTS

## I-1. GENERAL CONTEXT

### I-1.1. Introduction

Addressing water shortages is a difficult challenge for many countries due to population growth and the increasing need for water to support industry, agriculture and urban development. Innovative water management strategies are certainly needed to preserve water resources. But they may not be sufficient. Throughout the world, many highly populated regions face frequent and prolonged droughts. In these areas, where, for some reason, the natural hydrologic cycle cannot provide people with water, desalination is used to provide people with potable water. Desalination systems fall into two main design categories, namely thermal and membrane types. Thermal designs –including MSF and MED- use flashing and evaporation to produce potable water while membrane designs use the method of RO.

Desalination is the main technology being used to augment fresh water resources in water scarce coastal regions. With almost 64.4 million $m^3$/day (GWI 2012) of worldwide desalination water production capacity, about two third is produced by thermal distillation, mainly in the Middle East. Outside this region, membrane-based systems predominate. Both processes are energy-intensive (Fig. I-1.). Even if power consumption has been reduced as technological innovations, such as energy recovery systems and variable frequency pumps (reverse RO plants), are introduced, it remains the main cost factor in water desalination. Traditionally, fossil fuels such as oil and gas have been the major energy sources. However, fuel price hikes and volatility as well as concerns about long term supplies and environmental release is prompting consideration of alternative energy sources for seawater desalination, such as nuclear desalination and the use of renewable energy sources. Replacing fossil fuel by renewable (solar, wind, geothermal, biomass) or nuclear energy, could reduce the impacts on air quality and climate.

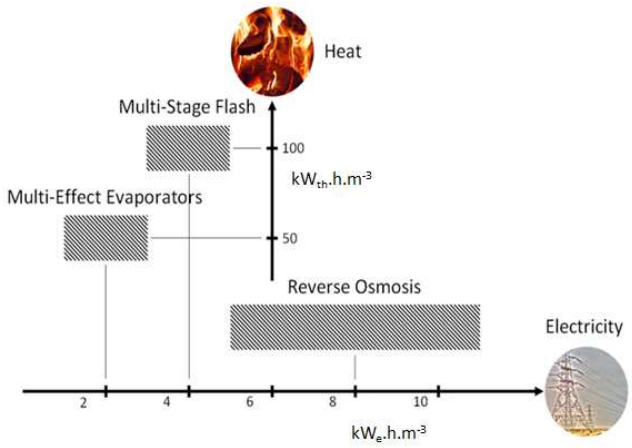


*FIG. I-1. Typical energy consumption of technologically mature desalination processes.*

The idea of using nuclear energy to desalinate seawater is not new. Since the USS nautilus was commissioned more than a half century ago, the drinking water on nuclear submarines has come from reactor-powered desalination systems. Today, nuclear desalination is being

used by a number of countries, including India and Japan, to provide fresh water for growing populations and irrigation. Commercial uses are also being considered in Europe, the Middle East and South America. The IAEA has always been an important contributor to the R&D effort in nuclear desalination. In 2009, it launched a coordinated research programme entitled "New Technologies for Seawater Desalination using Nuclear Energy", focusing on the introduction of innovative nuclear desalination technologies, producing desalted water at the lowest possible cost and in a sustainable manner.

The French atomic and alternative energies commission (CEA) expressed interest in participating to the CRP. A research proposal, aiming at using CEA software tools to develop optimized nuclear desalination systems was established and submitted to the IAEA. The studies focused on the development of optimized nuclear desalination systems producing large amounts of desalinated water while minimizing the impact on the efficiency of power conversion. Technologically mature desalination processes viz. MEE and RO have been considered for the study. Each of these systems will be modelled using innovative techniques developed in CEA. Models would first be validated (against experimental results published in literature, or obtained through bilateral collaborations involving CEA) and then applied to optimize the energy use in the integrated power and water plants.

## I-2. STATE OF THE ART OF MEE PLANT MODELING

### I-2.1. Description of the MEE process

Multieffect distillation is the oldest and most commonly used method of desalination. The world's first land-based desalination plant was a 60 $m^3$/day MEE unit installed in Curaçao (Netherlands Antilles), an island in the southern Caribbean Sea, in 1928. The MEE process consists of a number of effects (or cells) maintained at decreasing levels of pressure and temperature (Fig. I-2.).

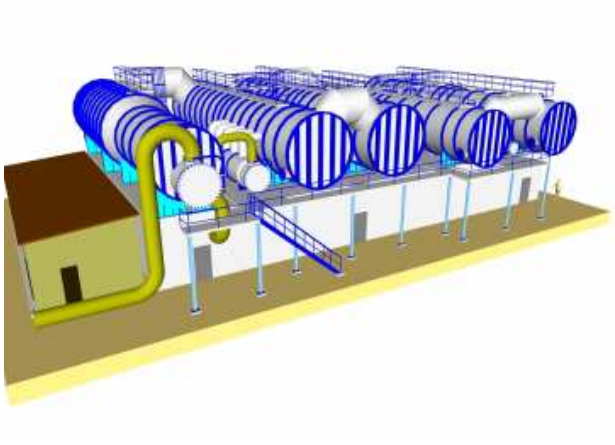

*FIG. I-2. Typical layout of an MEE plant (image: entropie.com).*

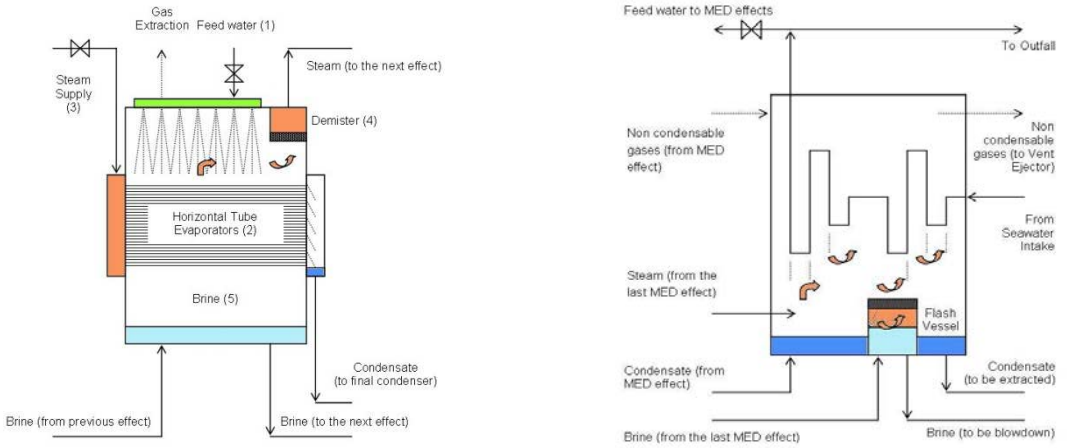


*FIG. I-3. Typical architecture of MEE evaporators (left) and final condenser (right).*

In each cell (Fig. I-3.), the feedwater (1), sprayed on a bank of HT (2), partially evaporates (4) and then flows down by gravity (5). As steam from the previous effect (3) condensates inside the tubes, seawater partially evaporates. The generated steam is first purified in the demister (4), and then used as a heat source for the next effect, maintained at a lower pressure. The unevaporated brine (5) is cascaded to the next effect. The evaporation–condensation cycle is repeated successively throughout the plant. The steam generated in the last evaporator flows towards the condenser (Fig. I-3.) –a conventional shell and tubes heat exchanger- where it transfers its latent heat to the incoming seawater. Currently, MED processes with the highest technical and economic potential are the LTHT MED process and the vertical tube evaporation process (VTE). In LTHT MED plants, evaporation tubes are arranged horizontally and evaporation occurs by spraying the brine over the outside of the HT creating a thin film from which steam evaporates. In VTE plants, evaporation takes place inside vertical tubes. MEE plants also include auxiliary systems exhausting air and non-condensable gases (creating and maintaining a vacuum within the evaporators), extracting, cooling brine and distilled water, filtering and preheating the incoming seawater. The MEE process produces ultrapure water (specific conductance less than 5.5 μS/cm) from seawater at 15–5°C and 30 000–40 000 ppm TDS. The quantity (kilos) of distillate produced per one kilo of steam introduced to the system is referred to as the gain output ratio (GOR). It is a measure of the efficiency of the process.

## I-3. A NEW MODELING APPROACH

### I-3.1. Process description using networks of links and well-stirred control volumes

The new modelling approach assumes that the desalination plant components can be represented using networks of well-stirred volumes and links. Well-stirred volumes evaluate the instant temperatures, pressures and salinities in different regions. The next two paragraphs (I-3.2. to I-3.3.) describe the models associated to the following circuits: non-condensable gas extraction (vacuum system), seawater preheat. Links calculate the flows of mass and energies between different volumes. The heat exchanger described in paragraph I-3.3.5. provides an illustration of the modelling technique. Paragraph I-3.4. describes the methods adopted for the evaluation of the thermo physical properties correlations of dry air and (sub-cooled and saturated) pure water. The numerical techniques used for the calculation of the different well-stirred volumes are discussed in paragraph I-3.5.

### I-3.2. Vacuum system

The vacuum system extracts air and non-condensable gases from MEE evaporators, which maintains a vacuum within the desalination system. It generally consists of a hydro-ejector, a separation drum and a recirculation pump organized in a closed loop. The dynamics of system depressurization can be simulated modelling MEE evaporators and the components of the vacuum loop. A simpler approach consists of representing MEE evaporators using a structure "air volume" having the same free volume and filled with (dry) air. "Air volume" refers to a delimited space with a given volume of (dry) air at a uniform temperature and pressure. The instant values of these two (state) variables can be evaluated applying the mass Eq. (I-1) and energy Eq. (I-2) conservation principles:

$$\frac{dM}{dt} = V\frac{d\rho}{dt} = V\left(\frac{\partial\rho}{\partial T}\frac{dT}{dt} + \frac{\partial\rho}{\partial P}\frac{dP}{dt}\right) = \delta\dot{m} \qquad \text{Eq. (I-1)}$$

$$\frac{d(\bar{h}M)}{dt} = \bar{h}\frac{dM}{dt} + M\frac{d\bar{h}}{dt} = \bar{h}\frac{dM}{dt} + M\left(\frac{\partial\bar{h}}{\partial T}\frac{dT}{dt} + \frac{\partial\bar{h}}{\partial P}\frac{dP}{dt}\right) = \delta\left(\dot{Q} + \bar{h}\dot{m}\right) \qquad \text{Eq. (I-2)}$$

where

$M$ is the mass of matter within the control volume (kg);

$t$ is the time (s);

$V$ is the volume of matter within the control volume ($m^3$) (constant);

$\rho$ is the density ($kg.m^{-3}$);

$T$ is the temperature (°C);

$P$ is the pressure (bar);

$\dot{m}$ is the rate of mass flow ($kg.s^{-1}$);

$\delta\dot{m}$ is the difference between the flow rates of matter entering and flowing out the control volume ($kg.^{-1}$);

$$\delta\dot{m} = \sum \dot{m}_{in} - \sum \dot{m}_{out} \qquad \text{Eq. (I-3)}$$

$\bar{h}$ is the enthalpy ($kJ.kg^{-1}$);

$\dot{Q}$ is the thermal power (kW);

$\delta(\dot{Q} + \bar{h}\dot{m})$ is the difference between the power entering and leaving the control volume (kW);

$$\delta\left(\dot{Q} + \bar{h}\dot{m}\right) = \sum\left(\dot{Q} + \bar{h}\dot{m}\right)_{in} - \sum\left(\dot{Q} + \bar{h}\dot{m}\right)_{out} \qquad \text{Eq. (I-4)}$$

The volume is assumed to be well-stirred: the enthalpy of air flowing out of the volume is equal to that of the air inside the volume. Applying this assumption and combining Eq. (I-1), Eq. (I-2), Eq. (I-3) and Eq. (I-4), the following system of equations is obtained:

$$a_{11}\frac{dT}{dt} + a_{12}\frac{dP}{dt} = u_1 \qquad \text{Eq. (I-5)}$$

$$a_{21}\frac{dT}{dt} + a_{22}\frac{dP}{dt} = u_2 \qquad \text{Eq. (I-6)}$$

$$a_{11} = V\frac{\partial\rho}{\partial T} \qquad \text{Eq. (I-7)}$$

$$a_{12} = V\frac{\partial\rho}{\partial P} \qquad \text{Eq. (I-8)}$$

$$a_{21} = \rho V\frac{\partial\bar{h}}{\partial T} \qquad \text{Eq. (I-9)}$$

$$a_{22} = \rho V\frac{\partial\bar{h}}{\partial P} \qquad \text{Eq. (I-10)}$$

$$u_1 = \delta\dot{m} \qquad \text{Eq. (I-11)}$$

$$u_2 = \delta\dot{Q} + \sum\dot{m}_{in}\left(\bar{h}_{in} - \bar{h}\right) \qquad \text{Eq. (I-12)}$$

The system of ODE is solved using different variants of the Euler (numerical) method (cf. paragraph I-3.5.). The evaluation of the thermo physical properties of (dry) air (density, enthalpy and their *T*, *P* derivatives) is discussed in paragraph I-3.5.1.

## I-3.3. Seawater preheating section

The devices used for the preheating of the incoming seawater (pipes, valves, pumps, heat exchangers, etc.) are modelled using "sub-cooled brine volume" and links.

### *I-3.3.1. Sub-cooled brine volumes*

"Sub-cooled brine volume" refers to a delimited space with a given volume of saline water at a uniform temperature (T), pressure (P) and salinity €. The instant values of these three (state) variables can be evaluated applying the total Eq. (I-13) and species Eq. (I-15) mass and energy Eq. (I-17) conservation principles:

$$\frac{dM}{dt} = V\frac{d\rho}{dt} = V\left(\frac{\partial\rho}{\partial T}\frac{dT}{dt} + \frac{\partial\rho}{\partial P}\frac{dP}{dt} + \frac{\partial\rho}{\partial C}\frac{dC}{dt}\right) = \delta\dot{m} \qquad \text{Eq. (I-13)}$$

$$\delta\dot{m} = \sum \dot{m}_{in} - \sum \dot{m}_{out} \qquad \text{Eq. (I-14)}$$

$$\frac{d(CM)}{dt} = C\frac{dM}{dt} + M\frac{dC}{dt} = \delta(C\dot{m}) \qquad \text{Eq. (I-15)}$$

$$\delta(C\dot{m}) = \sum (C\dot{m})_{in} - \sum (C\dot{m})_{out} \qquad \text{Eq. (I-16)}$$

$$\frac{d(\bar{h}M)}{dt} = \bar{h}\frac{dM}{dt} + M\frac{d\bar{h}}{dt} = \delta(\dot{Q} + \bar{h}\dot{m}) \qquad \text{Eq. (I-17)}$$

$$\delta(\dot{Q} + \bar{h}\dot{m}) = \sum (\dot{Q} + \bar{h}\dot{m})_{in} - \sum (\dot{Q} + \bar{h}\dot{m})_{out} \qquad \text{Eq. (I-18)}$$

The volume is assumed to be well stirred. Eq. (I-13), Eq. (I-15) and Eq. (I-17) lead to a system of ODE. The system is solved using different variants of the Euler (numerical) method (cf. paragraph I-3.6.). The evaluation of the thermo physical properties of brine (density, enthalpy and their *T*, *P*, *C* derivatives) is discussed in paragraph I-3.4.

### *I-3.3.2. Links (pipes)*

Links are used to evaluate the mass flow rate between two volumes. To establish the relation between the mass flow rate within the link and the pressure difference between the two volumes, we will consider the inclined pipe illustrated by Fig. I-4.

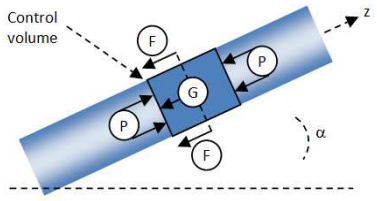


| | |
|---|---|
| Diameter (m) | D |
| Section ($m^2$) | $A = 0.25\ \pi\ D^2$ |
| Length (L) | L |
| Angle | α |

*FIG. I-4. Inclined pipe.*

The control volume shown in Fig. I-4. Is assumed to be in mechanical equilibrium. In these conditions, the sum of the forces associated to friction (*F*), gravity (*G*) and pressure (*P*) is equal to zero:

$$-dF_f - dMg\sin(\alpha) - A(P+\rho u^2)_{z+dz} + A(P+\rho u^2)_z = 0 \qquad \text{Eq. (I-19)}$$

$dF_f$ (*N*) is the force due to friction, $dM = \rho A\, dz$ is the mass (kg) of the control volume, $g$ is the Earth's gravity constant (9.81 $N \cdot kg^{-1}$) and $u$ is the brine velocity ($m \cdot s^{-1}$).

The rate of change of pressure with the axial coordinate $z$ is deduced from Eq. (I-20):

$$\frac{dP}{dz} = -\frac{1}{A}\frac{dF_f}{dz} - \rho g\sin(\alpha) - \frac{d(\rho u^2)}{dz} \qquad \text{Eq. (I-20)}$$

The total pressure difference consists of three terms:

$$\Delta P = \Delta P_f + \Delta P_g + \Delta P_a \qquad \text{Eq. (I-21)}$$

The friction term is $\Delta P_f$:

$$\Delta P_f = -\left(\lambda\frac{L}{D} + \sum K\right)\frac{\rho u^2}{2} \qquad \text{Eq. (I-22)}$$

$\lambda$ is the linear pressure drop coefficient (dimensionless). $\sum K$ is the sum of the singular pressure drop coefficients (dimensionless).

The friction term is a function of the mass flow rate of brine.

The gravity term is $\Delta P_g$:

$$\Delta P_g = -\int_0^L \rho g \sin(\alpha)\, dz \qquad \text{Eq. (I-23)}$$

The acceleration term is $\Delta P_a$:

$$\Delta P_a = -((\rho u^2)_L - (\rho u^2)_0) \qquad \text{Eq. (I-24)}$$

The acceleration term is a function of the mass flow rate of brine. The mass flow rate through the link is obtained solving Eq. (I-24). The transport properties of saline water, required for the calculations, are evaluated as described in paragraph I-3.5.2.

*I-3.3.3. Valves*

Valves are represented by a singular pressure drop. The associated model is deduced from that of the link (cf. paragraph I-3.3.2). An additional correlation (real position vs. position) is introduced as a parameter to take the type of the valve into account (first order linear, quick-opening non-linear, etc.).

*I-3.3.4. Centrifugal pumps*

Centrifugal pump are represented by a link (cf. paragraph I-3.3.2.) for which the total pressure difference, Eq. (I-24); include an additional term representing the pump static head. This term is obtained by multiplying the design static head and the square of normalized pump speed. Pump degradation and fluid density changes are taken into account. Pump performance diagrams (power vs. mass flow rate) provided by manufacturer are taken into account. The available net positive suction head (NPSH) is calculated and compared to the required NPSH.

*I-3.3.5. Heat exchangers*

The internal fluid is described by thermo hydraulic volumes related by thermo hydraulic links. The internal heat transfer coefficient is evaluated by these links. Thermal links calculate the amount of heat exchanged between the thermo hydraulic volumes and the masses that represent the tube structure. A similar approach is considered for the shell side.

## I-3.4. Thermo physical properties evaluation

This paragraph presents the method used to evaluate the thermo physical properties of (dry) air, pure and saline water (sub-cooled and saturated).

*I-3.4.1. Dry air*

A (C++) class has been developed to calculate the thermodynamic properties of air assuming a real fluid behaviour: Enthalpy = *fcn*(*T*,*P*) (kJ/kg), Density = *fcn* (*T*,*P*) (kg/m) and their *T*, *P* derivatives = *fcn* (*T*,*P*). The temperature, *T* (°C), ranges from 5 to 105°C. The pressure,

*P* (bar), may vary from 0.05 bar to 1.05 bar. The EES software built-in functions, implementing the E.W. Lemmon et al. fundamental equation of state, were used to build 22 polynomials of degree 6:

— 11 correlations describe how Enthalpy, Density and their *T*, *P* derivatives change with *T* for *P* = 0.05, 0.15, 0.25, 0.35, 0.45, 0.55, 0.65, 0.75, 0.85, 0.95 and 1.05 (bar)
— 11 correlations describe how Enthalpy, Density and their T, P derivatives change with *P* for *T* = 5, 15, 25, 35, 45, 55, 65, 75, 85, 95 and 105 (°C)

For a couple of temperature and pressure, the evaluation of the thermodynamic property F (Enthalpy or Density) and its *T*, *P* derivative is achieved following the steps described below:

— For the lists above, we identify $T_1$, $T_2$, $P_1$ and $P_2$ for which the condition (*T* in ($T_1$,$T_2$) and *P*in ($P_1$,$P_2$)) is true;
— The *T* derivative of *F* is calculated using Eq. (I-25):

$$\frac{dF}{dT} = (1-\alpha)\frac{dC_{P1}(T)}{dT} + \alpha\frac{dC_{P2}(T)}{dT} \qquad \text{Eq. (I-25)}$$

$C_{Pi}(T)$ is the correlation expressing the variation of *F* with *T* for $P=P_i$. $\alpha$ is a proportionality coefficient calculated using Eq. (I-26):

$$\alpha = \frac{P - P_1}{P_2 - P_1} \qquad \text{Eq. (I-26)}$$

— A first value of *F*, $F^{(1)}$, is calculated using Eq. (I-27):

$$F^{(1)} = (1-\alpha)C_{P1}(T) + \alpha C_{P2}(T) \qquad \text{Eq. (I-27)}$$

— The *P* derivative of *F* is calculated using Eq. (I-28):

$$\frac{dF}{dP} = (1-\beta)\frac{dC_{T1}(P)}{dP} + \beta\frac{dC_{T2}(P)}{dP} \qquad \text{Eq. (I-28)}$$

$C_{Ti}(P)$ is the correlation expressing the variation of *F* with *P* for $T=T_i$. $\beta$ is a proportionality coefficient calculated using Eq. (I-29):

$$\beta = \frac{T - T_1}{T_2 - T_1} \qquad \text{Eq. (I-29)}$$

- A second value of $F$, $F^{(2)}$, is calculated using Eq. (I-30):

$$F^{(2)} = (1-\beta)C_{T1}(P) + \beta C_{T2}(P) \quad \text{Eq. (I-30)}$$

- The value of $F$ is calculated using Eq. (I-31):

$$F = \frac{F^{(1)} + F^{(2)}}{2} \quad \text{Eq. (I-31)}$$

*I-3.4.2. Sub-cooled pure and saline water*

The thermodynamic and transport properties of sub-cooled pure and saline water are evaluated using the same methodology as for dry air. The temperature, $T$ (°C), ranges from 5 to 95°C. The pressure, $P$ (bar), may vary from 1 to 10 bars. The EES software built-in functions were used to build a series of polynomials of degree 6 evaluating the properties of pure water. These polynomials were implemented in a C++ class as for dry air. The thermodynamic properties correlations built-in in EES are based on the 1995 Formulation for the Thermodynamic Properties of Ordinary Water Substance for General and Scientific Use, issued by the International Association for the Properties of Water and Steam (IAPWS). The thermal conductivity, viscosity, and surface tension correlations are based on Kestin et al. [66]. The range of applicability for these transport correlations is the same as for the thermodynamic properties. The properties of saline water are deduced from the characteristics of pure water assuming the dissolved salts-water solution to be ideal.

*I-3.4.3. Saturated pure and saline water*

The properties of saturated pure and saline water are evaluated on the same basis as for the sub-cooled condition. An additional correlation evaluating the boiling point elevation (BPE) of saline water is also implemented.

**I-3.5. ODEs solving**

$$a_{11}\frac{df_1}{dt} + a_{12}\frac{df_2}{dt} + \cdots + a_{1n}\frac{df_n}{dt} = u_1 \quad \text{Eq. (I-32)}$$

$$a_{21}\frac{df_1}{dt} + a_{22}\frac{df_2}{dt} + \cdots + a_{2n}\frac{df_n}{dt} = u_2 \quad \text{Eq. (I-33)}$$

$$a_{n1}\frac{df_1}{dt} + a_{n2}\frac{df_2}{dt} + \cdots + a_{nn}\frac{df_n}{dt} = u_n \quad \text{Eq. (I-34)}$$

This paragraph presents the numerical technique, based on the Euler method, used to solve the ODE describing the dynamics of well-stirred control volumes:

In this system of equations, the coefficients $\{a_{ij}\}$ and $\{u_i\}$ are functions of unknowns $\{f_1, f_2, \ldots f_n\}$:

$$a_{ij} = a_{ij}(f_1, f_2, \ldots, f_n) \qquad \text{Eq. (I-35)}$$

$$u_i = u_i(f_1, f_2, \ldots, f_n) \qquad \text{Eq. (I-36)}$$

The value of $\{f_k^* = f_k(t+\Delta t)\}$ can be estimated from that of $\{f_k = f_k(t)\}$ applying either an explicit or an implicit scheme. Let vector $\{v\}$ be the result of the multiplication of vector $\{u\}$ by the inverse of matrix $\{a_{ij}\}$.

*I-3.5.1. Explicit scheme*

According to the explicit scheme, $\{f_k^*\}$ is evaluated applying Eq. (I-37):

$$f_k^* = f_k + v_k \Delta t \qquad \text{Eq. (I-37)}$$

The terms on the right of the equal sign in Eq. (I-37) are evaluated at time $\{t\}$. The error introduced can be given by the difference between Eq. (I-37) and the Taylor representation (a sum of terms calculated from the values of derivatives at time $\{t\}$) of $\{f_k^*\}$:

$$\frac{1}{2!}\frac{d_{vk}}{dt}\Delta t^2 + O(\Delta t^3) \qquad \text{Eq. (I-38)}$$

Eq. (I-38) suggests that the error introduced at each time step $\{\Delta t\}$ is proportional to the value of the time derivative of $\{v_k\}$ and to $\{\Delta t^2\}$. This error $\{\varepsilon_k\}$ can also be expressed as the difference between the numerical solution $\{f_k\}$ and the exact one $\{\varepsilon_k\}$. Applying (Eq. I-38), we may write:

$$e_k^* + \epsilon_k^* = e_k + \epsilon_k + v_k(e_k + \epsilon_k)\Delta t \qquad \text{Eq. (I-39)}$$

Replacing, in Eq. (I-39), $\{v_k\}$ by its Taylor representation limited to the first order[1], we obtain:

$$e_k^* + \epsilon_k^* = e_k + \epsilon_k + v_k(e_k)\Delta t + \epsilon_k \frac{d_{vk}}{de_k}(e_k)\Delta t \qquad \text{Eq. (I-40)}$$

If the exact solution $\{\varepsilon_k\}$ obeys to Eq. (I-37) then we may write:

$$\frac{\epsilon_k^*}{\epsilon_k} = 1 + \frac{dv_k}{de_k}(e_k)\Delta t \qquad \text{Eq. (I-41)}$$

To ensure stability, the error at $\{t+\Delta t\}$, $\{\varepsilon_k^*\}$ has to be lower than that introduced at $\{t\}$, $\{\varepsilon_k\}$. This condition is satisfied when:

$$\frac{dv_k}{de_k} < 0 \qquad \text{Eq. (I-42)}$$

and

$$\left|\frac{dv_k}{de_k}\right| \Delta t < 2 \qquad \text{Eq. (I-43)}$$

The Euler explicit scheme is, in fact, conditionally stable.

*I-3.5.2. Implicit scheme*

According to the implicit scheme, $\{f_k^*\}$ is evaluated using Eq. (I-44):

$$f_k^* = f_k + v_k^* \Delta t \qquad \text{Eq. (I-44)}$$

Applying the same error propagation analysis as in the explicit scheme we obtain:

[1] To ease the error propagation analysis, we consider a system of ODEs reduced to one equation.

$$\frac{\epsilon_k^*}{\epsilon_k} = \frac{1}{1 - \frac{dv_k}{de_k}(e_k^*)\Delta t} \qquad \text{Eq. (I-45)}$$

When the problem is well formulated, the derivative of $\{v_k\}$ in Eq. (I-45) is negative and the scheme is stable regardless of the value given to the time step. One drawback of the implicit Euler scheme is the fact that the term $\{v_k^*\}$ on the right of the equal sign in Eq. (I-44) is evaluated at the current time – $\{t+\Delta t\}$. This implicit (nonlinear) character can be eliminated by replacing the term $\{v_k^*\}$ by its Taylor representation limited to the first order:

$$v_k^* = v_k + \frac{\partial v_k}{\partial f_1}(f_1^* - f_1) + \frac{\partial v_k}{\partial f_2}(f_2^* - f_2) + \frac{\partial v_k}{\partial f_n}(f_n^* - f_n) \qquad \text{Eq. (I.46)}$$

Replacing, in Eq. (I-44), $\{v_k^*\}$ by it expression given by Eq. (I.46), rearranging, we can demonstrate that $\{f_k^*\}$ is the solution of the following (linear) system of equations:

$$b_{11}f_1^* + b_{12}f_2^* + \cdots + b_{1n}f_n^* = w_1 \qquad \text{Eq. (I-47)}$$

$$b_{21}f_1^* + b_{22}f_2^* + \cdots + b_{2n}f_n^* = w_2 \qquad \text{Eq. (I-48)}$$

...

$$b_{n1}f_1^* + b_{n2}f_2^* + \cdots + b_{nn}f_n^* = w_n \qquad \text{Eq. (I-49)}$$

The expressions of coefficients $\{b_{ij}\}$ and $\{w_i\}$ are given by Eq. (I-50) to Eq. (I-52).

$$b_{ij;j\neq i} = \frac{\partial v_i}{\partial f_j}\Delta t \qquad \text{Eq. (I-50)}$$

$$b_{ii} = -1 + \frac{\partial v_i}{\partial f_i}\Delta t \qquad \text{Eq. (I-51)}$$

$$w_i = -v_i\Delta t + \left(-1 + \frac{\partial v_i}{\partial f_i}\Delta t\right)f_i + \sum_{j\neq i}\frac{\partial v_i}{\partial f_j}\Delta t f_j \qquad \text{Eq. (I-52)}$$

## I-4. CONCLUSION

A new modelling approach was developed to simulate the dynamics of multieffect evaporators. The methodology is based on the representation of plant components using networks of well-stirred volumes and links. Well-stirred volumes evaluate the instant temperatures, pressures and salinities in different regions. Links calculate the flows of mass and energies between different volumes. The corresponding models are analytical: they derive from basic mass, momentum and energy conservation principles applied to process subsystems. They also include correlations for heat transfer coefficients and thermo physical properties of pure and saline water. The new models introduced are associated to the following circuits: non-condensable gas extraction, seawater preheat, distilled water and brine extraction, and multieffect evaporators. They represent components like booster pumps, variable speed pumps, shell and tube heat exchangers, plate-type heat exchangers, evaporators and condensers. The thermo physical properties correlations of (sub-cooled and saturated) pure water, and dry air, are based on the EES software built-in functions. The properties of saline water are deduced from the characteristics of pure water assuming the dissolved salts–water solution to be ideal.

The physical models, the related correlations, the explicit and implicit variants of the Euler (numerical) method, were used to build a C++ code implementing an OOP approach. This program is now being used to simulate the dynamics of an existing MEE plant. The simulation results will be compared to experimental data. Once validated, the model will be enriched to include options like mechanical and thermal vapour compression, and then applied to plants operated by our partners. Many of the unitary operations used in MSF and RO plants (tanks, ducts, tees, pumps, heat exchangers, etc.) were already modelled in the context of this study. U unified modelling approach for both thermal and membrane-based desalination processes can be developed on the base of the work, extending the MEE models and validating the new modules.

# ANNEX II
# NEW FINANCIAL MODELING FOR FEASIBILITY OF COGENERATION PROJECTS: NET PRESENT VALUE ANALYSIS FINANCIAL MODELING TOOL

II-1. GENERAL CONTEXT

## II-1.1. Introduction

This annex develops the net present value model for a co-located water and electricity plant using nuclear fuel. The emphasis of the model is to determine the threshold of combined average water and electricity demand that, given costs, can make the project break-even. In this work, we will ignore the complication of time varying demand or growth in demand over time. The model developed here is implemented in an excel spreadsheet.

## II-1.2. Inputs for the model

The followings are required inputs by the model:

$K_j$ is overnight capital cost of sitting the plant for product $j$, $j \in (e, w)$ wherein $e$ denotes electricity, and $w$ denotes water;

$D_j$ is decommissioning costs for plant $j$ to be incurred at the end of the project (assumed to be equity financed);

$L_j$ is operational life of the plant $j$;

$T_j$ is construction period in years rounded to nearest integer. $T \geq 1$;

$F_j$ is annual fixed maintenance cost of the plant $j$;

$d_j$ is proportion of overnight capital cost that is debt financed for plant $j$;

$r_j^d$ is interest rate on the debt for plant $j$;

$r_j^e$ is discount rate on equity for plant $j$;

$I_j$ is loan payment per year per dollar of debt (includes both interest cost and repayment of principal) for plant $j$;

$E$ is gross capacity of the electricity plant including the inputs into production of water;

$W$ is gross capacity of the water plant including any water needed for production of electricity;

$\beta_e$ is quantity of electricity needed to produce 1 unit of water;

$\beta_w$ is quantity of water required to produce 1 unit of electricity;

$Q_j^k$ is quantity sold of product *j* to customer class *k*;

$Q_j$ is total quantity of product *j* sold to all customer classes combined in the base year;

$$Q^j = \Sigma_k \, Q_k^j \qquad \text{Eq. (II-1)}$$

$V_j$ is variable cost of producing *1* unit of product[2] *j*;

$P_j^k$ is price charged for product *j* to customer class $k \in (t,c,i,h,a,x)$ *k,* wherein:

- *t* denotes tourist use;
- *c* denotes commercial use;
- *i* denotes industrial use;
- *h* denotes residential use;
- *a* denotes agricultural use;
- *x* denotes exports.

### II-1.3. The supply side

We first derive the MPP frontier of the plant, and the marginal costs.

*II-1.3.1. Maximum possible production*

$$Q_e + \beta_e Q_w \leq E \qquad \text{Eq. (II-2)}$$

$$Q_w + \beta_w Q \leq W \qquad \text{Eq. (II-3)}$$

MPP represents all possible combinations of electricity and water that it can sell to final consumers i.e. net of any electricity required to produce water and vice versa within the plant. MPP is given by the combination of $Q_e$, $Q_w$ that satisfies both conditions above. To determine the corner point of the PPF, we solve for $Q_e$, $Q_w$ that just exhausts the capacities E, W. The solution is illustrated by Fig. II-1. And following equations:

[2] Variable cost is independent of end user. However, in the spreadsheet implementation of the model, we assume that the variable cost depends on whether only one or both plants are sited. This is because production of water requires electricity and potentially vice versa. If the investor were to own both the water and electricity plants he can avail of energy or water component of inputs and marginal costs. However, if he were to own only one plant he will have to buy the other input at market prices which are likely to exceed marginal costs.

$$Q_e = \frac{E - \beta_e W}{1 - \beta_e \beta_w} \qquad \text{Eq. (II-4)}$$

$$Q_w = \frac{W - \beta_w E}{1 - \beta_e \beta_w} \qquad \text{Eq. (II-5)}$$

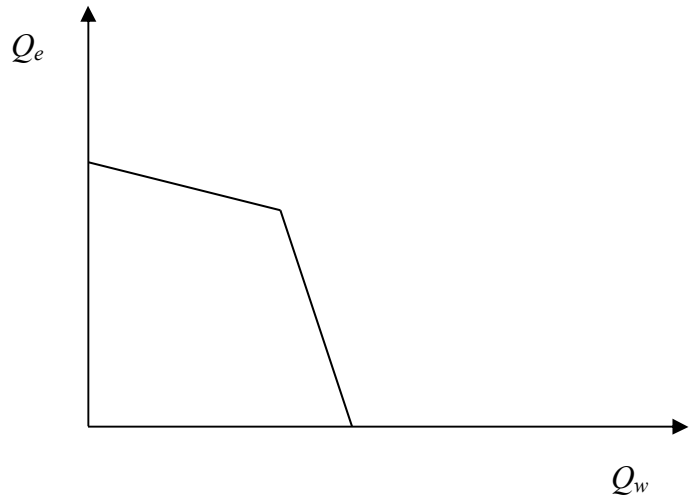


*FIG. II-1. MPP line.*

*II-1.3.2. Variable costs*

Consider the scenario in which production of water requires electricity and that electricity requires water. Then to compute the variable cost of water, the plant operator needs to figure out the variable cost of electricity, but that in turn is unknown since production of electricity requires water. In this scenario, true variable costs are computed as follows in a simultaneous equation system.

The variable cost of production, of say water, can be modelled as follows:

$$V = V_w^{other} + \beta_e V_e \qquad \text{Eq. (II-6)}$$

Where:

$V_w^{other}$ is cost of the inputs that go into the production of water other than electricity;

$V_e$ is marginal cost of one unit of electricity;

$\beta_e$ is quantity of electricity required to produce one unit of water.

Analogously, for electricity:

$$V_e = V_e^{other} + \beta_w V_w \qquad \text{Eq. (II-7)}$$

Solving the previous two equations, we get true variable costs:

$$V_w = \frac{V_w^{other} + \beta_e V_e^{other}}{(1-\beta_e\beta_w)} \qquad \text{Eq. (II-8)}$$

$$V_e = \frac{V_e^{other} + \beta_w V_w^{other}}{(1-\beta_e\beta_w)} \qquad \text{Eq. (II-9)}$$

### II-1.4. The demand side: Net present value model

We can write the *NPV* model of the project *j* (*j* is either water or electricity) as evaluated at the beginning of its operational period as follows:

$$NPV_j = -(1-d_j)\sum_{t=1}^{T_j}\frac{K_j}{T_j}(1+r_j^e)^t - \sum_{t=1}^{L_j}\frac{F_j}{(1+r_j^e)^t} - \sum_{t=1}^{L_j}\frac{I_j}{(1+r_j^e)^t}(d_j\sum_{t=1}^{T_j}\frac{K_j}{T_j}(1+r_j^d)^t \qquad \text{Eq. (II-10)}$$

$$-\frac{D_j}{(1+r^e)^{L_j}} + \sum_{k\in(t,c,i,h,a,x)}\sum_{t=1}^{L_j}\frac{(P_j^k - V_j)}{(1+r_e)^t}Q_j^k \qquad \text{Eq. (II-11)}$$

On the first line of the above expression, the first term on the right hand side is *NPV* of the equity outlay during the construction period, the second term is the *NPV* of the annual fixed costs and the third term is the *NPV* of the debt service payments over the life of the debt which is assumed to be the same as the operational life of the plant. All these terms are expected to be negative. On the second line, the first term is the discounted value of the decommissioning costs and the summation in the second term is over the operational cash flows from the sale of each product to each customer class in each year discounted to the beginning of the operations.

We now use the following well-known formulae concerning the sum of geometric series to simply the above expression for *NPV*.

$$\sum_{t=1}^{T}(1+r)^t = \frac{(1+r)}{r}[(1+r)^T - 1] \qquad \text{Eq. (II-12)}$$

$$\sum_{t=1}^{L}\frac{1}{(1+r_e)^t} = \frac{1-(1+r_e)^{-L}}{r_e} \qquad \text{Eq. (II-13)}$$

The expression for *NPV* now reduces to:

$$NPV_j = -(1-d_j)\frac{K_j}{T_j}\frac{(1+r_j^e)}{r_j^e}[(1+r_j^e)^{T_j} - 1] - \frac{1-(1+r_j^e)^{-L_j}}{r_j^e}[F_j - \frac{K_j}{T_j}\frac{(1+r_j^d)}{r_j^d}\{(1+r_j^d)^{T_j} - 1\}I_j d_j]$$

$$-\frac{D_j}{(1+r_j^e)^{L_j}} + \sum_{k\in(t,c,i,h,a,x)}\frac{1-(1+r_j^e)^{-L_j}}{r_j^e}(P_j^k - V_j)Q_j^k$$

Eq. (II-14) and Eq. (II-15)

We will now denote the following cash flow multipliers. All these are constants for a given interest rate and time period.

$$m_j^e = \frac{(1+r_j^e)}{r_j^e}[(1+r_j^e)^{T_j} - 1] \qquad \text{Eq. (II-16)}$$

$$m_j^d = \frac{(1+r_j^d)}{r_j^d}[(1+r_j^d)^{T_j} - 1] \qquad \text{Eq. (II-17)}$$

$$m_j^l = \frac{1-(1+r_j^e)^{-Lj}}{r_j^e} \qquad \text{Eq. (II.18)}$$

Substituting in the expression for *NPV*:

$$NPV_j = -(1-d_j)\frac{K_j}{T_j}m_j^e - m_j^l(F_j - m_j^d\frac{K_j}{T_j}I_j d_j) - \frac{D}{(1+r_j^e)^{L_j}} + m_j^l \sum_{k\in(t,c,i,h,a,x)}(P_j^k - V_j)Q_j^k$$

Eq. (II-19)

Lastly, denoting the sum of quantity invariant terms in the above expression for *NPV*, namely:

$$-(1-d_j)\frac{K_j}{T_j}m_j^e - m_j^l(F_j - m_j^d\frac{K_j}{T_j}I_j d_j) - \frac{D}{(1+r_j^e)^{L_j}} \qquad \text{Eq. (II.20)}$$

as $-C_j$, we get:

$$NPV_j = -C_j + m_j^l \sum_{k\in(t,c,i,h,a)}(P_j^k - V_j)Q_j^k \qquad \text{Eq. (II-21)}$$

Summing over the two plants, we get the *NPV* of the combined project as:

$$NPV = \sum_{j\in(e,w)} NPV_j = -\sum_{j\in(e,w)} C_j + \sum_{j\in(e,w)} m_j^l \times \sum_{k\in(t,c,i,h,a)} (P_j^k - V_j)Q_j^k \qquad \text{Eq. (II-22)}$$

This is the version of the *NPV* equation that is used in the accompanying spread sheet.

Setting the above expression for *NPV* to 0, we get the equation of the hyper-plane that divides the space of possible demand (characterized by the vector) into two regions. In one region given by NPV>0, the project is in the profitable proposition. In the other region given by NPV< 0, the project is a loss proposition.

We will now reduce the dimension of the solution space by imposing some feasibility constraints on the demand vector. We postulate that both for electricity and for water demand

for each customer class is a constant fraction of total demand, though the fractions can vary between the two products.

Denoting:

- Total demand for product $j \in (e, w)$ as , $Q_j = \sum_k Q_j^k$
- Share of customer class $k \in (t, c, i, h, a)$ in total demand for product $j$ as $a_j^k$

We impose the restrictions:

$$Q_w^k = \alpha_w^k Q_w \text{, where } k \in (t, c, i, h, a, x); \qquad \text{Eq. (II-23)}$$

$$Q_e^k = \alpha_e^k Q_e \text{, where } k \in (t, c, i, h, a, x); \qquad \text{Eq. (II-24)}$$

Using these restrictions, and denoting weighted average revenue per unit of product $j$ as $P_j^\alpha = \sum_k \alpha_j^k P_j^k$ , the expression for *NPV*, reduces to:

$$NPV = -C_w - C_e + m_e^l (P_e^\alpha - V_e) Q_e + m_w^l (P_w^\alpha - V_w) Q_w \qquad \text{Eq. (II-25)}$$

Our solution space is now only two-dimensional. Setting the equation to zero, we can delineate the region in which the co-project is in the money starting from the inputs listed in the beginning of this document.

$$-C_w - C_e + m_e^l (P_e^\alpha - V_e) Q_e + m_w^l (P_w^\alpha - V_w) Q_w = 0 \qquad \text{Eq. (II-26)}$$

A typical graphical representation of the above equation, which we call the *NPV* = 0 line, is shown in Fig. II-2. For the project to break demand for water and electricity must lie to the right of the line.

### II-1.5. Viability analysis

In order to determine whether the operating regions lie below or above the NPV line, a comparison is made using the MPP curve of water and electricity for given project sizes and annual load (Fig. II-3. and Table II-1.).

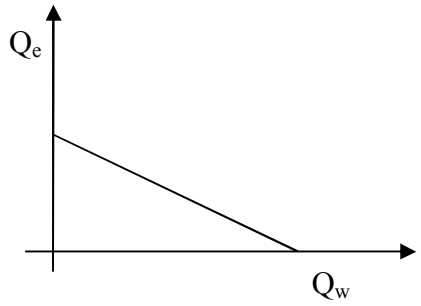


*FIG. II-2. NPV line at Breakeven.*

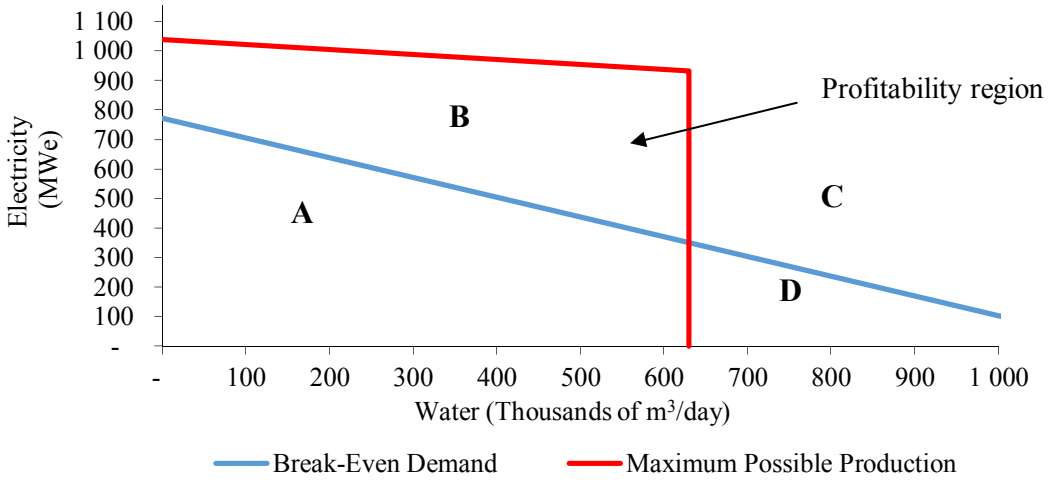


*FIG. II-3. MPP curve of water and electricity.*

The region between the NPV line and the MPP curve is the profitability region. The NPV line separates all the combinations of water production and direct electricity sales that are financially viable (above the line) from those that are not (below). The MPP curve identifies all the combinations of water production and direct electricity sales that are physically possible with the technology, all combinations inside (below) the red line are possible to produce.

The table below (Table II-1.) illustrates the possible combinations of physically and economically viable projects.

TABLE II-1. VIABILITY ANALYSIS

| | Economically viable | Physically viable |
|---|---|---|
| Region A | No | Yes |
| Region B | Yes | Yes |
| Region C | Yes | No |
| Region D | No | No |

### II-1.6. Shifting of the NPV line

The trends in shifts of the NPV line are a function of specific variations in key model parameters. A parallel shift in the NPV line occurs due to a change in any of the non-variable (or fixed) costs (fixed costs capital, decommissioning and other fixed costs). This can be concluded directly from the NPV equation. If any of these non-variable costs increase, the NPV line would shift outwards, reducing the region of profitability between the NPV and MPP lines and vice versa. The slope of the NPV line is given by the ratio (P–V) water / (P–V) electricity. Thus, if the variable cost or price of any of the two product changes, it will change the slope of the NPV line unless the price or variable cost of the other product also changes in a compensating way so as to maintain the same ratio. Indeed, it will be demonstrated that in

the exports scenario, the surplus from water sales will increases proportionately more than the surplus from electricity causing an increase in the slope of the NPV line.

## II-2. ARGONNE'S FINANCIAL MODEL PARAMETERS

The "power law rule" is used to calculate the capital cost of the varying water plant capacities. Using the power law formulation and available values from the literature, a set of water plant capacities and their respective capital costs were calculated (Table II-2.). Also, typical unit production costs are listed in Table II-2. All other model input parameters and the basis for choosing specific values are summarized in Tables II-3., II-4., II-5., and II-6.

TABLE II-2. RO WATER DESALINATION PLANT SIZES AND CORRESPONDING CAPITAL COSTS

| Water plant size (maximum production capacity in $m^3$/day) | Capital cost (million $) | Unit production cost ($) | Basis |
|---|---|---|---|
| 10 000 | 20.1 | 0.95 | From Wittholz et al., *Desalination,* 229 (2008). |
| 50 000 | 74 | 0.70 | |
| 275 000 | 293 | 0.50 | |
| 500 000 | 476.7 | 0.45 | |

TABLE II-3. ELECTRICITY PARAMETERS

| Parameters | Value | Basis |
|---|---|---|
| Plant Life | 40 years | Prototype EPR |
| Capacity | 1154 MW | |
| Plant load factor | 0.85 | Design |
| Construction period | 5 years | The economic future of nuclear power, August 2004 |
| Overnight capital cost | Variable | |
| Annual fixed maintenance cost | $69.3 /kW | The economic future of nuclear power, August 2004 |
| Decommissioning costs | 10% of overnight capital costs | |
| Variable costs | $5.687 /kW·h | |

TABLE II-4. DESALINATION PLANT PARAMETERS

| | Value | Basis |
|---|---|---|
| Plant life | 40 years | Economic life of power plant |
| Consumption rate | 0.004 MW·h/ $m^3$ | Bruno Sauvet-Goichon, *Desalination*, 203 (2007) |
| Capacity | 250 500 or 750 thousand $m^3$/day | Typical sizes of large desalination plants |
| Plant load factor | 0.9 | Typical annual availability of desalination plants |

| | Value | Basis |
|---|---|---|
| Unit production cost | Variable | Table III-3. |
| Construction period | 2 years | Typical value |
| Capital and fixed costs | | |
| Overnight capital cost | Variable | |
| Annual fixed maintenance cost | 4% of total operating costs (or unit production cost) | Semiat, R., *Desalination,* 25 (2000) |
| Decommissioning costs | 10% of overnight capital cost | Typical assumption |
| Variable costs | | |
| Maintenance + parts + consumables | 15% of unit production cost | Semiat, R., *Desalination,* 25 (2000) |

TABLE II-5. COST COMPONENT FOR A TYPICAL SEAWATER RO DESALINATION PLANT

| Cost component | % of Total operating cost | Basis |
|---|---|---|
| Maintenance and parts (variable ) | 7 | Semiat, R., *Desalination,* 25 (2000) |
| Membrane replacement (variable ) | 5 | |
| Consumables (variable ) | 3 | |
| Labor (fixed cost) | 4 | |
| Capital and other fixed costs | 37 | |
| Electrical consumption (variable ) | 44 | |

TABLE II-6. GENERAL FINANCIAL PARAMETERS

| Parameter | Value | Basis |
|---|---|---|
| Discount rate on equity | 8%, 14% or 20% | Chosen to yield a range of weighted average capital cost (discount rate) values: 8%, 14% and 20% for the current analysis |
| Interest rate on debt | 4%, 10% or 16% | |
| Debt fraction | 0.5 | The economic future of nuclear power, August 2004 |

# ANNEX III
# LIFE CYCLE ASSESSMENT FOR POWER AND DESALINATION PLANT IMPACTS ON CLIMATE CHANGE

## III-1. GENERAL CONTEXT

### III-1.1. Introduction

The energy chain, from primary energy extraction to end-use, is one of the main sources of GHG emissions. The key GHG emitted by human activities are (Fig. III-1.(a)):

— *Carbon dioxide ($CO_2$)* — Fossil fuel use is the primary source of $CO_2$. The way in which people use land is also an important source of $CO_2$, especially when it involves deforestation;
— *Methane($CH_4$)* — Agricultural activities, waste management, and energy use all contribute to CH4 emissions;
— *Nitrous oxide($N_2O$)* — Agricultural activities, such as fertilizer use;
— *Fluorinated gases (F-gases)* — Industrial processes, refrigeration, and the use of a variety of consumer products contribute to emissions of F-gases, which include hydrofluorocarbons (HFCs), perfluorocarbons (PFCs), and sulphur hexafluoride (SF6).

—

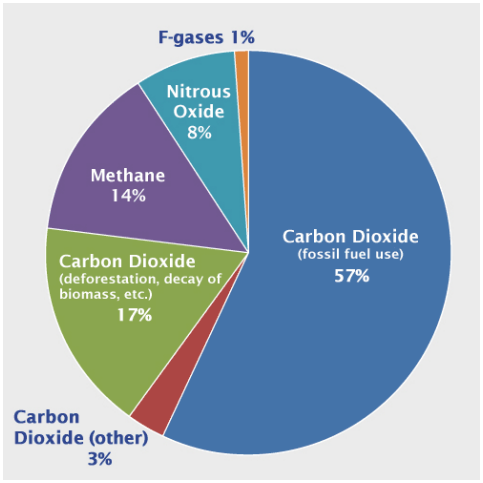


*(a) Global GHG emissions by gas.*

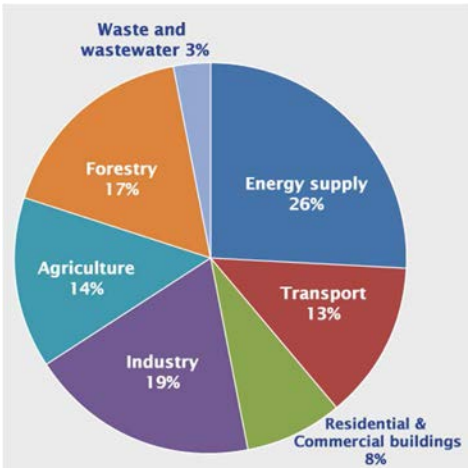


*(b) Global GHG emissions by source (ratio of 2004 global GHG emissions).*

*FIG. III-1. Global GHG emissions.*

Global GHG emissions can also be broken down by the economic activities that lead to their production (Fig.III-1.(b)). Carbon dioxide is the main GHG, because of their potential risk to induce global warming and climate change. Global carbon emissions from fossil fuels have significantly increased since 1900. Emissions increased by over 16 times between 1900 and 2008 and by about 1.5 times between 1990 and 2008 (Fig. III-2.).

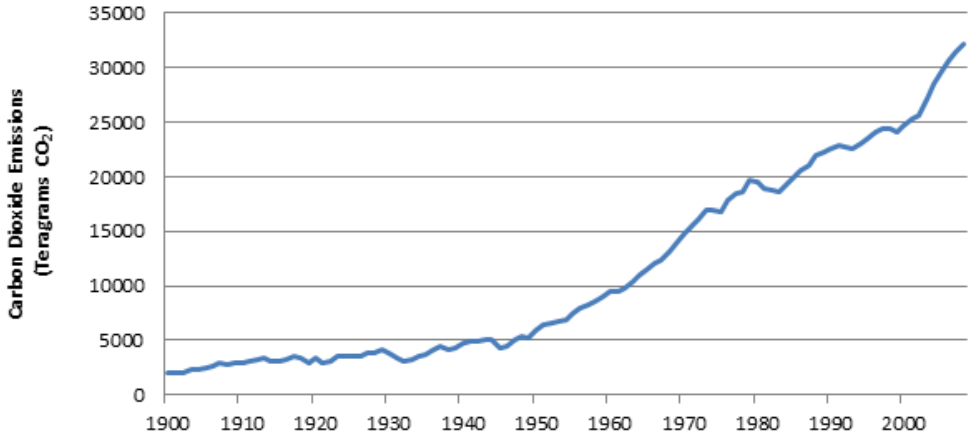


*FIG. III-2. Global carbon dioxide emissions from fossil-fuels 1990–2008.*

Owing to the fact that the burning of fossil fuels contributes about three quarters of man-made GHG emissions, the implementation of less carbon intensive energy systems is high in the list of possible measures for reducing GHG emissions. In this connection, "new and renewable forms of energy" are mentioned explicitly in the Kyoto Protocol.

Indeed, there are a number of technical options that could help in reducing, or at least slowing the increase of, GHG emissions from the energy sector. The list of options includes:

— Improving the efficiency of energy conversion and end-use processes;
— Shifting to less carbon intensive energy sources (e.g. shifting from coal to nuclear);
— Developing carbon-free or low-carbon energy sources;
— Carbon sequestration (e.g. planting forests or capturing and storing carbon dioxide).

However, when the technological readiness and costs of the various options are taken into account, there are only a few options that could be implemented in the short and medium terms at an acceptable cost. The nuclear variants as well as results from a number of other studies show that technically and economically feasible nuclear development paths could contribute significantly to alleviating the risks associated with global climate change. Recognizing that up to now it has proven to be difficult to meet the GHG emission reduction targets proposed at international or national levels, it is important to keep open all the options that could help in achieving those objectives.

Nuclear power is one of the few options that are:

— Currently available on the market;
— Competitive in a number of countries, especially if global costs to society of alternative options are considered;
— Alleviating the risk of global climate change and its potential contribution to GHG emissions reduction;
— Practically carbon-free; and sustainable at large-scale deployment (i.e. large energy supply can be supported by natural resources which are plentiful and have no other use).

The production of energy by burning fossil fuels generates pollutants and some GHG. Since current electricity production heavily relies on fossil fuels, it is envisioned that expanding generation technologies based on nuclear power and renewable energy sources would dramatically reduce future GHG emissions. However, all anthropogenic means of energy production, including nuclear generate pollutants when their entire life cycle is accounted for.

Solar (or renewable energy) and nuclear electricity generation technologies often are deemed "carbon-free" because of their operation does not generate any carbon dioxide. However, this is not so when considering their entire lifecycle of energy production, carbon dioxide and other gases are emitted during the extraction, processing, and disposal of associated materials.

We determined the greenhouse-gas emissions, namely, $CO_2$, $CH_4$, $N_2O$, and chlorofluorocarbons due to materials and energy flows throughout all stages of the life of commercial technologies for solar electric and nuclear power generation, based on data from 12 photovoltaic (PV) companies, and reviews of nuclear-fuel life cycles in the United States, Europe, and Japan. Previous GHG estimates vary widely, from 40 to 180 $CO_2$equ./kW·h for PV, and 3.5 to 100 $CO_2$equ./kW·h for nuclear power. Country-specific parameters account for many of these differences, which are exacerbated by outdated information.

The fuel LCA is used as a tool for evaluation of potential environmental impacts of a product, process, or activity. An LCA study involves data collection and calculation to quantify relevant inputs and outputs or environmental loads of a product system. Environmental loads represent resources consumed and emissions released into the environment. One of the most significant contributors to environmental loads of most systems is energy that is essential to operate and run unit processes for the production of products and services in all industrial systems.

Building LCA software package for energy production system is important in order to improve environmental performance of an electricity generation system itself as well as to provide industries with a basic database required to carry out LCA studies for their own products. Building LCA software package for power production is valuable for effective environmental management of power producers as well as industrial systems that use electricity. In addition, since the power production sector is being subjected to increasingly stringent environmental regulations, establishing environmental loads data for power production is important to identify and improve its environmental aspects.

LCA investigates the environmental impacts throughout the full lifecycle of product or system. Since environmental awareness and regulations are growing, LCA can improve the efficacy of environmental regulation since it can pinpoint with great certainty the source of, for example, environmental pollution or resource use of upstream and downstream processes. GHG LCA can provide information during which stage of the lifecycle significant emissions occur and therefore aid policymakers and stakeholders in focusing efforts where they are most effective in reducing GHG emissions. Comparing between two or more alternatives, LCA can help decision-makers to compare the total cumulative emissions originating from a choice of technologies per unit of electricity. In addition to their use as a tool for decision-making LCA can be used for informing consumers, education, marketing etc. (e.g. environmental labelling, environmental product declaration).

This study discusses the results of the assessed LCAs, as well as highlighting the most significant processes of GHG (carbon dioxide ($CO_2$), nitrogen oxides ($NO_x$), sulphur oxides ($SO_x$), methane ($CH_4$), carbon monoxide (CO), ammonia ($NH_3$), hydrogen sulphide ($H_2S$), formaldehyde ($CH_2O$), non-methane hydrocarbons (NMHCs) and particulates) release for the technologies under consideration. The GHG emission estimates presented here reflect the assessment methodology, conversion efficiency, practices in fuel preparation and transport, technology and fuel choice, the fuel mix assumed for electricity requirements related to plant construction and manufacturing of equipment, and the assessment boundary (i.e. what processes are included in the analysis and which ones are not). Analysing upstream and downstream processes and its associated GHG emissions, of the power plant (i.e. electricity generation stage), is important since otherwise the GHG emissions resulting from electricity generation of the various fuel options are underestimated.

The goal of this study was to build a computer program by using the engineering equation tool to present and analyse the economics of the lifecycle greenhouse emission of electricity generation and water production chains (coal, natural gas, oil and nuclear). A sensitivity analysis for the computer program was performed to find the effectiveness of assumptions and to find the key factors (variables) influencing the life cycle energy use and greenhouse emissions. The GHG are classified under global warming category and the GWP per functional unit is calculated in $CO_2$ equivalent units. The annual GHG emissions for the two future electricity supply and water production options in Egypt's plan and the total GHG emissions over the expansion plan (2007/2008–2026/2027) for the two future electricity supply and water production options are estimated.

The results in the present study are generic, since the comparison of results presents an overview of emissions that can be usually expected. However, variations exist according to site-specific conditions (e.g. technology, carbon content of fuel, climatic conditions, etc.) This comparison can be practical for policymakers, since policy decisions are often required before detailed site-specific information becomes available.

The work on this project was started in 2010 as a coordinated research project with the IAEA. The main objective of the project was to develop an economic assessment tool for power and desalination plants impacts on climate.

The goal of the study is to provide decision makers with simple, soundly based, indicators of cost performance for a range of different electricity generation and water production technologies and fuels.

The main objectives of the study are:

1. Build a computer program by using the EES tool to present and analyse the lifecycle greenhouse emission cost for the electricity generation and the water production chains (coal, natural gas, oil and nuclear);
2. A sensitivity analysis for the computer program (program verification) will perform to find the effectiveness of assumptions and to find the key factors (variables) influencing the life cycle energy use and greenhouse emissions;
3. The global worming potential (GWP) per kW·h of electricity production will calculate in $CO_2$ equivalents unit;

4. To calculate annual GHG emissions for 1000 MW€ power plant (coal, NG, oil, nuclear);
5. To calculate the global worming potential (GWP) per $m^3$ of water production in $CO_2$ equivalents unit;
6. Annual 200 000 $m^3$/day MED, MSF and RO desalination plants GHG emissions will calculate;
7. The cost of the GHG for electricity generation and water production will calculate.

The work plan has been as the following:

(IV) The first Year (2010) developing computer software:

— Modelling of life time chain cycle;
— Developing the computer software;
— Testing the software through the sensitivity analysis;
— Progress report.

(B) The second year (2011) case study:

— Evaluating the global worming for electricity and water desalination for a nuclear desalination plant using a case study of Egypt.

€ Attached work done:

— Modelling of GHG life time chain cycle;
— Developing the computer software;
— Testing the software through the sensitivity analysis.

III-2. MATHEMATICAL MODEL

**III-2.1. Basic methodology**

LCA seeks to make general statements about the GHG emissions of a particular type of coal, oil, natural gas and nuclear life cycles stages.

For electricity generation, LCA would account for GHG emissions at the following stages:

— Energy resource exploration, extraction and processing;
— Raw materials extraction for technology and infrastructure;
— Production of infrastructure and fuels;
— Production and construction of technology;
— Transport of fuel;
— Other related transport activities (e.g. during construction, decommissioning;
— Conversion to electricity or heat or mechanical energy; and waste management and waste management infrastructure (e.g. radioactive waste depositories, ash disposal.

The rate of emission of GHG is influenced by numerous factors. The dominant parameters for each fuel type are:

***Fossil fuels***

- Fuel characteristics such as carbon content and caloric value;
- Type of mine;
- Fuel extraction practices (affecting transport requirements and methane releases);
- Transmission losses for natural gas;
- Conversion efficiency;
- Fuel mix for electricity needs associated with fuel supply and plant construction/ decommissioning.

***Nuclear power (light water reactor)***

- Energy use for fuel extraction, conversion, enrichment and construction/ decommissioning;
- Fuel enrichment by gas centrifuge, which is an energy less intensive process that can decrease GHG releases by an order of magnitude when compared to enrichment by diffusion;
- Emissions from the enrichment step, which are highly country-specific since they depend on the local fuel mix.

Some basic features of the methodology:

- It covers the complete fuel life cycle chain (fuel extraction and conversion, transportation, electricity generation and waste management). All chains are described on a "cradle to grave" basis, with each step in the cycle being decomposed into construction, operation and dismantling;
- It covers not only direct (concentrated) emissions from the life cycle but also indirect (grey or diffuse) ones that are considered in order to provide as complete as possible representation of the total environmental fluxes;
- Material inputs are considered in connection with all steps of a fuel cycle, also construction efforts and materials for the infrastructure are included in the analysis;
- A consistent set of data for material (concrete, steel) used in construction, production and decommissioning was developed to be used by all energy chains;
- For electricity inputs resulting from the Egyptian generation mixes were used through analysis;
- Only air pollutants ($CO_2$, $CH_4$, $NO_x$, $H_2S$, $NH_3$, CO, $CH_2O$, NMHCs, $SO_x$ and particulates) are considered;
- The impact of carbon dioxide emissions costs have taken into consideration in the analysis. A range of costs has been considered, i.e. \$50 per $CO_2$equ.·tonne.

LCA computer program uses a simplified version of the process analysis technique to perform the assessment of full energy chains. Process analysis is a microanalysis in which complex system is divided into well-defined process steps and sub-systems.

The energy uses of some upstream fuel life cycles processes were gathered from various literature sources. Electricity production for use in upstream process was assumed to be the generation mix of Egypt. The LCA for the fuel life cycles of electricity generation (coal, natural gas, fuel oil and nuclear) are computed by using the engineering equation solver software, EES.

The life cycle primary energy use is estimated as the sum of the energy consumed in the life cycle processes, which includes energy consumed in exploration, extraction, processing, manufacturing, decommissioning, severe accidents and disposal of all the materials associated with the power generation system.

By tracing the primary sources of energy, a major GHG, namely, $CO_2$, $CH_4$, $NO_x$, and others gases $H_2S$, $NH_3$, CO, $CH_2O$, NMHCs, $SO_x$ and particulates are estimated. The different fuel life cycles analysis results are compared. Carbon dioxide $CO_2$, methane $CH_4$ and nitrous oxide $N_2O$ are the main contribution to atmospheric warming. The specific contribution of $CH_4$ and $N_2O$ have been assessed respectively as 21 and 310 time that of $CO_2$. The GHG are classified under global warming category and the GWP per functional unit is calculated in $CO_2$ equivalents unit. Also, the climate warming rise temperature in the area centred by the power plant is calculated.

III-3. LIFE CYCLE CHAIN CALCULATIONS

**III-3.1. Coal life cycle chain**

The coal life cycle chain covered all the processes in the life cycle of the product, starting from the extraction of raw materials from nature and finishing with the delivery of electricity.

In coal-fired power plants, the largest part of lifecycle GHG emissions arises at the power plant. For presently operating plants, emissions at the operating stage range between 800–1000 $gCO_2$equ./kW€·h, whereas cumulative emissions for the same plants range between approximately 950–1250 $gCO_2$equ./kW€·h. The d difference arises at up and downstream stages, which have been recorded to lie between roughly 50–300 $gCO_2$equ./kW€·h. While GHG emissions from construction, decommissioning and waste disposal are negligible, emissions relating to coal mining and coal transport can be significant. The coal life cycle chain is represented in Fig. III-3.

The following processes were included in the inventory:

- Mining and processing of the hard coal;
- Manufacturing of the raw materials;
- All transportation processes for which emission data were to be obtained;
- Conversion of hard coal into electricity in the power plant;
- electricity and heat generation related to the hard coal mining, and to produce raw materials;

— Savings in the external processes through waste recovery.

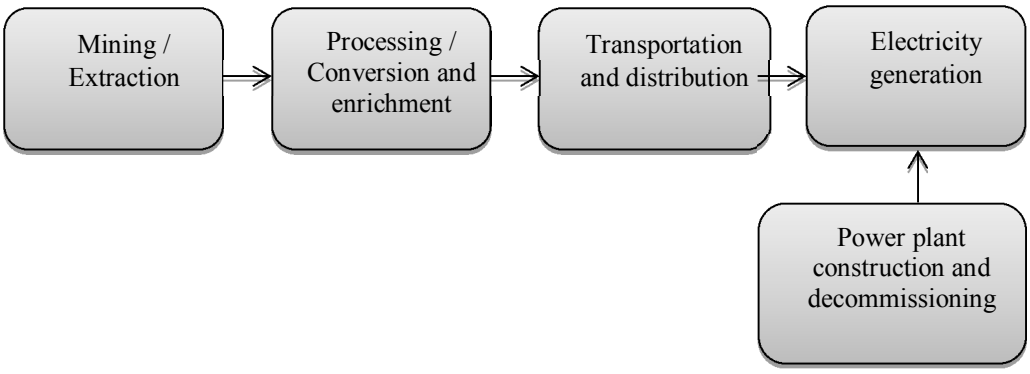


*FIG. III-3. The coal life cycle chain.*

Material and energy flows were quantified for each process. The specifications required for calculation include the coal characteristics (low calorific value, carbon content, sulphur content, nitrogen content, ash content, moisture content), technology designation and average transport distance. Information on power plant size (MW€), plant efficiency (%), equivalent full power of operation hours (h/year) are also required.

Calculations are carried out from mining (level II) to electricity generation (level VI). The energy uses of some upstream processes were gathered from various literature sources. Electricity production for use in upstream process was assumed to be the generation mix of Egypt.

### III-3.2. Mass flow calculations

The mass flow of the primary energy sources was calculated starting from power plant and working backward through each front-end process. Then the waste generated is calculated based on the fuel requirements at the power plant. The mass flows in the coal life cycle chain are represented in Fig. III-4.

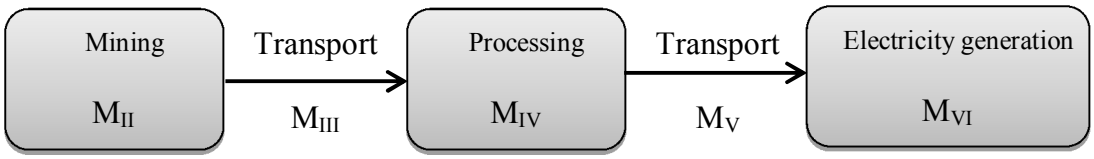


*FIG. III-4. Mass flow in the coal life cycle chain.*

*III-3.2.1. Power plant coal requirements (level VI)*

The quantity of coal required at the power plant per kW·h electricity produced is based on the characteristic of the power plant and the coal:

$$M_{VI} = \frac{360\ 000}{LHV \times \eta} \qquad \text{Eq. (III-1)}$$

Where:

$M_{VI}$ is quantity of coal burned at power plant (g/kW·h);

$LHV$ is lower heating value of coal (MJ/kg);

$\eta$ is power plant thermal efficiency (%).

*III-3.2.2. Power plant annual coal requirements*

The quantity of coal required at power plant per year produced is based on the characteristics of the power plant and the fuel:

$$M_{VI}a = \frac{P \times H \times M_{VI} \times f_{fi}}{1000} \qquad \text{Eq. (III-2)}$$

Where:

$M_{VI}a$ is quality of coal required at power plant per year (g/kW·h);

$P$ is plant net output capacity (MW€);

$H$ is equivalent full power of operation (h/year);

$f_{fi}$ is fraction of coal burned.

*III-3.2.3. Transportation of processed coal (level V)*

The losses in transportation are considered in calculating the mass flow:

$$M_V = M_{VI} \times (1 + L_V \times D_V \times 10^{-6}) \qquad \text{Eq. (III-3)}$$

Where:

$M_V$ is transportation mass flow (g/kW·h);

$L_V$ is losses in transportation of the processed coal (g/t·km);

$D_V$ is transportation distance (km).

*III-3.2.4. Coal processing (level IV)*

The losses during processing are considered using the efficiency of the process:

$$M_{IV} = M_V / \eta_{IV} \qquad \text{Eq. (III-4)}$$

Where:

$M_{IV}$ is processing mass flow (g/kW·h);

$\eta_{IV}$ is processing efficiency.

*III-3.2.5. Transportation of raw coal (level III)*

The losses in transportation of the raw coal are considered in calculating mass flow:

$$M_{III} = M_V \times (1 + L_{III} \times D_{III} 10^{-6}) \qquad \text{Eq. (III-5)}$$

Where:

$M_{III}$ is transportation of raw coal mass flow (g/kW·h);

$L_{III}$ is losses in transportation of the raw coal (g/t·km);

$D_{III}$ is transportation distance (km).

*III-3.2.6. Mining (level II)*

The losses at the mining site (e.g. handling, storage) are accounted for using a mining factor:

$$M_{II} = M_{III} \times MF \qquad \text{Eq. (III-6)}$$

Where:

$M_{II}$ is mining mass flow in (g/kW·h);

$MF$ is mining factor;

*III-3.2.7. Solid waste generation by the power plant*

The fly ash generated is calculated using the following formula:

$$M_{VIA} = \frac{ACF}{100} \times M_{VI} (1 - \frac{IC_{ASH}}{100}) \qquad \text{Eq. (III-7)}$$

Where:

$M_{VIA}$ is fly ash generated mass flow (g/kW·h);

$IC_{ASH}$ is the inherent of the technology (fraction of the bottom ash from total in coal);

$ACF$ is ash content in primary coal (%).

**III-3.3. Calculation of emission factors**

*III-3.3.1. Direct (concentrated) emissions*

The direct emissions generated from the coal life cycle process (mining, processing, electricity generation) itself are calculated using the formula:

$$EF_{Di} = M_p \times EF_i / 1000 \qquad \text{Eq. (III-8)}$$

Where:

$EF_{Di}$ is direct emissions of the pollutant i generated from a certain process (g/kW·h);

$EF_i$ is emission factor of the pollutant *i* (g/kg);

$M_P$ is coal mass flow at a certain process (g/kW·h).

*III-3.3.2. Indirect (grey) emissions*

The indirect emissions factors associated to the production of the materials used in the construction of the facility are distributed over the life cycle processes during the economic life time of the facility. The emissions factors are:

$$EF_{IDi} = \frac{1}{H \times L} \sum EF_{im} \times REQ \qquad \text{Eq. (III-9)}$$

Where:

$EF_{Idi}$ is indirect emissions of the pollutant i generated from a certain process (g/kW·h);

$H$ is equivalent full hours of operation per year;

$L$ is economic lifetime of the facility;

$EF_{im}$ is emissions factors for the pollutant i associated with the production of the materials;

$REQ = HREQ + MREQ$ where (*HREQ* and *MREQ* are the heat and mechanical power requirements in a production of materials).

## III-3.4. Natural gas life cycle chain

Natural gas is a naturally occurring mixture of hydrocarbon and non-hydrocarbon gases found in porous geologic formations beneath the earth's surface. The chemical composition of natural gas varies from site to site. The principal component of natural gas is methane ($CH_4$) often representing between 70% and 95% of the raw mix. The natural gas life cycle chain covered all the processes in the life cycle of the product, starting from the gas recovery and finishing with the delivery of electricity (Fig. III-5.).

The majority of GHG emissions from gas-fired power plants arise during the operation of the power plant and range according to the literature between 360–575 g$CO_2$equ./kW€·h for present technologies. No significant emissions arise during the construction and decommissioning of the power plant. However, significant fuel-cycle GHG emissions exist. They are mainly from gas processing, venting wells, pipeline operation (mainly compressors) and system leakage in transportation and handling. Because these factors vary amongst

countries, the import structure can be an important factor in determining cumulative emissions.

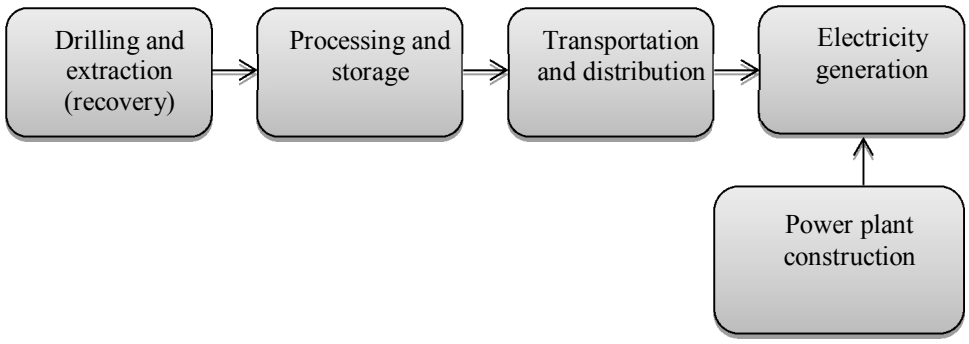


*FIG. III-5. Natural gas life cycle chain.*

The following processes were included in the inventory:

- Recovery and purification of the natural gas;
- Manufacturing of the raw materials;
- All transportation processes for which emission data were obtainable;
- Conversion of the natural gas into the electricity in the power plant;
- Electricity and heat generation related to the natural gas recovery and purification, and to produce raw materials.

The specifications required for calculations include natural gas characteristics (low calorific value, methane and other gases content), technology designation and average transport distance. Information on power plant size (MW€), plant efficiency (%), equivalent full power of operation hours (h/year) are also required.

Calculations are carried out from gas drilling (level II) to electricity generation (level VI). The energy uses of some upstream processes were gathered from various literature sources. Electricity production for use in upstream process was assumed to be the generation mix of Egypt.

### III-3.5. Natural gas volume flow calculations

The volume flow of the natural gas in the life cycle chain is calculated from power plant (level VI) and working backwards through each front-end step. The gas volume flows in the natural gas life cycle chain are represented in Fig. III-6.

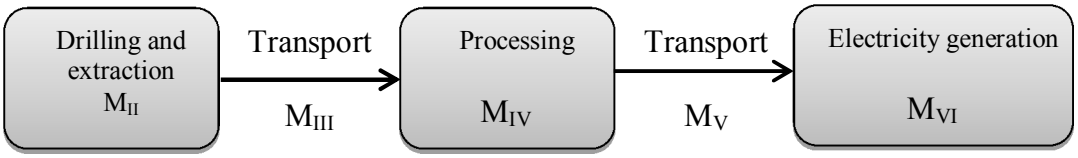


*FIG. III-6. Mass flow in the natural gas life cycle chain.*

*III-3.5.1. Power plant natural gas requirements (level VI)*

The volume of natural gas required at the power plant per kW·h electricity was computed based on the energy conversion efficiency, heat rate and lower heating calorific value (LHV) of combusted natural gas:

$$M_{VI} = \frac{360\,000}{LHV \times \eta} \qquad \text{Eq. (III-10)}$$

Where:

$M_{VI}$ is quantity of natural gas burned at power plant ($m^3$/MW·h);

$LHV$ is lower heating value of natural gas (MJ/$m^3$);

$\eta$ is power plant thermal efficiency (%).

*III-3.5.2. Power plant annual natural gas requirements*

The quantity of natural gas required at power plant per year was calculated based on the characteristic of the power plant and the fuel:

$$M_{VI}a = \frac{P \times H \times M_{VI} \times f_{fi}}{1000} \qquad \text{Eq. (III-11)}$$

Where:

$P$ is plant net output capacity (MW€);

$H$ is equivalent full power of operation (h/year);

$f_{fi}$ is fraction of Natural gas burned.

*III-3.5.3. Natural gas distribution net (level V)*

The losses in distribution net must be incorporated in calculating the gas volume flow:

$$M_V = M_{VI} \times (1 + L_V \times D_V) \times (1 + S_V/100) \qquad \text{Eq. (III-12)}$$

Where:

$M_V$ is natural gas requirements in power plant ($m^3$/MW·h);

$L_V$ is losses of natural gas in distribution net ($m^3$/$m^3$·km);

$D_V$ is transportation distance in distribution net (km);

$S_V$ is self-consumption of the gas turbine (%).

*III-3.5.4. Natural gas processing and storage (level IV)*

Some fraction of natural gas volume is stored in underground cavities. The natural gas consumption in the GT, driving the appropriate compressors represents one of the gas volume losses. The other losses are related to the underground storage process. Total volume of natural gas on the input of the national distribution node is expressed as follows:

$$M_{IV} = M_V \times [1 + SF \times (1 + \frac{L_{IV}}{100}) \times (1 + GREQ_{IV})] \qquad \text{Eq. (III-13)}$$

Where:

$M_{IV}$ is volume of gas on the output from national pipeline ($m^3$);

$SF$ is fraction of natural gas processed by underground storage;

$L_{IV}$ is losses of gas during underground storage (%);

$GREQ_{IV}$ is self-consumption of gas to drive the gas turbine in appropriate compressor station in $m^3/m^3$.

*III-3.5.5. Transportation of natural gas in pipeline (level III)*

The equivalent volume of gas on the input of national pipeline is influenced by the losses in pipeline as well as by the gas consumption in appropriate compressor stations.

$$M_{III} = M_{IV} \times (1 + L_{III} \times D_{III}) \times (1 + GREQ_{III} \times D_{III}) \qquad \text{Eq. (III-14)}$$

Where:

$M_{III}$ is natural gas volume on the input of pipeline ($m^3$);

$L_{III}$ is natural gas losses in pipeline ($m^3/m^3 \cdot km$);

$GREQ_{III}$ is gas requirements to drive the appropriate compressor station in ($m^3/m^3$ km);

$D_{III}$ is distance of pipeline in (km).

*III-3.5.6. Natural gas drilling (level II)*

The losses at the drilling site are accounted for using the mining factor.

$$M_{II} = M_{III} \times MF$$

Where:

$M_{II}$ is mining mass flow (g/kW·h);

$MF$ is mining factor.

## III-3.6. Calculations of emission factors

As for the coal life cycle chain, the emissions factors per kW·h can be calculated on the basis of the natural gas volume at individual levels. In the natural gas life cycle chain the following emissions are considered.

*III-3.6.1. Direct emissions*

The direct emissions factors for the pollutant *i* are:

$$EF_{IIDi} = EF_i \times \frac{M_{II}}{1000} \qquad \text{Eq. (III-15)}$$

Where:

$EF_{IIDi}$ is facility emissions factor of pollutant *i* associated with the total volume of gas produced (g/kW·h);

$EF_i$ is emissions (g/m$^3$).

*III-3.6.2. Indirect emissions*

Emissions associated with electricity generation (on site or from grid) should be considered together with the steam required at drilling process. For electricity generation on the site (gas turbine) the greenhouse gases should be considered; in the case of grid electricity, the fuel mix should be used. The indirect emissions associated with the pollutant *i* are:

$$EF_{IIiDI} = M_{II} \times \left( EF_E \frac{EREQ_{II}}{10^6} + EF_Q \frac{HREQ_{II}}{10^9} \right) \qquad \text{Eq. (III-16)}$$

Where:

$EF_{IIiDi}$ is indirect emissions factor for drilling (g/kW·h);

$EF_E$ is aggregated emissions factor (g/kW·h);

$EREQ_{II}$ is electricity requirements (Wh/m$^3$);

$EF_Q$ is aggregated emissions factor (g/GJ);

$HREQ_{II}$ is heat (steam requirements at drilling) (kJ/m$^3$).

## III-3.7. Transportation of natural gas in pipeline

*III-3.7.1. Direct emissions*

The direct emissions for the pollutant *i* are:

$$EF_{IIIDi} = EF_i \frac{M_{III} \times D_{III}}{1000} \quad \text{Eq. (III-17)}$$

Where:

$EF_{IIIDi}$ is emissions factor of pollutant *i* (g/km·m$^3$).

*III-3.7.2. Indirect emissions*

The indirect emissions for the pollutant *i* are:

$$EF_{IIIiDi} = M_{III} \times LHV_{gas} \times EF_{gas} \times GREQ_{III} \times D_{III} \times 10^{-6} \quad \text{Eq. (III-18)}$$

Where:

$EF_{IIIiDi}$ is indirect emissions factor for pipeline (g/kW·h);

$LHV_{gas}$ is lower heating value of gas (MJ/m$^3$);

$EF_{gas}$ is emissions factor of gas combustion in gas turbine (g/GJ).

**III-3.8. Natural gas processing and storage (underground storage)**

*III-3.8.1. Direct emissions*

The direct emissions for the pollutant *i* are:

$$EF_{IVDi} = EF_i \times M_{IV} \times \frac{RF}{1000} \quad \text{Eq. (III-19)}$$

Where:

$EF_{IVDi}$ is emissions factor of pollutant *i* (g/ m$^3$);

$RF$ is fraction of gas in underground storage.

*III-3.8.2. Indirect emissions*

The emissions are connected with the natural gas combustion in GT used by compressor stations as well as with electricity and heat requirements. The indirect emissions for the pollutant *i* are:

$$EF_{IV_iD_i} = M_V \times RF\left(LHV_{gas} \times EF_{gas} \times GREQ_{IV} \times D_{III} \times 10^{-6} + EF_E \times EREQ_{II} \times 10^{-6} + EF_Q \times HREQ_{II} \times 10^{-6}\right)$$

Eq. (III-20)

Where:

$EF_{IviDi}$ is indirect emissions factor of the processing (g/kW·h);

$RF$ is fraction of gas in underground storage;

$M_V$ is Natural gas requirements in power plant ($m^3$/MW·h);

$LHV_{gas}$ is lower heating value of gas (MJ/$m^3$);

$EF_{gas}$ is emissions factor of gas combustion in gas turbine (g/GJ);

$EF_E$ is aggregated emissions factor (g/kW·h);

$EREQ_{II}$ is electricity requirements (W·h/$m^3$);

$EF_Q$ is aggregated emissions factor (g/GJ);

$HREQ_{II}$ is heat required for generating steam at drilling (kJ/$m^3$);

$GREQ_{III}$ is gas requirements to drive the appropriate compressor station ($m^3$/$m^3$·km).

*III-3.8.3. Distribution net (pipeline)*

The direct emissions for the pollutant *i* are:

$$EF_{VDi} = EF_i \times M_V \frac{D_V}{1000} \qquad \text{Eq. (III-21)}$$

Where:

$EF_{Vi}$ is emissions factor of pollutant *i* (g/km·$m^3$);

$M_V$ is volume of gas transported ($m^3$/MW·h);

$D_V$ is distance of pipeline (km).

*III-3.8.4. Power plant operation*

The direct emissions from the power plant operation are calculated from:

$$EF_{VI} = EF_i \times M_{VI} \qquad \text{Eq. (III-22)}$$

Where:

$EF_{IV}$ is emissions for the pollutant *i* (g/$m^3$);

$EF_i$ is emissions factor of pollutant *i* (g/$m^3$).

*III-3.8.5. Power plant construction and decommissioning*

The emissions during the power plant construction and decommissioning are calculated related to the energy uses due to the activities associated with land preparation, drilling and blasting, ground excavation, earth moving, and the building of the power plant. The emissions are calculated from:

$$EF_{CD} = EF_i \times E \times EREQ \qquad \text{Eq. (III-23)}$$

Where:

$EF_{CD}$ is emissions for the pollutant *i* (g/m$^3$);

$EF_i$ is emissions factor of pollutant *i* (g/GJ);

$E$ is Energy uses in the construction and decommissioning (GJ);

$EREQ$ is electricity required in (W·h/m$^3$).

**III-3.9. The crude oil life cycle chain**

Crude oil is essentially a complex mixture of hydrocarbons with very different chemical and physical properties. The processing of crude oil is aimed at separating the mixture into groups of chemicals with similar properties for use in particular applications. The route from extraction of the crude to use of the individual refined components is long and complex.

The crude oil life cycle chain covered all the processes in the life cycle of the product, starting from the extraction of raw materials from nature and finishing with the delivery of electricity (Fig. III-7.).

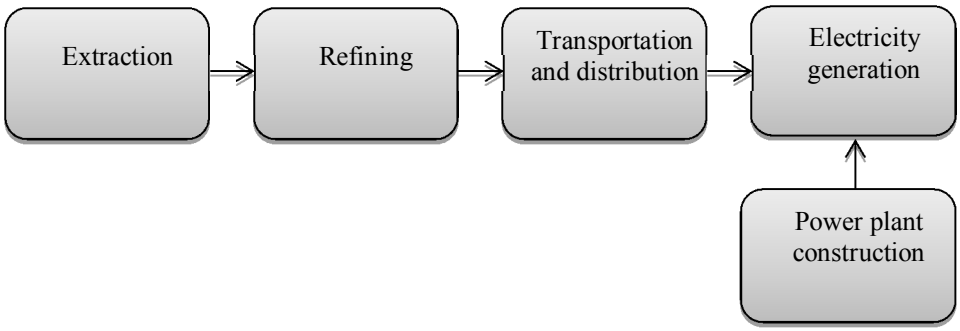


*FIG. III-7. Crude oil life cycle chain.*

Most of the GHG lifecycle emissions arise from the operation of the power plant, which range between roughly 700–800 g$CO_2$equ./kW€·h. GHG emissions from power plant construction and decommissioning are negligible, and significant upstream emissions arise mainly at the stages of oil transport, refinery, exploration and extraction, which are in the range of 40–110 g$CO_2$equ./kW€·h.

The following processes were included in the inventory:

— Extraction and refining of the crude oil;
— Manufacturing of the raw materials;
— All transportation processes for which emission data were to be obtained;
— Conversion of the crude oil into the electricity in the power plant;
— Electricity and heat generation related to the crude oil extraction and refining to produce raw materials.

The specifications required for calculations include the natural gas characteristics (low calorific value, methane and other gases content), technology designation and average transport distance. Information on power plant size (MW€), plant efficiency (%), equivalent full power of operation hours (h/year) are also required.

The calculations are carried out from oil extraction (level II) to electricity generation (level VI). The energy uses of some upstream processes were gathered from various literature sources. Electricity production for use in upstream process was assumed to be the generation mix of Egypt.

**III-3.9. Crude oil mass flows calculations**

The mass flow of the primary energy sources was calculated starting from power plant and working backward through each front-end process. The mass flows in the crude oil life cycle chain are represented in Fig. III-8.

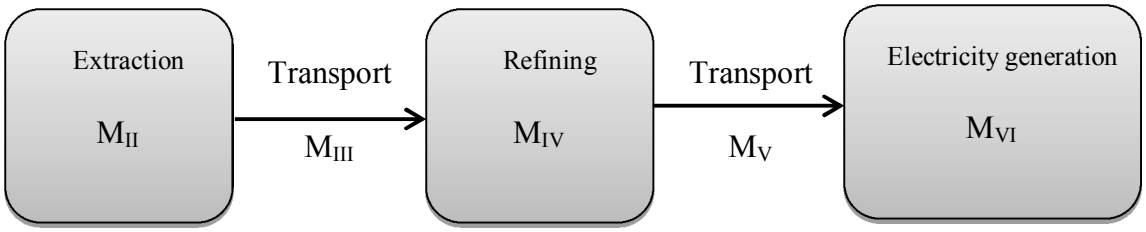


*FIG. III-8. Mass flow in the life cycle chain.*

*III-3.9.1. Power plant oil requirements (level VI)*

The mass flow required at the power plant per kW·h electricity was calculated based on the energy conversion efficiency, heat rate LHV of combusted oil.

$$M_{VI} = \frac{360\,000}{LHV \times \eta} \qquad \text{Eq. (III-24)}$$

Where:

$M_{VI}$ is quantity of oil burned at power plant (g/kW·h);

$LHV$ is lower heating value of oil (MJ/kg);

$\eta$ is power plant thermal efficiency (%).

*III-3.9.2. Power plant annual oil requirements*

The quantity of oil mass required at power plant per year was calculated based on the characteristics of the power plant and the fuel:

$$M_{VI}a = \frac{P \times H \times M_{VI} \times f_{fi}}{1000} \qquad \text{Eq. (III-25)}$$

Where:

$P$ is plant net output capacity (MW€);

$H$ is equivalent full power of operation (h/year);

$f_{fi}$ is fraction of oil burned.

*III-3.9.3. Oil distribution net (level V)*

The losses in distribution net must be incorporated in calculating the oil mass flow:

$$M_V = M_{VI} \times (1 + L_V \times D_V) \times (1 + S_V / 100) \qquad \text{Eq. (III-26)}$$

Where:

$M_V$ is oil requirements in power plant (g/kW·h);

$L_V$ is losses of oil in distribution net (kg/kg·km);

$D_V$ is transportation distance in distribution net (km);

$S_V$ is self-consumption of the gas turbine (%).

*III-3.9.4. Oil refining (level IV)*

Some fraction of oil mass is stored in underground cavities. The oil consumption in the GT, driving the appropriate compressors represents one of the oil mass flow losses. Oil mass flow on the input of the distribution node is expressed as follows:

$$M_{IV} = M_V \times (1 + \frac{L_{IV}}{100}) \times (1 + GREQ_{IV}) \qquad \text{Eq. (III-27)}$$

Where:

$M_{IV}$ is mass flow of oil on the output from pipeline (g/kW·h);

$L_{IV}$ is losses of oil during refining (%);

$GREQ_{IV}$ is self-consumption of oil to drive the GT in appropriate compressor station (kg/kg).

*III-3.9.5. Transportation of oil in pipeline (level III)*

The equivalent mass flow of oil on the input of national pipeline is influenced by the losses in pipeline as well as by the oil consumption in appropriate compressor stations.

$$M_{III} = M_{IV} \times (1 + L_{III} \times D_{III}) \times (1 + GREQ_{III} \times D_{III}) \quad \text{Eq. (III-28)}$$

Where:

$M_{III}$ is oil mass flow of pipeline (g/kW·h);

$L_{III}$ is oil losses in pipeline in (kg/kg·km);

$GREQ_{III}$ is oil requirements to drive the appropriate compressor station in ($m^3/m^3$·km);

$D_{III}$ is distance of pipeline in (km).

*III-3.9.6. Oil extraction (level II)*

The losses at the extraction site are accounted for using the extraction factor.

$$M_{II} = M_{III} \times MF \quad \text{Eq. (III-29)}$$

Where:

$M_{II}$ is oil extraction mass flow (g/kW·h);

$MF$ is oil extraction factor.

**III-3.10. Emissions factors calculations — oil extraction**

The emissions factors per kW·h can be calculated on the basis of the oil mass flow at individual levels. In the oil life cycle chain the following emissions are considered:

*III-3.10.1. Direct emissions*

The direct emissions factors for the pollutant *i* are:

$$EF_{IIDi} = EF_i \times \frac{M_{II}}{1000} \quad \text{Eq. (III-30)}$$

Where:

$EF_{IIDi}$ is facility emissions factor of pollutant *i* associated with the total mass of oil produced (g/kW·h);

$EF_i$ is emissions ($g/m^3$).

*III-3.10.2. Indirect emissions*

Emissions associated with electricity generation (on site or from grid) should be considered together with the steam required at extraction process. For electricity generation on the site, the GHG should be considered; in the case of grid electricity, the fuel mix should be used. The indirect emissions associated with the pollutant *i* are:

$$EF_{IIiDI} = M_{II} \times (EF_E \frac{EREQ_{II}}{10^6} + EF_Q \frac{HREQ_{II}}{10^9}) \qquad \text{Eq. (III-31)}$$

Where:

$EF_{IiiDi}$ is indirect emissions factor for extraction (g/kW·h);

$EF_E$ is aggregated emissions factor (g/kW·h);

$EREQ_{II}$ is electricity requirements (W·h/m$^3$);

$EF_Q$ is aggregated emissions factor (g/GJ);

$HREQ_{II}$ is heat (steam requirements at extraction) (kJ/m$^3$).

**III-3.11. Transportation in pipeline**

*III-3.11.1. Direct emissions*

The direct emissions for the pollutant *i* are:

$$EF_{IIIDi} = EF_i \frac{M_{III} \times D_{III}}{1000} \qquad \text{Eq. (III-32)}$$

Where:

$EF_{IIIDi}$ is emissions factor of pollutant *i* (g/km·m$^3$).

*III-3.11.2. Indirect emissions*

The indirect emissions for the pollutant *i* are:

$$EF_{IIIiDi} = M_{III} \times LHV_{gas} * EF_{gas} \times GREQ_{III} \times D_{III} \times 10^{-6} \qquad \text{Eq. (III-33)}$$

Where:

$EF_{IIIiDi}$ is indirect emissions factor for national pipeline (g/kW·h);

$LHV_{gas}$ is lower heating value of gas (MJ/m$^3$);

$EF_{gas}$ is emissions factor of oil combustion in gas turbine (g/GJ).

## III-3.12. Oil refining

*III-3.12.1. Direct emissions*

The direct emissions for the pollutant *i* are:

$$EF_{IVDi} = EF_i \times M_{IV} \times \frac{RF}{1000} \qquad \text{Eq. (III-34)}$$

Where:

$EF_{IVDi}$ is emissions factor of pollutant *i* (g/m$^3$);

$RF$ is fraction of oil refining.

*III-3.12.2. Indirect emissions*

The emissions are connected with the oil combustion in GT used by compressor stations as well as with electricity and heat requirements. The indirect emissions for the pollutant *i* are:

$$EF_{IV_iD_i} = M_V \times RF\left(LHV_{gas} \times EF_{gas} \times GREQ_{IV} \times D_{III} \times 10^{-6} + EF_E \times EREQ_{II} \times 10^{-6} + EF_Q \times HREQ_{II} \times 10^{-6}\right)$$

Eq. (III-35)

Where:

$EF_{IviDi}$ is indirect emissions factor of the extraction (g/kW·h);

$RF$ is fraction of oil refining;

$M_V$ is oil requirements in power plant (m$^3$/MW·h);

$LHV_{gas}$ is lower heating value of gas (MJ/m$^3$);

$EF_{gas}$ is emissions factor of oil combustion in gas turbine (g/GJ);

$EF_E$ is aggregated emissions factor in g/kW·h);

$EREQ_{II}$ is electricity requirements (W·h/m$^3$);

$EF_Q$ is aggregated emissions factor (g/GJ);

$HREQ_{II}$ is heat required for generating steam at extraction (kJ/m$^3$);

$GREQ_{III}$ is oil requirements to drive the appropriate compressor station (m$^3$/m$^3$·km).

*III-3.12.3. National distribution net*

The direct emissions for the pollutant *i* are:

$$EF_{VDi} = EF_i \times M_V \frac{D_V}{1000} \qquad \text{Eq. (III-36)}$$

Where:

$EF_{Vi}$ is emissions factor of pollutant *i* (g/km.m$^3$);

$M_V$ is mass of oil transported (m$^3$/MW·h);

$D_V$ is distance of pipeline (km).

*III-3.12.4. Power plant operation*

The direct emissions from the power plant operation are calculated from:

$$EF_{VI} = EF_i * M_{VI}$$

Where:

$EF_{IV}$ is emissions for the pollutant *i* (g/m$^3$);

$EF_i$ is emissions factor of pollutant *i* (g/m$^3$).

*III-3.12.5. Power plant construction and decommissioning*

The emissions during the power plant construction and decommissioning are calculated related to the energy uses due to the activities associated with land preparation, drilling and blasting, ground excavation, earth moving, and the building of the power plant. The emissions are calculated from:

$$EF_{CD} = EF_i \times E \times EREQ \qquad \text{Eq. (III-37)}$$

Where:

$EF_{CD}$ is emissions for the pollutant *i* (g/m$^3$);

$EF_i$ is emissions factor of pollutant *i* (g/GJ);

$E$ is Energy uses in the construction and decommissioning (GJ);

$EREQ$ is electricity required (W·h/m$^3$).

**III-3.13. Nuclear fuel life cycle chain**

Differences in the GHG emissions for nuclear energy chains, amongst others, can be attributed to the enrichment technology used, as well as the nuclear energy technology type

(PWR, BWR). For example, enrichment using diffusion technology rather than centrifuge technology is more energy-intensive and depending on GHG emissions relating to the electricity supply mix of the country where enrichment is taking place can significantly impact on the cumulative GHG lifecycle. A typical chain for nuclear would, for example, consist of uranium mining (open pit and underground), milling, conversion, enrichment (diffusion and centrifuge), fuel fabrication, power plant, reprocessing, conditioning of spent fuel, interim storage of radioactive waste, and final repositories.

So the nuclear fuel life cycle chain can be divided into three main stages:

— The so-called front-end which extends from the mining of uranium ore unit to the delivery of fabricated fuel elements to the reactor site (level I to level V).
— Fuel use in the reactor, where fission energy is employed to produce electricity, and temporary storage at the reactor site (level VI).
— The so-called back-end, which starts with the shipping of spent fuel away from reactor storage or to a reprocessing plant and ends with the final disposal of wastes from reprocessing or the encapsulated spent fuel itself. Figure III-9. Shows the nuclear life cycle chain processes.

*III-3.13.1. Nuclear mass flows calculations*

The mass flow of the primary energy sources was calculated starting from power plant and working backward through each front-end process. The mass flows in the nuclear life cycle chain are represented in Fig. III-9.

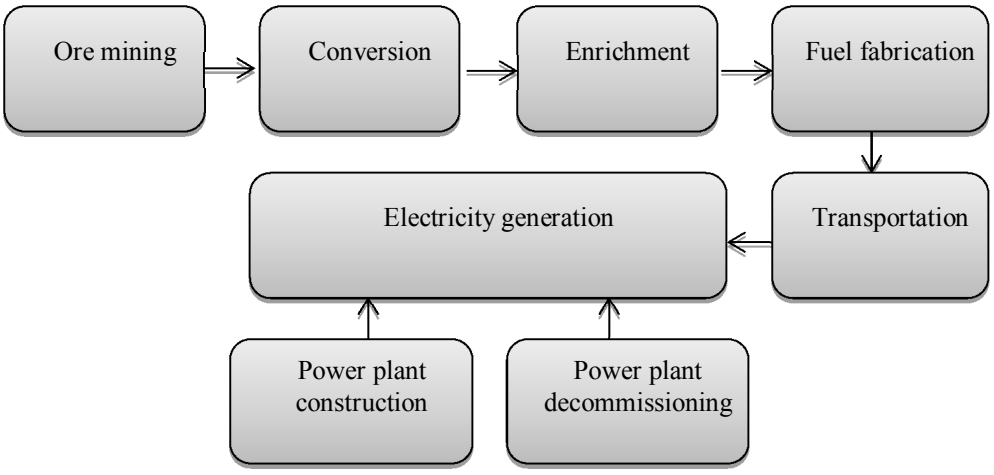


*FIG. III-9. Nuclear fuel life cycle chain (without reprocessing).*

*III-3.13.2. Equilibrium consumption of nuclear fuel (one cycle)*

Equilibrium is reached when nuclear fuel charges and discharges are proportional to the electricity generated. It is assumed that this is the case one year after start-up. Although some reactors need more time to reach equilibrium, the differences in the fuel requirements and

The annual equilibrium fuel requirement in kg per GW·h of electricity is calculated from:

$$M_{IVCe} = \frac{10^5}{24 \times B \times \eta} \qquad \text{Eq. (III-38)}$$

Where:

$M_{IVCe}$ is the annual equilibrium fuel requirement (kg/GW);

$B$ is burn up (MW·d/kg);

$\eta$ is net thermal efficiency of the power plant (%).

*III-3.13.3. Lifetime fuel requirement*

The lifetime equilibrium fuel requirement was calculated from:

$$M_L = M_i + 0.001 \times M_{IVCe} \times P \times H \times L \qquad \text{Eq. (III-39)}$$

Where:

$M_L$ is lifetime equilibrium fuel requirement (kg);

$M_i$ is first core mass (kg);

$P$ is net electrical capacity (MW);

$H$ is utilization (h/year);

$L$ is economic lifetime (years);

*III-3.13.4. Power plant mass requirement (level VI)*

Distribution of the initial fuel loading over the economic lifetime of power plant results in an average fuel requirement (Fig. III-10.).

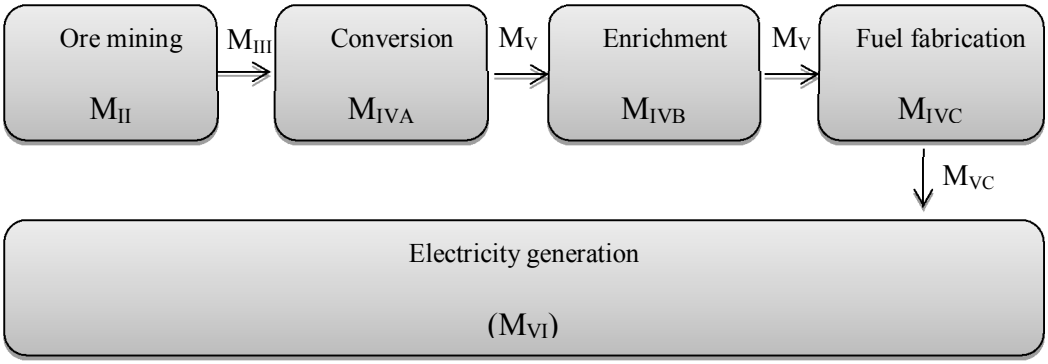


*FIG. III-10. Mass flow in the nuclear fuel life cycle chain.*

$$M_{VI} = M_{IVCe} + 1000 \frac{M_i}{P \times H \times L} \qquad \text{Eq. (III-40)}$$

Where:

$M_{VI}$ is average fuel requirement in the power plant (g/GW·h).

*III-3.13.5. Transportation of fuel requirement (level VC)*

The fuel mass during transportation was calculated from:

$$M_{VC} = M_{VI} + L_{VC} \times d_{VC} \times 10^{-6} \qquad \text{Eq. (III-41)}$$

Where:

$L_{VC}$ is losses factors in transportation of the fuel (g/t·km);

$d_{VC}$ is transportation distance (km).

*III-3.13.6. Fuel fabrication (level IVC)*

The required uranium input in the fabrication process is calculated for the once through cycle from:

$$M_{IVC} = M_{VC} \times \frac{1}{f_{IVC}} \qquad \text{Eq. (III-42)}$$

Where:

$f_{IVC}$ is fabrication efficiency.

*III-3.13.7. Transportation of UO2 (level VB)*

The fuel mass during transportation of $UO_2$ was calculated from:

$$M_{VB} = M_{IVC} + L_{VB} \times d_{VB} \times 10^{-6} \qquad \text{Eq. (III-43)}$$

Where:

$L_{VB}$ is losses in transportation of the $UO_2$ (kg/t·km);

$d_{VB}$ is transportation distance (km).

*III-3.13.8. Uranium enrichment (level IVB)*

The uranium feed to the enrichment plant is calculated from:

$$M_{IVB} = M_{VB} \frac{1}{f_{IVB}} \times \frac{(e_p - e_t)}{(e_f - e_t)} \qquad \text{Eq. (III-44)}$$

Where:

$M_{IVB}$ is uranium feed to the enrichment plant (kg/GW·h);

$f_{IVB}$ is enrichment efficiency (%);

$e_p$ is fraction of $U^{235}$ in fresh equilibrium fuel;

$e_f$ is fraction of $U^{235}$ in the feed;

$e_t$ is fraction of $U^{235}$ in the tails.

The required separative work units SW are calculated from:

$$SW = M_{IVC} \times V_p + M_t \times V_t - M_{IVB} \times V_f \qquad \text{Eq. (III-45)}$$

Where:

$$M_t = M_{IVB} \times f_{IVC} - M_{IVC} \qquad \text{Eq. (III-46)}$$

$$V_x = (2.e_x - 1) \times \ln \frac{e_x}{1 - e_x} \qquad \text{Eq. (III-47)}$$

Where $x$ is subscript of: $f$, $p$ or $t$.

*III-3.13.9. Transportation of UF6 (level VA)*

The fuel losses during transportation are calculated from:

$$M_{VA} = M_{IVB} + L_{VB} \times d_{VB} \times 10^{-6} \qquad \text{Eq. (III-48)}$$

Where:

$M_{VA}$ is UF6 fuel mass (kg/GW·h);

$L_{VB}$ is losses in transportation of the $UF_6$ (kg/t·km);

$d_{VB}$ is transportation distance (km).

*III-3.13.10. Uranium conversion (level IVA)*

The natural uranium feed to the conversion plant is calculated from:

$$M_{IVA} = M_{VA} \frac{f_{IVA}}{100} \qquad \text{Eq. (III-49)}$$

Where:

$M_{IVA}$ is natural uranium feed to conversion plant (kg/GW·h);

$f_{IVA}$ is conversion efficiency (%).

*III-3.13.11. Transportation of UF6 (level III)*

The fuel losses during transportation are calculated from:

$$M_{III} = M_{IVA} + L_{III} \times d_{III} \times 10^{-6} \qquad \text{Eq. (III-50)}$$

Where:

$M_{III}$ is UF6 mass (kg/GW·h);

$L_{III}$ is losses in transportation of the UF6 (kg/t·km);

$d_{III}$ is transportation distance (km).

*III-3.13.12. Uranium mining (level II)*

The amount of uranium ore to be mined is:

$$M_{II} = M_{III} \frac{f_{II}}{100} \qquad \text{Eq. (III-51)}$$

Where:

$M_{II}$ is amount of uranium ore (kg/GW·h);

$f_{II}$ is mine-specific ratio of ore mined to uranium product after milling.

*III-3.13.13. Emissions calculations*

The emissions during the nuclear life cycle chain processes are calculated related to the energy uses in these processes. The emissions are calculated:

$$EF_{IDi} = \frac{1}{H \times L} \sum EF_{im} \times REQ \qquad \text{Eq. (III-52)}$$

Where:

$EF_{Idi}$ is indirect emissions of the pollutant i generated from a certain process (g/kW·h);

$H$ is equivalent full hour of operation per year (hours);

$L$ is economic lifetime of the facility (years);

$EF_{im}$ is emissions factors for the pollutant i associated with the production of the materials;

$REQ = HREQ + MREQ$ (*HREQ* and *MREQ* are the heat and mechanical the power requirements in production of materials).

**III-3.14. Global warming potential calculations**

Carbon Dioxide $CO_2$, Methane $CH_4$ and Nitrous Oxide $N_2O$ are the main contributors to atmospheric warming. The specific contribution of $CH_4$ and $N_2O$ have been assessed respectively as 21 and 230 (in Sec III-6 it is mentioned as 310) time that of $CO_2$ (IPCC, 1988). The GHG are classified under global warming category and the GWP per functional unit is calculated in $CO_2$ equivalents unit as follows:

$$GWP = E_{CO2} \times 1 + E_{CH4} \times 21 + E_{N2O} \times 320 \qquad \text{Eq. (III-53)}$$

Where

*GWP* is global warming potential greenhouse gas emissions, ($gCO_2equ./kW{\cdot}h$);

$E_{CO2}$ is $CO_2$ emissions ($g/kW{\cdot}h$);

$E_{CH4}$ is $CH_4$ emissions ($g/kW{\cdot}h$);

$E_{N2O}$ is $N_2O$ emissions ($g/kW{\cdot}h$).

*III-3.14.1. Greenhouse gases cost calculations*

The cost of GWP per functional unit of electricity generation and water production is calculated in $CO_2$ equivalents unit as follows:

$$GWPC = GWP \times CCO_2 \qquad \text{Eq. (III-54)}$$

Where

*GWPC* is cost of global warming potential greenhouse gas emissions, ($/kW·h);

*GWP* is global warming potential greenhouse gas emissions, ($gCO_2equ./kW{\cdot}h$);

$CCO_2$ is in ($/ $gCO_2equ$).

## ANNEX IV
## NEW ROBUST THERMODYNAMIC MODULES IN DEEP

IV-1. GENERAL CONTEXT

### IV-1.2. Introduction

In order to enhance the performance of thermal desalination process, typically a vapour compression system is added. Such addition will help increase the steam temperature of the desalination process. In general, there are two different ways for the addition of vapour compression: MVC and thermal vapour compression (TVC). In this work, both methods will be discussed: the thermodynamic analysis of the thermal vapour compression with the TVC/MEE design, and the thermodynamic analysis of the MVC. In the first scheme, the design includes the Thermodynamic analysis of the evaporator (i.e. distillation effects), as well as the steam jet ejector. Whereas in the second one, our work will highlight the TVC/MEE design and details of the economic model. In the following sections, the mathematical model will be presented, and DEEP software modification in terms of a new MED/TVC template will be discussed. The thermodynamic analysis of MED/TVC will details modelling of performance, evaluation of economics and development of a template of renewable energy source using solar energy.

### IV-1.3. New gain output ratio calculation

The amount of produced water, $M_d$ is:

$$M_d = \sum_{j=1}^{n} D_j + \sum_{j=2}^{n} d_j \qquad \text{Eq. (IV-1)}$$

The amount of vapour formed by boiling in the effect $i$ is:

$$D_i = \frac{D_{i-1} \times \lambda_{i-1}}{\lambda_i} \qquad \text{Eq. (IV-2)}$$

The amount of vapour formed by brine flashing in the effect $i$ equal:

$$d_i = \left( M_f - \sum_{j=1}^{i-1} D_j - \sum_{j=2}^{i-1} d_j \right) \cdot C_P \cdot \frac{T_{i-1} - T_i'}{\lambda_i} \qquad \text{Eq. (IV-3)}$$

Where $M_h$ can be determined by the following equations:

$$Q_1 = D_1 \lambda_1 = M_h \lambda_h = Q_{th} \rightarrow M_h = D_1 \lambda_1 / \lambda_h \qquad \text{Eq. (IV-4)}$$

$$D_i = D_1 \lambda_1 / \lambda_i \text{ , with } i = 2 \text{ to } n \qquad \text{Eq. (IV-5)}$$

$$D_1 = M_d / ( 1 + \lambda_1/\lambda_2 + ..... + \lambda_1/\lambda_{n-1} + \lambda_1/\lambda_n) \qquad \text{Eq. (IV-6)}$$

### IV-1.4. Gain output ratio (GOR) calculation in DEEP

The GOR in MED systems is calculated in DEEP as follows:

$$GOR \approx 0.8 \times N_{emed} \quad \text{Eq. (IV-7)}$$

Where $N_{emed}$ is the number of effects.

For the old version of DEEP, the overall working temperature is also equal to the sum of the temperature differences over all effects (or is equal to the product of the number of effects and the average temperature difference per effect):

$$DT_{do} = N_{emed} \times DT_{ae} \quad \text{Eq. (IV-8)}$$

The average temperature difference per effect, $DT_{ae}$, is a function of the overall working temperature $DT_{do}$:

$$DT_{ae} = 1.65 + (0.0185 \times DT_{do})/ 0.85 \quad \text{Eq. (IV-9)}$$

The number of effects for the MED plant was therefore:

$$N_{emed} = \text{integer}\ (DT_{do} / DT_{ae}) + 1 \quad \text{Eq. (IV-10)}$$

The gain output ratio, *GOR*, is calculated by the following expression:

$$GOR = \frac{Q_{rh}}{\left(Q_{rm} \times DT_{ae}/DT_{ao} + 4.019 \times \left(\mathrm{d}T_{ph} + \mathrm{d}T_{be}\right)\right)} \quad \text{Eq. (IV-11)}$$

Where $Q_{rh}$. Is the latent heat of heating vapour, $\mathrm{d}T_{ph}$ is the temperature increase in feedwater preheater, $\mathrm{d}T_{be}$ is the average BPE.

### IV-1.5. Gain output ratio results comparison

Deep was run for MED case with different top brine temperature and equivalent number of effects as result GOR and specific heat consumption were obtained as in Table IV-1. And the same was carried out using the new GOR macro and the water cost as shown in Figs (IV-1. To IV-6.). Figures IV-1. To IV-6. Show diagrams for GOR and specific heat consumption for different top brine temperature and equivalent number of effects. It can be concluded that in low top brine temperature and low number of effects DEEP and GOR macro agree with each other for both GOR and specific heat consumption, while in high TBT or high number of effects DEEP calculates GOR using a simple linear equation ignoring the changes in the latent heat of vapour at different temperatures and the same is for the number of effects.

In case of DEEP, water cost is shown increasing with temperature. This trend is not acceptable.

TABLE IV-1. GAIN OUTPUT RATIO AND SPECIFIC HEAT CONSUMPTION FOR DIFFERENT TEMPERATURE

| Top brine temperature [°C] | Number of effects | GOR | | Specific heat consumption [kW·h/m³] | | Water cost [$/m$^3$] | |
|---|---|---|---|---|---|---|---|
| | | DEEP | MACRO | DEEP | MACRO | DEEP | MACRO |
| 110 | 28 | 22.4 | 17.85 | 27.47 | 34.18 | 1.1489 | 0.9031 |
| 105 | 26 | 20.8 | 17 | 29.75 | 36 | 1.1255 | 0.9117 |
| 100 | 24 | 19.2 | 16.2 | 32.41 | 38.14 | 1.1011 | 0.9209 |
| 95 | 22 | 17.6 | 15.3 | 35.55 | 40.66 | 1.0756 | 0.9328 |
| 90 | 20 | 16 | 14.31 | 39.32 | 43.6 | 1.0491 | 0.9428 |
| 85 | 18 | 14.4 | 13.28 | 43.94 | 47.39 | 1.0215 | 0.9671 |
| 80 | 16 | 12.8 | 12.16 | 49.7 | 52.02 | 0.9926 | 0.9921 |
| 75 | 14 | 11.2 | 10.97 | 57.11 | 58 | 0.9626 | 1.0251 |
| 70 | 12 | 9.6 | 9.7 | 66.99 | 65.93 | 0.9413 | 1.0705 |
| 65 | 10 | 8 | 8.32 | 80.83 | 77.06 | 0.9087 | 1.1396 |
| 60 | 8 | 6.4 | 6.9 | 101.58 | 93.76 | 0.8747 | 1.2349 |

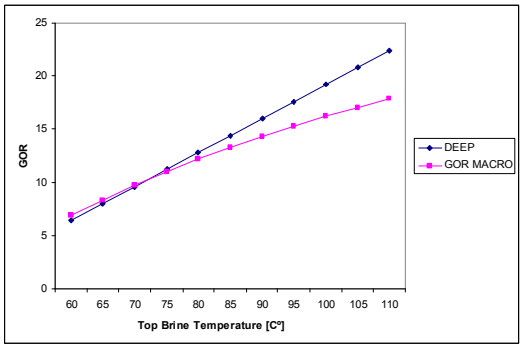


*FIG. IV-1. Top brine temperature vs. GOR.*

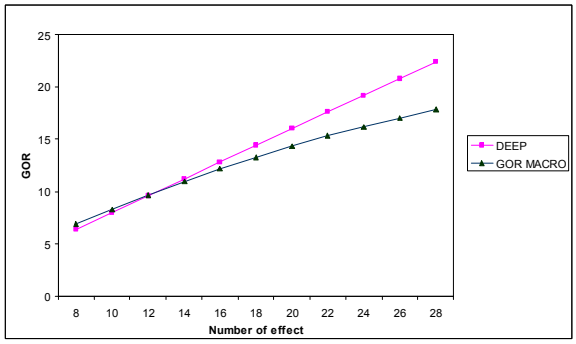


*FIG. IV-2. Number of effects vs. GOR.*

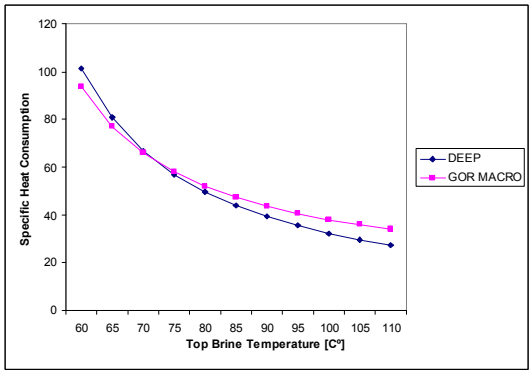


*FIG. IV-3. Specific heat consumption vs top brine temperature.*

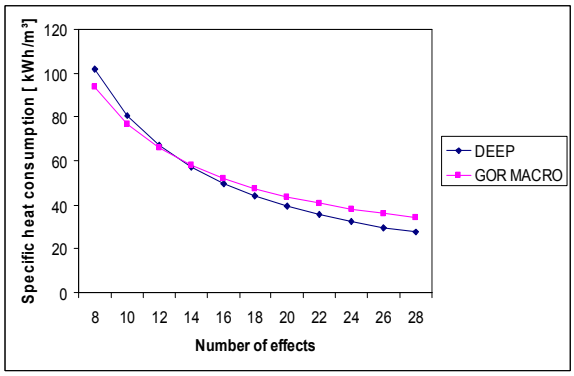


*FIG. IV-4. Specific heat consumption vs number of effects.*

Figure IV-5. shows that DEEP water cost decreases with increasing temperature. This is exactly opposite to the trend shown in Table IV-1., and GOR macro cost trends to decrease and increase with increasing in temperature, whereas Table IV-1. Shows continuous decreasing trend with temperature. Figure IV-6. Shows that DEEP water cost decreases with increasing number of effects. This is exactly opposite to the trend shown in Table IV-1. GOR

macro cost trends to decrease and increase with increasing in number of effects whereas Table IV-1. Shows continuous decreasing trend with temperature.

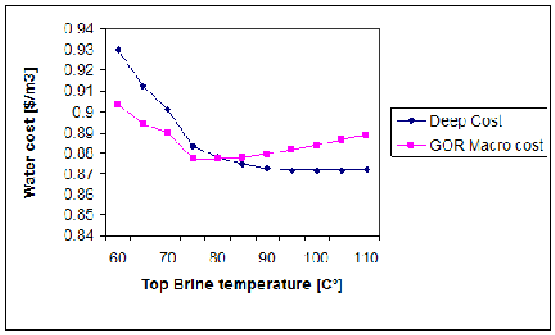


*FIG. IV-5. Water cost vs. top brine temperature.

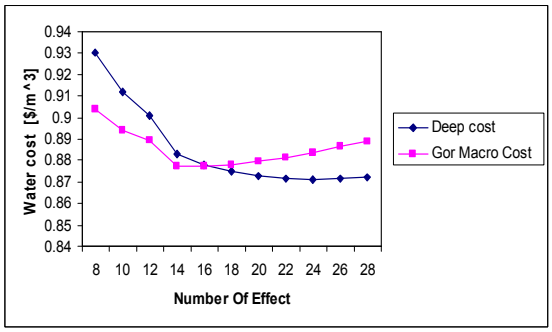


**FIG. IV-6. Water cost vs. number of effects.

As it is shown, while the top brine temperature increases GOR increases as well, this leads to the decrease the plant heat consumption and, in other word, heat cost decreases. The differences in the behaviour between DEEP and GOR Macro can be explained: the water plant specific power use $Q_{sdp}$ in DEEP is defined:

$$Q_{sdp} = 2.5+0.1\times (GOR-10) \qquad \text{Eq. (IV-12)}$$

This leads to more increases in the water cost at high temperature or high number of effect in the GOR MACRO. In addition, DEEP has ignored the changes in the vapour latent heat at different temperature.

## IV-1.6. New module for water desalination with solar power as energy source

| | | | | | | | | |
|---|---|---|---|---|---|---|---|---|
| Latitude angle | Ø | 35 | | Solar Calculations | | | | |
| Number of the year day counted from January 1 | n | 21 | | | | | | |
| Feed water flow rate | m | 8 | m^3 /day | | | | | |
| Efficiency of the collector | η | 0.75 | | | | | | |
| tob brine temperature | tbt | 70 | | | | | | |
| last effect temperature | tn | 45 | | | | | | |
| The temperature difference for feed water | ΔT1 | 25 | | | | | | |
| Heat capacity of feed water | Cp | 4.18 | kJ/kg.C^0 | | | | | |
| Solar time started from 12:00 at night | t | 10 | | | | | | |
| The slope surface angle | S | 45 | | | | | | |
| The surface direction angle | γ | -45 | | | | | | |
| solar heating system plant life | NP | 20 | | | | | | |
| Discount Rate | r | 0.08 | | | | | | |
| | | | | | | | | |
| The declination angle of the sun | δ | -20.13801482 | | | | | | |
| The angle of solar hours ( in the middle of the day w=0) | w | -30 | | | | | | |
| Elevation angle | sinα | 0.468565207 | | | | | | |
| | α | 27.94120129 | | | | | | |
| The incidence angle of beam radiation on a horizontal surfa | cosθz | 0.372393711 | | | | | | |
| | θz | 68.1366804 | | | | | | |
| The angle of solar hours at the sun sety | wss | 75.12171671 | | | | | | |
| Duration of the day | Td | 10.0162289 | Hours | | | | | |
| The incidence angle of beam radiation | cosθ | 0.432441484 | | | | | | |
| | θ | 64.3773971 | | | | | | |
| The vertdirect solar flux striking the horizontal surface outsi | Gon | 1394.763244 | W/m^2 | | | | | |
| The direct solar flux striking the horizontal surface outside t | Go | 519.4010606 | W/m^2 | | | | | |
| Avearge daily amount of global solar energy received by 1 r | H0 | 17.8526308 | MJ/m^2 | | | | | |
| Total solar radiation on horizontal surface | G | | W/m^2 | | | | | |
| Required heat energy for feed water | Q | 9.675925926 | kW | | | | | |
| Solar collectoe area | A | | m^2 | | | | | |
| Earth reflectivity | ρgr | 0.146446609 | | | | | | |
| | rb | 1.161248084 | | | | | | |
| | ar | 0.101852209 | | | | | | |
| | Cca | 16.29635341 | | | | | | |
| | Co | 17.11117108 | | | | | | |
| specific construction cost | Scc | 0.380248246 | | | | | | |
| Solar system construction cost | sscc | 1655 | $/m^3 | | | | | |
| Solar collector cost | scc | 160 | $/m^2 | | | | | |
| Total cost | TC | 13240 | $ | | | | | |

| | A1 [W/m^2] | B | C |
|---|---|---|---|
| Jan | 1085 | 0.207 | 0.136 |
| Feb | 1107 | 0.201 | 0.122 |
| Mar | 1151 | 0.177 | 0.092 |
| Apr | 1192 | 0.16 | 0.073 |
| May | 1220 | 0.149 | 0.063 |
| Jun | 1233 | 0.142 | 0.057 |
| Jul | 1230 | 0.142 | 0.058 |
| Aug | 1214 | 0.144 | 0.06 |
| Sept | 1185 | 0.156 | 0.071 |
| Oct | 1135 | 0.18 | 0.06 |
| Nov | 1103 | 0.196 | 0.071 |
| Dec | 1088 | 0.205 | 0.097 |

| | Gho [W/m^2] | Aho [m^2] | Gb.n [W/m^2] | Gd [W/m^ | F | Gt [W/m^2] | At [m^2] |
|---|---|---|---|---|---|---|---|
| Jan | 316.3891202 | 30.58235985 | 622.3309085 | 84.637 | 0.9284388 | 363.59379 | 35.482549 |
| Feb | 322.8043835 | 29.97458034 | 645.2627545 | 78.72206 | 0.9405278 | 373.31425 | 34.558645 |
| Mar | 332.3073953 | 29.11739571 | 715.5725568 | 65.83268 | 0.9607533 | 388.98329 | 33.166552 |
| Apr | 345.4812616 | 28.0070933 | 775.6761104 | 56.62436 | 0.9731368 | 408.04038 | 31.617544 |
| May | 356.0201732 | 27.17802713 | 817.6970959 | 51.51492 | 0.9790629 | 422.5913 | 30.52887 |
| Jun | 361.5887824 | 26.75947484 | 842.091472 | 47.99921 | 0.9823787 | 430.53085 | 29.965877 |
| Jul | 361.5490469 | 26.7624158 | 840.0425876 | 48.72247 | 0.9818397 | 430.25938 | 29.984784 |
| Aug | 356.5839572 | 27.13505678 | 824.6742447 | 49.48045 | 0.980745 | 423.91159 | 30.433786 |
| Sept | 345.6025483 | 27.99726441 | 779.4484666 | 55.34084 | 0.9743588 | 408.58468 | 31.575424 |
| Oct | 302.6599188 | 31.96963101 | 699.9637389 | 41.99782 | 0.980745 | 359.806 | 35.856085 |
| Nov | 288.9250109 | 33.4894023 | 651.6218061 | 46.26515 | 0.9743588 | 341.5783 | 37.769479 |
| Dec | 294.5033525 | 32.85506206 | 627.4122245 | 60.85899 | 0.957296 | 343.95764 | 37.508208 |

*FIG. IV-7. The solar collector work sheet.*

In order to evaluate the water cost, solar panel prices were obtained from several manufacturers.

| | | | | | |
|---|---|---|---|---|---|
| Solar cells | | | | | |
| Type | Cd Te | | | | |
| Short circuit current | Is/A | 50 | A/m^2 | | |
| Open circuit voltage | Voc | 1.4 | V | | |
| Temperature | T | 300 | K | | |
| Electric pumping power | Pout required | 123457000 | W | | |
| Electron chargr | e | 1.602*(10^-19) | J/v | | |
| Boltzman constant | K | 1.381*10^-23 | J/K | | |
| The reserved sayuration current | Io/A | 1.54374E-22 | A/m^2 | | |
| the voltage that maximize the power | Vmp | 1.2 | V | | |
| The load current that maximize the power | Imp/A | 48.94517349 | A/m^2 | | |
| The maximum power | Pmax/A | 58.73420819 | W/m^2 | | |
| The cell area | A | 2101960.745 | m^2 | | |
| | | | | | |
| **solar cells** | | | | | |
| **Modules types** | **Pmax W** | **Vmp V** | **Imp A** | **Voc V** | **Isc A** |
| Micromorph Tandem Thin Film Solar Moule 130 W | 132 | 118.6 | 1.11 | 146 | 1.27 |
| CSI Black-Framed Poly Solar Module 230 W | 230 | 29.6 | 7.78 | 36.8 | 8.34 |
| CSI Mono Module 245 W | 245 | 30.3 | 8.09 | 37.4 | 8.61 |
| DMSOLAR Solar Module 280 W | 280 | 36.4 | 7.7 | 44.5 | 8.3 |
| CSI Mono Module 295 W | 295 | 36.4 | 8.11 | 44.9 | 8.63 |
| | | | | | |
| **Batteries** | **voltage V** | **Amper Ah** | **Price $** | | |
| | 12 | 100 | 134.288 | | |
| | 12 | 100 | 120.12 | | |
| | 12 | 40 | 52.36 | | |
| | | | | | |
| **Charger** | **voltage V** | **Amper A** | **Outs** | **Price $** | |
| | 24 | 100 | 3 | 1118.54 | |
| | 12 | 45 | 3 | 215.99 | |
| | 24/12 | 40 | | 130.81 | |
| | | | | | |
| **Charger controller** | **voltage V** | **Amper Ah** | **Price $** | | |
| | 12/24 V | 10 | 22.87 | | |
| | | | | | |
| **Inverter** | **voltage V** | **Power W** | **Price $** | **effeciency %** | |
| | 24/230 | 300 | 127.5 | 85 | |
| | 12 | 300 | 225.25 | 90 | |
| | 24 | 2500 | 106.3 | 92 | |
| | 12 | 3200 | 826 | 92 | |
| | | | | | |
| **Switch** | **No. of arrays** | **Price $** | | | |
| | 1 | 131.67 | | | |
| | 2 | 225.61 | | | |
| | 4 | 443.52 | | | |
| | | | | | |
| **Fixing System** | **No. of modules** | **Price $** | | | |
| | 2 | 48.2636 | | | |
| | 3 | 5165.93 | | | |
| | 4 | 80.3572 | | | |
| | 5 | 102.5178 | | | |
| | 6 | 106.5372 | | | |
| | 7 | 111.1495 | | | |
| | 8 | 143.9669 | | | |
| | 9 | 160.7991 | | | |
| | 10 | 165.4037 | | | |
| | | | | | |
| **Wire** | **Dia mm** | **Length m** | **Price $** | | |
| | 4 | 100 | 67.2826 | | |
| | | | | | |
| Cost of PV System (1 Module) | 995.5562 | $ | | | |
| Number of Modules | 385018 | | | | |
| Total Cost of PV System | 383307057 | $ | | | |
| | | | | | |
| Land Cost | 40000 | $ | | | |
| | | | | | |
| Plant availability ( f) | 0.9 | | | | |
| Plant life | 25 | years | | | |
| Operating and Mentenance cost | 1916535.285 | $/yr | | | |
| Intrest rate (i) | 0.08 | | | | |
| Cells replacement cost | 7666141.14 | $/yr | | | |
| Amortization factor ( a ) | 0.093678779 | yr^-1 | | | |
| Annual fixed chareges A fixed | 35907737.1 | $/yr | | | |
| Total annual cost Atot | 45530413.53 | $/yr | | | |
| **Power product cost unit** | **1.12** | **$/kW** | | | |
| | 0.001122666 | | | | |

*FIG. IV-8. The solar collector work sheet.*

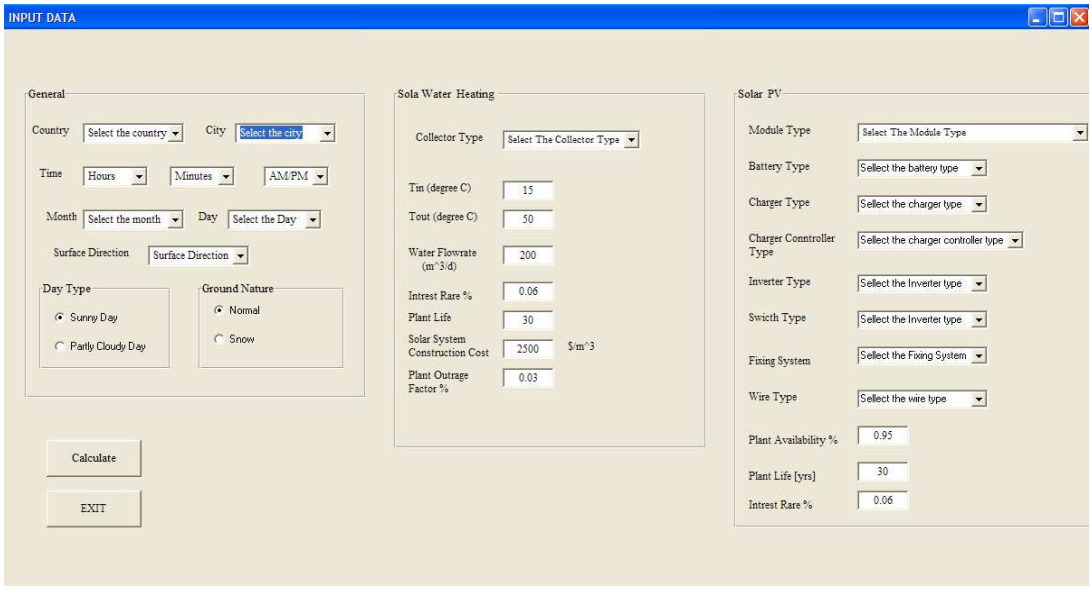


*FIG. IV-9. The solar cell input Macro.*

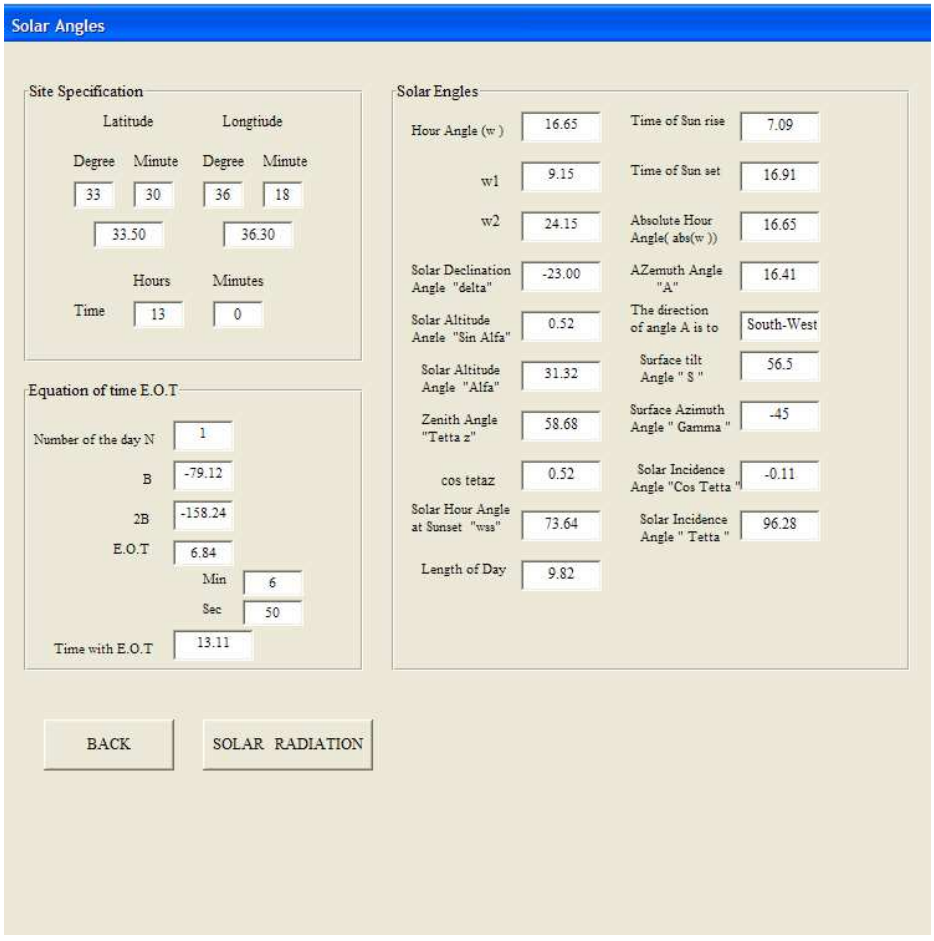


*FIG. IV-10. The solar cell output macro.*

## LIST OF ABBREVIATIONS

| | |
|---|---|
| ALARA | As low as reasonably achievable |
| AP1000 | Advanced pressurized water reactor, 1000 MW(e) |
| BARC | Bhabha Atomic Research Centre |
| Bbl | Barrel of oil (or equivalent barrel of oil) |
| BPE | Boiling point elevation |
| BTU | British thermal unit |
| BWRO | Brackish water reverse osmosis |
| CANDU | Canada deuterium uranium (reactor) |
| CC | Combined cycle |
| CEA | Commissariat à l'énergie atomique et aux énergies alternatives (Atomic Energy and Alternative Energies Commission) |
| CFM | Cubic feet per metre |
| CRP | Coordinated research project |
| DEEP | Desalination economic evaluation program |
| DG TREN | Directorate General for Transport and Energy |
| DM | Demineralised (water) |
| ED | Electro dialysis |
| EDR | Electro dialysis reversal |
| EES | Engineering equation solver |
| FBR | Fast breeder reactor |
| FGD | Flue gas desulphurization |
| GCR | Gas cooled reactor |
| GHG | Greenhouse gas(es) |
| GOR | Gain output ratio |
| GT | Gas turbine |
| GWP | Global warming potential |
| HF | Hollowfibre |
| HT | Horizontal tube |
| HTGR | High temperature gas reactor |

| | |
|---|---|
| HTTF | Horizontal tube thin film |
| HWR | Heavy water reactor |
| IAEA | International Atomic Energy Agency |
| IAPWS | International Association for the Properties of Water and Steam |
| ICRP | International Commission on Radiological Protection |
| KANUPP | Karachi Nuclear Power Plant |
| LCA | Life cycle assessment |
| LHV | Lower heating value |
| LT | Low temperature |
| LTE | Low temperature evaporation |
| LTF | Low temperature flash |
| LTHT MED | Low temperature horizontal tube multieffect distillation |
| LWR | Light water reactor |
| MBTU | One thousand BTU |
| MED | Multieffect desalination |
| MEE | Multieffect evaporation |
| MF | Microfiltration |
| MGD | Million gallon per day |
| MHR | Modular helium reactor |
| MIGD | Million imperial gallons per day |
| MIMO | Multi-input multi-output |
| MPa | Mega pascal |
| MPP | Maximum possible production |
| MSF | Multistage flash |
| MW(e) | Megawatt electric |
| MW(th) | Megawatt thermal |
| MVC | Mechanical vapour compression |
| NEQS | National environment quality standards |
| ND | Nuclear desalination |
| NDDP | Nuclear desalination demonstration plant |

| | |
|---|---|
| NF | Nanofiltration |
| NPSH | Net positive suction head |
| NPV | Net present value |
| ODE | Ordinary differential equations |
| OOP | Object oriented programming |
| PBMR | Pebble bed modular reactor |
| PCW | Primary cooling water |
| PHWR | Pressurized heavy water reactor |
| PID | Proportional-integral-derivative (controller) |
| PPM | Parts per million |
| PR | Performance ratio |
| PWR | Pressurized water reactor |
| RDC | Research and Development Centre |
| R&D | Research and Development |
| RO | Reverse osmosis |
| ROE | Return on equality |
| SEWA | Sharjah Electricity and Water Authority |
| SMR | Small and medium reactors |
| SW | Spiralwound |
| SWCC | Saline water conversion corporation |
| SWRO | Seawater reverse osmosis (desalination) |
| TBT | Top brine temperature |
| TDS | Total dissolved salts |
| TVC | Thermo vapour compression |
| TWG-ND | Technical working group on nuclear desalination |
| UF | Ultrafiltration |
| UNFCCC | United Nations Framework Convention on Climate Change |
| VC | Vapour compression |
| VTE | Vertical tube evaporator (MED system) |
| WHO | World Health Organisation |

| | |
|---|---|
| WLHP | Wraparound loop heat pipe |

## CONTRIBUTORS TO DRAFTING AND REVIEW

| | |
|---|---|
| El-Desoky Ibrahim, A-H | Nuclear Power Plants Authority, Egypt |
| Nisan, S. | Nisan Desalination Services, France |
| Dardour, S. | Centre d'Études Cadarache, France |
| Goswami, D. | Bhabha Atomic Research Centre, India |
| Sudi, A. | National Nuclear Energy Agency, Indonesia |
| Kim, S.S. | Korea Atomic Energy Research Institute, Republic of Korea |
| Muhammad, A. | Pakistan Atomic Energy Commission, Pakistan |
| Suleiman, S. | Atomic Energy Commission of Syria, Syria |
| Jouhara, H. | Brunel University London, United Kingdom |
| Faibish, R. | Argonne National Laboratory, United States of America |
| Belkaid, A. | Commissariat a l'Énergie Atomique, Algeria |
| Rao, I. | Bhabha Atomic Research Centre, India |
| Meenai, J.A. | Pakistan Atomic Energy Commission, Pakistan |
| Tewari, P.K. | Bhabha Atomic Research Centre, India |

## RESEARCH COORDINATION MEETINGS

Vienna, Austria: 27–28 October 2009, 4–5 October 2010, 17–18 October 2011

## CONSULTANTS MEETINGS

Vienna, Austria: 24–26 October 2013

IAEA
International Atomic Energy Agency

No. 23

# ORDERING LOCALLY

In the following countries, IAEA priced publications may be purchased from the sources listed below or from major local booksellers.

Orders for unpriced publications should be made directly to the IAEA. The contact details are given at the end of this list.

**AUSTRALIA**
***DA Information Services***
648 Whitehorse Road, Mitcham, VIC 3132, AUSTRALIA
Telephone: +61 3 9210 7777 • Fax: +61 3 9210 7788
Email: books@dadirect.com.au • Web site: http://www.dadirect.com.au

**BELGIUM**
***Jean de Lannoy***
Avenue du Roi 202, 1190 Brussels, BELGIUM
Telephone: +32 2 5384 308 • Fax: +32 2 5380 841
Email: jean.de.lannoy@euronet.be • Web site: http://www.jean-de-lannoy.be

**CANADA**
***Renouf Publishing Co. Ltd.***
5369 Canotek Road, Ottawa, ON K1J 9J3, CANADA
Telephone: +1 613 745 2665 • Fax: +1 643 745 7660
Email: order@renoufbooks.com • Web site: http://www.renoufbooks.com

***Bernan Associates***
4501 Forbes Blvd., Suite 200, Lanham, MD 20706-4391, USA
Telephone: +1 800 865 3457 • Fax: +1 800 865 3450
Email: orders@bernan.com • Web site: http://www.bernan.com

**CZECH REPUBLIC**
***Suweco CZ, spol. S.r.o.***
Klecakova 347, 180 21 Prague 9, CZECH REPUBLIC
Telephone: +420 242 459 202 • Fax: +420 242 459 203
Email: nakup@suweco.cz • Web site: http://www.suweco.cz

**FINLAND**
***Akateeminen Kirjakauppa***
PO Box 128 (Keskuskatu 1), 00101 Helsinki, FINLAND
Telephone: +358 9 121 41 • Fax: +358 9 121 4450
Email: akatilaus@akateeminen.com • Web site: http://www.akateeminen.com

**FRANCE**
***Form-Edit***
5 rue Janssen, PO Box 25, 75921 Paris CEDEX, FRANCE
Telephone: +33 1 42 01 49 49 • Fax: +33 1 42 01 90 90
Email: fabien.boucard@formedit.fr • Web site: http://www.formedit.fr

***Lavoisier SAS***
14 rue de Provigny, 94236 Cachan CEDEX, FRANCE
Telephone: +33 1 47 40 67 00 • Fax: +33 1 47 40 67 02
Email: livres@lavoisier.fr • Web site: http://www.lavoisier.fr

***L'Appel du livre***
99 rue de Charonne, 75011 Paris, FRANCE
Telephone: +33 1 43 07 50 80 • Fax: +33 1 43 07 50 80
Email: livres@appeldulivre.fr • Web site: http://www.appeldulivre.fr

**GERMANY**
***Goethe Buchhandlung Teubig GmbH***
Schweitzer Fachinformationen
Willstätterstrasse 15, 40549 Düsseldorf, GERMANY
Telephone: +49 (0) 211 49 8740 • Fax: +49 (0) 211 49 87428
Email: s.dehaan@schweitzer-online.de • Web site: http://www.goethebuch.de

**HUNGARY**
***Librotade Ltd., Book Import***
PF 126, 1656 Budapest, HUNGARY
Telephone: +36 1 257 7777 • Fax: +36 1 257 7472
Email: books@librotade.hu • Web site: http://www.librotade.hu

**INDIA**
***Allied Publishers***
1st Floor, Dubash House, 15, J.N. Heredi Marg, Ballard Estate, Mumbai 400001, INDIA
Telephone: +91 22 2261 7926/27 • Fax: +91 22 2261 7928
Email: alliedpl@vsnl.com • Web site: http://www.alliedpublishers.com

***Bookwell***
3/79 Nirankari, Delhi 110009, INDIA
Telephone: +91 11 2760 1283/4536
Email: bkwell@nde.vsnl.net.in • Web site: http://www.bookwellindia.com

**ITALY**
***Libreria Scientifica "AEIOU"***
Via Vincenzo Maria Coronelli 6, 20146 Milan, ITALY
Telephone: +39 02 48 95 45 52 • Fax: +39 02 48 95 45 48
Email: info@libreriaaeiou.eu • Web site: http://www.libreriaaeiou.eu

**JAPAN**
***Maruzen Co., Ltd.***
1-9-18 Kaigan, Minato-ku, Tokyo 105-0022, JAPAN
Telephone: +81 3 6367 6047 • Fax: +81 3 6367 6160
Email: journal@maruzen.co.jp • Web site: http://maruzen.co.jp

**NETHERLANDS**
***Martinus Nijhoff International***
Koraalrood 50, Postbus 1853, 2700 CZ Zoetermeer, NETHERLANDS
Telephone: +31 793 684 400 • Fax: +31 793 615 698
Email: info@nijhoff.nl • Web site: http://www.nijhoff.nl

***Swets Information Services Ltd.***
PO Box 26, 2300 AA Leiden
Dellaertweg 9b, 2316 WZ Leiden, NETHERLANDS
Telephone: +31 88 4679 387 • Fax: +31 88 4679 388
Email: tbeysens@nl.swets.com • Web site: http://www.swets.com

**SLOVENIA**
***Cankarjeva Zalozba dd***
Kopitarjeva 2, 1515 Ljubljana, SLOVENIA
Telephone: +386 1 432 31 44 • Fax: +386 1 230 14 35
Email: import.books@cankarjeva-z.si • Web site: http://www.mladinska.com/cankarjeva_zalozba

**SPAIN**
***Diaz de Santos, S.A.***
Librerias Bookshop • Departamento de pedidos
Calle Albasanz 2, esquina Hermanos Garcia Noblejas 21, 28037 Madrid, SPAIN
Telephone: +34 917 43 48 90 • Fax: +34 917 43 4023
Email: compras@diazdesantos.es • Web site: http://www.diazdesantos.es

**UNITED KINGDOM**
***The Stationery Office Ltd. (TSO)***
PO Box 29, Norwich, Norfolk, NR3 1PD, UNITED KINGDOM
Telephone: +44 870 600 5552
Email (orders): books.orders@tso.co.uk • (enquiries): book.enquiries@tso.co.uk • Web site: http://www.tso.co.uk

**UNITED STATES OF AMERICA**
***Bernan Associates***
4501 Forbes Blvd., Suite 200, Lanham, MD 20706-4391, USA
Telephone: +1 800 865 3457 • Fax: +1 800 865 3450
Email: orders@bernan.com • Web site: http://www.bernan.com

***Renouf Publishing Co. Ltd.***
812 Proctor Avenue, Ogdensburg, NY 13669, USA
Telephone: +1 888 551 7470 • Fax: +1 888 551 7471
Email: orders@renoufbooks.com • Web site: http://www.renoufbooks.com

**United Nations**
300 East 42nd Street, IN-919J, New York, NY 1001, USA
Telephone: +1 212 963 8302 • Fax: 1 212 963 3489
Email: publications@un.org • Web site: http://www.unp.un.org

## Orders for both priced and unpriced publications may be addressed directly to:

IAEA Publishing Section, Marketing and Sales Unit, International Atomic Energy Agency
Vienna International Centre, PO Box 100, 1400 Vienna, Austria
Telephone: +43 1 2600 22529 or 22488 • Fax: +43 1 2600 29302
Email: sales.publications@iaea.org • Web site: http://www.iaea.org/books

International Atomic Energy Agency
Vienna
ISBN 978–92–0–100115–3
ISSN 1011–4289